



HAL
open science

Phosphaalcènes, phosphaallènes : synthèse, structure et calculs théoriques

Petronela Maria Petrar

► **To cite this version:**

Petronela Maria Petrar. Phosphaalcènes, phosphaallènes : synthèse, structure et calculs théoriques. Chimie. Université Paul Sabatier - Toulouse III, 2007. Français. NNT: . tel-00391985

HAL Id: tel-00391985

<https://theses.hal.science/tel-00391985>

Submitted on 5 Jun 2009

HAL is a multi-disciplinary open access archive for the deposit and dissemination of scientific research documents, whether they are published or not. The documents may come from teaching and research institutions in France or abroad, or from public or private research centers.

L'archive ouverte pluridisciplinaire **HAL**, est destinée au dépôt et à la diffusion de documents scientifiques de niveau recherche, publiés ou non, émanant des établissements d'enseignement et de recherche français ou étrangers, des laboratoires publics ou privés.

THESE

présentée devant l'Université Babes-Bolyai de Cluj-Napoca (Roumanie)

en vue de l'obtention du **Doctorat de l'Université Paul Sabatier** et du **Doctorat Roumain** dans le cadre d'une procédure de co-tutelle.

Spécialité : Chimie Moléculaire

par

Petronela Maria PETRAR

Phosphaalkenes, Phosphaallenes : Synthesis, Structure and Theoretical Investigations

Soutenue le 14 décembre 2007 devant la commission d'examen :

Mme. E. Hey-Hawkins	Professeur à l'Université de Leipzig (Allemagne)	Rapporteur
M. D. Horvath	Chargé de Recherche CNRS, Université de Lille (France)	Rapporteur
M. I. Haiduc	Professeur à l'Université Babes Bolyai, Cluj-Napoca (Roumanie)	Examineur
M. R. Poteau	Professeur à l'Université P. Sabatier, Toulouse (France)	Examineur

Directeurs de thèse:

M. I. Silaghi-Dumitrescu	Professeur à l'Université Babes Bolyai, Cluj-Napoca (Roumanie)	Examineur
M. J. Escudié	Directeur de Recherche CNRS, Université P. Sabatier, Toulouse (France)	Examineur

Table of Contents

<i>Introduction</i>	5
Introduction.....	7
I. Review on heteroallenes	
<i>Revue sur les hétérocumulenes</i>	9
1-Phosphaallenes -P=C=C<.....	16
1, 3 – Diphosphaallenes -P=C=P-.....	22
1-Arsaallenes –As=C=C<.....	27
1-Phospha-3-arsaallenes -As=C=P-.....	30
1, 3 – Diarsaallenes -As=C=As-.....	31
1-Silaallenes >Si=C=C<.....	32
1-Phospha-3-silaallenes –P=C=Si<.....	36
1,2,3-Trisilaallene >Si=Si=Si<.....	37
1-Germaallenes >Ge=C=C<.....	40
1-Phospha-3-germaallenes >Ge=C=P-.....	44
1,2,3- Trigermaallenes >Ge=Ge=Ge< and 1,3-digerma-2-silaallenes >Ge=Si=Ge<.....	46
1,2,3- Tristannaallenes >Sn=Sn=Sn<.....	48
Cumulenenic compounds containing doubly-bonded heavy group 14 or/and 15 elements.....	49
<i>References</i>	51
II. Theoretical Characterization of Group 14 Heavy Heteroallenes	
<i>Etude théorique des hétéroallènes lourds de la groupe 14</i>	55
1) Structural minima in the isomeric space of model 1-phospha-3-germaallenes...59	
2) Investigations of model phosphagermaallenes isomers through higher correlated methods.....	66
3) Theoretical Study of 1-Phospha-3-Silaallene Isomers.....	59

4) The influence of Ge-substituents on phosphagermaallenes – a measure for the stability of the P=C=Ge unit.....	72
<i>References</i>	81
III. 1, 3-Digermacyclobutanes with exocyclic C=P and C=P=S double bonds	
<i>1,3-digermacyclobutanes à doubles liaisons P=C et P=C=S exocycliques</i>	85
1) Synthesis and characterisation of a novel halogermylchlorophosphaalkene 4 ...	91
2) Action of <i>t</i> BuLi on derivative 4 . Synthesis of the novel 2, 4-diphosphylydene 1,3-digermacyclobutanes 5a,b	94
3) Mechanism of formation of 5a and 5b	98
4) Synthesis and characterization of the first bis(methylenethioxophosphoranes) bridged by germanium atoms.....	101
5) Theoretical investigation of compounds 5 and 8	106
<i>Experimental Section</i>	114
<i>References</i>	122
<i>Recapitulative list of synthesized compounds</i>	125
IV. Phosphagerma-, phosphasila- and phosphastannapropenes	
<i>Phosphagerma-, phosphasila- et phosphastannapropènes</i>	111
Phosphagermapropenes.....	131
1) Synthesis and characterization of phosphagermapropenes	
Mes*P=C(Cl)Ge(Tip)X ₂	131
2) Synthesis and characterization of the phosphagermapropene	
Mes*P=C(Cl)-Ge(Tip) ₂ X (X = Cl, F)	136
3) Synthesis and characterization of	
Mes*P=C(Cl)-GeCl(<i>t</i> Bu)C ₆ H ₄ - <i>o</i> -CH ₂ -NMe ₂	138
Phosphasilapropenes.....	144
Phosphastannapropenes.....	147
<i>Experimental Section</i>	157
<i>References</i>	169
<i>Recapitulative list of synthesized compounds</i>	171

V. A new phospharsaallene: the arsenylidenebis(methylenephosphorane)	
$(\text{Me}_3\text{Si})_2\text{C}=\text{P}(\text{Mes}^*)=\text{C}=\text{AsMes}^*$	
<i>Un nouveau phospharsaallene: L'arsenylidenebis(methylenephosphorane)</i>	
$(\text{Me}_3\text{Si})_2\text{C}=\text{P}(\text{Mes}^*)=\text{C}=\text{AsMes}^*$	173
1) Synthesis and characterization of the first arsenylidene-bis(methylene)- phosphorane 38	181
2) Action of tBuLi on the arsanyl-bis(methylene)phosphorane 38	187
<i>Experimental Section</i>	190
<i>References</i>	196
<i>Recapitulative list of synthesized compounds</i>	199
<i>Conclusion</i>	201
General Conclusions.....	205
<i>Annex 1</i>	207
<i>Annex 2</i>	211
<i>Annex 3</i>	215

INTRODUCTION

La chimie des phosphaalènes et des phosphallaènes a suscité beaucoup d'intérêt dans la communauté scientifique au cours des dernières décennies. Toutefois, les systèmes hétéroalléniques contenant à la fois des éléments lourds des groupes 14 et 15 du type $E_{14}=C=E_{15}$ sont très peu connus, en raison de leur instabilité ; ce sont des systèmes particulièrement intéressants du point de vue de la recherche fondamentale (par exemple étude de la géométrie, de la détermination des charges, de la ressemblance ou non avec les allènes purement carbonés), mais aussi pour leurs applications potentielles : ainsi les composés contenant l'entité $E=C=P$ pourraient s'avérer d'excellentes précurseurs de polymères organométalliques susceptibles de présenter des propriétés particulières liées à la présence des hétéroatomes. Une amélioration des propriétés optiques, mécaniques, et en particulier électriques de ce type de polymères serait également possible.

Au début de ce travail, il n'y avait pratiquement aucune étude théorique sur les systèmes hétéroalléniques contenant à la fois des éléments lourds des groupes 14 et 15, et il y avait seulement deux phosphagermaallènes $-P=C=Ge<$ (dont un transitoire) et un phosphasilaallène $-P=C=Si<$ caractérisé à basse température, décrits dans la littérature. Notons également qu'il n'existait que de rares dihalogénophosphamétallapropènes, $-P=C(X)-E(X')<$ ($X, X' = \text{halogène}, E = \text{Si, Ge, Sn}$) précurseurs potentiels des hétéroallènes par réaction de déshalogénéation.

Notre travail de thèse a porté sur la synthèse et l'étude de ces dérivés.

Le premier chapitre est une revue bibliographique sur les composés insaturés du type $E=C=E'$ (où E et E' sont des éléments lourds des groupes 14 ou 15).

Le deuxième chapitre est une analyse théorique sur les phosphagermaallènes et les phosphasilaallènes.

-P=C=Ge< et -P=C=Si<. A ce jour, il n'existait aucune étude théorique consacrée à ces composés. La stabilité relative de leurs isomères possibles a été étudiée par plusieurs méthodes théoriques DFT.

La tentative de synthèse d'un nouveau phosphagermaallène, $t\text{Bu}_2\text{Ge}=\text{C}=\text{PMes}^*$, est décrite dans le chapitre 3, avec la caractérisation des composés résultants et l'étude de leur réactivité vis-à-vis du soufre.

Le quatrième chapitre de la thèse décrit la synthèse de plusieurs précurseurs de phosphagermaallènes, principalement des germaphosphapropènes ; les tentatives visant à obtenir les hétéroallènes correspondants seront également discutées. D'autres précurseurs de systèmes alléniques seront également décrits ainsi que les tentatives pour obtenir les premiers phosphasila- et phosphastannaallènes.

Enfin, le chapitre V porte sur la synthèse d'un nouveau type de système hétérocumulénique possédant l'entité $\text{C}=\text{P}=\text{C}=\text{As}$ ainsi que sur la caractérisation de ses précurseurs.

INTRODUCTION

The chemistry of phosphalkenes and phosphallenes has received increasing interest from the scientific community in the last decades. However, heteroallenic systems containing both heavier group 14 and 15 elements are not well known, due to their instability, but there are interesting systems, from the point of view of fundamental research, as well as for their potential applications. Thus, the study of doubly bonded derivatives of the kind mentioned before provides insight in the nature of multiple bonding for heavier main group elements, a challenge that issued from the great difference between the behavior of carbon and that of its congeners. As far as the potential applications are concerned, compounds containing the E=C=P unit can be excellent precursors in the synthesis of organic polymers, that would have special properties due to the presence of the heteroatoms. An improvement of the optical, mechanical and especially the electrical properties of this kind of polymers is foreseen.

Before the beginning of this study, there was practically no work done on the theoretical investigation of heteroallenic systems and there were just two phosphagermaallenes described in the literature. We were concerned with the ways to stabilize the Ge=C=P unit and the study of the compounds deriving from dimerization reactions occurring at the Ge=C bond. Also, several potential precursors of heteroallenic and heterocumulenic systems were synthesized.

The first chapter reviews unsaturated compounds of the type E=C=E' (where E and E' are a group 14 or 15 element) described in the literature. An emphasis is put on their solid state structure, and their reactivity is also discussed. The instability of compounds of the type >E₁₄=C=P- is evidenced by the small number of such compounds that were synthesized and the rapid reactions undergone at the E₁₄=C double bond.

The second chapter consists in a theoretical analysis of phosphagermaallenes --P=C=Ge< . Up to date, there is no such study described in the literature dedicated to these compounds. The possible isomers of model phosphagermaallenes were investigated through DFT methods. The explanation for the chemical reactivity of the Ge=C bond in phosphagermaallenes resides in the electronic structure of the derivatives and the best ways to stabilize this bond are also indicated as a result of the theoretical study.

The attempted synthesis of the novel phosphagermaallene $t\text{Bu}_2\text{Ge=C=PMes}^*$ is described in chapter 3, together with the characterization of the resulting compounds, formal dimers of the heteroallene. Further functionalization of the novel 2,4-diphosphinylidene-1,3-digermacyclobutanes leads to the synthesis of new bis(methylenethiophosphoranes) with potential applications in coordination chemistry.

The fourth chapter of the thesis describes the synthesis of several precursors of phosphagermaallenes, mainly germyl-substituted phosphalkenes. The isolation and purification of these derivatives often proved to be difficult, but NMR spectroscopy provides the means for their characterization in solution. Attempts to obtain the Ge=C=P unit will also be discussed. Other precursors of allenic systems are also synthesized while trying to obtain the first phosphasila- and phosphastannaallene known to date.

Finally, chapter 5 deals with derivatives involved in the synthesis of new types of heterocumulenic systems of group 15 elements. The synthetic route leading to the first arsenyl-bis(methylene)phosphorane is described, together with the full characterization of the precursor to this derivative. Evidence for the formation of the first compound containing the C=P=C=As unit is also discussed.

CHAPTER I

REVIEW ON HETEROALLENES

Chapitre I

Revue sur les hétérocumulènes

Le premier chapitre est une revue bibliographique sur les composés insaturés du type $E=C=C<$, $E=C=E'$ et $E=E=E$ (où E et E' sont des éléments lourds des groupes 14 ou 15) décrits dans la littérature jusqu'à présent. L'accent est mis sur leur synthèse et leur structure à l'état solide, mais leur réactivité est également rapportée.

Plusieurs voies de synthèse conduisant aux phosphallènes $-P=C=C<$ et diphosphallènes $-P=C=P-$ sont présentées et la réactivité de ces dérivés est également passée en revue. Les structures à l'état solide déterminées pour plusieurs phosphallènes sont examinées ; elles montrent que ces dérivés possèdent une structure proche d'une structure allénique, avec toutefois des angles PCC et PCP inférieurs d'environ 10 à 15° aux 180° attendus pour une structure allénique purement carbonée. Quelques arsaallènes, dérivés du type $-As=C=X$, ont déjà été synthétisés; comme pour tous les hétéroallènes, les méthodes employées pour leur stabilisation comprennent principalement l'effet stérique de groupes organiques volumineux (c'est par exemple le cas de $Mes^*As=C=CR_2$, $Mes^* = 2,4,6\text{-tri-}tert\text{-butylphényle}$, $CR_2 = \text{fluorényle}$) ou la complexation avec des métaux de transition. Un seul 1,3-phosphaarsaallène stable ($Mes^*P=C=AsMes^*$) et un seul 1,3-diarsaallène ($Mes^*As=C=AsMes^*$) sont connus à ce jour.

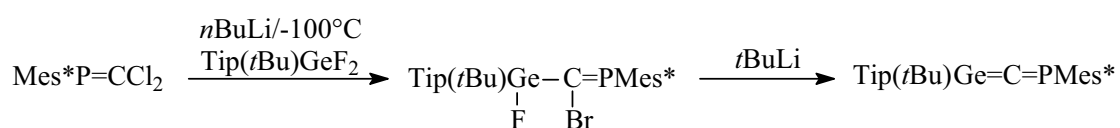
Les dérivés insaturés du silicium et du germanium contenant des doubles liaisons cumulées sont également présentés dans ce chapitre.

Plusieurs silaallènes $>Si=C=C<$ ont été obtenus depuis la synthèse du premier exemple stable par West en 1993 ; leur réactivité est bien illustrée dans la littérature. Par contre, les tentatives pour préparer des phosphasilaallènes ont connu moins de succès et un seul 1,3-phosphasilaallène transitoire a été mis en évidence, $Mes^*P=C=Si(Ph)Tip$ ($Tip = 2,4,6\text{-triisopropylphényle}$). La difficulté bien plus grande d'obtenir des dérivés

alléniques d'un élément du groupe 14 que du groupe 15 vient en particulier du fait que la liaison E₁₄=C est nettement plus réactive que celle de la liaison E₁₅=C.

La synthèse des dérivés du germanium à doubles liaisons contiguës s'avère également difficile, comme celle des silaallènes. Ainsi, seulement deux germaallènes stables ont été décrits à ce jour, le premier par West en 1998 et le second par Okazaki

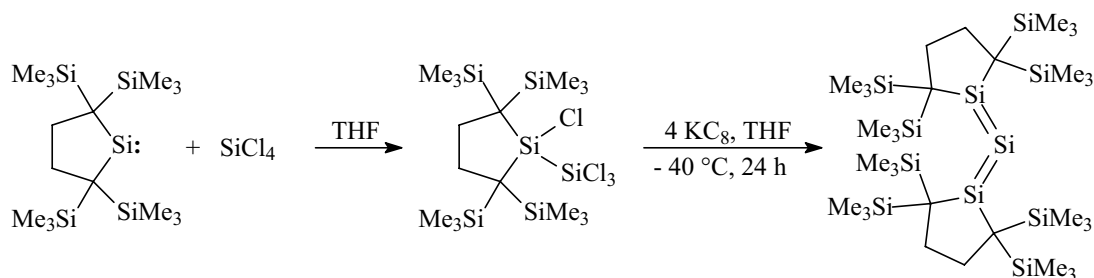
Le seul phosphagermaallène -P=C=Ge< stable a été synthétisé selon le schéma I.1 et sa réactivité a été étudiée, notamment dans des réactions de cycloaddition avec des aldéhydes et des cétones.



Schema I.1

L'instabilité des hétéroallènes du type >E₁₄=C=P- est attestée par le petit nombre de ces composés qui ont été synthétisés : elle est notamment liée à la difficulté de trouver les substituants adéquats pour la stabilisation de la double liaison E₁₄=C : assez volumineux pour empêcher la dimérisation mais permettant néanmoins le couplage des deux entités métallées et phosphorées et par la rapidité des réactions de la double liaison E₁₄=C.

Un 1,2,3-trisilaallène, le 1,3-bis(1,1,4,4-tetrakis(trimethylsilyl)butane-1,4-diyl)trisilaallène, analogue silicié d'un allène, a été obtenu en 2003 par Kira et al. (schéma I.2) et sa structure à l'état solide a été déterminée.



Schema I.2

Des analogues germaniés et des dérivés mixtes siliciés et germaniés ont également été obtenus par le même auteur. On doit cependant noter que tous ces dérivés

avec 3 éléments lourds du groupe 14 présentent une structure assez éloignée de celle des allènes purement organiques, avec un angle $E_{14}=E_{14}=E_{14}$ inférieur de plus de 50° aux 180° attendus.

Les analogues de ces dérivés avec l'étain sont inconnus ; le seul composé de l'étain avec des doubles liaisons cumulées est le tristannaallène $R_2Sn=Sn=SnR_2$ ($R = tBu_3Si$).

Beaucoup de 1-phosphabutatriènes $-P=C=C=C<$ et de 1,4-diphosphabutatriènes $-P=C=C=P-$ sont connus, mais peu de progrès a été accompli dans le cas des arsa- et silabutatriènes. Seuls un 1-silabutatriène et un arsabutatriène transitoires ont été décrits. Des dérivés analogues du germanium ou de l'étain n'ont jamais été obtenus.

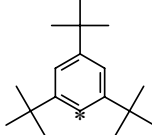
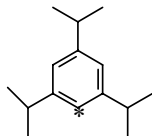
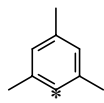
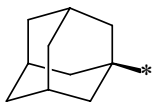
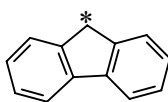
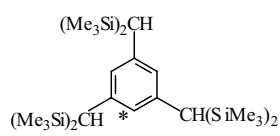
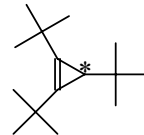
Alors que presque toutes les combinaisons possibles de $>E_{14}=C=C<$ ($E_{14} = Si, Ge$), $>E_{14}=C=P-$, $>E_{15}=C=C<$ ($E_{15} = P, As$) et $-E_{15}=C=E_{15}$ aient été obtenues jusqu'à présent (à l'exception de $E_{14} = Sn$), on ne peut pas en dire de même pour les dérivés cumuléniques. Leur chimie est encore nouvelle, même si quelques tentatives pour synthétiser des dérivés du type $E_{14/15}=C=C=C<$ ont déjà été faites.

There is a high interest shown by chemists in comparing the carbon chemistry with that of heavier elements of the same group. The quest for the silicon, germanium or tin analogues derivatives of alkenes, allenes and even cumulenes has resulted in hundreds of publications over the last decades. This has expanded to group 15 elements, as well, and it has been three decades since the first stable diphosphene [1] -P=P- and disilene [2] >Si=Si< have been obtained. Since then, almost every structure of the type $\text{E}=\text{E}'$ ($\text{E} = \text{C}, \text{Si}, \text{Ge}, \text{Sn}$; $\text{E}' = \text{N}, \text{P}, \text{As}$) has been synthesized, so focus has been put recently on the obtaining of derivatives containing the $\text{E}=\text{C}=\text{E}'$ or $\text{E}=\text{C}=\text{C}=\text{E}'$ units. Escudié and coworkers wrote a review on the subject in 2000 [3], and their classification of these types of compounds will be kept throughout this paper.

Increasing the unsaturation number while maintaining the stability of the compound became a real challenge and indeed the synthesis of systems as $\text{E}_{14}=\text{C}=\text{Y}$, where E_{14} = group 14 element and Y = group 15 to 16 element was attempted. The presence of two adjacent double bonds only made the task more difficult, but it has been proven that bulky substituents are useful in the stabilization of such compounds. Another solution is the formation of a π -complex by coordinating one of the double bonds to a transition metal. Such methods of stabilization work very well for $\text{Y}=\text{C}=\text{Y}$ ($\text{Y} = \text{C}, \text{N}, \text{P}$), for which η^1 and η^2 coordination occurs.

The substituents on E and E' play a major role in the stabilization of the multiple bonded group 14 and 15 element derivatives. Polymerization is prevented by both the increase in the activation energy to the polymerization process by steric crowding (kinetic stabilization), and the decrease in the stability of the polymers through increased steric crowding (thermodynamic stabilization). Some of the most common organic substituents used for this purpose are listed in Table I.1.

Table I.1. Bulky substituents used for steric protection of reactive multiple bonds

R	Structural Formula	Notation
2,4,6-Tri(<i>tert</i> -butyl)phenyl		Mes*
2,4,6-Tri-isopropylphenyl		Tip
2,4,6-Trimethylphenyl(mesityl)		Mes
Phenyl		Ph
Trisyl	(Me ₃ Si) ₃ C	Tsi
Tri(<i>tert</i> -butyl)silyl	^t Bu ₃ Si	
Trimethylsilyl	Me ₃ Si	
Adamantyl		Ad
Fluorenyl		CR ₂
<i>o</i> -Tolyl		<i>o</i> -Tol
2,4,6-Tri(bisyl)phenyl		Tbt
<i>Tert</i> -butyl	(CH ₃) ₃ C	<i>t</i> Bu
1,2,3-Tri- <i>tert</i> -butyl-cyclopropenyl		

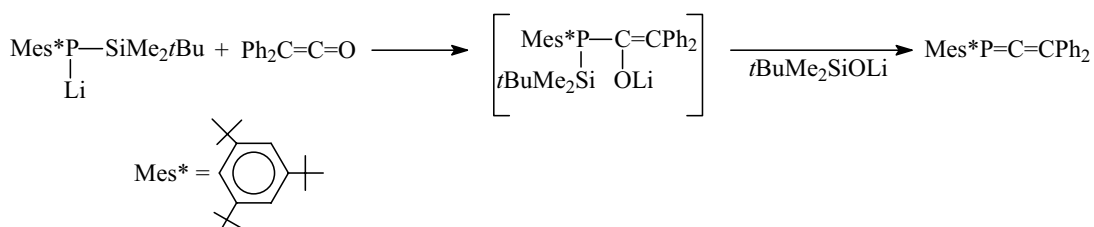
The chapter presents literature data reviewed up to 2007 on unsaturated derivatives of the type $>E_{14}=C=C<$ (1- E_{14} -allenes), $>E_{14}=C=E_{14}<$ (1,3- E_{14} -allenes), $>E_{14}=C=P-$ (1- E_{14} -phosphaallenes), $>E_{15}=C=C<$, and $>E_{15}=C=E_{15}$, where $E_{15} = \sigma^3\lambda^2\text{-P}$, -As. Some cumulenic-type derivatives will also be reviewed. Synthetic routes, spectroscopic data and the reactivity of these compounds are presented. All X-Ray structural data were taken from the *Cambridge Crystallographic Database* or from supplementary materials given by the authors. The crystallographic files were opened with ORTEP [4] and rendered with POV-Ray [5].

1-Phosphaallenes -P=C=C<

1. Synthesis of phosphaallenes

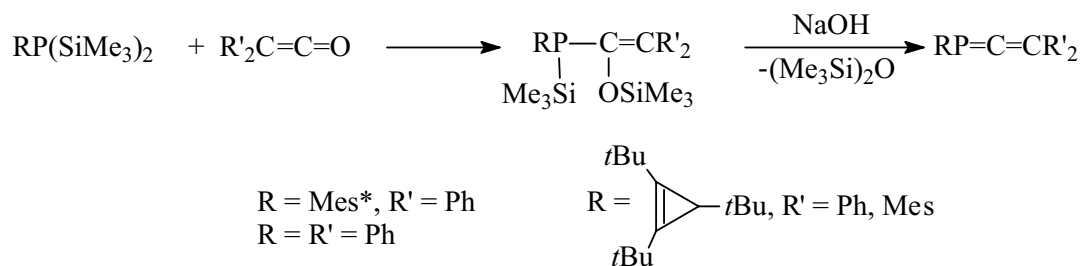
There are various synthetic routes to phosphaallenes; some of the most used ones are presented below.

The first stable compound of this type was obtained in 1984 by Yoshifuji and coworkers, through the reaction of a ketene with the lithium derivative of a silyl-substituted phosphine (scheme I.1) [6, 7].



Scheme I.1

This type of reaction has also been employed in the synthesis of several other transient or stable phosphaallenes. An alternative is the use of disilylphosphines, instead of the lithium derivatives, where the elimination of linear siloxanes in the presence of sodium hydroxide is the driving force of the reaction (scheme I.2) [8, 9].

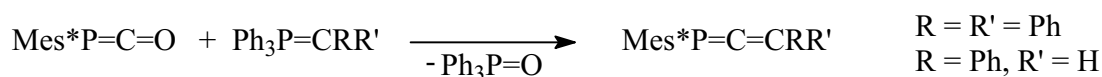


Scheme I.2

In the absence of a sufficient steric hindrance on the phosphorus atom ($\text{R} = \text{R}' = \text{Ph}$), dimerization of the formed phosphaallene is instantaneous, with the formation of the

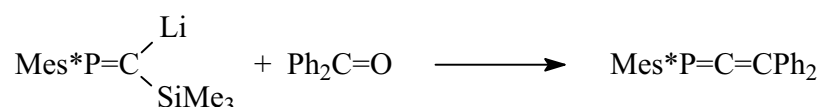
head-to-tail dimer, and the phenyl groups on the phosphorus atoms in an anti orientation [10].

Another commonly employed method is a Wittig type reaction which allowed the synthesis of several phosphallenes (scheme I.3) starting from the sterically crowded Mes*P=C=O [1]:



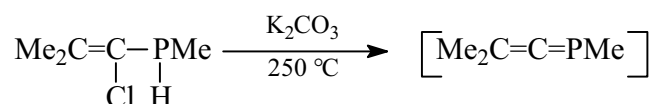
Scheme I.3

Mes*P=C=CPh₂ was also obtained by the reaction of benzophenone with 1-silyl-2-phosphavinyl lithium, as shown below (scheme I.4) [9]:



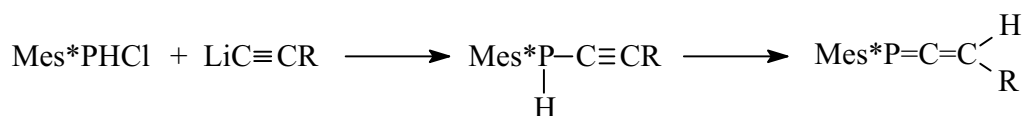
Scheme I.4

Some transient phosphallenes have been evidenced in the dehydrochlorination of 1-chlorovinylphosphines in the presence of DBU [11, 12], at low temperatures, or K₂CO₃ in gas phase at 250°C, but the reaction is always followed by an allene-alkyne rearrangement. The resulting products oligomerize on warming up to -20 °C. This kind of rearrangement can be avoided by the lack of hydrogen on the vinyl group. When a pure (but transient) phosphallene is obtained in the gas phase [12], it also undergoes subsequent oligomerization (scheme I.5):



Scheme I.5

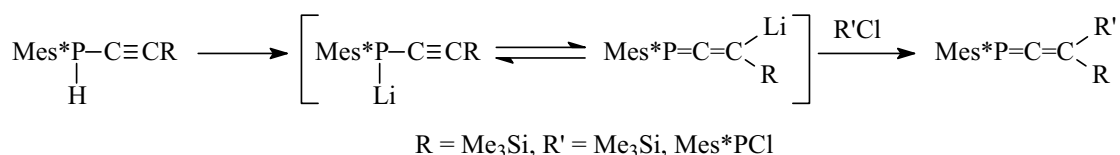
The alkyne-allene reaction was employed in the synthesis of various phosphallenes $\text{Mes}^*\text{P}=\text{C}=\text{CHR}$ ($\text{R} = \text{Ph}, \text{tBu}, \text{Me}$ and $\text{CR}'\text{R}''\text{OSiMe}_3$, where $\text{R}' = \text{R}'' = \text{H}, \text{Me}, \text{Ph}$; $\text{R}' = \text{Ph}, \text{R}'' = \text{Me}, 4\text{-MeC}_6\text{H}_4, \alpha\text{-naphthyl}$). The corresponding alkynylphosphine is prepared according to the scheme I.6 [13]:



Scheme I.6

The use of the lithium derivatives for the obtaining of alkynylphosphines seems to be necessary; in the case of the corresponding reaction with Grignard reagent the formation of the phosphallenes does not occur. This is explained in terms of the difference in basicity between the magnesium and lithium derivatives: the former, being less basic, stabilizes the alkyne and does not induce the rearrangement.

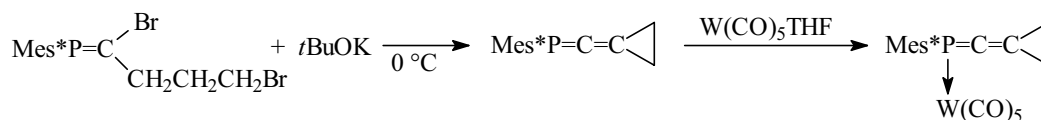
An alternative to the synthetic route discussed above is the treatment of a stable alkynylphosphine with lithium derivatives, like MeLi [14] or $n\text{BuLi}$ [15]. It is believed [15] that the afforded lithium phosphide is in equilibrium with the lithiated allene, and a subsequent reaction with $\text{R}'\text{Cl}$ derivatives leads to the formation of novel phosphallenes (scheme I.7).



Scheme I.7

Stabilization of the $\text{P}=\text{C}=\text{C}$ moiety seems to require steric hindrance mainly on the phosphorus atom, since the synthesis of such derivatives with small groups on the sp^2 carbon has been performed. However, further stabilization is afforded by the use of transition metals, when P coordinates to the metallic centre with the formation of complexes which are easier to characterize in solid state, due to their tendency to crystallize. Thus, a phosphallene containing a cyclopropylidene unit has been obtained

in an excellent yield by a dehalogenation reaction [16] and it readily reacts with $W(CO)_5THF$ (scheme I.8). The structure of the resulting complex is discussed below.



Scheme I.8

2. Structural characterization of phosphallenes

NMR spectroscopy appears very useful in the characterization of such compounds, with signals in ^{31}P NMR at higher fields, compared to those of phosphalkenes, between 40 and 95 ppm, depending on the nature of the substituents on both the phosphorus and the carbon atoms [3]. The chemical shifts of the sp hybridized carbon atom appear in the expected area, from 209 to 250 ppm, while those of the sp^2 carbon atom are observed between 93 and 157 ppm. The $^1J_{CP}$ and $^2J_{CP}$ coupling constants display values between 23-30 Hz, and 10-18 Hz, respectively [3].

Phosphaallenes are colorless substances, very few are pale yellow. The solid state structure has been determined for several phosphallenes (see table I.2). An ORTEP diagram for $Mes^*P=C=CPh_2$ is shown in figure I.1, and relevant geometrical parameters for several other phosphallenes are given in Table I.2.

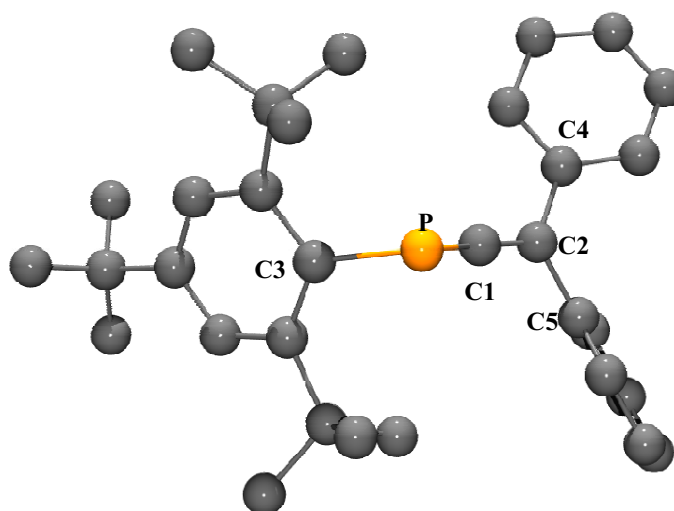
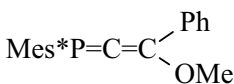
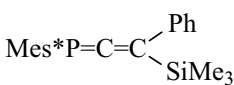
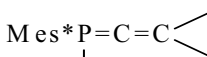
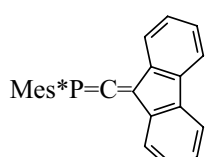


Figure I.1. Molecular structure of $Mes^*P=C=CPh_2$ [17]

Table I.2. Geometrical data for phosphaalenes in the solid state

Molecule	P-C1 (Å)	C1-C2 (Å)	P-C1-C2 (degrees)	C1-P-C3 (degrees)	C2-C1-P-C3 (degrees)	P-M (Å)	Ref.
Mes*P=C=CPh ₂	1.628	1.310	167.70	103.90	171.32		17
Mes*P=C=CH ₂	1.637	1.337	174.27	101.44	152.30		18
Mes*P=C=C ₂ 	1.623	1.340	163.06	105.75	178.87		19
Mes*P=C=C ₂ 	1.629	1.313	170.95	102.93	160.76		20
Mes*P=C=CPh ₂ ↓ Ni(CO) ₃	1.615	1.318	171.51	102.39	155.56	2.234	21
Mes*P=C=C ₂  ↓ W(CO) ₅	1.636	1.269	171.63	102.53	167.45	2.531	16
Mes*P=C=CPh ₂ ↓ W(CO) ₅	1.630	1.311	171.41	103.38	161.11	2.531	22
Mes*P=C=C ₂ 	1.628	1.335	169.94	104.78	171.80		23

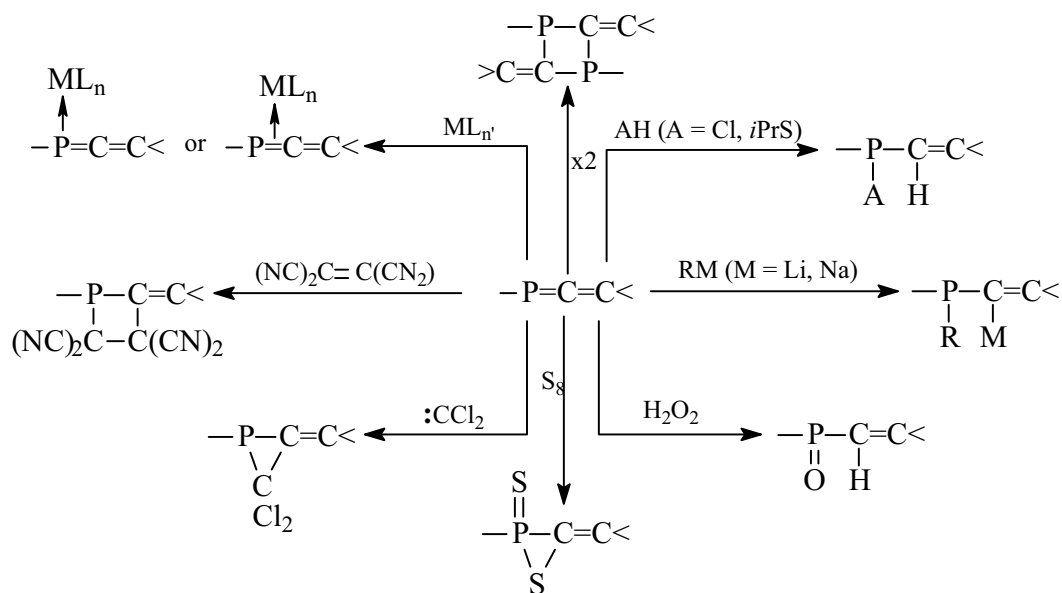
It can be noticed that the P=C bond lengths are a bit shorter than those in phosphaalenes, which vary between 1.64 and 1.69 Å. An explanation can be the presence of the *sp* hybridized carbon atom. The same considerations apply for the C=C bond. The P-C-C angle deviates from the expected linearity, but the steric hindrance of the bulky substituents cannot be the only reason, as analogue phosphaalenes complexes with transition metals exhibit the same deviation. We can assume that crystal packing must play an important role in this structural characteristic, but the electronic effects should also be considered, as *ab initio* calculations predict a bent P=C=C skeleton for

simpler, model compounds [24]. By contrast, the sp^2 carbon barely deviates from the ideal trigonal geometry.

3. Reactivity of phosphallenes

As expected, the P=C double bond is the most reactive site in the molecule, and most of the addition reactions occurring involve this bond. The phosphorus atom is also a reactive centre, and complexation with transition metals is easily carried out, with different outcomes, depending on the nature of the metal and the experimental conditions.

The following scheme summarizes the types of reactions undergone by phosphallenic derivatives [3]:

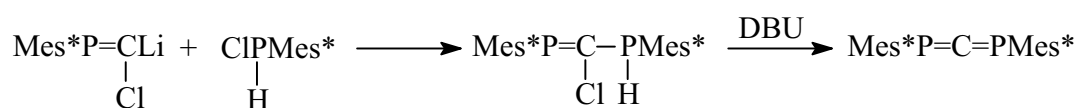


Scheme I.9

1,3 – Diphosphaallenes -P=C=P-

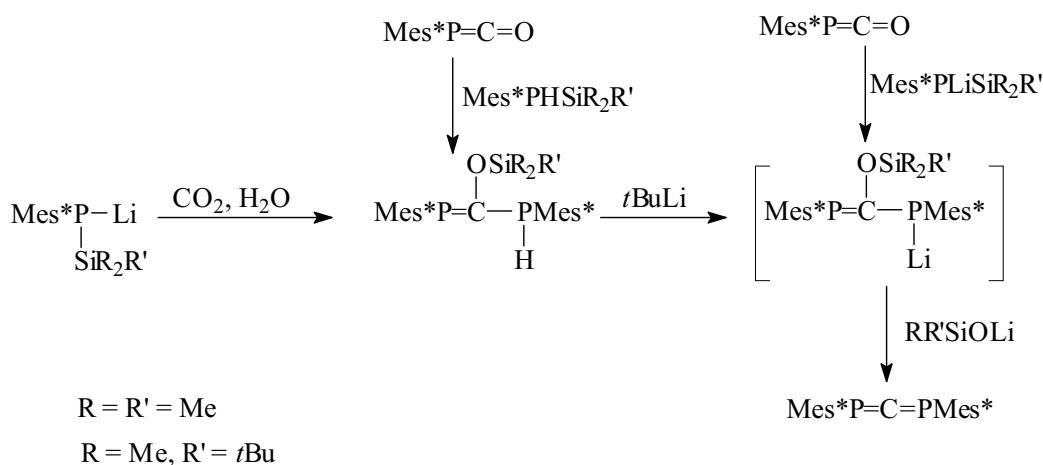
1. Synthesis of diphosphaallenes

Very few diphosphaallenes are known to date [3], but a series of synthetic routes are described in the literature. The first representative type, $\text{Mes}^*\text{P}=\text{C}=\text{PMes}^*$ was prepared by dehydrohalogenation reactions in the presence of DBU or *t*BuOK, as shown in scheme I.10.



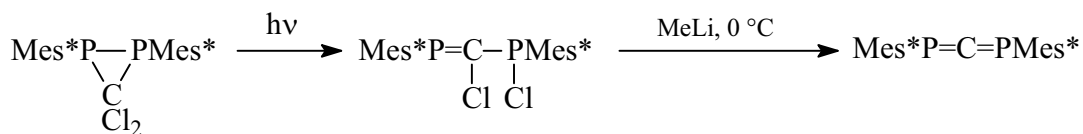
Scheme I.10

Elimination of lithium silanolates from the corresponding substituted diphosphapropenes was also used to prepare the symmetrical diphosphaallenes [17, 25] (scheme I.11).



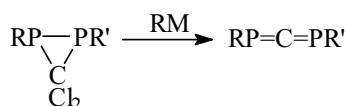
Scheme I.11

3,3-Dichloro-1,2-diphosphiranes undergo a photolytic ring opening to afford dihalodiphosphapropenes, which are suitable precursors of diphosphaallenes [26, 27]. The dehalogenation reaction is carried out in the presence of lithium derivatives, using Et_2O as a solvent, at low temperature. This synthetic route has also been employed in the preparation of $\text{Mes}^*\text{P}=\text{C}=\text{PMes}^*$ (scheme I.12).



Scheme I.12

Diphosphirane ring opening can also be achieved by alkyllithium reagents or anions of transition metal complexes [28]: in this case, it affords diphosphaallenes through a mechanism that reasonably involves a 1, 3-diphosphaallyl anion [29] (scheme I.13).



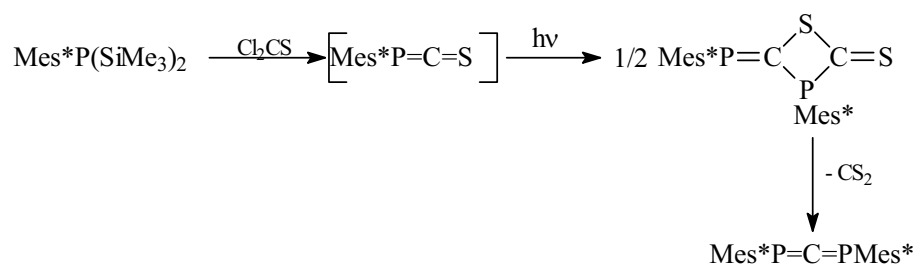
RM = MeLi, *n*BuLi, Cp(CO)₃MoNa, Cp(CO)₃WNa, Cp(CO)₂FeNa, (CO)₄CoNa,

R = R' = Mes*, 2,4,6-(CMe₂Et)₃C₆H₂, 2,6-*t*Bu-C₆H₄

R = Mes*, R' = 2,4,6-(CMe₂Et)₃C₆H₂

Scheme I.13

The transient phosphathioketene Mes*P=C=S dimerizes with the formation of a four membered thiophosphaethane ring which decomposes under UV irradiation [30] to afford Mes*P=C=PMes* and CS₂, as shown in scheme I.14.



Scheme I.14

2. Structural characterization of diphosphaallenes

NMR chemical shifts for the phosphorus atoms in diphosphaallenes are as expected at lower field than those of phosphoallenes, with values between 141 and 169 ppm. The ^{13}C spectra show signals at 270-280 ppm, with $^2J_{\text{CP}}$ coupling constants around 58 Hz [3].

Solid state diffraction studies were performed for $\text{Mes}^*\text{P}=\text{C}=\text{PMes}^*$ [31] and its η^1 -pentacarbonyltungsten complex [32]. The structures are shown in figures I.2 and I.3, and some relevant geometrical data are also given.

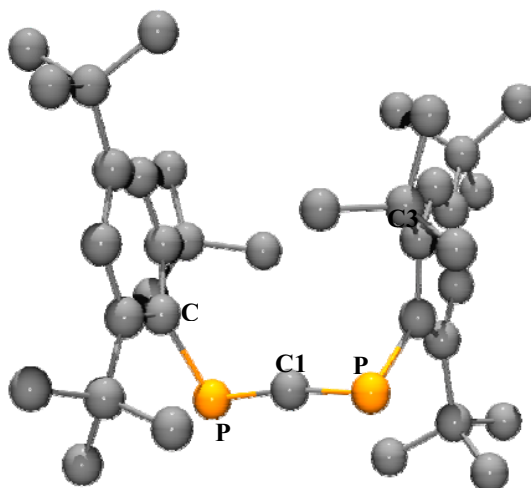


Figure I.2. Molecular structure of $\text{Mes}^*\text{P}=\text{C}=\text{PMes}^*$ [31]

Geometrical parameters: P1-C1 (1.639 Å), P1-C2 (1.876 Å), P1-C1-P2 (172.52°),
C1-P1-C2 (99.85°), C2-P1-C1-P2 (135.86°)

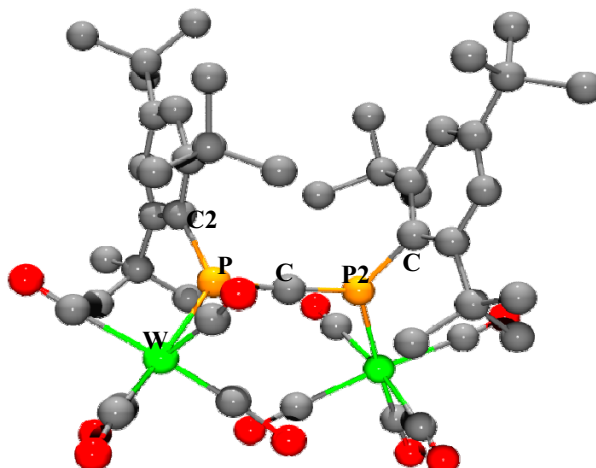
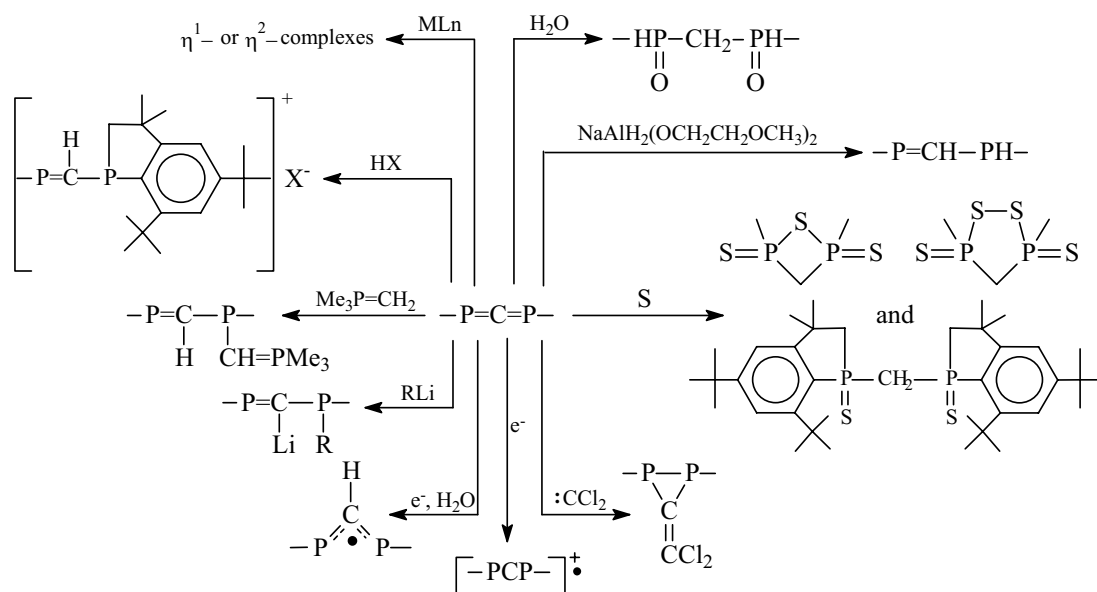


Figure I.3. Molecular structure of $(\text{CO})_5\text{W}(\text{Mes}^*)\text{P}=\text{C}=\text{P}(\text{Mes}^*)\text{W}(\text{CO})_5$ [32]
 Geometrical parameters: P2-C1 (1.640 Å), P2-C3 (1.851 Å), P2-W (2.517 Å), P1-C1-P2 (170.91°), C1-P2-C3 (109.82°), C3-P2-C1-P1 (-28.45°)

The C2-P1-C1 and C1-P2-C3 dihedral angle is 81.79° for the free diphosphaallene and even smaller, of 72.73° , in the case of the tungsten complex. This corresponds to a smaller value than that for the phosphaaallenes, where the deviation from the ideal allenic system was less than 5° . It is interesting to note also that the P=C bond length has similar values for both classes of derivatives.

3. Reactivity of diphosphaallenes

Scheme I.15 summarizes the main reactions undergone by diphosphaallenes [3]. The presence of two double P=C bonds complicates the reaction outcome, but it can still be seen that the carbon atom is the negatively charged centre of the molecule, a fact that has been confirmed by theoretical calculations [3].



Scheme I.15

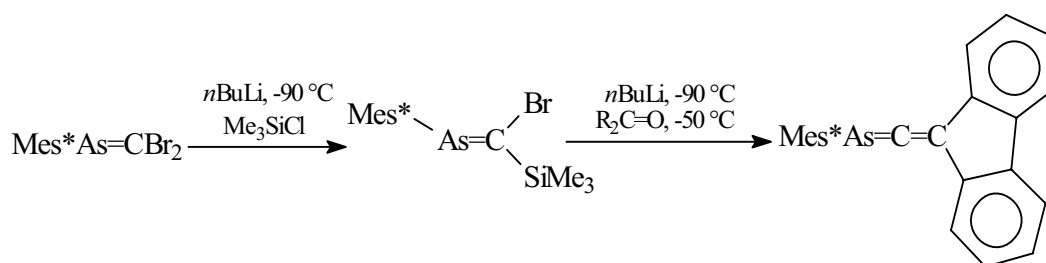
In the case of less hindered derivatives, head-to-tail dimerization occurs with the formation of an almost planar 1,3-cyclodiphosphaethane [33].

The behavior towards transition metals varies, depending on the nature of the metallic atom: η^1 -complexes are obtained in the case of W [32], η^2 - coordination is preferred for Ni, Pd and Pt [34, 35, 36], and even η^3 when Co is used. Iron induces cyclization involving one of the *o*-*t*Bu groups [37] on the phosphorus atom, but coordination from the other one is still possible. The versatility towards complexation of diphosphaallenes makes them of great interest as potential ligands in the chemistry of transition metals.

1-Arsaallenes –As=C=C<

Only two transient arsaallenes have been reported previously to the synthesis of the stable $\text{Mes}^*\text{As}=\text{C}=\text{CR}_2$ by Bouslikhane and coworkers in 2002 [38]. One was postulated as an intermediate in an alkyne-allene rearrangement similar to that discussed for 1-phosphaallenes [39]. A cumulene-like compound $\text{TsiAs}=\text{C}=\text{C}=\text{CPh}_2$ was also stated [40].

The low temperature synthetic route used for the preparation of the stable arsaallene employs $\text{Mes}^*\text{As}=\text{CBr}_2$ as a starting material and is carried out as shown in scheme I.16:



Scheme I.16

The first step of the reaction involves the formation of the sole *Z* isomer, as evidenced by the formation of the corresponding arsaalkene, characterized by NMR spectroscopy and X-ray diffraction in the solid state. After the addition of fluorenone, elimination of Me_3SiOLi readily occurs on warming up the reaction mixture to room temperature.

The ^{13}C NMR spectrum of the arsaallene shows the expected very low field signal at 255.8 ppm for the *sp* hybridized carbon atom and the characteristic value of 129.1 ppm for the one belonging to the fluorenylidene group.

The sterically hindered arsaallene is stable in air and no change is recorded when exposed to moisture. Colorless crystals are readily obtained from pentane and the molecular structure in the solid state was determined by means of X-ray diffraction. An ORTEP diagram is presented in figure I.4, together with relevant data [38].

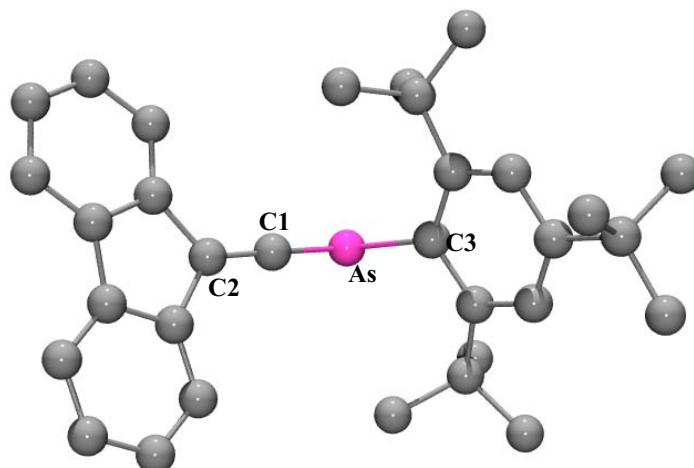
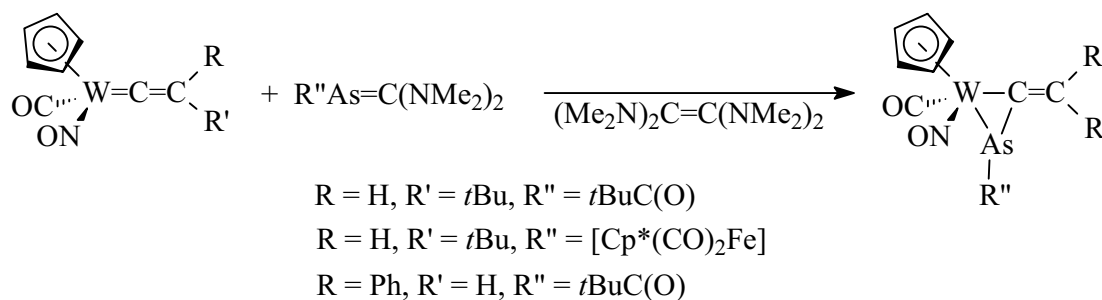


Figure I.4. Molecular structure of Mes*As=C=CR₂ [38]

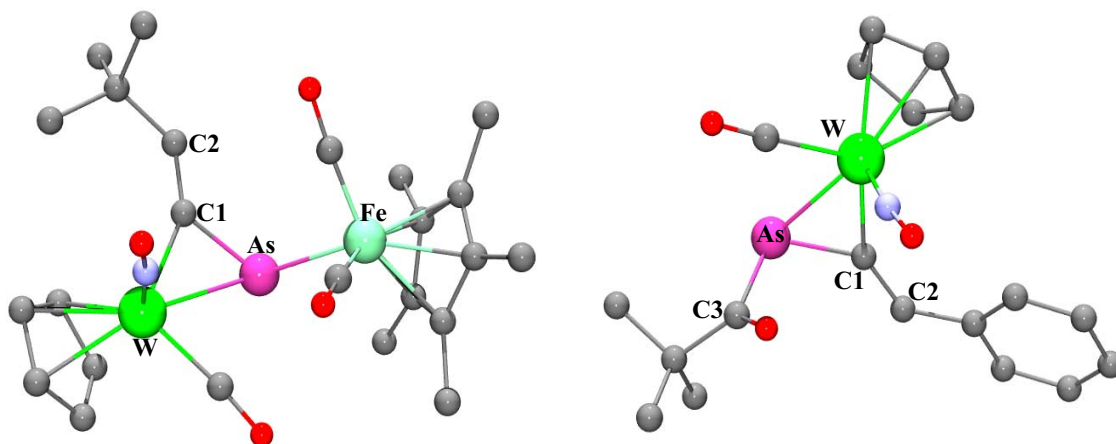
Geometrical parameters: As-C1 (1.754 Å), C1-C2 (1.314 Å), As-C3 (1.996 Å), As-C1-C2 (169.73°), C1-As-C3 (101.95°), C2-C1-As-C3 (-175.83°)

Very recently, three novel η^2 -1-arsaallenes transition metal complexes were obtained from reactions of tungsten complexes with equimolecular quantities of arsaalkene (scheme I.17) [41]. These complexes are obtained in good yields and are sensitive to air and moisture. This proof of the capacity of arsaallenes to act as a ligand towards transition metals comes as another incentive in the study of this kind of allenic derivatives.



Scheme I.17

Solid state structures for two of these derivatives are available (Figure I.5) [41]. The value of the As-C bond length in these compounds, around 1.900 Å, indicates that it can be envisaged as a double bond elongated by π -coordination to the metal centre. Lengths for As=C bonds reported in the literature vary from 1.789 to 1.867 Å [42].



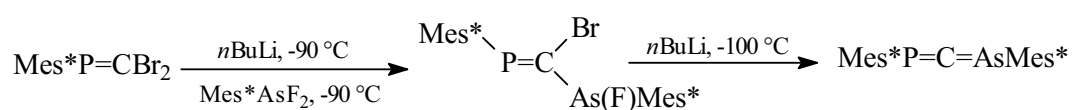
(a) As-C1 (1.911 Å), C1-C2 (1.348 Å), As-Fe (2.442 Å), As-W (2.714 Å), C1-W (2.164 Å), As-C1-C2 (128.94°), C1-As-Fe (112.94°), C2-C1-As-Fe (69.08°)

(b) As-C1 (1.909 Å), C1-C2 (1.360 Å), As-C3 (2.065 Å), As-W (2.690 Å), C1-W (2.134 Å), As-C1-C2 (131.62°), C1-As-C3 (95.37°), C2-C1-As-C3 (79.70°)

Figure I.5. Molecular structures of $[\text{Cp}(\text{CO})(\text{NO})\text{W}\{\eta^2\text{-}[\text{Cp}^*(\text{CO})_2\text{Fe}]\text{AsC}=\text{C}(\text{H})\text{tBu}\}]$ (a) and $[\text{Cp}(\text{CO})(\text{NO})\text{W}\{\eta^2\text{-tBuC}(\text{O})\text{AsC}=\text{C}(\text{H})\text{tBu}\}]$ (b) [41]

1-Phospha-3-arsaallenes -As=C=P-

The only phosphaarsaallene known to date, Mes*As=C=PMes* was prepared by Escudié and coll. in 1998 [43] following the series of reactions represented in scheme I.18. The first step is similar to that used in the synthesis of the 1-arsaallene described above. Again, only one isomer of the phosphaalkene lithium derivative seems to be obtained during the lithiation step.



Scheme I.18

The signal for the phosphorus atom in ^{31}P NMR appears as expected at low field (159.7 ppm) and the shift for the carbon atom is characteristic for allenic systems [44], at 299.54 ppm. A $^1J_{\text{CP}}$ coupling constant of 75.1 Hz was found.

The phosphaarsaallene was crystallized from pentane as yellow, air- and moisture-stable crystals. The space group found was $C2/c$, and the P and As atoms occupy symmetry-equivalent positions. Even though the structure could not be refined (so atom coordinates are not given in the paper) the P=C=As moiety was evidenced [43].

1,3 – Diarsaallenes -As=C=As-

A similar synthetic route as that employed for the preparation of $\text{Mes}^*\text{As}=\text{C}=\text{PMes}^*$ was used in order to obtain the first diarsaallene, $\text{Mes}^*\text{As}=\text{C}=\text{AsMes}^*$ [45], starting from the arsaalkene $\text{Mes}^*\text{As}=\text{CBr}_2$. Again, the use of very sterically-challenging organic groups on the arsenic atom makes the compound extremely stable to air and moisture. The solid-state molecular structure was determined by X-ray diffraction and an ORTEP diagram is shown in figure I.6.

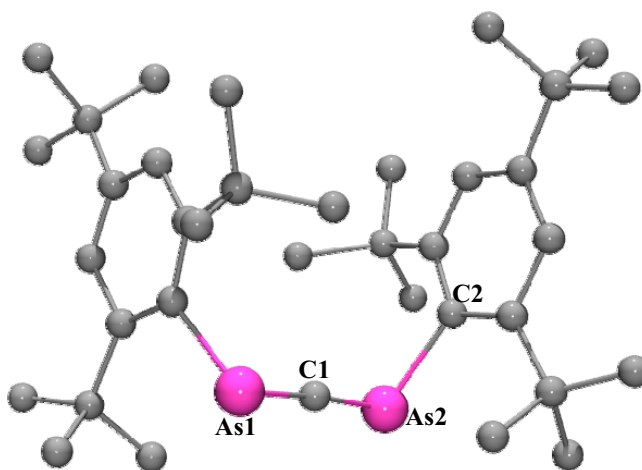


Figure I.6. Molecular structure of $\text{Mes}^*\text{As}=\text{C}=\text{AsMes}^*$ [45]

Geometrical parameters: As1-C1 (1.759 Å), As2-C2 (2.022 Å), As1-C1-As2 (175.58°),
C1-As2-C2 (97.43°), As1-C1-As2-C2 (-141.40°)

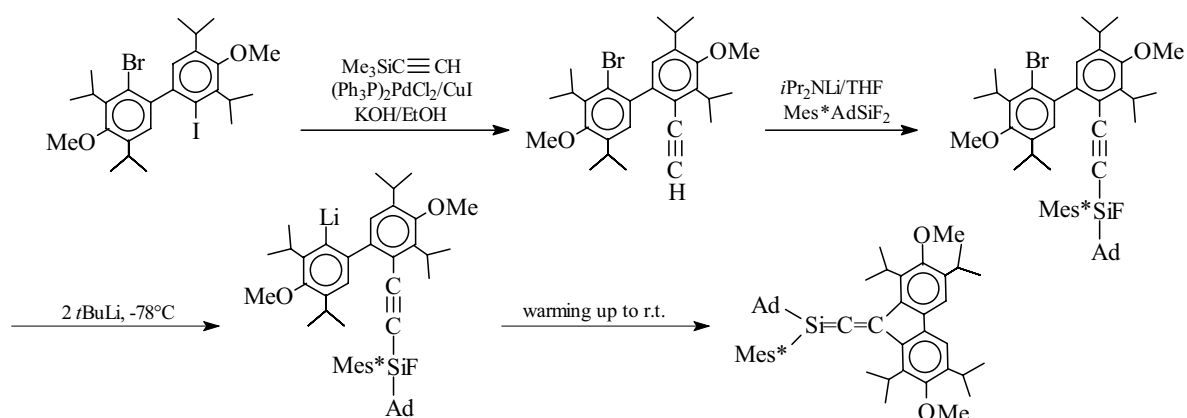
The molecule has a two-fold symmetry axis, which contains the *sp*-hybridized carbon atom. The As=C bond length is comparable to that found in the 1-arsaallene $\text{Mes}^*\text{As}=\text{C}=\text{CR}_2$. The angle between the planes containing the As=C and the C=C bonds is 77.13° (smaller than that reported for the arsaallene, of 83.94°), and the As-C-As angle is very close to the ideal value of 180°.

1-Silaallenes >Si=C=C<

Several transient silaallenes were postulated two decades ago in photolysis or thermolysis of silirenes and ethynyldisilanes [3]. They readily undergo dimerization or addition reactions involving the solvent. However, using trapping agents, it was possible to evidence the formation of these short-lived molecules. An approach in stabilizing silaallenes was the complexation with transition metals. For instance, in the presence of nickel complexes, alkynylpolysilanes undergo a transformation to afford a mixture of silaallene-nickel complexes and nickelasilacyclobutenes as intermediates. The final products of the reaction greatly depend on substituents on the silicon or carbon atom.

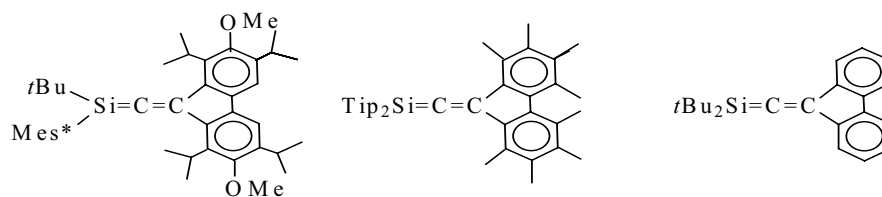
1. Synthesis of 1-silaallenes

The first stable silaallene was obtained by West in 1993 [46], following the synthetic route presented in scheme I.19.



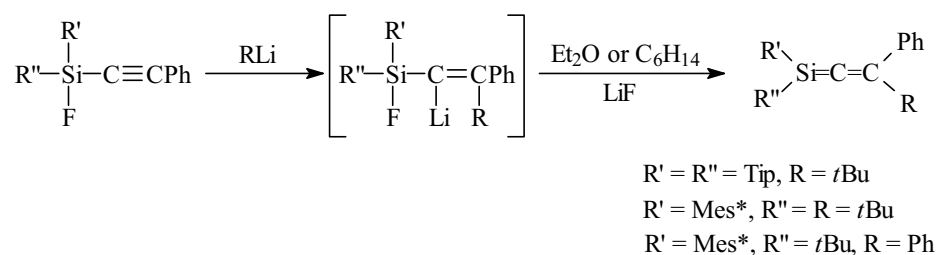
Scheme I.19

This method was used in the synthesis of other similar silaallenes, containing substituted fluorenylidene groups, like the ones presented below [47, 48]:



Scheme I.20

Another variant of this method, allowing a wider choice for the substituents on the carbon atom, involves the addition of organolithium compounds to a halosilyl-substituted alkyne, followed by elimination of lithium halide (scheme I.21) [48, 49]. The competing attack of the lithium derivative to the silicon atom can be avoided by using bulky organic groups which also stabilize the newly-formed silaallene.



Scheme I.21

The ^{29}Si NMR spectra of silaallenes show signals between 48 and 58 ppm close to the chemical shifts of silenes. In ^{13}C NMR, expected deshielded signals for the *sp* carbon atom, at chemical shifts between 216 and 230 ppm [44], are found. The solid state structures of $\text{Mes}^*(\text{Ad})\text{Si}=\text{C}=\text{CR}_2$ [46] ($\text{CR}_2 = 3,3',5,5'$ -tetraisopropyl-4,4'-dimethoxy-1,1'-biphenyl-2,2'-diyl) and $\text{Tip}_2\text{Si}=\text{C}=\text{C}(\text{Ph})\text{tBu}$ [49] have been determined by X-ray diffraction. The molecular structures for both compounds are given in figures I.7 and I.8.

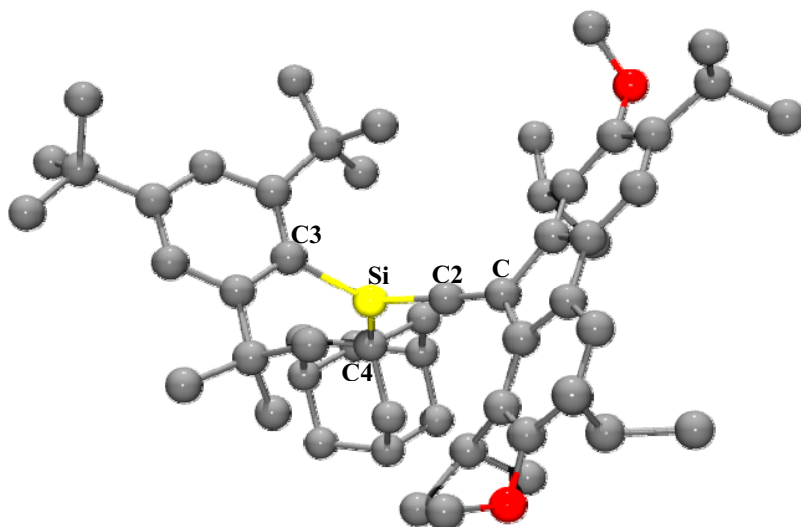


Figure I.7. Molecular structure of Mes*AdSi=C=CR₂ [46]

Geometrical parameters: Si-C2 (1.704 Å), C1-C2 (1.324 Å), Si-C3 (1.920 Å), Si-C2-C1 (173.50°), C2-Si-C3 (120.89°), C2-Si-C4 (117.50°).

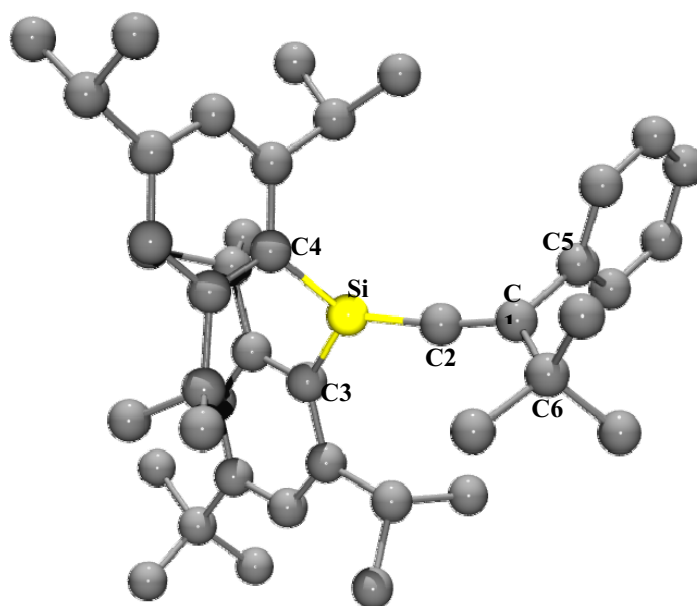


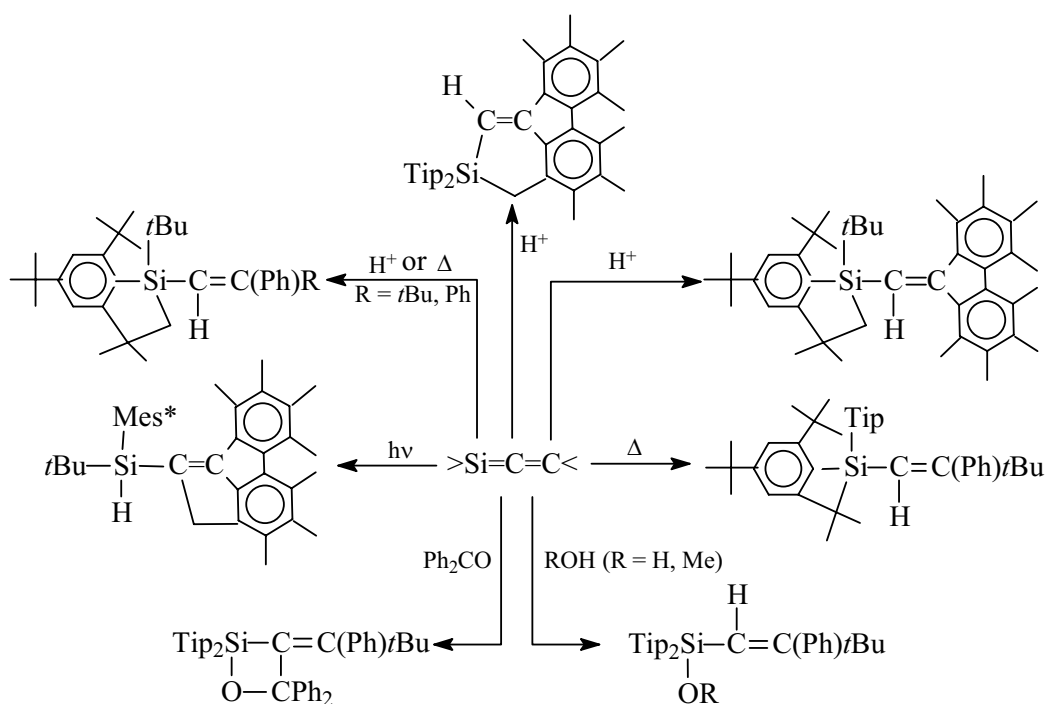
Figure I.8. Molecular structure of Tip₂Si=C=C(Ph)*t*Bu [49]

Geometrical parameters: Si-C2 (1.693 Å), C1-C2 (1.324 Å), Si-C3 (1.880 Å), C1-C5 (1.510 Å), Si-C2-C1 (172.00°), C2-C1-C5 (119.52°), C2-C1-C6 (123.50°), C2-Si-C3 (115.18°).

The bond lengths in both compounds are similar, with extremely short values for the Si=C bond (1.693 and 1.704 Å), compared to those found in silenes (1.74-2.17 Å) [42]. This is no doubt due to the *sp* hybridization of the central carbon atom. A slight elongation of this bond in Tip₂Si=C=C(Ph)*t*Bu can be explained in terms of a higher steric hindrance. The dihedral angles determined by the Si=C and C=C planes are about 77°, very much deviated from the ideal allenic geometry, although the silicon atom seems to be *sp*² hybridized.

2. Reactivity of silallenes

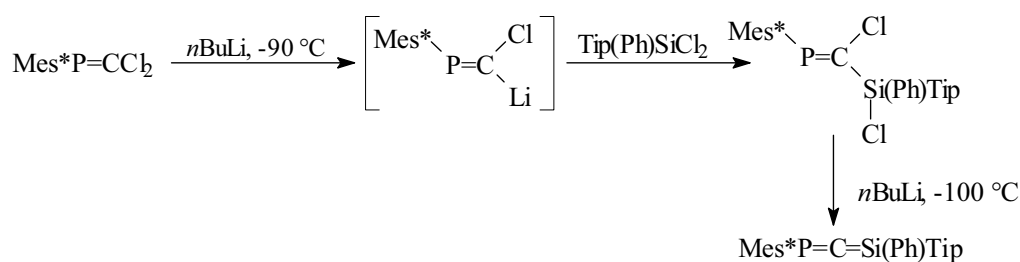
Many of the reactions undergone by these compounds are rearrangements by cyclizations involving the silicon atom and the organic substituents on it. Many silaallenes are stable toward air-oxygen for days, due to the important steric hindrance around the >Si=C=C< moiety. Addition reactions occur at the Si-C bond, with the carbon atom bearing a partial negative charge, as expected. The reactivity of silallenes is summarized in scheme I.22 [3].



Scheme I.22

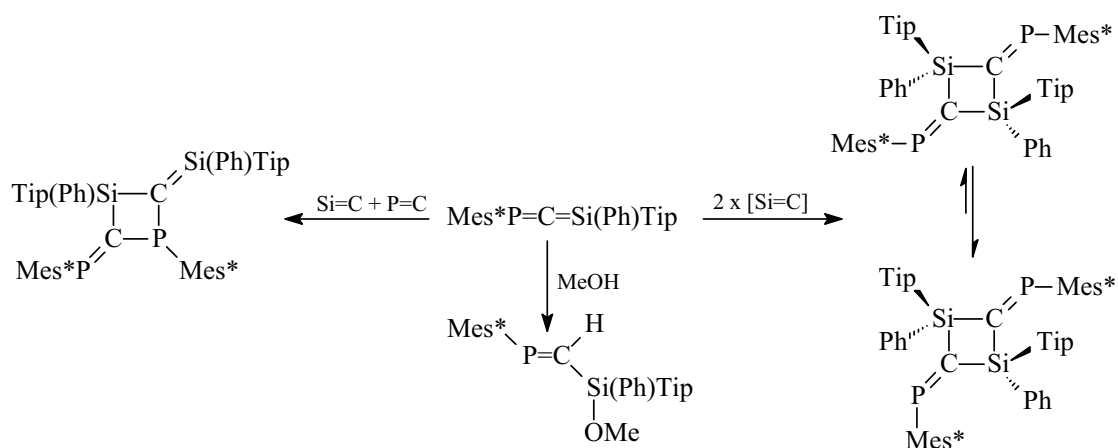
1-Phospha-3-silaallenes –P=C=Si<

The only phosphasilaallene known to date has been prepared by Escudié and coworkers in 1999, by a dehalogenation reaction of a 2,3-dichlorophosphasilapropene, as shown in scheme I.23 [50].



Scheme I.23

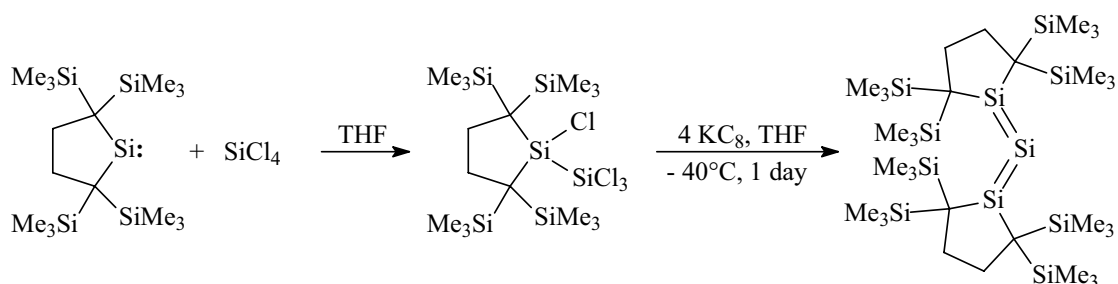
The phosphasilaallene thus obtained is only stable up to $-40\text{ }^\circ\text{C}$, above this temperature it slowly dimerizes affording two types of cyclic compounds. The reactivity of the $>\text{Si}=\text{C}=\text{P}-$ moiety involves, as expected, the $\text{Si}=\text{C}$ bond; addition of methanol to the metastable allene results in the formation of only the *E* –phosphaalkene (scheme I.24).



Scheme I.24

1,2,3-Trisilaallene >Si=Si=Si<

A 1,2,3-trisilaallene, the 1,3-bis(1,1,4,4-tetrakis(trimethylsilyl)butane-1,4-diyl)trisilaallene, the silicon-based analogue of an allene, was obtained in 2003 by Ishida and coworkers [51] through the series of reactions given in scheme I.25. Bulky substituents on the silicon atoms were used to protect the very fragile Si=Si=Si unit:



Scheme I.25

The dark green silaallene isolated was characterized through the usual spectroscopic methods. ²⁹Si NMR data were also collected and the signal for the *sp*-hybridized atom appears at 157 ppm, while the marginal Si atoms have a chemical shift of 196.6 ppm. The *sp* hybridization is actually only formal; as expected, the Si=Si=Si skeleton is significantly bent, and not linear, like for carbon-based allenes. This is no doubt due to the poor overlapping of *pπ-pπ* orbitals, a well-known fact for heavier elements of group 14. The solid-state structure of the derivative confirms the bent geometry, but also indicates the presence of four isomers (**A-D**) generated by disorders of the central Si atom over four different positions at temperatures higher than -100 °C. Their populations are strongly temperature-dependent. For instance, at 0 °C, isomers **A** to **D** are in a percentage of 46, 23, 22 and 10, while at 150°C, they can be found in a 76, 18, 7 and 0 percentage. Figure I.9 presents the molecular structure measured at -100 °C for the 1,2,3-trisilaallene [51], with the four identified positions for the central silicon atom. Geometrical data are given for the **A** isomer.

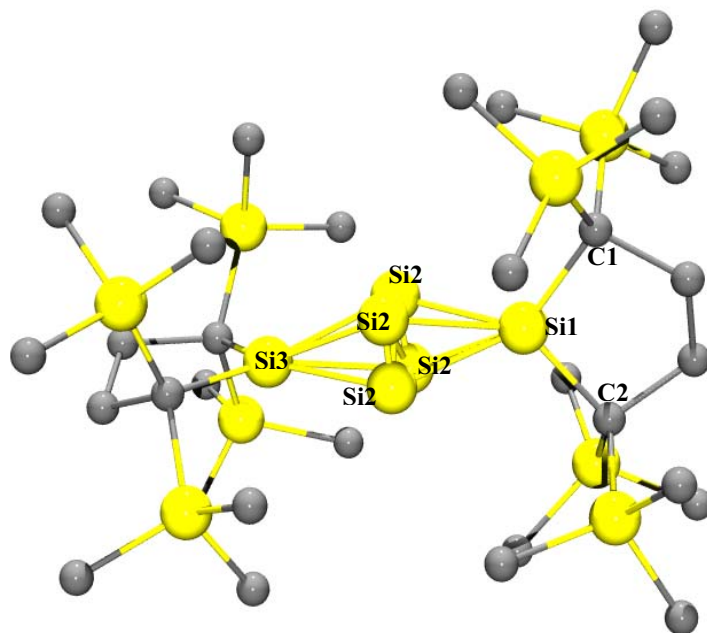
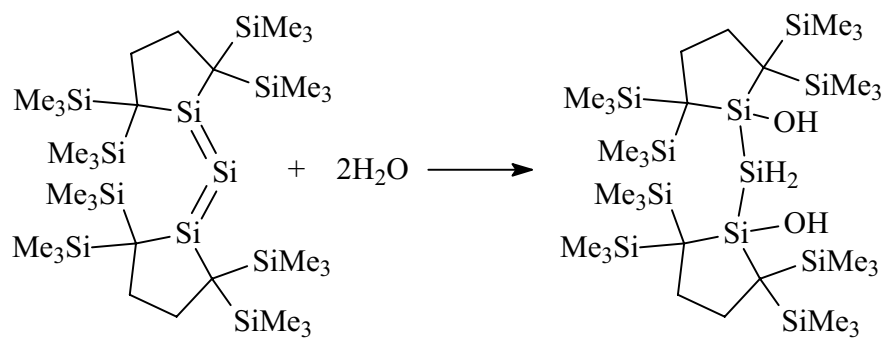


Figure I.9. Molecular structure for 1,3-bis(1,1,4,4-tetrakis(trimethylsilyl)butane-1,4-diy)trisilaallene [51]

Geometrical parameters: Si1-Si2A (2.179 Å), Si2A-Si3 (2.181 Å), Si1-C1 (1.895 Å), Si1-C2 (1.900 Å), Si1-Si2A-Si3 (137.17°), Si2A-Si1-C1 (116.72°), Si2A-Si1-C2 (138.37°), Si3-Si2A-Si1-C1 (149.30°)

Both Si=Si double bonds have values in the range 2.14-2.25 Å, typical for stable silenes [42]. The geometry of the marginal silicon atoms of the Si=Si=Si unit is not planar, but pyramidal, which can be expected from the important steric hindrance and the strain imposed by the 5-atom-rings. The two cycles are almost perpendicular to each other, and it can be noted that the orientation of the trimethylsilyl substituents affords an important steric protection of the Si=Si=Si moiety, which explains the stability of the trisilaallene. Theoretical calculations have shown that they also influence the electronic structure of the compound, by forcing the overlapping between twisted $p\pi$ -type orbitals at the terminal silicon atoms with both $p\pi$ -type and in-plane orbitals at the central silicon atom, resulting in the bent-allenic electronic structure [51].

The trisilaallene readily reacts with two molecules of water, leading to the addition product depicted in scheme I.26.

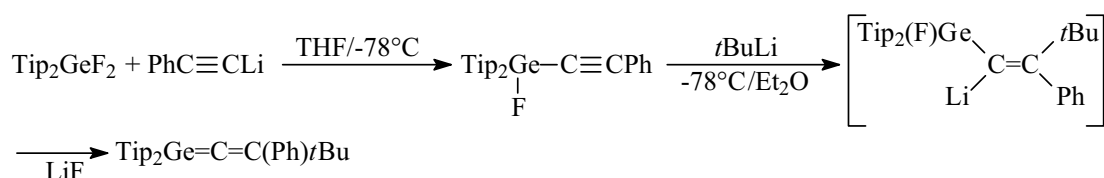


Scheme I.26

1-Germaallenes >Ge=C=C<

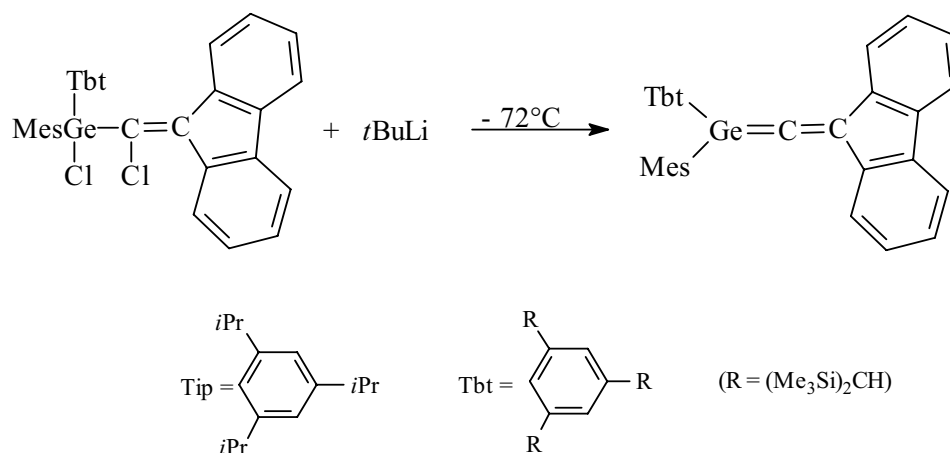
The synthesis of germaallenes has proved to raise more issues than that of silaallenes, no doubt because of the higher reactivity of the Ge=C bond as compared to the Si=C one. Thus, only two germaallenes have been reported up to date, the first one being synthesized by West in 1998 [52] and the second one by Okazaki [53].

The preparation [52] was achieved as for the corresponding silaallene through the addition of a lithium derivative to a fluoroalkynylgermane, followed by subsequent elimination of lithium fluoride, as shown in scheme I.27.



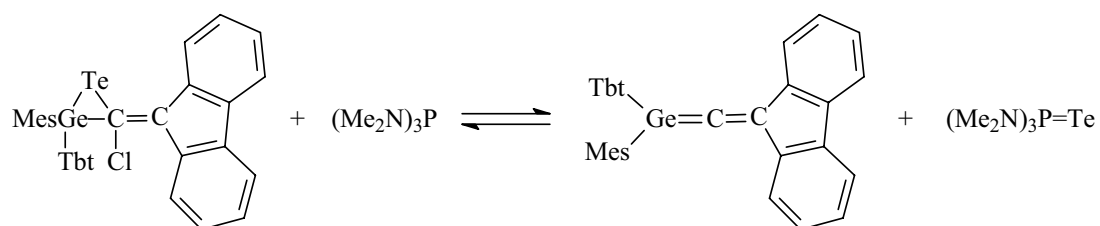
Scheme I.27

Dehalogenation by means of a lithium derivative of (haloalkenyl)halogermanes also affords germaallenes[53]. This route was used in the synthesis of Tbt(Mes)Ge=C=CR₂ (CR₂ = fluorenyl) (scheme I.28):



Scheme I.28

The same 1-germaallene is obtained through the reaction of a very large excess of $(\text{Me}_2\text{N})_3\text{P}$ to a telluragermirane [53] (scheme I.29). The isolation of the germaallene is not possible due to the existence of an equilibrium between the reactants and the products, but by trapping of the germaallene using additions at the $\text{Ge}=\text{C}$ bond, the equilibrium is modified to a nearly quantitative formation of $\text{Tbt}(\text{Mes})\text{Ge}=\text{C}=\text{CR}_2$.



Scheme I.29

The ^{13}C NMR spectra show characteristic shifts for the central carbon atom in both cases: 235.1 ppm for $\text{Tip}_2\text{Ge}=\text{C}=\text{C}(\text{Ph})t\text{Bu}$ and 143.5 ppm for $\text{Tbt}(\text{Mes})\text{Ge}=\text{C}=\text{CR}_2$ [52, 53].

The solid-state structure of $\text{Tip}_2\text{Ge}=\text{C}=\text{C}(\text{Ph})t\text{Bu}$ was determined by X-ray diffraction and showed a bent geometry for the $\text{Ge}=\text{C}=\text{C}$ moiety. In the case of the silaallene analogue, a similar geometry is found, but the $\text{Si}-\text{C}-\text{C}$ angle is about 12° wider. We can conclude then that the deviation from the expected linearity of allenes increases with the increase of the quantum number n . In figure IX.1, the molecular structure of $\text{Tip}_2\text{Ge}=\text{C}=\text{C}(\text{Ph})t\text{Bu}$ is presented.

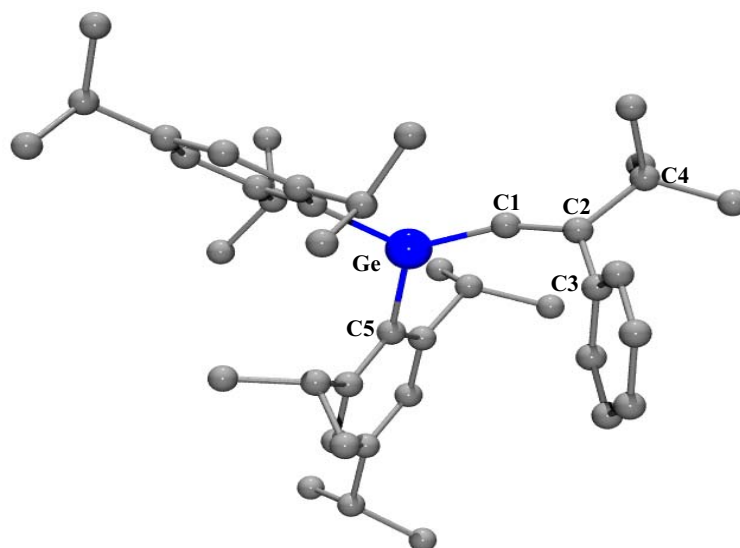
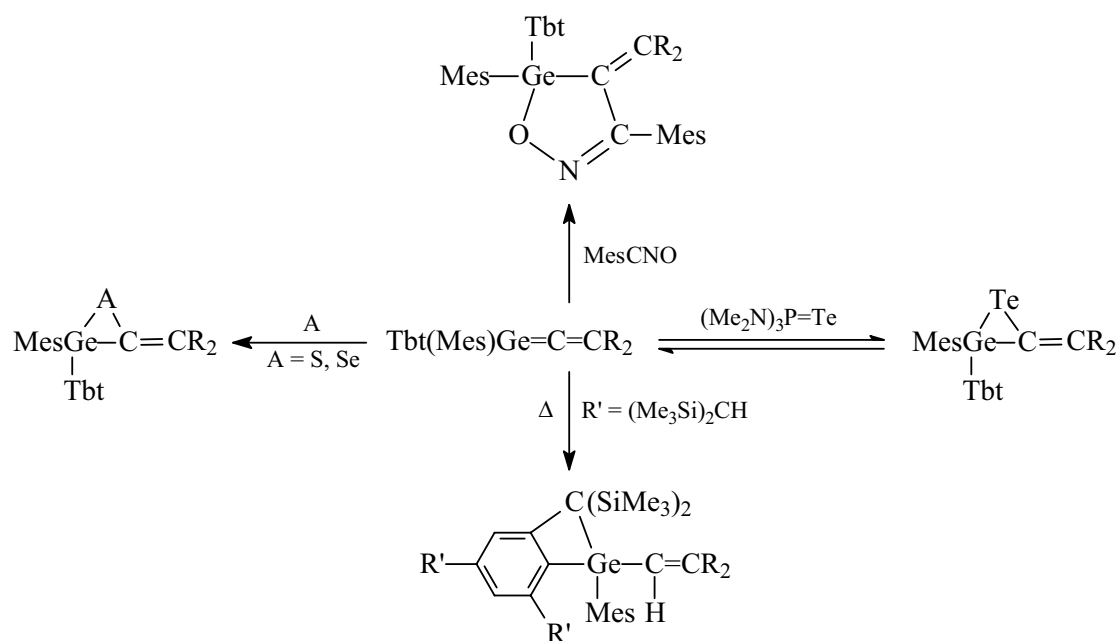


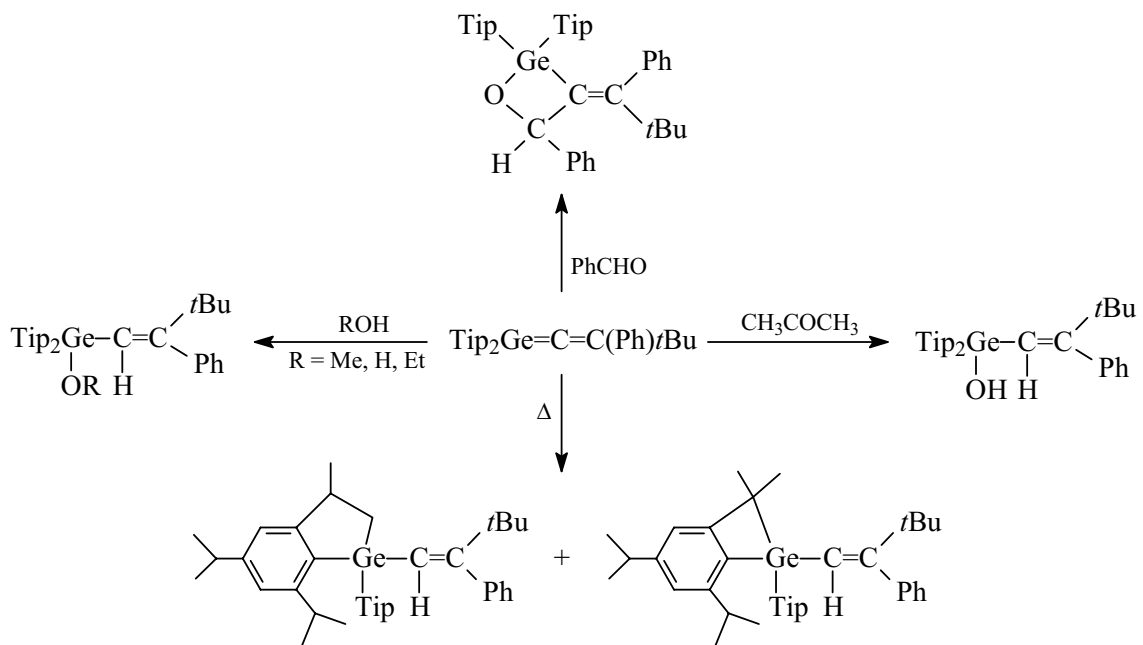
Figure I.10. Molecular structure of $\text{Tip}_2\text{Ge}=\text{C}=\text{C}(\text{Ph})t\text{Bu}$ [52]

Geometrical parameters: Ge-C1 (1.783 Å), Ge-C6 (1.950 Å), Ge-C5 (1.951 Å), C1-C2 (1.314 Å), C2-C3 (1.498 Å), C2-C4 (1.537 Å); Ge-C1-C2 (159.2°, C1-Ge-C6 (123.15°), C1-Ge-C5 (111.24°), C1-C2-C3 (119.9°), C1-C2-C4 (121.6°), C3-C2-C4 (118.42°)

The reactivity of the two germaallenes is summarized in schemes I.30 and I.31 [54].



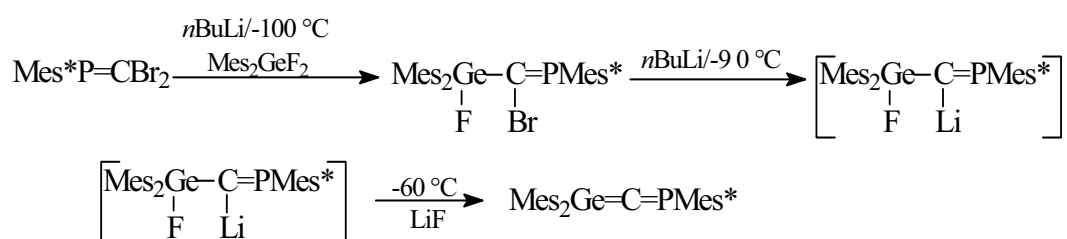
Scheme I.30



Scheme I.31

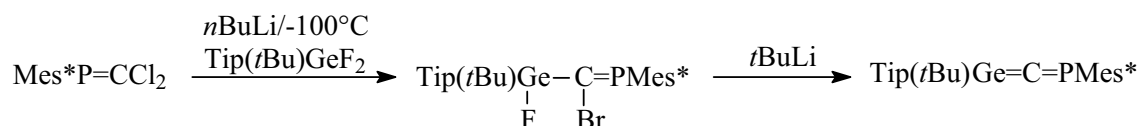
1-Phospha-3-germaallenes >Ge=C=P-

The first metastable phosphagermaallene was obtained by Escudié and coworkers in 1996 [55, 56], using a similar synthetic route to that proposed for the phosphasilaallenes. The starting product is the dibromophosphaalkene Mes*P=CBr₂ and bulky Mes groups on the germanium atom are used to sterically protect the labile Ge=C bond (scheme I.32).



Scheme I.32

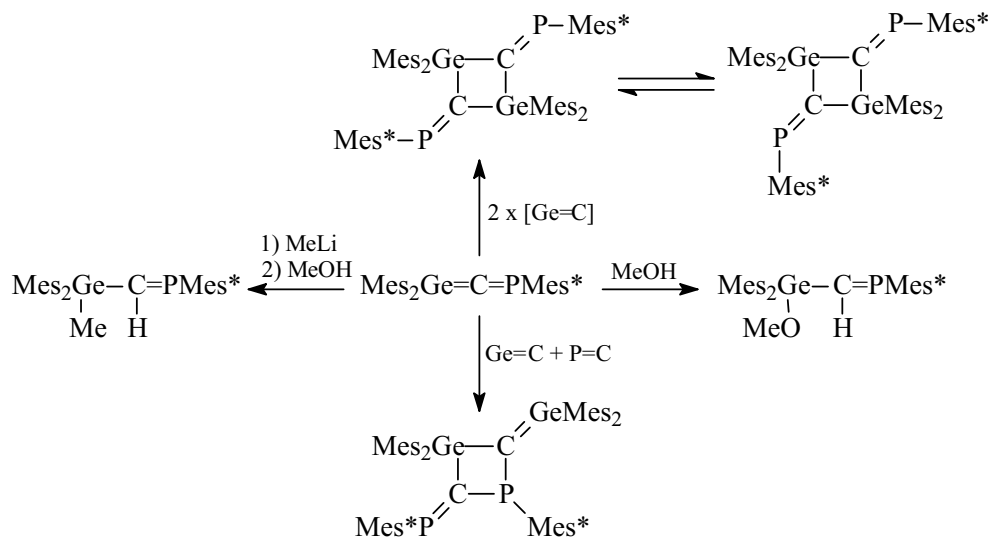
The first stable phosphagermaallene, Tip(*t*Bu)Ge=C=PMes* was obtained by the same group in 2002 [57], following the same synthetic route (scheme I.33), but using bulkier organic groups on the germanium atom. The yield of the final step is almost quantitative, and an orange solution of the allene in THF is obtained.



Scheme I.33

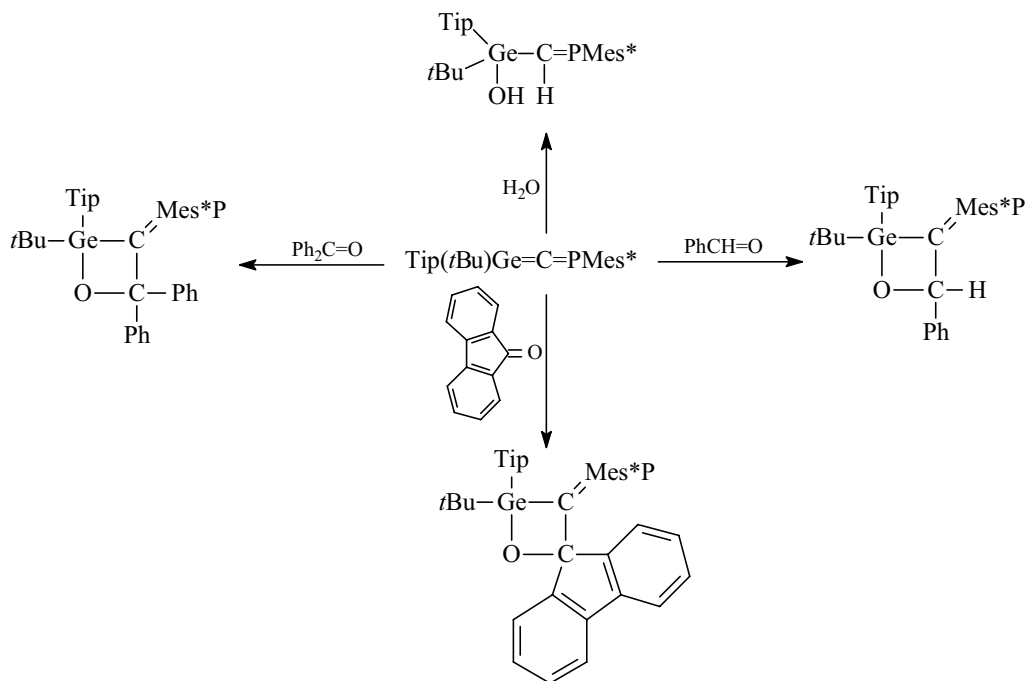
Although Mes₂Ge=C=PMes* is stable only up to -30°C and was never isolated, it has been characterized through NMR spectroscopy and its reactivity has been studied. A chemical shift of 240 ppm has been found for the ³¹P NMR signal. The *sp* carbon atom appears at low shifts (280.9 ppm) with a *J*_{CP} coupling constant of about 54 Hz. By comparison, Tip(*t*Bu)Ge=C=PMes* is stable in solution at room temperature for several days, but as expected, is extremely air- and moisture-sensitive. Characteristic chemical shifts have been found in ³¹P (280.4 ppm) and ¹³C NMR (249.9 ppm, *J*_{CP} = 62.1 Hz).

Some reactions of $\text{Mes}_2\text{Ge}=\text{C}=\text{PMes}^*$ are presented in scheme I.34.



Scheme I.34

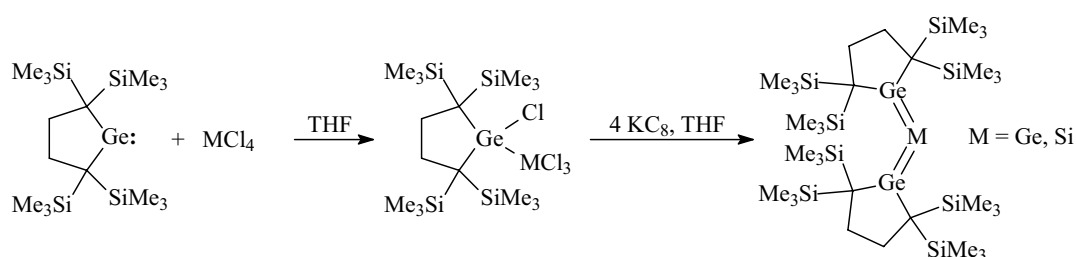
The reactivity of the stable $\text{Tip}(t\text{Bu})\text{Ge}=\text{C}=\text{PMes}^*$ was more difficult to study, mainly because of the presence of the prochiral germanium atom. Cycloaddition reactions were observed with carbonyl compounds (scheme I.35).



Scheme I.35

1,2,3- Trigermaallenes $>Ge=Ge=Ge<$ and 1,3-Digerma-2-silaallenes $>Ge=Si=Ge<$

A stable trigermaallene and a 1,3-digermasilaallene have been recently synthesized [58] (scheme I.36) following the same route as that for the trisilaallene described before (see scheme I.25) The yields of the reactions are about 20%. Both compounds are thermally stable, but air sensitive, and they are obtained as dark blue-green crystals.



Scheme I.36

The compounds were characterized in solution through NMR spectroscopy; the chemical shift for the central silicon atom in the 1,3-digermasilaallene is of 236.6 ppm, very much shifted compared to the trisilaallene analogue (157 ppm). The solid-state structures of the unsaturated derivatives have also been determined through X-ray diffraction. The bent geometry for the $Ge=M=Ge$ was found, as in the case of the trisilaallene, but unlike the latter, no disorder of the central atom has been observed. Figures I.11 and I.12 show the molecular structure of the two heteroallenes, together with significant geometrical parameters [58].

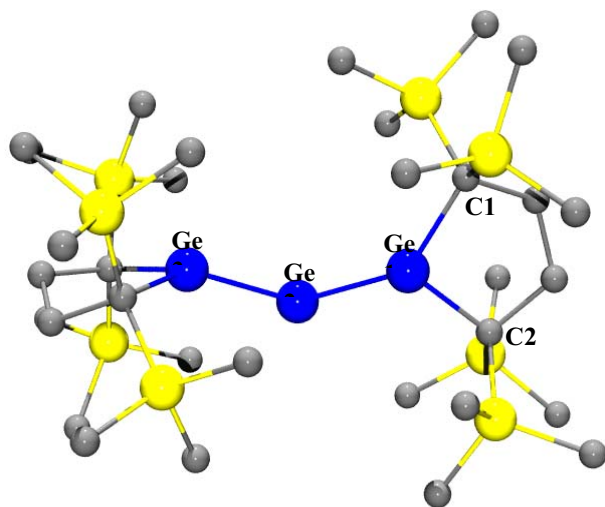


Figure I.11. Molecular structure for
 1,3-bis(1,1,4,4-tetrakis(trimethylsilyl)butane-1,4-diyl)trigerma-allene [51]
 Geometrical parameters: Ge1-Ge2 (2.321 Å), Ge2-Ge3 (2.330 Å), Ge1-C1 (1.994 Å), Ge1-C2
 (1.999 Å), Ge1-Ge2-Ge3 (122.61°), Ge2-Ge1-C1 (137.11°), Ge2-Ge1-C2 (115.26°), Ge3-Ge2-
 Ge1-C1 (-68.06°)

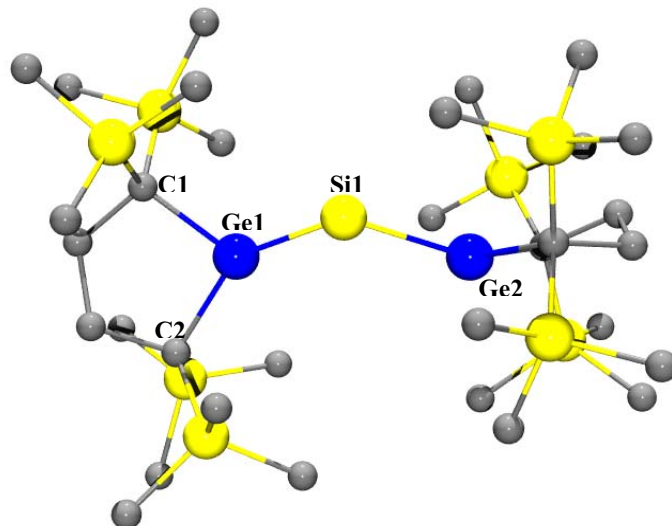
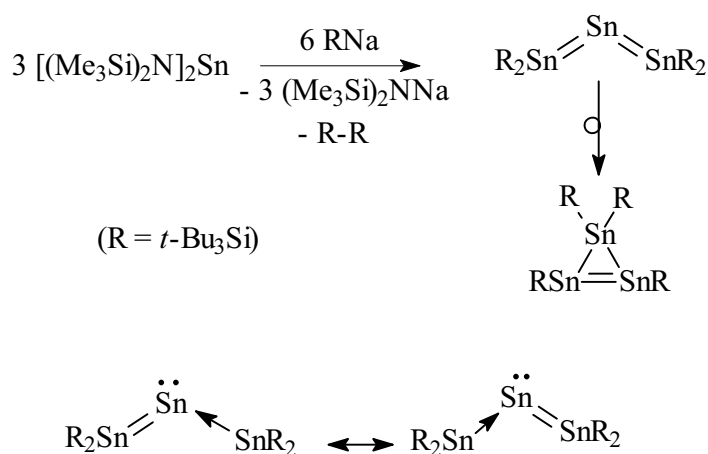


Figure I.12. Molecular structure for
 1,3-bis(1,1,4,4-tetrakis(trimethylsilyl)butane-1,4-diyl)1,3-digerma-2-silaallene[51]
 Geometrical parameters: Ge1-Si1 (2.269 Å), Ge1-C1 (2.007 Å), Ge1-C2 (2.001 Å), Ge1-Si1-Ge2
 (125.72°), Si1-Ge1-C1 (138.27°), Si1-Ge1-C2 (115.15°), Ge2-Si1-Ge1-C1 (66.00°)

The Ge1-Ge2 and Ge2-Ge3 distances in the trigermaallene are slightly different but in the range of usual Ge-Ge bond lengths (2.21-2.46 Å) [59]. The Ge1- Si1 distance in the 1,3-digerma-2-silaallene is slightly larger than that of a 1,2-disila-3-germyl-cyclopenta-2,4-diene (2.250 Å) [60]. It should be noted that the angle between the two double bonds decreases from the trisilaallene (137.17°) to the digermasilaallene (125.72°) and becomes even smaller for the Ge=Ge=Ge moiety (122.61). The pyramidalization at the marginal germanium atoms is more significant (the sum of the bond angles around Ge is about 348°) than in the case of the corresponding atoms in the trisilaallene analogue (the sum of the bond angles around Si is about 354°).

1,2,3- Tristannaallenes >Sn=Sn=Sn<

Tristannaallene $R_2Sn=Sn=SnR_2$ [61] obtained from stannylene $[(Me_3Si)_2N]_2Sn$ and RNa ($R = t-Bu_3Si$) has been isolated. It rearranges at ambient temperature to the corresponding cyclotristannene and according to its ^{119}Sn NMR spectrum and X-ray structural analysis, its bonding situation in $R_2Sn=Sn=SnR_2$ is best described by the resonance formulae (Scheme I.37).

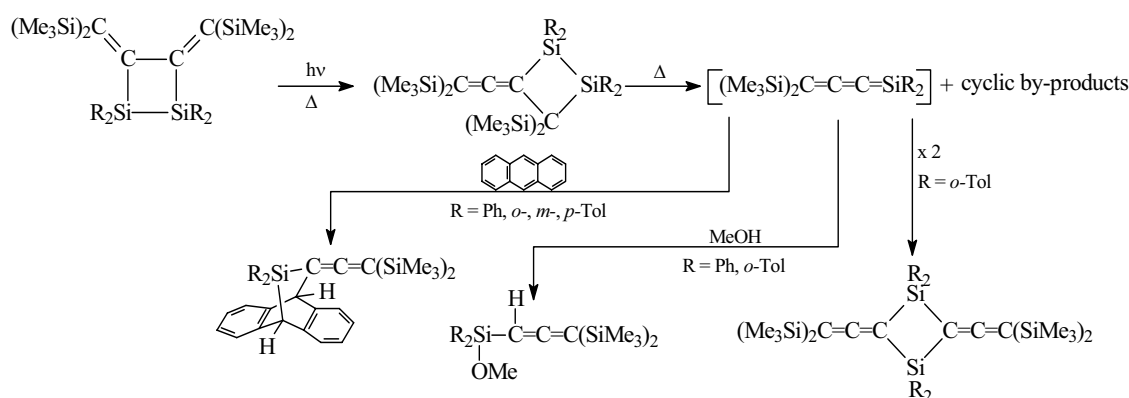


Scheme I.37.

Cumulenic compounds containing doubly-bonded heavy group 14 or/and 15 elements

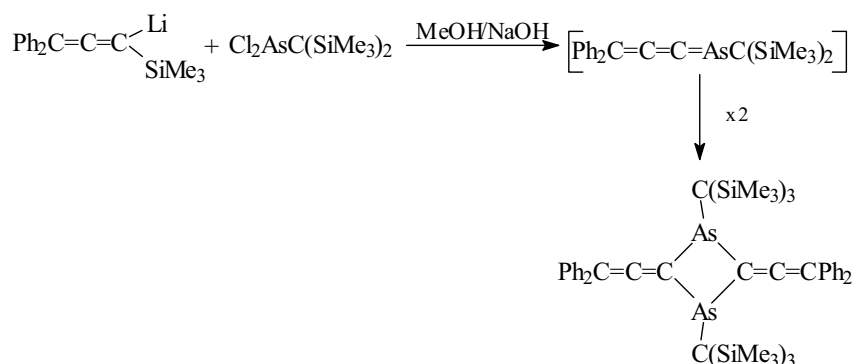
Group 15 derivatives containing three cumulated double bonds are of great interest because of their potential applications as versatile ligands for transition metals complexes and as building block in the synthesis of polymers with special properties due to the presence of the heteroelement. Many 1-phosphabutatrienes $-P=C=C=C<$ and 1,4-diphosphabutatrienes $-P=C=C=P-$ [3, 62] are known, but little progress has been made in the case of arsa- and silabutatrienes, and germanium or tin analogues of such derivatives have never been obtained.

Transient 1-silabutatrienes are formed in the thermolysis of 1,2-disilacyclobutanes[63, 64]. Their existence can be proved by reactions with trapping agents, like methanol or by the dimerization products that result. Scheme I.38 shows the synthetic route used in the preparation and evidencing of the first silabutatriene.



Scheme I.38

The only transient arsa-butatriene evidenced so far, $(Me_3Si)_3C-As=C=C=CPh_2$ [65], quickly dimerizes to form a 1,3-dia-silacyclobutane ring, and is obtained as an intermediate in a reaction starting from $(Me_3Si)_3CAsCl_2$ (scheme I.39).



Scheme I.39

There are no cumulenenic compounds described in the literature containing doubly-bonded germanium. Thus, the synthesis of group 14 and 15 elements derivatives containing more than two cumulated double bonds remains a challenge.

The synthesis of derivatives with cumulated double bonds in which a group 14 or 15 element is involved can be achieved by various synthetic routes, provided that the steric hindrance is important enough to protect the very reactive $\text{E}_{14/15}=\text{C}$ double bond of the $\text{E}_{14/15}=\text{C}=\text{E}_{14/15}$ moiety. Another way to stabilize this bond is by coordination to transition metals, leading to complexes with possible applications in homogeneous catalysis [3]. Spectroscopic data for such allenic compounds are available in the literature. Solid state structures have also been determined for several of these derivatives; however, crystallization is not always possible and disorders on the heavy atoms are often encountered.

While almost every possible combination of the type $>\text{E}_{14}=\text{C}=\text{C}<$ ($\text{E}_{14} = \text{Si}, \text{Ge}$), $>\text{E}_{14}=\text{C}=\text{E}_{14}<$, $>\text{E}_{14}=\text{C}=\text{P}<$, $>\text{E}_{15}=\text{C}=\text{C}<$ ($\text{E}_{15} = \text{P}, \text{As}$), and $>\text{E}_{15}=\text{C}=\text{E}_{15}<$ was obtained so far (except for $\text{E}_{14} = \text{Sn}$), the same cannot be said about cumulenenic compounds. Their chemistry is still a new one, although attempts to synthesize $\text{E}_{14/15}=\text{C}=\text{C}=\text{C}<$ derivatives have already been made.

References

1. Yoshifuji, M.; Shima, I.; Inamoto, N.; Hirotsu, K.; Higuchi, T.; *J. Am. Chem. Soc.* **1981**, *103*, 4587.
2. West, R.; Fink, M. J.; Michl, J.; *Science*, **1981**, *214*, 1343.
3. Escudié, J.; Ranaivonjatovo, H.; Rigon, L.; *Chem.Rev.*, **2000**, *100*, 3639.
4. Farrugia, L. J.; *J. Appl. Cryst.*, **1997**, *30*, 565.
5. *Persistence of Vision Raytracer Pty. Ltd.*, Windows version Copyright © **1996-2003**, C. Cason.
6. Yoshifuji, M.; Toyota, K.; Shibayama, K.; Inamoto, N. *Tetrahedron Lett.*, **1984**, *25*, 1809.
7. Yoshifuji, M.; Toyota, K.; Shibayama, K.; Hashida, T.; Inamoto, N. *Phosphorus Sulfur*, **1987**, *30*, 527.
8. Hafner, M.; Wegemann, T.; Regitz, M.; *Synthesis*, **1993**, 1247.
9. Yoshifuji, M.; Sasaki, S.; Inamoto, N.; *Tetrahedron Lett.*, **1989**, *30*, 839.
10. Appel, R.; Winkhaus, V.; Knoch, F.; *Chem. Ber.*, **1986**, *119*, 2466.
11. Guillemin, J.-C.; Janati, T.; Denis, J.-M.; *J. Chem. Soc, Chem. Commun.*, **1992**, 415.
12. Guillemin, J.-C.; Janati, T.; Denis, J.-M.; Guenot, P; Savignac, P.; *Tetrahedron Lett.* , **1994**, *35*, 245.
13. (a) Märkl, G.; Reitingner, S.; *Tetrahedron Lett.*, **1988**, *29*, 463. (b) Märkl, G.; Herold, U.; *Tetrahedron Lett.*, **1988**, *29*, 2935.
14. Märkl, G.; Kreitmeier, P.; *Angew. Chem., Int. Ed. Engl.*, **1988**, *27*, 1360.
15. Märkl, G.; Kreitmeier, P.; Nöth, H.; Polborn, K.; *Angew. Chem., Int. Ed. Engl.*, **1990**, *29*, 927.
16. Ito, S.; Kimura, S.; Yoshifuji, M.; *Org. Lett.*, **2003**, *5*, 1111.
17. Appel, R.; Folling, P.; Josten, B.; Siray, M.; Winkhaus, V.; Knoch F.; *Angew. Chem., Int. Ed. Engl.*, **1984**, *23*, 619.
18. Ito, S.; Sekiguchi, S.; Yoshifuji, M.; *Eur. J. Org. Chem.*, **2003**, 4838.
19. Ito, S.; Sekiguchi, S.; Yoshifuji, M.; *J. Org. Chem.*, **2004**, *69*, 4181.

20. Ito, S.; Sekiguchi, S.; Freytag, M.; Yoshifuji, M.; *Bull. Chem. Soc. Jpn.*, **2005**, 78, 1142.
21. Appel, R.; Knoch, F.; Winkhaus, V.; *J. Organomet. Chem.*, **1986**, 307, 93.
22. Yoshifuji, M.; Toyota, K.; Miyahara, T.; Hirotsu, K.; *J. Organomet. Chem.*, **1993**, 461, 81.
23. Chentit, M.; Sidorenkova, H.; Choua, S.; Geoffroy, M.; Ellinger, Y.; Bernardinelli G.; *J. Organomet. Chem.*, **2001**, 634, 136.
24. Nguyen, M. T.; Vansweevelt, H.; Vanquickenborne, L. G.; *Chem. Ber.*, **1992**, 125, 923.
25. Yoshifuji, M.; Toyota, K.; Inamoto, N.; *J. Chem. Soc., Chem. Commun.*, **1984**, 689.
26. Gouygou, M.; Koenig, M.; Escudié, J.; Couret, C.; *Heteroatom. Chem.*, **1991**, 2, 221.
27. Gouygou, M.; Tachon, C.; El Ouatib, R.; Ramarijaona, O.; Etemad-Moghadam, G.; Koenig, M.; *Tetrahedron Lett.*, **1989**, 30, 177.
28. El-Ouatib, R.; Ballivet-Tkatchenko, D.; Etemad-Moghadam, G.; Koenig, M.; *J. Organomet. Chem.*, **1993**, 453, 77.
29. Liu, M.; Bachrach, S. M.; *Phosphorus, Sulfur, Silicon, Relat. Elem.*, **1990**, 53, 7.
30. Appel, R.; Fölling, P.; Krieger, L.; Siray, M.; Knoch, F.; *Angew. Chem., Int. Ed. Engl.*, **1984**, 23, 970.
31. Karsch, H. H.; Reisacher, H.-U.; Müller, G.; *Angew. Chem., Int. Ed. Engl.*, **1984**, 23, 618.
32. Yoshifuji, M.; Toyota, K.; Niitsu, T.; Inamoto, N.; Hirotsu, K.; *J. Organomet. Chem.*, **1990**, 389, C12.
33. Appel, R.; *Multiple Bonds and Low Coordination in Phosphorus Chemistry*; Regitz, M.; Scherer, O. J.; Eds.; Thieme: Stuttgart, **1990**, 157.
34. Karsch, H. H.; Appelt, A.; Reisacher, H.-U.; Müller, G.; *Phosphorus Sulfur*, **1987**, 30, 417.
35. Akpan, C. A.; Meidine, M. F.; Nixon, J. F.; Yoshifuji, M.; Toyota, K.; Inamoto, N.; *J. Chem. Soc., Chem. Commun.*, **1985**, 946.
36. Nixon, J. F.; *Phosphorus Sulfur*, **1987**, 30, 471.
37. Akpan, C. A.; Hitchcock, P. B.; Nixon, J. F.; Yoshifuji, M.; Niitsu, T.; Inamoto, N.; *J. Organomet. Chem.*, **1988**, 338, C35.

38. Bouslikhane, M.; Gornitzka, H.; Ranaivonjatovo, H.; Escudié, J.; *Organometallics*, **2002**, *21*, 1531.
39. Guillemin, J.-C.; Lassalle, L.; Drean, P.; Wlodarczak, G.; Demaison, J.; *J. Am. Chem. Soc.*, **1994**, *116*, 8930.
40. Märkl, G.; Reithinger, S.; *Tetrahedron Lett.*, **1990**, *31*, 6331.
41. Weber, L.; Bayer, P.; Noveski, G.; Stammer, H.-G.; Neumann, B.; *Eur. J. Inorg. Chem.*, **2006**, *11*, 2299.
42. Power, P.P.; *Chem. Rev.*, **1999**, *99*, 3465.
43. Ranaivonjatovo, H.; Ramdane, H.; Gornitzka, H.; Escudié, J.; Satgé, J.; *Organometallics*, **1998**, *17*, 1631.
44. Dean, J. A.; *Lange's Handbook of Chemistry*, McGraw&Hill Inc., **1999**, 7100.
45. Bouslikhane, M.; Gornitzka, H.; Escudié, J.; Ranaivonjatovo, H.; Ramdane, H.; *J. Am. Chem. Soc.*, **2000**, *122*, 12880.
46. Miracle, G. E.; Ball, J. L.; Powell, D. R.; West, R.; *J. Am. Chem. Soc.*, **1993**, *115*, 11598.
47. Eichler, B. E.; Miracle, G. E.; Powell, D. R.; West, R.; *Main Group Met. Chem.*, **1999**, *22*, 147.
48. Miracle G. E.; Ball, J. L.; Bielmeier, S. R.; Powell, D. R.; West, R.; *Progress in Organosilicon Chemistry*; Marciniak, B., Chojnowski, J., Eds.; Gordon and Breach Science Publishers: Basel, **1995**, 83.
49. Trommer, M.; Miracle, G. E.; Eichler, B. E.; Powell, D. R.; West, R.; *Organometallics*, **1997**, *16*, 5737.
50. Rigon, L.; Ranaivonjatovo, H.; Escudié, J.; Dubourg, A.; Declercq, J. P.; *Chem. Eur. J.*, **1999**, *5*, 774.
51. Ishida, S.; Iwamoto, T.; Kabuto, C.; Kira, M.; *Nature*, **2003**, *421*, 725.
52. Eichler, B. E.; Powell, D. R.; West, R.; *Organometallics*, **1998**, *17*, 2147.
53. Tokitoh, N.; Kishikawa, K.; Okazaki, R.; *Chem. Lett.*, **1998**, *8*, 811.
54. Eichler, B. E.; Powell, D. R.; West, R.; *Organometallics*, **1999**, *18*, 540.
55. Ramdane, H.; Ranaivonjatovo, H.; Escudié, J.; Mathieu, S.; Knouzi, N.; *Organometallics*, **1996**, *15*, 3070.

56. Escudié, J.; Ranaivonjatovo, H.; Bouslikhane, M.; El Harouch, Y.; Baiget, L.; Cretiu Nemes, G.; *Russ. Chem. Bull.*, **2004**, 53, 1020.
57. El Harouch, Y.; Gornitzka, H.; Ranaivonjatovo, H.; Escudié, J.; *J. Organomet. Chem.*, **2002**, 643-644, 202.
58. Iwamoto, T.; Masuda, H.; Kabuto, C.; Kira, M.; *Organometallics*, **2005**, 24, 197.
59. Escudié, J.; Ranaivonjatovo, H.; *Adv. Organomet. Chem.*, **1999**, 44, 113.
60. Lee, V. Y.; Ichinohe, M.; Sekiguchi, A.; *J. Am. Chem. Soc.*, **2000**, 122, 12604.
61. Wiberg, N.; Lerner, H.-W.; Vasisht, S.-K. Wagner, S; Karaghiosoff, K.; Nöth, H.; Ponikwar, W. *Eur. J. Inorg. Chem.* **1999**, 1211.
62. Nixon, J. F.; *Chem. Rev.*, **1988**, 8, 1327.
63. Kerst, C.; Ruffolo, R.; Leigh, W. J.; *Organometallics*, **1997**, 16, 5804.
64. Kerst, C.; Rogers, C. W.; Ruffolo, R.; Leigh, W. J.; *J. Am. Chem.Soc.*, **1997**, 119, 466.
65. Baudler, M.; Saykowski, F.; Hintze, M.; Tebbe, K. F.; Heinlein, T.; Vissers, A.; Feher, M.; *Chem. Ber.*, **1984**, 117, 1542.

CHAPTER II

***THEORETICAL CHARACTERIZATION OF GROUP 14 HEAVY
HETEROALLENES***

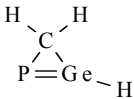
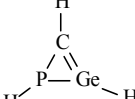
Chapitre II

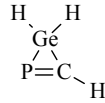
Etude théorique des hétéroallènes lourds de la groupe 14

Dans ce chapitre, nous présentons une étude théorique DFT sur la stabilité de phosphagerma- et de phosphasilaallènes $-P=C=E<$ ($E = Si, Ge$) et de ses isomères de formule brute CH_3GeP afin de déterminer quelles sont les structures les plus stables.

La géométrie de tous ces isomères a été optimisée au niveau B3LYP/6-31G (d, p), à l'aide du programme Spartan. L'analyse vibrationnelle a également été effectuée afin de s'assurer que toutes les géométries trouvées correspondent à un minimum. L'état triplet du phosphagermaallène a également été étudié afin de voir si la préférence pour l'état singulet est conservée en passant de $Ge=C$ à $Ge=C=P$. Le tableau 1 montre les énergies totales et relatives en fonction du minimum global de la série pour les isomères optimisés.

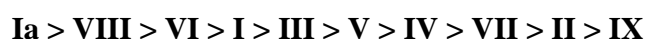
Tableau 1. Energies totales et relatives pour les isomères optimisés

Molecule	HP=C=GeH ₂ I	HP=C=GeH ₂ Ia (triplet)	H ₃ Ge-C≡P II
Total Energy (au)	-2457.92568	-2457.891415	-2457.97514
ΔE (kcal/mol)	46.64	68.14	15.60
Molecule	 III	 IV	H ₂ C=Ge=PH V
Total Energy (au)	-2457.951919	-2457.960168	-2457.957917
ΔE (kcal/mol)	30.17	24.99	26.41

Molécule	$\text{H}_2\text{P}-\text{C}\equiv\text{GeH}$ VI	 VII	$\text{HC}\equiv\text{Ge}-\text{PH}_2$ VIII
Total Energy (au)	-2457.913166	-2457.965443	-2457.911001
ΔE (kcal/mol)	54.49	21.69	55.85

Molécule	$\text{P}\equiv\text{Ge}-\text{CH}_3$ IX
E (HF)	-2458.000005
ΔE (kcal/mol)	0.00

L'ordre des énergies données par la méthode DFT est:



Cette étude théorique effectuée en utilisant des méthodes à plus haute corrélation a conduit à des résultats similaires ; elle a été étendue au phosphagermaallène substitué par des groupements méthyles $\text{MeP}=\text{C}=\text{GeMe}_2$ et à tous ses isomères dans lesquels les atomes d'hydrogène ont été remplacés par des groupes méthyles ainsi qu'au phosphasilaallène $\text{HP}=\text{C}=\text{SiH}_2$ et à ses isomères.

Dans tous les cas, l'isomère le plus stable est un dérivé avec une triple liaison PGe (ou PSi) $\text{P}\equiv\text{E}-\text{CR}_3$ (E = Si, Ge; R = H, Me); la différence d'énergie entre l'isomère à triple liaison GeP et le phosphagermaallène est moins importante lorsque H est remplacé par un méthyle. Ceci correspond à l'expérience puisqu'en protégeant l'entité $\text{P}=\text{C}=\text{Ge}$ par des groupes très volumineux tels que Tip (2,4,6-triisopropylphényl), *t*Bu et Mes* (2,4,6,tri-*tert*-butylphényl) on peut isoler le phosphagermaallène. Même si les effets stériques sont le moyen le plus efficace pour protéger une double liaison et empêcher sa dimérisation, une autre méthode consiste à faire varier les effets électroniques ; une étude NBO a donc été réalisée afin de déterminer l'influence de la nature de plusieurs substituants (groupes à effet inductif +I ou -I ou mésomère +M ou -M) sur la liaison double $\text{C}=\text{Ge}$. Des composés modèles $\text{HP}=\text{C}=\text{GeR}_2$ et $\text{HP}=\text{C}=\text{GeRR}'$ ont été étudiés (R = BH_2 , CH_3 , SiH_3 , NH_2 , OMe, F; R' = H). Il a été constaté que l'interaction principale

contribuant à l'affaiblissement de la double liaison Ge=C est un transfert de densité électronique du doublet libre de l'atome de phosphore vers l'orbitale moléculaire antiliante localisée sur la liaison Ge-C (schéma 1).

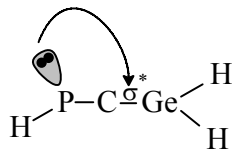


Schéma 1

Les substituants avec des atomes possédant des doublets libres ou des orbitales p vacantes induisent d'autres types de transfert de charge qui aboutissent également à l'affaiblissement de l'ordre de liaison Ge=C, tandis que les groupes contenant des éléments du groupe 14 tels que Si et C sont jugés "inertes". Une distinction entre les substituants aromatiques et aliphatiques n'a pas pu être faite à ce niveau de la théorie, mais l'influence de l'effet stérique a déjà été prouvée expérimentalement. Donc, il apparaît à partir de cette étude que l'utilisation de substituants encombrants organiques et silylés constitue le meilleur choix pour la stabilisation de l'entité P=C=Ge.

The instability of unsaturated compounds of group 14 elements makes computational chemistry a useful tool in the study of their structure and properties, providing the means to investigate them. Not too many attempts to use theoretical methods in the study of phosphagermallenes have been made: Escudié and coworkers rationalized the dimerization outcome of $\text{Mes}^*\text{P}=\text{C}=\text{GeMe}_2$ using HF calculations, which favors the head-to-tail dimerization of two $\text{Ge}=\text{C}$ bonds or a $\text{Ge}=\text{C}$ and a $\text{P}=\text{C}$ bonds in contrast with the experimentally determined behavior [1]. However, the calculated difference in energy was only 1 and 6 kcal/mol respectively. Due to the experimental use of very bulky mesityl and supermesityl (2,4,6-tri-*tert*-butylphenyl) groups, the discrepancy with the calculations are not surprising since the large steric hindrance of substituents disfavor the head-to-tail dimers. Phospha- and diphosphaallenes were intensely reviewed and attempts to explain their electronic properties through theoretical chemistry have been made [2]. The models for double bonding of elements with the principal quantum number higher than 3 are discussed by Power in 1999 [3].

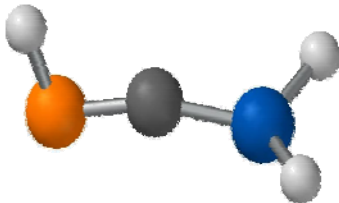
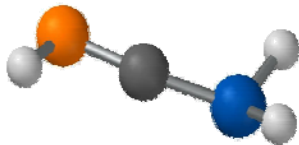
1) Structural minima in the isomeric space of model 1-3-phosphagermaallenes

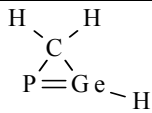
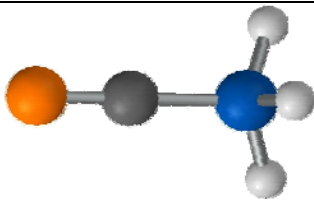
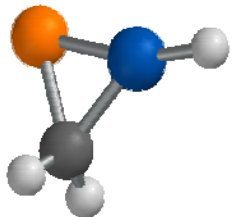
In this section, we present a DFT theoretical study on the stability of phosphasilaallenes and phosphagermaallenes, in an attempt to explain the small number of such derivatives described to date [2, 4].

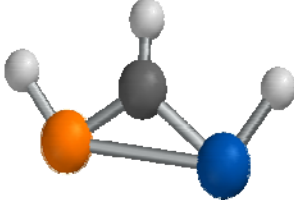
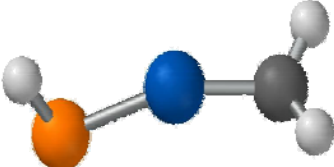
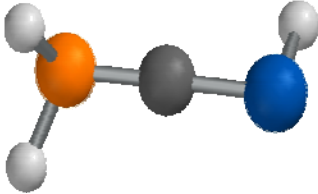
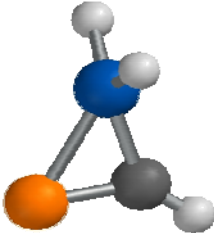
The geometries of all possible isomers of the model compound PCGeH_3 were optimized at the B3LYP/6-31G(d,p) [5] level of the theory, using the Spartan package of programs [6]. A vibrational analysis was also carried out in order to ensure that all the geometries found correspond to minima. The triplet state of the phosphagermaallene was also investigated in order to see whether the preference for the single state is kept while

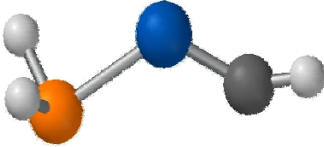
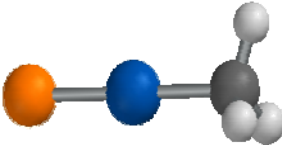
going from Ge=C to Ge=C=P. The results are reproduced in table II.1; some relevant geometrical parameters are also given. The relative energies (ΔE) compared to the global minimum of the series are given in kcal/mol.

Table II.1. Calculated B3LYP/6-31G(d,p) energies and geometrical parameters for HP=C=GeH₂ isomers

Molecule	HP=C=GeH ₂ I	HP=C=GeH ₂ Ia (triplet state)
Optimized geometry		
Total Energy (au)	-2457.92568	-2457.891415
ΔE (kcal/mol)	46.64	68.14
Ge-C (Å)	1.779	1.868
P-C (Å)	1.641	1.650
Ge-C-P (°)	156.71	159.18

Molecule	P≡C-GeH ₃ II	 III
Optimized geometry		
Total Energy (au)	-2457.97514	-2457.951919
ΔE (kcal/mol)	15.60	30.17
Ge-C (Å)	1.922	1.953
P-C (Å)	1.553	1.988
Ge-C-P (°)	179.81	65.002

Molecule	$ \begin{array}{c} \text{H} \\ \\ \text{C} \\ / \quad \backslash \\ \text{P} \quad \text{Ge} \\ \quad \\ \text{H} \quad \text{H} \end{array} $ <p style="text-align: center;">IV</p>	$ \begin{array}{c} \text{HP}=\text{Ge}=\text{CH}_2 \\ \mathbf{V} \end{array} $
Optimized geometry		
Total Energy (au)	-2457.960168	-2457.957917
ΔE (kcal/mol)	24.99	26.41
Ge-C (Å)	1.989	1.796
P-Ge (Å)	3.109	2.149
P-Ge-C (°)	29.427	150.00
Molecule	$ \begin{array}{c} \text{H}_2\text{P}-\text{C}\equiv\text{GeH} \\ \mathbf{VI} \end{array} $	$ \begin{array}{c} \text{H} \quad \text{H} \\ \backslash \quad / \\ \text{Ge} \\ \\ \text{P}=\text{C}-\text{H} \\ \mathbf{VII} \end{array} $
Optimized geometry		
Total Energy (au)	-2457.913166	-2457.965443
ΔE (kcal/mol)	54.49	21.69
Ge-C (Å)	1.809	1.924
P-C (Å)	1.670	1.683
Ge-C-P (°)	178.13	79.9

Molecule	H ₂ P-Ge≡CH VIII	P≡Ge-CH ₃ IX
Optimized geometry		
Total Energy (au)	-2457.911001	-2458.000005
ΔE (kcal/mol)	55.85	0.00
Ge-C (Å)	1.727	1.967
P-Ge (Å)	2.359	2.024
P-Ge-C (°)	122.19	179.897

So the estimated energy for the isomers of model compound H₃CGeP decreases as follows:



The most stable isomer is unexpectedly **IX**, containing the P≡Ge triple bond. This comes as a surprise, considering that the instability of multiple bonded germanium derivatives usually increases with the degree of unsaturation, and even the isomer containing the P=Ge bond is thermodynamically less stable than **IX**. In fact, previous calculations reported in the literature are in agreement with our results: the phosphorus-germanium triple bonds are computed to be energetically more favored than the double one [7, 8]. Electronegative substituents on the germanium atom increase the strength of the triple bond, while electropositive ones weaken it. The reason for which triple bonded germanium compounds are so scarce (and there are no known derivatives containing the P≡Ge unit reported up to date) must be of kinetical nature; no doubt, the use of bulky substituents providing a proper steric protection could lead to the isolation of such derivatives.

Since experimentally we start from the P=C-Ge skeleton to synthesize 1-3-phosphagermaallenes, we were more interested in the isomers containing the P-C-Ge

sequence. The phosphagermirene **IV** is theoretically more likely to form than the phosphagermaallene **I**, but no such compound has been previously reported. The energy difference of about 20 kcal/mol between **V** and **I** can be easily covered by the ring opening of the cycle to afford the linear structure.

From all the model-compounds given in table II.1, only **VII** has a precedent [9] in the literature to be characterized by X-ray crystallography, and the DFT method affords very close geometrical parameters (see Scheme II.1), indicating that this computational method is accurate enough in describing such derivatives.



Scheme II.1.

The bent geometry obtained for **I** is not surprising for such compounds, since heavier group 14 elements are known to prefer a bent structure when involved in multiple bonding [10]. A molecular orbital analysis of **I** reveals that the frontier orbitals have a pronounced antibonding character between the phosphorus and carbon atom in the P=C=Ge unit. The HOMO is mainly localized on the P=C double bond (see Figure II.1).

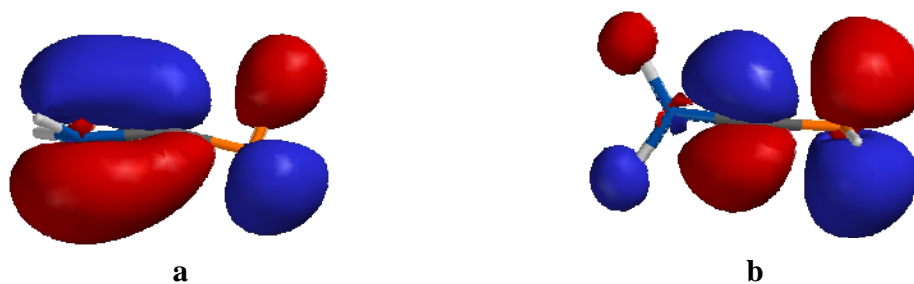
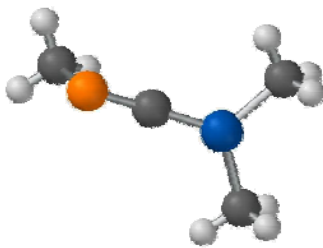
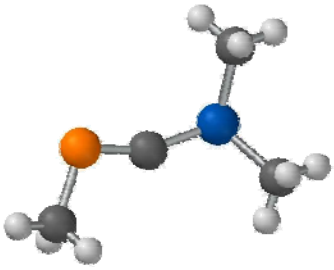


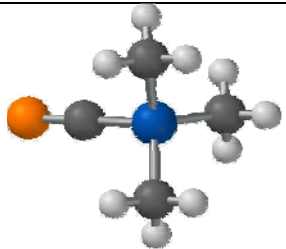
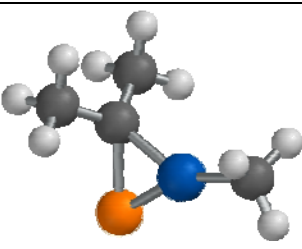
Figure II.1. HOMO (a) and LUMO (b) orbitals of **I**

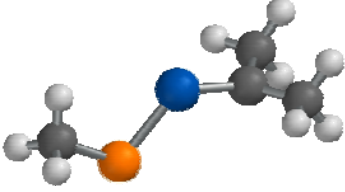
The same shapes of the frontier orbitals are also found for all the other isomers, the HOMO being mainly localized on the Ge-C bond, while the LUMO has an even more pronounced antibonding character (with three nodal planes) and is localized on the P-C fragment. The HOMO-LUMO energy separation for **I** is more than 4 eV. This gap is

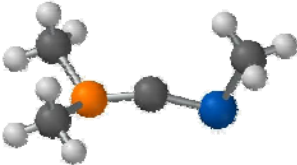
smaller for the cyclic structures **III** and **IV** (3 eV), but increases again for **VII**, which indicates that the isolation of **VIIa** is partially due to its smaller kinetic liability compared to the other isomeric rings. The use of sterically hindering substituents on the germanium and phosphorus atoms should afford the stabilization needed for the linear structure. With this in mind, we have slightly increased the steric congestion on the P-C-Ge unit, performing calculations on the isomers of the model phosphagermaallene $\text{MeP}=\text{C}=\text{GeMe}_2$ at the same DFT level. The results are given in table II.2.

Table II.2. Calculated B3LYP/6-31G(d,p) parameters for $\text{MeP}=\text{C}=\text{GeMe}_2$ isomers

Molecule	I-Me₃	Ia-Me₃ (triplet)
Optimized geometry		
Total Energy (au)	-2575.906811	-2575.871256
ΔE (kcal/mol)	32.89	55.20
Ge-C (Å)	1.771	1.883
P-C (Å)	1.638	1.646
Ge-C-P (°)	167.478	157.945

Molecule	II-Me₃	III-Me₃
Optimized geometry		
Total Energy (au)	-2575.95922	-2575.917116
ΔE (kcal/mol)	0.00	26.42
Ge-C (Å)	1.942	1.968
P-C (Å)	1.556	2.016
Ge-C-P (°)	179.837	64.457

Molecule	IV-Me ₃	V-Me ₃
Optimized geometry		
Total Energy (au)	-2575.930853	-2575.915250
ΔE (kcal/mol)	17.80	27.59
Ge-C (Å)	1.997	1.874
P-Ge (Å)	3.070	2.176
P-Ge-C (°)	30.709	123.202

Molecule	VI-Me ₃	VII-Me ₃
Optimized geometry		
Total Energy (au)	-2575.892586	-2575.94575
ΔE (kcal/mol)	41.81	8.45
Ge-C (Å)	1.834	1.933
P-C (Å)	1.642	1.698
Ge-C-P (°)	158.911	79.415

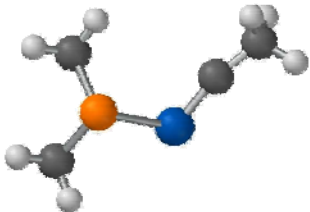
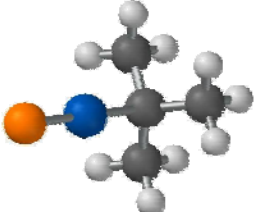
Molecule	VIII-Me ₃	IX-Me ₃
Optimized geometry		
Total Energy (au)	-2575.887026	-2575.947134
ΔE (kcal/mol)	45.30	7.58
Ge-C (Å)	1.752	2.026
P-Ge (Å)	2.407	2.029

Table II.3. Calculated CCSD/6-31G(d, p) and *MP4/6-31G(d, p)* (*italics*) parameters for the phosphagermaallene isomers **I-IX**

Isomer	I	Ia
Total Energy (au)	-2453.839071	-2453.725295
	<i>-2453.838522</i>	<i>-2453.724823</i>
ΔE (kcal/mol)	48.74	<i>120.09</i>
	<i>48.46</i>	119.86
Ge-C (Å)	1.784	1.758
	<i>1.789</i>	<i>1.790</i>
P-C (Å)	1.648	1.648
	<i>1.650</i>	<i>1.645</i>
Ge-C-P (°)	164.04	163.97
	<i>162.56</i>	<i>160.05</i>

Isomer	II	III
Total Energy (au)	-2453.898196	-2453.869169
	<i>-2453.898768</i>	<i>-2453.867939</i>
ΔE (kcal/mol)	10.93	30.28
	<i>11.36</i>	29.58
Ge-C (Å)	1.917	1.941
	<i>1.918</i>	<i>1.953</i>
P-C (Å)	1.556	1.972
	<i>1.560</i>	<i>1.987</i>
Ge-C-P (°)	179.84	65.30
	<i>179.82</i>	<i>58.28</i>

Isomer	IV	V
Total Energy (au)	-2453.867485	-2453.869561
	<i>-2453.866262</i>	<i>-2453.868517</i>
ΔE (kcal/mol)	31.33	29.92
	<i>30.63</i>	29.33
Ge-C (Å)	1.972	1.792
	<i>1.971</i>	<i>1.792</i>

P-Ge (Å)	3.105 <i>3.099</i>	2.140 <i>2.136</i>
P-Ge-C (°)	29.23 <i>29.40</i>	157.86 <i>156.79</i>
<hr/>		
Isomer	VI	VII
Total Energy (au)	-2453.811658 <i>-2453.808344</i>	-2453.884057 <i>-2453.88359</i>
ΔE (kcal/mol)	67.68 <i>65.67</i>	20.46 <i>20.23</i>
Ge-C (Å)	1.778 <i>1.801</i>	1.915 <i>1.913</i>
P-C (Å)	1.717 <i>1.666</i>	1.686 <i>1.687</i>
Ge-C-P (°)	170.35 <i>177.84</i>	79.87 <i>79.82</i>
<hr/>		
Isomer	VIII	IX
Total Energy (au)	-2453.823081 <i>-2453.819879</i>	-2453.91631 <i>-2453.916201</i>
ΔE (kcal/mol)	60.44 <i>58.50</i>	0.00 <i>0.00</i>
Ge-C (Å)	1.732 <i>1.723</i>	1.953 <i>1.953</i>
P-Ge (Å)	2.3298 <i>2.316</i>	2.028 <i>2.031</i>
P-Ge-C (°)	129.16 <i>136.31</i>	179.92 <i>179.91</i>
<hr/>		

The correlation methods give similar geometries to those found by DFT, and seem to favor more the cyclic structures. For instance, both higher methods indicate a smaller total energy for isomer **VI**. Still, isomer **IX** is calculated to be the most stable one.

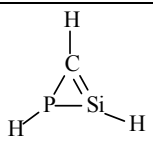
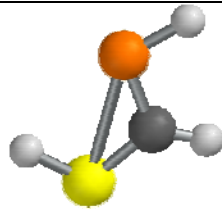
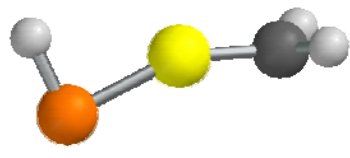
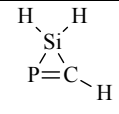
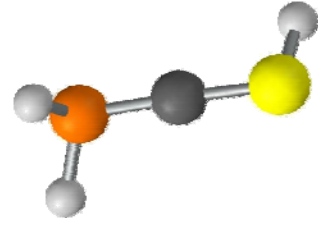
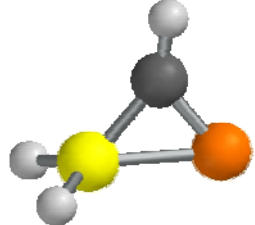
3) Theoretical study of 1-3-phosphaallene isomers

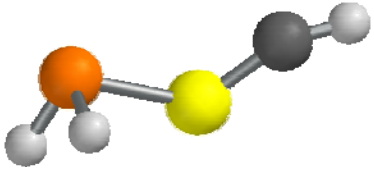
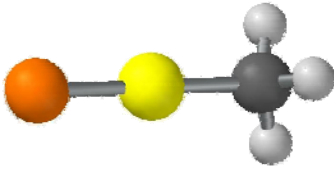
For comparison, the same study has been undergone for model compounds of phosphaallenes, and the results are shown in table II.4. The optimized geometries, together with relevant parameters are given. The order found for the germanium analogues is generally kept, especially for the DFT method. The most stable isomer is **II**, but isomer **IX** has a very close calculated energy relative to the global minimum.

Table II.4. Calculated B3LYP/6-31G(d,p) geometrical data and energies for HP=C=SiH₂ isomers

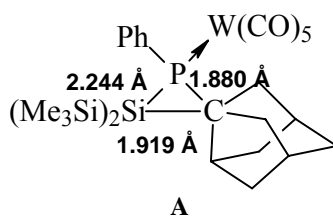
Molecule	HP=C=SiH ₂ I	HP=C=SiH ₂ Ia (triplet)
Optimized Geometry		
Total Energy (au)	-670.655873	-670.618473
ΔE (kcal/mol)	33.53	57.00
Si-C (Å)	1.699	1.759
P-C (Å)	1.641	1.658
Si-C-P (°)	171.64	166.14

Molecule	P≡C-SiH ₃ II	 III
Optimized Geometry		
Total Energy (au)	-670.709306	-670.675632
ΔE (kcal/mol)	0.00	21.13
Si-C (Å)	1.844	1.8449
P-C (Å)	1.553	2.0271
Si-C-P (°)	179.85	45.7420

Molecule	 <p style="text-align: center;">IV</p>	$\text{HP}=\text{Si}=\text{CH}_2$ <p style="text-align: center;">V</p>
Optimized Geometry		
Total Energy (au)	-670.662687	-670.670547
ΔE (kcal/mol)	29.25	24.32
Si-C (Å)	1.883	1.7126
P-Si (Å)	3.053	2.0811
P-Si-C (°)	29.523	156.5615
Molecule	$\text{H}_2\text{P}-\text{C}\equiv\text{SiH}$ <p style="text-align: center;">VI</p>	 <p style="text-align: center;">VII</p>
Optimized Geometry		
Total Energy (au)	-670.625539	-670.700568
ΔE (kcal/mol)	52.56	5.48
Si-C (Å)	1.7071	1.824
P-C (Å)	1.687	1.690
Si-C-P (°)	176.7902	78.594

Molecule	$\text{H}_2\text{P}-\text{Si}\equiv\text{CH}$	$\text{P}\equiv\text{Si}-\text{CH}_3$
	VIII	IX
Optimized Geometry		
Total Energy (au)	-670.623692	-670.707826
ΔE (kcal/mol)	53.72	0.93
Si-C (Å)	1.6494	1.8883
P-Si (Å)	2.2810	1.9659
P-Si-C (°)	122.0345	179.875

A search through the Crystallographic Cambridge Data Base resulted in only one solid state structure for the phosphasilirane **A** [14] (scheme II.2) coordinated to pentacarbonyltungsten and bearing bulky organic groups on carbon and silicon (trimethylsilyl), and as expected, no cyclic unsaturated analogues were ever characterized in solid state. The bond lengths corresponding to Si-C and C-P simple bonds obtained through the DFT geometry optimization are in fair agreement with those for compound **A**. So the crystalline packing in solid state does not affect too much this type of bonds and they are not too sensitive to the chemical environment.



Scheme II.2

The P=C bond length is also correctly rendered by the DFT method: the values reported in the literature for compounds containing the P=C-Si unit [15-21] are in the range 1.60-1.70 Å for P=C and 1.85-1.90 Å for the simple C-Si bond, so B3LYP seems to be an appropriate method for the estimation of geometries of phosphasilaallenes.

The higher correlation methods also indicate isomer **II** as the more stable of the series, and indicate a relative stability of **I** lower than that found through DFT, the energy difference between **II** and **I** being about 40 kcal/mol. Complete data is provided in Annex 2.

A theoretical study on 1,3-2-diphosphaallenes $P=Si=P$ gives similar results to those discussed above, showing that the allene is not the global minimum and that ring isomers are often favored, depending on the substituents on the silicon and the carbon atom [22]. However, isomers containing triple bonds are not taken into consideration.

In conclusion, quantum calculations predict the relative reduced stability of phosphasilaallenes and phosphagermaallenes previously observed experimentally. The high chemical reactivity of such compounds usually leads to rapid dimerization or addition reactions involving the $E_{14}=C=P$ skeleton. However, their stability could be modified and increased by using the appropriate substituents with both electronic and steric effect on the double bonds: for example, $Mes^*P=C=Ge(tBu)Tip$ is stable for months in an inert atmosphere at room temperature [23].

4) The influence of Ge-substituents on phosphagermaallenes – a measure for the stability of the $P=C=Ge$ unit

The electronic effect has been only little employed in order to stabilize systems containing the $P=C=Ge$ unit, but it could be a mean to avoid a steric hindrance that is likely to decrease or even block the reactivity of the double bonds. The electronic properties of the allenic core could be in theory tuned by using different substituents. This study aims to identify the influence that the nature (electron withdrawing or releasing) of several substituents would have on the strength of the $C=Ge$ bond in the $P=C=Ge$ unit, by means of a NBO analysis using the NBO 5.0 program [24] incorporated in Gaussian 98.

For the model phosphagermaallene $\text{HP}=\text{C}=\text{GeH}_2$, the optimized geometry is given in Figure II.3, along with geometrical data relevant to our study.

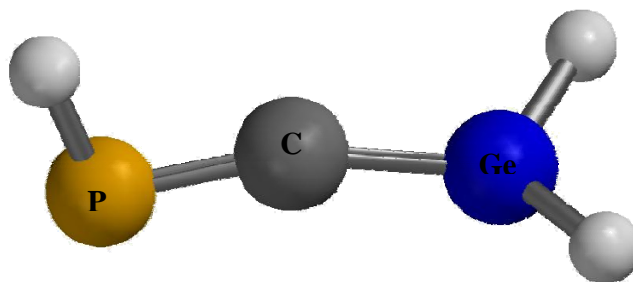
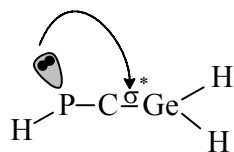


Figure II.2. B3LYP/6-311G(d,p) optimized geometry of $\text{HP}=\text{C}=\text{GeH}_2$ Ge-C: 1.78 Å, C-P: 1.64 Å, P-H: 1.44 Å, Ge-C-P: 160.4°

The C=Ge and C=P bond lengths are 1.78 and 1.64 Å, respectively. These values are in agreement with experimental data: a 1.78 Å bond length was reported for Ge=C in a 1-germaallene [25]. The P=C bond in phosphallenes is usually slightly shorter than 1.64 Å, as expected from the sp hybridization of the C atom [2]. The P=C=Ge () unit in the model compound is not linear, as it is the case for carbon-allenic structures; the GeCP angle has a value of 160.4°. An NBO analysis performed on the optimized structure indicates a sp hybridization for the carbon atom, together with the expected sp^2 hybridization for the germanium. The reason for the calculated deviation from linearity seems to be an hyperconjugation effect involving donation of electron density from the phosphorus lone pair to the antibonding orbital localized on the Ge-C bond (see scheme II.3), as revealed by a NBO analysis. This can also account for a smaller bond order than 2, as the calculated Wiberg bond index [26] for the Ge=C bond is 1.6575. Figure II.3 shows the shape of the lone pair orbital on the phosphorus and the σ -antibonding orbital on the Ge-C atom. The interaction energy is estimated by NBO analysis to be 10.22 kcal/mol.



Scheme II.3. Lone-pair- σ^* hyperconjugation in the case of the P=C=Ge unit

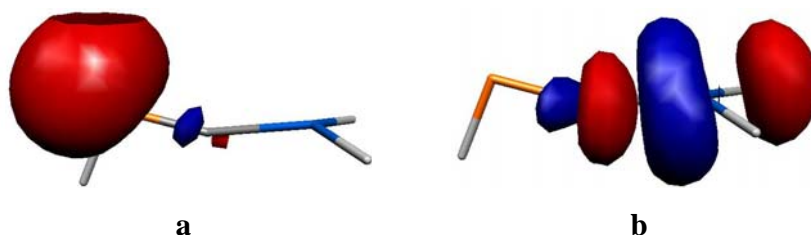


Figure II.3. Shape of the P lone pair (a) and the σ^* orbital on the Ge-C bond (b) involved in an hyperconjugative interaction in the case of HP=C=GeH₂

Another significant interaction with the same effect in the decrease of the Ge-C bond order is a charge transfer from a P-H bonding orbital to the π -symmetry antibonding orbital on the Ge-C bond (figure II.4a). The NB orbitals involved are also shown.

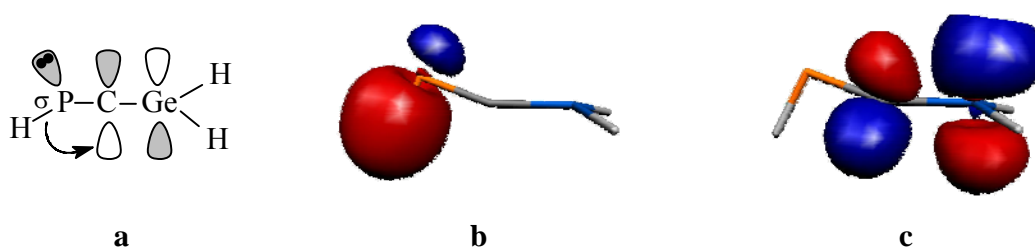
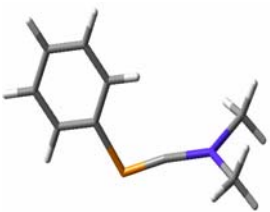
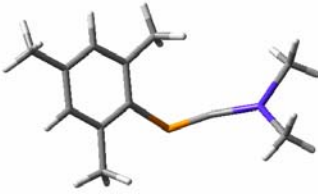
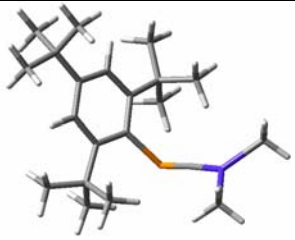


Figure II.4. σ - π^* interconjugation (a) between the P-H bond orbital (b) and the Ge-C antibonding NB orbital (c) in the model phosphagermaallene HP=C=GeH₂

In the case of aryl-substituted derivatives, with the aromatic groups on the phosphorus atom, other interactions complicate the influence of the hyperconjugative effect on the length of the Ge-C bond and the Ge-C-P angle. For instance, in the case of PhP=C=GeMe₂, this angle is calculated by B3LYP to be 171.70°, wider than in the case of the more crowded MesP=C=GeMe₂ (166.7°) (see table II.5). There is no direct

correlation between the volume of the organic group and the Ge=C bond order. For instance, in Mes*P=C=GeMe₂, the P-C-Ge angle is wider (no doubt due to the steric effect) and the calculated Wiberg bond order is smaller than in the case of PhP=C=GeMe₂, but MesP=C=GeMe₂ has a smaller value for the PCGe angle and a larger one for the Ge=C bond order.

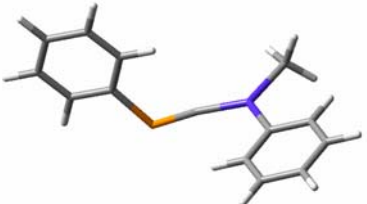
Table II.5. Calculated B3LYP data for aryl-P substituted phosphagermaallenes

Molecule			
Ge-C (Å)	1.764	1.767	1.765
C-P (Å)	1.636	1.636	1.633
P-C-Ge (°)	171.0	166.7	174.9
Ge-C bond order	1.562	1.5665	1.5529

The explanation seems to reside in the sum of all the hyperconjugative interactions possible in the molecule, as revealed by an NBO analysis. For instance, the donation of electron density from the lone pair on the phosphorus to antibonding orbitals on the Ge-C bond, which is supposed to elongate this bond and in the same time decrease the Ge-C-P angle, is counteracted by other interactions which contribute to the increase in the bond order. Other possible donations of electron density to the antibonding orbitals of the Ge-C bond in the case of the simplest model, HP=C=GeH₂, are in competition with conjugation effects over the aromatic groups for the aryl-substituted models. The same considerations are valid for phosphagermaallenes bearing aryl groups on the germanium atom. NBO analysis on optimized structures were carried out on PhP=C=GeMePh in comparison to the PhP=C=GeMe₂. The results are given in table II.6 together with the optimized geometry of the model compound. This proves that in the case of large substituents, it is often the electronic effect rather than the steric one that accounts for the

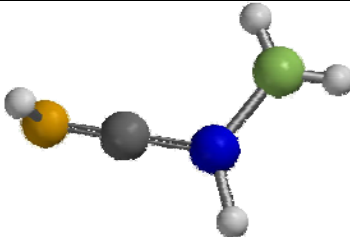
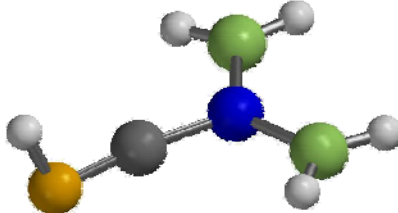
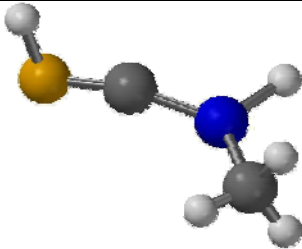
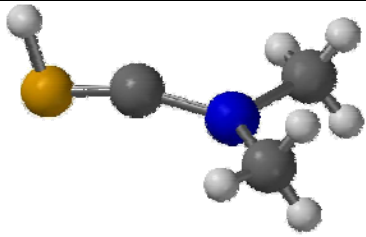
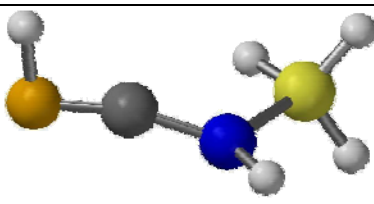
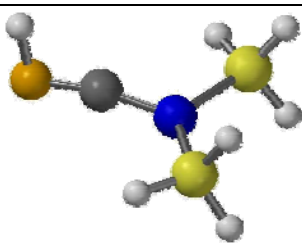
geometry, the molecular electronic density and ultimately, the reactivity of phosphagermaallenes.

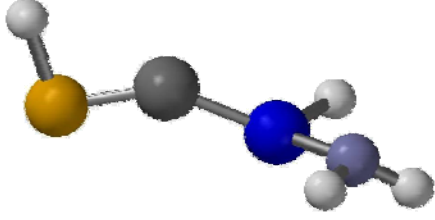
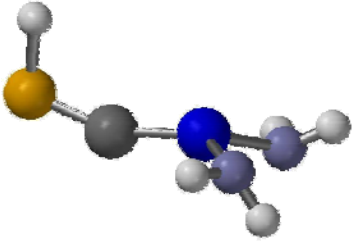
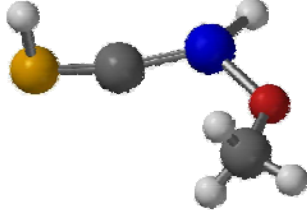
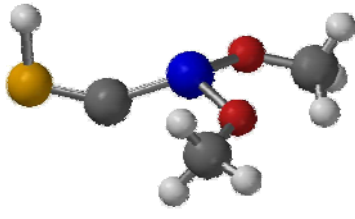
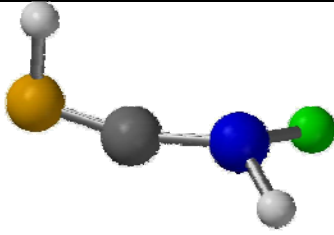
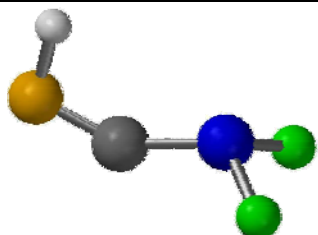
Table II.6. B3LYP data for PhP=C=GeMePh

Molecule	
	
Ge-C (Å)	1.766
C-P (Å)	1.634
P-C-Ge (°)	170.9
Ge-C bond order	1.5303

With this in mind, a comparative study was carried out to account for the effect that different substituents containing group 13 to 17 elements on the germanium atom would have on the bond order of the Ge-C bond in phosphagermaallenes. To this respect, calculations at the B3LYP/6-311G(d, p) level of the theory were carried out on several model compounds (see table II.7). First, geometry optimizations were performed and a vibrational analysis was carried out in order to determine if the optimized structure was indeed a true minimum on the potential surface. The results obtained are shown in table II.7, together with values for bond lengths and angles.

Table II.7. B3LYP/6-311G(d,p) structures and NBO analysis results for model phosphagermaallenes

Molecule		
	HP=C=Ge(BH ₂)H	HP=C=Ge(BH ₂) ₂
Ge-C (Å)	1.801	1.825
C-P (Å)	1.635	1.636
P-C-Ge (°)	170.8	171.9
Ge-C bond order	1.5182	1.4343
Molecule		
	HP=C=Ge(CH ₃)H	HP=C=Ge(CH ₃) ₂
Ge-C (Å)	1.779	1.779
C-P (Å)	1.641	1.642
P-C-Ge (°)	160.7	160.5
Ge-C bond order	1.6157	1.5679
Molecule		
	HP=C=Ge(SiH ₃)H	HP=C=Ge(SiH ₃) ₂
Ge-C (Å)	1.785	1.789
C-P (Å)	1.640	1.642
P-C-Ge (°)	163.5	166.1
Ge-C bond order	1.6443	1.6374

Molecule		
	HP=C=Ge(NH ₂)H	HP=C=Ge(NH ₂) ₂
Ge-C (Å)	1.796	1.797
C-P (Å)	1.647	1.643
P-C-Ge (°)	147.0	155.9
Ge-C bond order	1.5092	1.4031
Molecule		
	HP=C=Ge(OMe)H	HP=C=Ge(OMe) ₂
Ge-C (Å)	1.638	1.829
C-P (Å)	1.781	1.647
P-C-Ge (°)	167.0	147.6
Ge-C bond order	1.5061	1.3599
Molecule		
	HP=C=GeFH	HP=C=GeF ₂
Ge-C (Å)	1.790	1.859
C-P (Å)	1.683	1.643
P-C-Ge (°)	162.7	147.1
Ge-C bond order	1.5201	1.3434

It can be seen that the largest bond order is calculated for substituents containing group 14 elements, like CH_3 and SiH_3 . We repeated the calculation for a phosphagermaallene bearing a SiMe_3 group on the germanium atom to check if the Si-H bond is not the one determining the higher bond order through stabilizing hyperconjugation effects towards the $\text{Ge}=\text{C}$ unit, because SiH_3 would make a poor experimental choice. The results were similar for $\text{HP}=\text{C}=\text{Ge}(\text{SiMe}_3)_2$ with a calculated Wiberg bond order of 1.6396. The most important interaction that leads to the decrease in the $\text{Ge}=\text{C}$ bond strength remains the donation of electron density from the P lone pair to the sigma antibonding orbital.

The low bond order in the case of the model compound $\text{HP}=\text{C}=\text{GeF}_2$ is explained by supplementary interactions due to the presence of the fluorine atom, bearing electron lone pairs. The NBO analysis performed shows a strong delocalization of one of the lone pairs, the one oriented perpendicular to the Ge-F bond to the π^* orbital on the Ge-C bond. Both fluorine atoms display this type of interaction. Figure II.5 shows the shape of the NB orbitals involved. The other lone pair is oriented perpendicular to the π^* orbital and cannot contribute to the hyperconjugative effect.

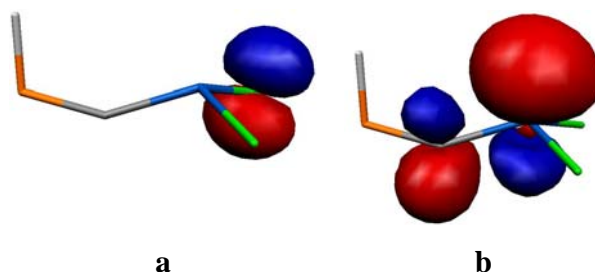


Figure II.5. Non Bonding orbitals involved in hyperconjugation leading to $\text{Ge}=\text{C}$ destabilization in $\text{HP}=\text{C}=\text{GeF}_2$ (a) lone pair on F, b) π^* orbital on the Ge-C bond)

In conclusion, the $\text{Ge}=\text{C}$ bond in phosphagermaallenes is weakened by an hyperconjugative effect directed from the P lone pair to the Ge-C bonding orbital. Substituents with atoms bearing lone pairs or vacant p orbitals induce other types of charge transfer which also result in the weakening of the $\text{Ge}=\text{C}$ bond order, while groups containing group 14 elements like Si and C are found to be “inert”. A distinction between

aromatic and aliphatic substituents could not be made at this level of the theory, but influence of the steric effect was already proven experimentally. So, bulky organic and silyl substituents are the best choice for the stabilization of the Ge=C=P unit.

References

1. Ramdane, H.; Ranaivonjatovo, H.; Escudié, J.; Mathieu, S.; Knouzzi, N. *Organometallics*, **1996**, *15*, 3070.
2. Escudié, J.; Ranaivonjatovo, H.; Rigon, L.; *Chem. Rev.*, **2000**, *100*, 3639.
3. Power, P.P.; *Chem. Rev.*, **1999**, *99*, 3465.
4. Escudié, J.; Ranaivonjatovo, H.; *Organometallics* **2007**, *26*, 1542.
5. a) Becke, A.D.; *J.Chem.Phys.*, **1993**, *98*, 5648; b) Lee, C.; Yang, W.; Parr, R.G.; *Phys. Rev. B*, **1988**, *37*, 785; c) Vosko, S.H.; Wilk, L.; Nusair, M.; *Can. J. Phys.*, **1980**, *58*, 1200; d) Stephens, P.J.; Devlin, F.J.; Chabalowski, C.F. ; Frisch, M.J.; *J. Phys. Chem.*, **1994**, *98*, 11623.
6. Wavefunction Inc.18401 Von Karman Avenue, Suite 370 Irvine, CA 92612.
7. Basch, H.; *Inorg. Chim. Acta*, **1996**, *252*, 265.
8. Chin-Hung Lai, C.L., Su, M.; Chu, S.Y.; *J. Phys. Chem. A*, **2002**, *106*, 575.
9. Cowley, A. H.; Hall, S. W.; Nunn, C.M.; Power, J. M.; *Chem. Commun.*, **1988**, 753.
10. Rappoport, Z. (Editor); *The Chemistry of Organic Germanium, Tin and Lead Compounds, Volume 2*, **2002**, John Wiley & Sons, Ltd.
11. a) Cizek, J.; *Adv. Chem. Phys.*, **1969**, *14*, 35; b) Purvis, G. D.; Bartlett, R. J.; *J. Chem. Phys.*, **1982**, *76*, 1910; c) Scuseria, G. E.; Janssen, C. L.; Schaefer III, H. F.; *J. Chem. Phys.*, **1988**, *89*, 7382; d) Scuseria, G. E.; Schaefer III, H. F.; *J. Chem. Phys.*, **1989**, *90*, 3700.
12. Krishnan, R.; Pople, J. A.; *Int. J. Quant. Chem.*, **1978**, *14*, 91.
13. *Gaussian 98, Revision A.11.3*, Frisch, M. J.; Trucks, G. W.; Schlegel, H. B.; Scuseria, G. E.; Robb, M. A.; Cheeseman, J. R.; Zakrzewski, V. G.; Montgomery Jr., J. A.; Stratmann, R. E.; Burant, J. C.; Dapprich, S.; Millam, J. M.; Daniels, A. D.; Kudin, K. N.; Strain, M. C.; Farkas, O.; Tomasi, J.; Barone, V.; Cossi, M.; Cammi, R.; Mennucci, B.; Pomelli, C.; Adamo, C.; Clifford, S.; Ochterski, J.; Petersson, G. A.; Ayala, P. Y ; Cui, Q.; Morokuma, K.; Malick, D. K.; Rabuck, A. D.; Raghavachari, K.; Foresman, J. B.; Cioslowski, J.; Ortiz, J. V.; Baboul, A. G.; Stefanov, B. B.; Liu, G.; Liashenko, A; Piskorz, P.; Komaromi, I.; Gomperts, R.; Martin, R. L.; Fox, D. J.; Keith, T.; Al-Laham,

- M. A.; Peng, C. Y.; Nanayakkara, A.; Gonzalez, C.; Challacombe, M.; Gill, P. M. W.; Johnson, B.; Chen, W.; Wong, M. W.; Andres, J. L.; Gonzalez, C.; Head-Gordon, M.; Replogle, E. S.; Pople, J. A.; Gaussian, Inc., Pittsburgh PA, **2002**.
14. Vlaar, M. J. M.; Ehlers, A. W.; de Kanter, F. J.; Schakel, M.; Spek, A. L.; Lutz, M.; Sigal, N.; Apeloig, Y.; Lammertsma, K.; *Angew. Chem., Int. Ed.*, **2000**, *39*, 4127.
15. Niecke, E.; Fuchs, A.; Nieger, M.; *Angew. Chem., Int. Ed.*, **1999**, *38*, 3028.
16. Cowley, A. H.; Jones, R. A.; Lasch, J. G.; Norman, N. C.; Stewart, C. A.; Stuart, A. L.; Atwood, J. L.; Hunter, W. E.; Zhang, H.-M.; *J. Am. Chem. Soc.*, **1984**, *106*, 7015.
17. Appel, R.; Menzel, J.; Knoch, F.; *Chem. Ber.*, **1985**, *118*, 4068.
18. Chernega, A.N.; Antipin, M.Yu.; Struchkov, Yu.T.; Boldeskul, I.E.; Kolodyazhnyi, O.I.; Shevchenko, I.V.; Kukhar, V.P.; *Zh. Obshch. Khim.*, **1987**, *57*, 1975.
19. Ito, S.; Nishide, K.; Yoshifuji, M.; *Organometallics*, **2006**, *25*, 1424.
20. Nemes, G.; Ranaivonjatovo, H.; Escudié, J.; Silaghi-Dumitrescu, I.; Silaghi-Dumitrescu, L.; Gornitzka, H.; *Eur. J. Inorg. Chem.*, **2005**, *6*, 1109.
21. Ito, S.; Jin, H.; Kimura, S.; Yoshifuji, M.; *J. Org. Chem.*, **2005**, *70*, 3537.
22. Pietschnig, R.; Orthaber, A.; *Eur. J. Inorg. Chem.*, **2006**, *22*, 4570.
23. El Harouch, Y.; Gornitzka, H.; Ranaivonjatovo, H.; Escudié, J.; *J. Organomet. Chem.*, **2002**, *643-644*, 202.
24. *NBO 5.0*, Glendening, E. D.; Badenhoop, J. K.; Reed, A. E.; Carpenter, J. E.; Bohmann, J. A.; Morales, C.M.; Weinhold, F.; Theoretical Chemistry Institute, University of Wisconsin, **2001**.
25. Eichler, B. E.; Powell, D. R.; West, R.; *Organometallics*, **1998**, *17*, 2147.
26. Wiberg, K.B.; *Tetrahedron*, **1968**, *24*, 1083.

CHAPTER III

***1,3-DIGERMACYCLOBUTANES WITH EXOCYCLIC
C=P AND C=P=S DOUBLE BONDS***

CHAPITRE III

1,3-digermacyclobutanes à doubles liaisons P=C et P=C=S exocycliques

L'action de *t*BuLi sur le (di-*tert*-butylfluorogermyle)chlorophosphapropène **1** (Mes* = 2,4,6-tri-*tert*-butylphényl) à basse température conduit à un nouveau 1,3-digermacyclobutane substitué par des groupements arylphosphanylidènes (schéma 1). Deux isomères géométriques, *cis* (**3a**) et *trans* (**3b**) par rapport à l'axe -P=C...C=P-, ont été identifiés par RMN ³¹P, l'isomère *cis* étant le plus abondant.

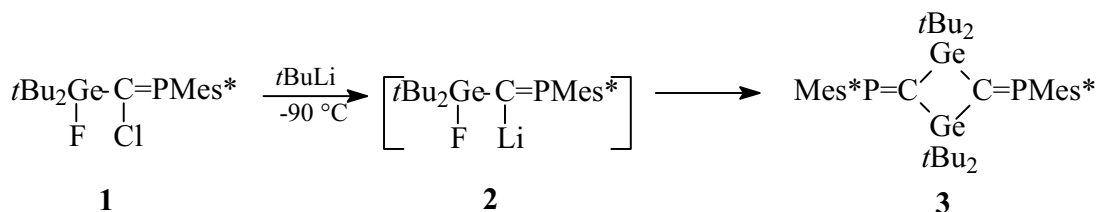


Schéma 1

Les structures cristallines de **3a**, **b** ont été déterminées. Elles présentent à peu près les mêmes caractéristiques structurales. La figure 1 présente la structure moléculaire du dérivé *cis*, ainsi que certaines données géométriques qui montrent notamment que le cycle à 4 chaînons est plan.

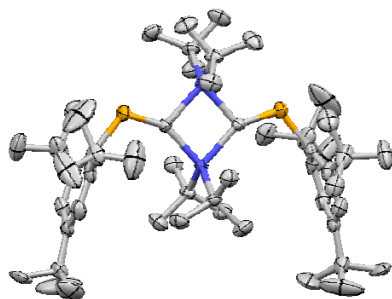


Figure 1. Structure moléculaire de **3a**

Distances (Å):

Ge-C: 2.008; C-P: 1.665; Ge-C*t*Bu: 2.016;
P-CMes*: 1.872 ;
Ge...Ge: 2.918; C...C: 2.755

Angles (°) :

C-Ge-C*t*Bu: 114.48; C-Ge-C: 86.71;
Ge-C-Ge: 93.72; Ge-C-P: 117.46; C-P-CMes*:
109.86

Angles de torsion (°):

C-Ge-C-Ge: 0.00, P-C-Ge-C: 178.65

Une étude de RMN ^{31}P à température variable a permis de prouver que les composés **3** n'étaient pas formés par dimérisation du phosphagermaallène $\text{Mes}^*\text{P}=\text{C}=\text{Ge}(t\text{Bu})_2$. Il semble qu'une élimination intramoléculaire de LiF ait lieu à partir des dérivés lithiés **2** pour conduire aux produits finaux.

Les dérivés soufrés **4a, b**, premiers composés avec deux entités $\text{P}=\text{C}=\text{S}$ dans une même molécule, sont facilement obtenus à partir de **3** par réaction avec S_8 à 60°C (schéma 2). Deux isomères géométriques ont également été obtenus, dans les mêmes proportions relatives que les produits de départ.

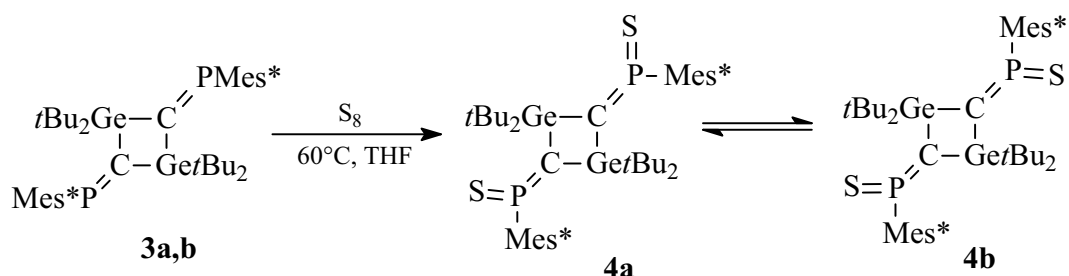


Schéma 2

Les structures par rayons X de ces dérivés ont également été déterminées. La figure 2 présente la structure moléculaire de l'isomère *trans* **4b**. Les longueurs et les angles de liaison sont en conformité avec des valeurs déjà rapportées dans la littérature pour des produits similaires.

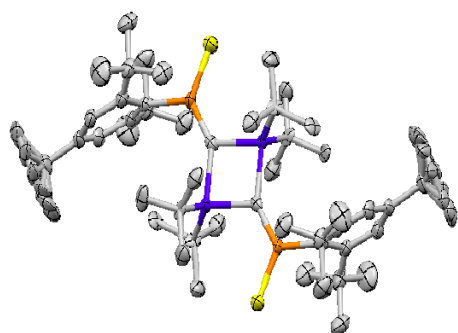


Figure 2. Structure moléculaire de **4b**

Distances (Å):

Ge-C: 2.004; C-P: 1.652; P-CMes*: 1.827 ;
P-S: 1.937; Ge...Ge: 2.956; C...C: 2.712;

Angles (°) :

C-Ge-C 85.07; C-Ge-C*t*Bu: 114.48; Ge-C-P:
121.90; C-P-CMes*: 118.30; S-P-C: 124.77

Angles de torsion (°):

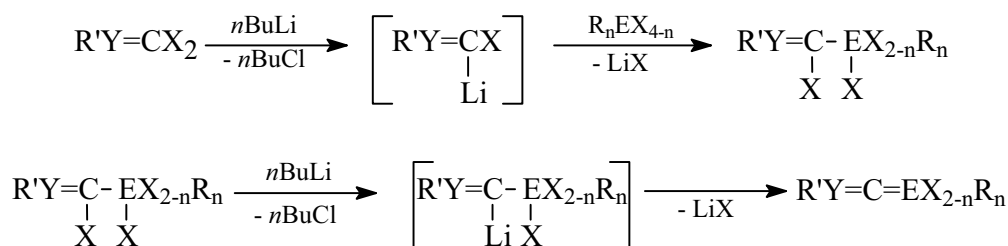
C-Ge-C-Ge: 0.00; P-C-Ge-C: 180.00
S-P-C-Ge: 0.00

Probablement en raison de l'encombrement stérique, les dérivés **4a, b** sont très stables et une isomérisation en thiaphosphiranes n'a pas été observée.

Des calculs théoriques ont été effectués sur des composés modèles de **3a, b** (H au lieu des groupements encombrants) au niveau B3LYP/6-31G (d); ils montrent une légère préférence pour l'isomère *trans* alors que l'isomère *cis* est expérimentalement prépondérant. Il semble que cette inversion soit due à un effet de solvant. Des calculs sophistiqués ont révélé que, bien qu'il n'y ait pas une conjugaison substantielle entre les deux liaisons P=C, la grande stabilité des composés **3a b**, peut être expliquée par des interactions des orbitales moléculaires à travers le cycle et les liaisons doubles.

Multiple bonded derivatives of heavier 14 group elements have been the subject of intense interest in the last few decades. Compounds containing only one double bond of silicon, germanium and tin are fairly well known and several synthesis methods have been employed to prepare relatively stable unsaturated compounds that bear one multiple bond of group 14 elements. Increasing the unsaturation degree while maintaining the stability of the compound became a real challenge and indeed the synthesis of systems as $E_{14}=C=Y$ where $Y =$ group 14, 15, 16 elements, has been attempted. As previously discussed, the presence of two adjacent double bonds made the task more difficult, and bulky substituents have proven to be useful for the stabilization of such compounds. Another way to stabilize such structures consists in their coordination onto a transition metal. Such methods of stabilization work very well for $Y=C=Y$ ($Y = C, P, N$), for which η^1 - and η^2 - coordination occur, but have not yet been employed for group 14 element-containing heteroallenes.

The great reactivity of $E_{14}=C$ bond is limiting with respect to the number of routes available in the synthesis of $E_{14}=C=Y$ unit. So it is better to first create the more stable $C=Y$ bond, and to form the more reactive π -bond by an elimination reaction in the next step. This means that both E_{14} and the carbon atom must have good leaving groups as substituents, E_{14} also bearing bulky radicals which provide sterical hindrance. A general route often employed in the synthesis of derivatives containing the $E=C=P$ unit is shown below (scheme III.1):



Scheme III.1

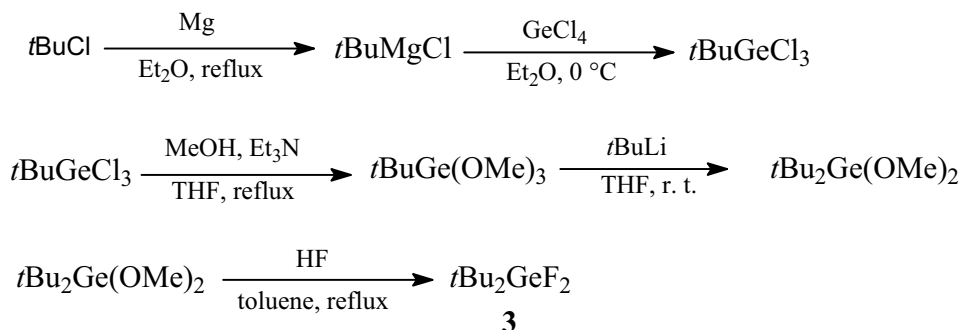
It follows that phosphapropenes of the type $\text{R}_2\text{E}(\text{X})-\text{C}(\text{X})=\text{PR}'$ are valuable precursors in the synthesis of group 14 element heteroallenes [1]. Although the lithium derivative $\text{R}_2\text{E}(\text{X})-\text{C}(\text{Li})=\text{PR}'$ is obtained by lithiation with $n\text{BuLi}$ at low temperatures the formation of the heteroallene depends on the nature of the substituents on the E_{14} atom, as well as that of the vicinal halogen and is not always observed, for example in $\text{RCl}_2\text{Si}-\text{C}(\text{Li})=\text{PMes}^*$ with $\text{R} = 9\text{-methylfluorenyl}$ [2].

Because most of the commercially available starting materials are chlorinated derivatives, the choice of chlorogermanes as precursors was obvious. However, fluorine is also often used as the halogen on the E_{14} atom because the higher bond energy of $\text{E}-\text{F}$ compared to the related $\text{E}-\text{Cl}$ prevents side reactions like direct alkylation of the germanium or reduction of the $\text{Ge}-\text{F}$ bond (see table III.1[3]). The employment of fluorine also allows an easier identification of the derivatives thanks to the NMR active ^{19}F isotope.

Table III.1. Bond energies and lengths for $\text{E}_{14}-\text{X}$

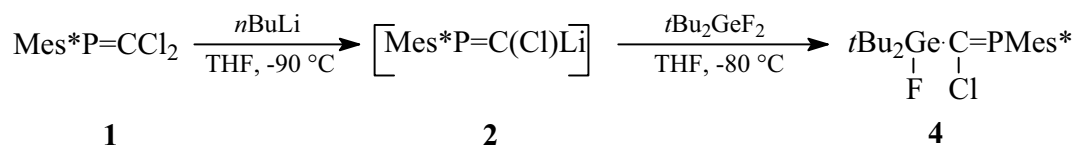
	D (kJ/mol)	r (Å)
Si-F	565	1.60
Si-Cl	381	2.02
Ge-F	470	1.68
Ge-Cl	349	2.10
Sn-F	414	
Sn-Cl	323	2.33
Sn-Br	273	2.50

The starting germanium derivative was obtained through a procedure described in scheme III.4 [5].



Scheme III.4

The reaction of the lithium phosphavinylcarbenoid **2** with $t\text{Bu}_2\text{GeF}_2$ **3** at low temperature leads to the formation of the novel phosphagermapropene $t\text{Bu}_2\text{Ge(F)-C(Cl)=PMes}^*$ **4**, as shown in scheme III.5.



Scheme III.5

After removal of the lithium salts, phosphagermapropene **4** was purified by precipitating it from methanol. The only signal observed at 293.5 ppm (d, $^3J_{\text{PF}} = 45.8$ Hz) in the ^{31}P NMR spectrum was assigned to the *E* isomer with respect to the P=C double bond. The ^1H NMR spectra of compound **4** reveals that the *t*Bu groups on the germanium atom are not equivalent, due to the high steric congestion which prevents the rotation of the (F)Ge-C(Cl) bond. To make sure that the two signals are not the result of the coupling with the fluorine atom, the spectrum was recorded at another frequency and showed a different value in Hz between the two signals. The fluorine spectrum showed one signal at the expected value of -135.4 ppm.

A detail of the ^{13}C NMR spectrum for **4** is given in figure III.1.

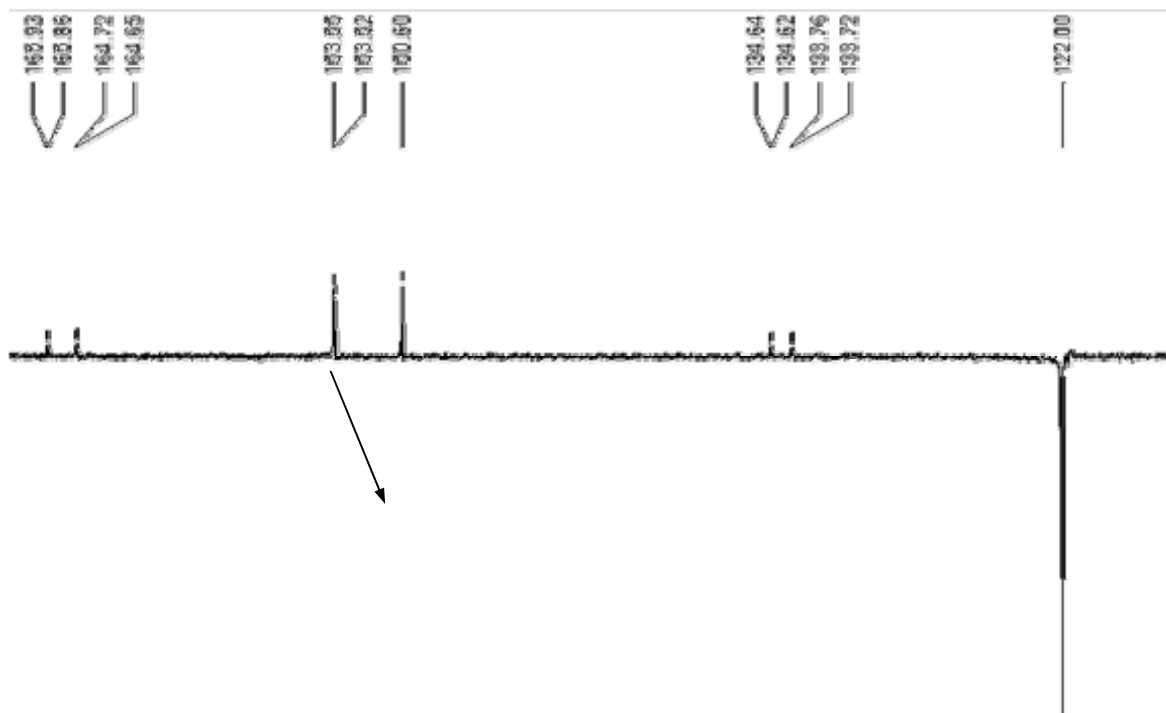
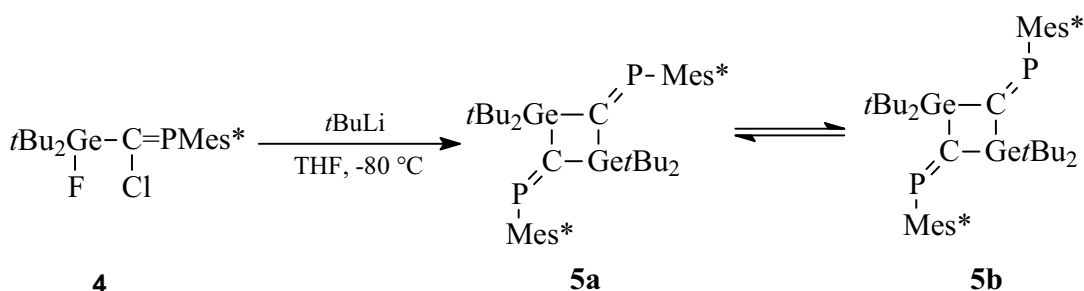


Figure III.1. Aromatic range of the ^{13}C NMR spectrum for compound **4**

The carbon atom involved in the double bond appears at 165.2 ppm (dd, $\text{C}=\text{P}$, $^1J_{\text{CP}} = 91$ Hz, $^2J_{\text{CF}} = 4.5$ Hz), as expected for this type of compounds. Two signals for the quaternary carbons of the *t*Bu groups appear at 32.9 and 33.0 ppm. The coupling of the fluorine atom with the *ipso* carbon from the supermesityl group can be seen, with a value of 2.3 Hz for $^4J_{\text{CF}}$.

2) Action of *t*BuLi on derivative 4. Synthesis of the novel 2,4-diphosphinylidene-1,3-digermacyclobutanes 5a,b

In an attempt to synthesize the new phosphagermaallene $t\text{Bu}_2\text{Ge}=\text{C}=\text{PMes}^*$, compound **4** was treated with *t*BuLi at low temperature. By warming to room temperature, the expected phosphagermaallene was not formed; instead the novel 2,4-diphosphinylidene-1,3-digermacyclobutanes **5a,b** were obtained, as shown in scheme III.6 [6].



Scheme III.6

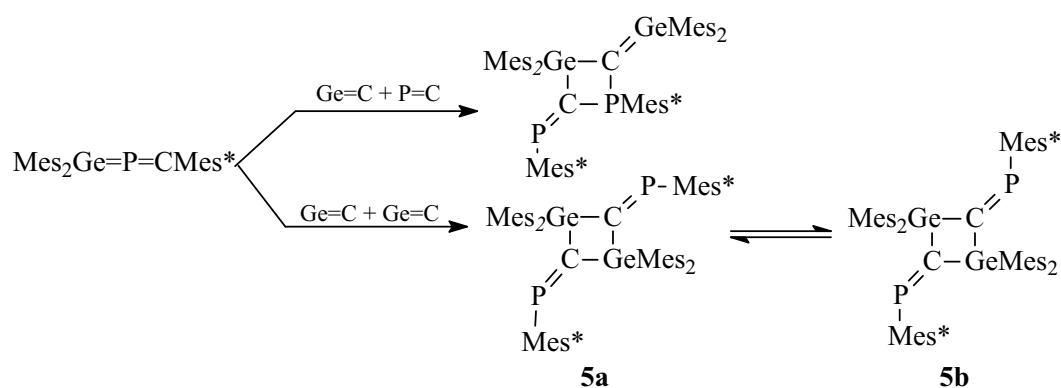
Both the *cis* and the *trans* isomer (derived from the different orientation of the Mes^* groups with respect to the $-\text{P}=\text{C}=\text{C}=\text{P}-$ axis) were obtained, in a 3/1 ratio in favor of the *cis* derivative. The equilibrium between the two geometrical isomers is quickly established in solution at room temperature; thus, by dissolving crystals of either **5a** or **5b**, the equilibrium ratio is achieved in less than an hour. This kind of geometrical isomerism has previously been described for similar compounds [7]. Although it was previously assumed that steric effects would favor the *trans* isomer, the *cis* form seems to be stabilized by interactions with the solvent.

Compounds **5a,b** were characterized through NMR spectroscopy; relevant data are given in Table III.2.

Table III. 2. NMR data for **5a,b**

	5a, cis	5b, trans
³¹ P	367.4 ppm	367.7 ppm
¹³ C	204.0 ppm (dd, C=P, ¹ J _{CP} = 25.7 Hz, ³ J _{CP} = 96.6 Hz)	204.3 ppm (dd, C=P, ¹ J _{CP} = 24.9 Hz, ³ J _{CP} = 92.0 Hz)
¹ H	7.07 ppm (H _{arom})	7.13 ppm (H _{arom})

The spectra of the cyclodigermane analogues [Mes₂Ge-C=PMes*]₂ present slightly more deshielded signals in ³¹P NMR, at 381 (for the *trans* isomer) and 374.7 ppm (for the *cis* form). The *trans* isomer is formed immediately after the reaction (scheme III.7), but after a few days at room temperature, a mixture of *trans/cis* isomers in 42/58 ratio is obtained. The *trans* derivative transforms into the *cis* isomer after irradiation for 2h [8].

**Scheme III.7**

Irradiating the mixture of **5a,b** did not lead to any transformation; the equilibrium once achieved could not be modified.

The crystal structure of both **5a** and **5b** was determined through X-ray diffraction [6]. The molecular structure of the *cis* isomer is given in Figure 2 and relevant geometrical data are shown in table III.3. The four-membered ring is planar, similar to that of the other 1,3-digermacyclobutanes described in the literature [9]. The Ge-C distance of 2.00 Å is within the range of 1.98-2.00 Å reported for analogue derivatives. The germanium atom has a distorted tetrahedral geometry. The Ge...Ge distance (around 2.90 Å) is slightly larger than those found in the literature (2.77 – 2.80 Å) for 1,3-

digermacyclobutanes without exocyclic double bonds [9b,c], while the C \cdots C distance decreases (2.755 Å in **5b** versus 2.904 Å) [9b]. This is no doubt a consequence of the geometry required by the sp^2 hybridization of the carbon atoms.

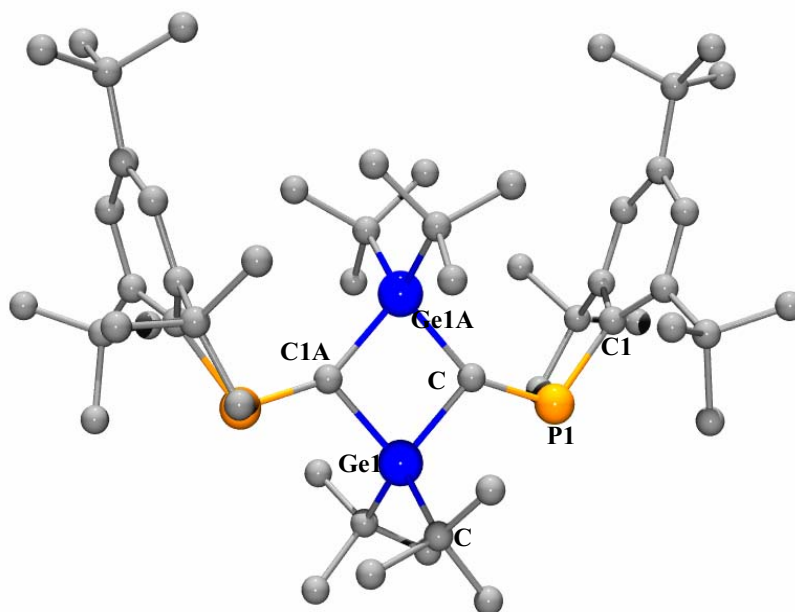


Figure III. 2. Molecular structure of **5a** (hydrogen atoms are omitted for clarity)

Table III.3. Selected bond distances and bond angles for **5a**

Interatomic lengths (Å)	Angles (°)
Ge(1)-C(1): 2.002(2)	C(1)-Ge(1)-C(1A): 86.29(11)
C(1)-P(1): 1.671(2)	Ge(1)-C(1)-Ge(1A): 93.70(11)
P(1)-C(10): 1.863(2)	Ge(1)-C(1)-P(1): 116.55(15)
Ge(1)-C(2): 2.014(2)	C(1)-Ge(1)-C(1A)-Ge(1A): 0
Ge(1) \cdots Ge(1A): 2.920	C(1)-Ge(1)-C(1A)-P(1A): -175.22
C(1) \cdots C(1A): 2.737	

The *trans* derivative was also characterized through single-crystal X-ray diffraction; its molecular structure is presented in Figure 3. The geometrical parameters are very similar to those of its *cis* isomer, as shown in Table III.4.

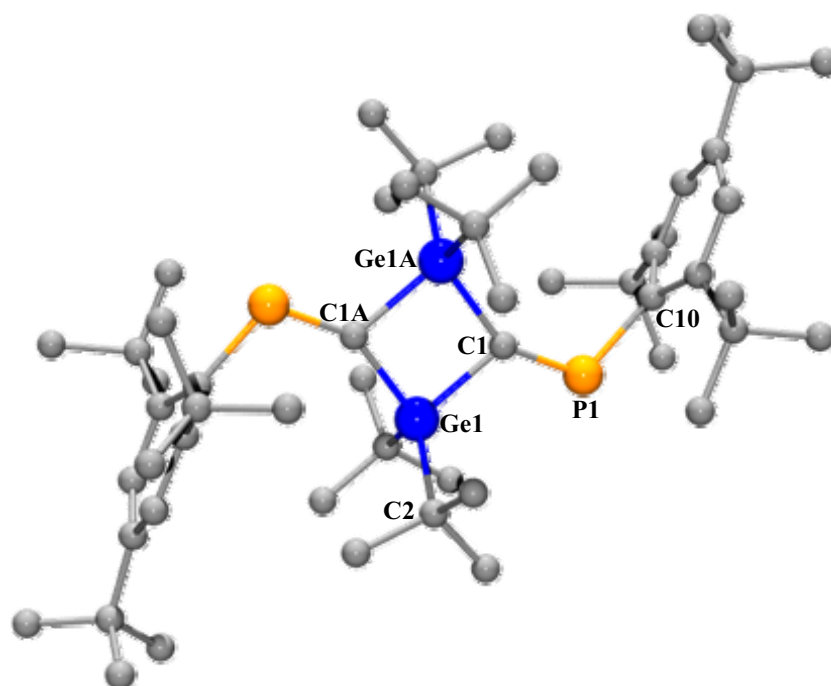


Figure III.3. Molecular structure of **5b** (hydrogen atoms are omitted for clarity)

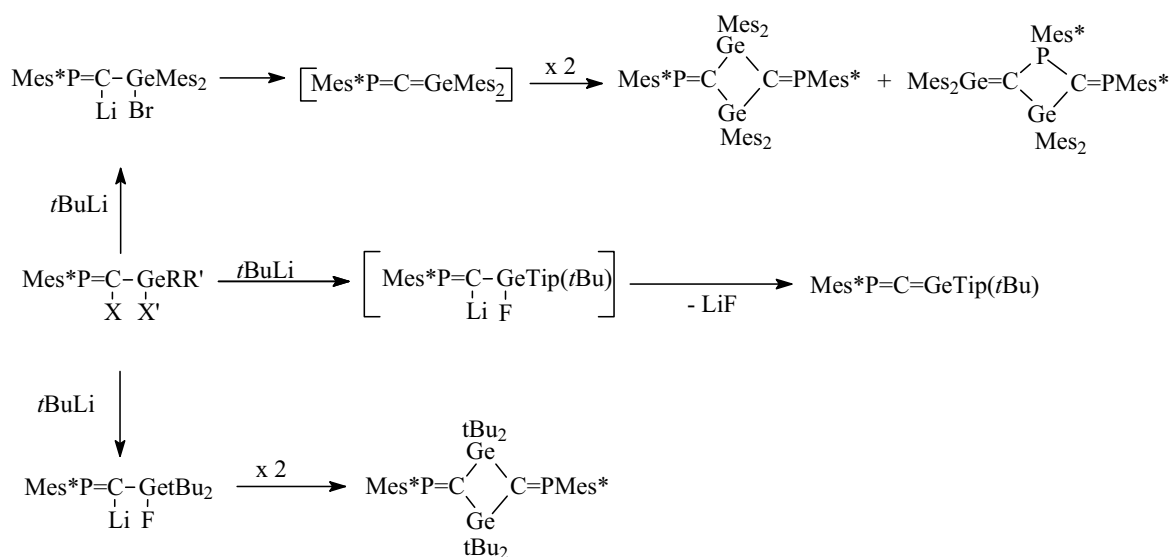
Table III.4. Selected bond distances and bond angles for **5b**

Interatomic lengths (Å)	Angles (°)
Ge(1)-C(1): 2.005(3)	C(1)-Ge(1)-C(1A): 86.71(11)
C(1)-P(1): 1.665(3)	Ge(1)-C(1)-Ge(1A): 93.29(11)
P(1)-C(10): 1.872(3)	Ge(1)-C(1)-P(1): 117.46(15)
Ge(1)-C(2): 2.016 (3)	C(1)-Ge(1)-C(1A)-Ge(1A): 0
Ge(1)···Ge(1A): 2.918	C(1)-Ge(1)-C(1A)-P(1A): 178.65
C(1)···C(1A): 2.755	

As it can be seen, the orientation of the Mes* group with respect to the diagonal of the cycle bears little consequence on the bond lengths and bond angles values and does not influence the planar conformation of the four-atom ring. The only immediate effect is the difference in polarity of the two isomers, which allows a better separation of the mixture. As said before, **5b** readily crystallizes from THF, while crystals of the less polar **5a** are obtained from pentane. Both derivatives exhibit a pronounced thermal stability and are stable in air.

3) Mechanism of formation of 5a and 5b

The action of *t*BuLi on phosphagermapropenes containing the Ge-C(X)=PMes* unit at low temperature leads to the formation of a lithium compound of the type >Ge-C(Li)=PMes*. Its evolution with the increase of temperature seems to vary a lot, depending on the nature of the groups on the germanium atom. As shown in scheme III.8, Mes₂Ge(Br)-C(Li)=PMes* undergoes an intramolecular elimination of the lithium halide to afford the metastable Mes₂Ge=C=PMes*. The formed phosphagermaallene then readily dimerizes according to schemes III.7 and III.8. The only known stable phosphagermaallene is obtained from Tip(*t*Bu)Ge(F)-C(Li)=PMes* which also undergoes the intramolecular elimination of LiF, to afford Tip(*t*Bu)Ge=C=PMes* [10]. Scheme III.8 summarizes this behavior. We investigated the possibility of the allene *t*Bu₂Ge=C=PMes* to be an intermediate in the synthetic route leading to compounds **5a** and **5b**, given that the overall steric hindrance at the germanium in the starting phosphagermapropene **4** is similar to that of the ones mentioned above.



Scheme III.8

The action of *t*BuLi on derivative **4** was monitored by ³¹P NMR spectroscopy from -90 °C to room temperature, using THF as a solvent (see Figure III. 4). The initial formation of the corresponding lithium compound **6** was observed immediately and in quantitative yield ($\delta^{31}\text{P}$: 381.6 ppm, $^3J_{\text{PF}} = 10.1$ Hz) (Scheme III.9). As the temperature raised to -60 °C, the signal at 381.6 ppm decreases and two doublets appear at 286.7 and 443.8 ppm ($J_{\text{PP}} = 38.9$ Hz). By increasing the temperature above -40 °C, these signals decrease and those of the final products **5a/5b** appear.

It seems we can propose an intermolecular elimination of LiF from two molecules of **6** to get intermediate **7** (scheme III.9). The most deshielded signal could correspond to the phosphorus atom of the P=C-Li unit. The coupling with the fluorine atom is not observed, but a small coupling of less than 5 Hz would be hard to be observed.

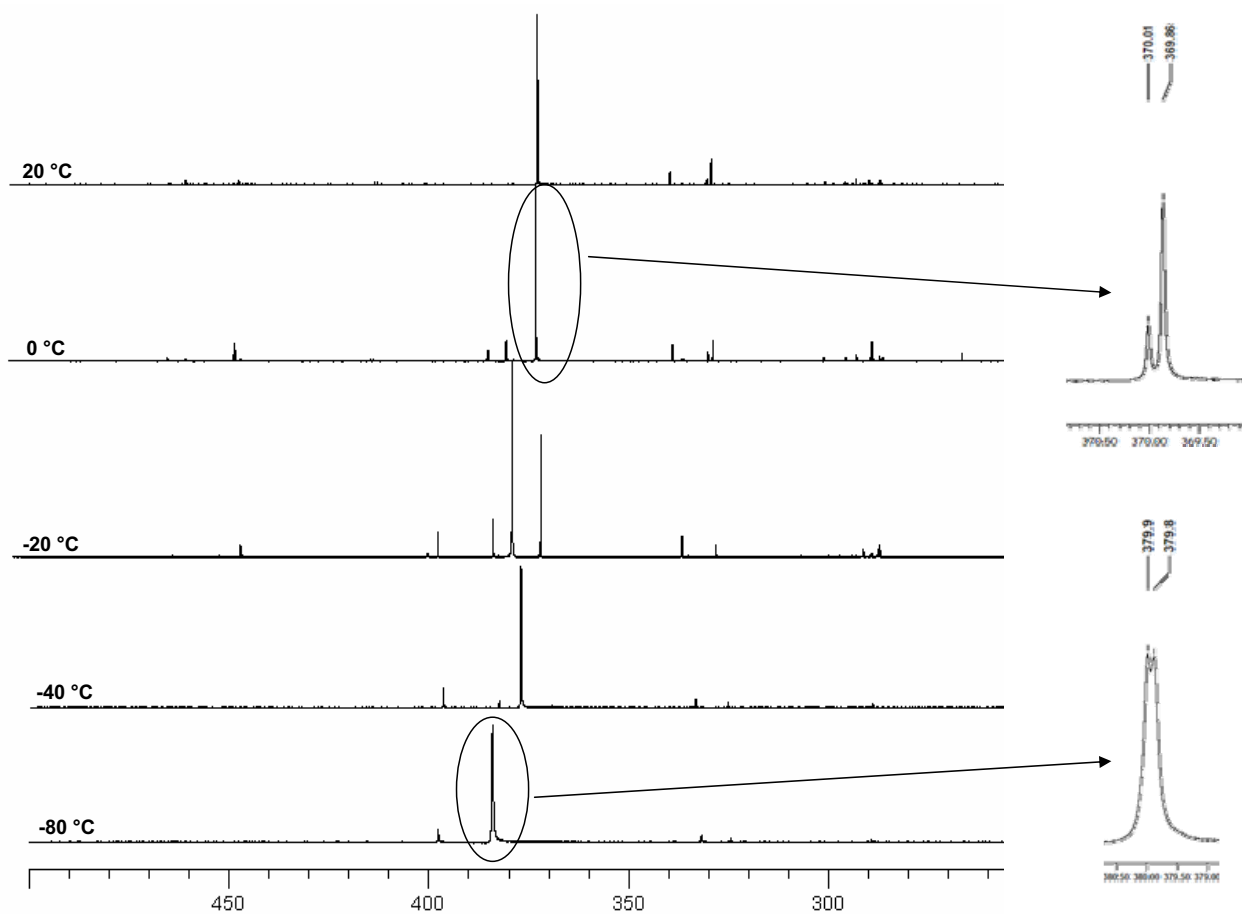
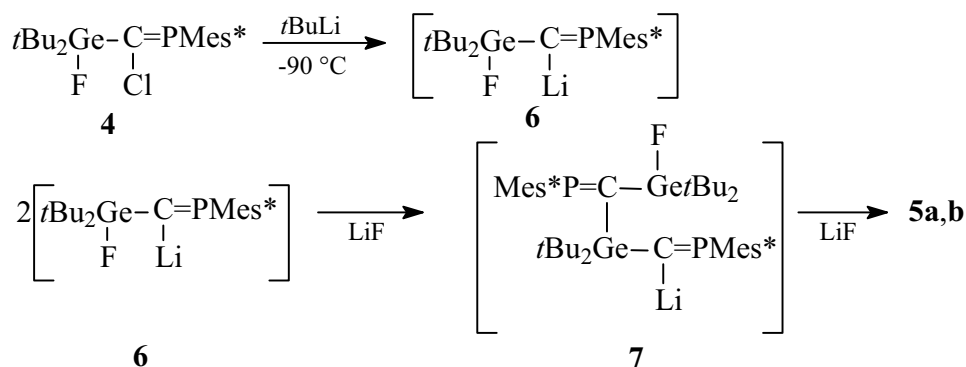


Figure III.4. Variable temperature NMR spectra for the formation of **5a, b**



Scheme III.9

Other intermediates can be envisaged, like zwitterions of the type $t\text{Bu}_2\text{Ge}^+-\text{C}^-\text{=PMes}^*$ which can dimerize to afford derivative **5**, but there is no real evidence to support their formation neither that of the corresponding $t\text{Bu}_2\text{Ge}=\text{C}=\text{PMes}^*$. For this kind of compounds we expect a signal in the range 240-250 ppm in ^{31}P NMR [10], which was never observed. The decrease of the lithium derivative peak coincides with the appearance of the signal for **7**.

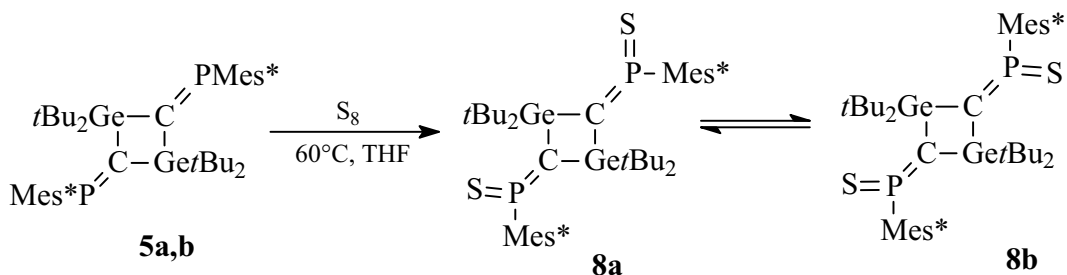
We therefore concluded that the formation of the germaphosphaallenic unit $\text{P}=\text{C}=\text{Ge}$ is greatly influenced by the organic groups on the germanium atom. It seems that the presence of an aromatic substituent favors the intramolecular elimination of LiF, by increasing the stability of the lithium derivative $\text{Ar}_2\text{Ge}(\text{F})\text{C}(\text{Li})=\text{PMes}^*$ (Ar = aryl) compared to the analogue $\text{R}_2\text{Ge}(\text{F})\text{C}(\text{Li})=\text{PMes}^*$ (R = alkyl). In order to sustain this theory, a theoretical study is in progress

4) Synthesis and characterization of the first bis(methylenethioxophosphoranes) bridged by germanium atoms

Due to the electronic properties of the $\text{P}=\text{C}$ unit (σ -donor and π -acceptor effects), there has been an increasing interest in using this structural brick as a ligand in the synthesis of novel transition metal complexes with use in catalysis [11]. The presence of two such units in derivatives **5a, b** should confer them potential intriguing characteristics,

like complexation of two different metals and communication between them by means of extensive conjugation involving the digermacyclobutane moiety. Further complexation of the P=C=S unit by a transition metal should increase their ability to act as ligands with potential applications in catalysis.

The synthesis of the bis(methylenethioxophosphanes) derivatives **8a,b** was carried out starting from the mixture of **5a,b** as shown in scheme III.10 with an excess of sulfur in THF. Reflux was necessary to get **8a,b** contrary to the case of Mes*P(S)=CTms₂ (Tms = SiMe₃) which could be obtained at room temperature by a similar procedure [12]. Derivatives **8a,b** are extremely thermally stable and do not undergo any transformation, even when exposed to air for several days. The high steric congestion in **8** might be responsible for its stability since in other instances, depending on the substituents on the C and P atom, the C=P=S moieties rearrange to a thiaphosphirane or give a further addition of sulfur [13-20].



Scheme III.10

The same mixture of the *cis* and *trans* isomers is obtained as in the non-sulfurated starting products **5a,b**. The ratio is kept, but the *cis* isomer is more deshielded (184.4 ppm) than the corresponding *trans* one (183.7 ppm). The electropositive germanium atoms (2.0 – 2.1 on the Pauling scale) bonded to the thioxophosphaalkene carbons cause the phosphorus nuclei in compound **8** to resonate at low fields, as in the case of Mes*P(S)=CTms₂ (190.9 ppm) [16] bearing two electropositive silicon atoms. The ³¹P NMR spectra of such compounds substituted by alkyl or aryl groups generally exhibit chemical shifts between 107 and 160 ppm [13-20]. For Mes*P(S)=CTms₂, the phosphorus signal at 190.9 ppm corresponds to a ~200 ppm shift upfield compared to the starting

phosphaalkene Mes*P=CTms₂. This is also the case for derivatives **8a** and **8b**, the shift from P=C to P=C=S being about 185 ppm.

The ¹H and ¹³C NMR spectra for the mixture of the two isomers were recorded; some relevant data are given in table III.5. The shifts for each individual derivative were not obtained because the equilibrium between the two geometrical isomers establishes too quickly in solution.

Table III.5. NMR chemical shifts for **8a, b**

	<i>cis/trans mixture</i>
³¹ P	184.4 ppm (<i>cis</i>), 183.7 ppm (<i>trans</i>)
¹³ C	121 and 122.60 (<i>m</i> -C of Mes*); 159.3-164.2 (<i>m</i> , C=P).
¹ H	7.24 – 7.46 (<i>m</i> , 4H, arom H).

Single crystals were obtained by taking advantage again of the difference in polarity. The *trans* isomer **8b** crystallized from a THF solution of the mixture kept at low temperature for several days. The *cis* derivative **8a** was obtained in crystalline form by slow evaporation of a pentane solution. Their molecular structures are presented in figures III.5 and III.6.

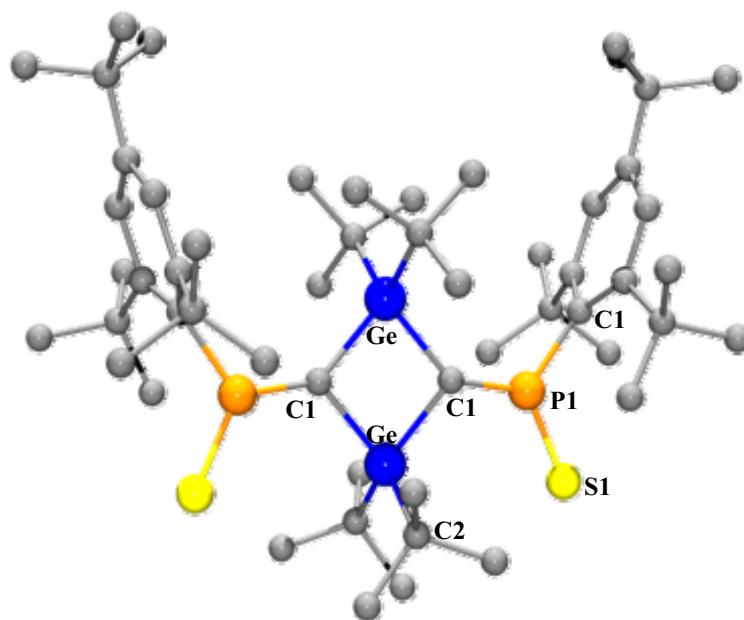


Figure III.5. Molecular structure of **8a** (hydrogen atoms were omitted for clarity)

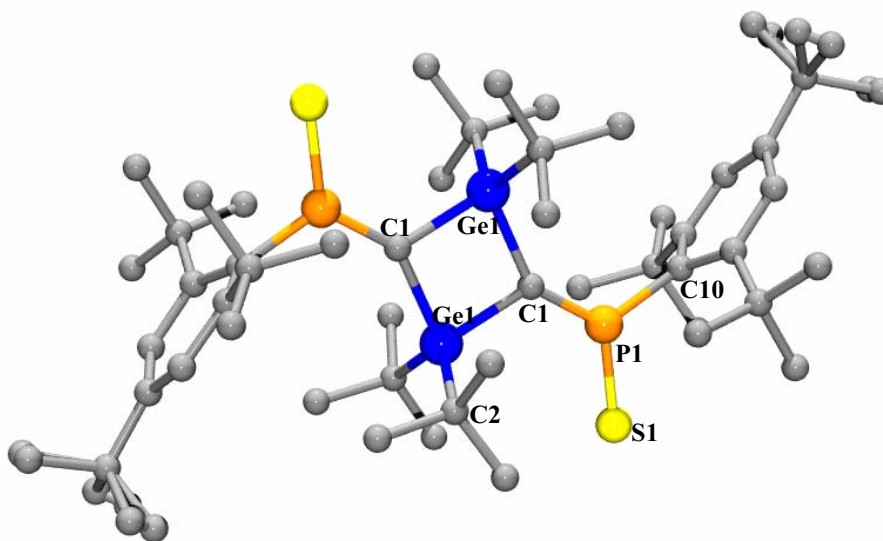


Figure III.6. Molecular structure of **8b** (hydrogen atoms were omitted for clarity)

Some relevant geometrical data are given in tables III.6 and III.7.

Table III.6. Selected bond distances and bond angles for **8a**

Interatomic lengths (Å)	Angles (°)
Ge(1)-C(1): 1.9977(18)	C(1)-Ge(1)-C(1A): 84.77(10)
C(1)-P(1): 1.6545(18)	Ge(1)-C(1)-Ge(1A): 95.61(8)
P(1)-C(10): 1.8202(19)	Ge(1)-C(1)-P(1): 139.66(10)
Ge(1)-C(2): 2.0195(19)	C(1)-Ge(1)-C(1A)-Ge(1A): 0
P1-S(1): 1.9369(7)	C(1)-Ge(1)-C(1A)-P(1A): 175.78
Ge(1)⋯Ge(1A): 2.971	
C(1)⋯C(1A): 2.693	

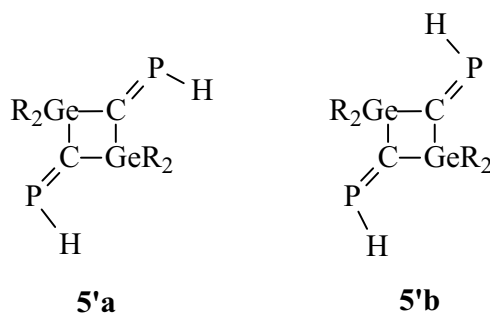
Table III.7. Selected bond distances and bond angles for **8b**

Interatomic lengths (Å)	Angles (°)
Ge(1)-C(1): 2.008(6)	C(1)-Ge(1)-C(1A): 85.1(3)
C(1)-P(1): 1.652(6)	Ge(1)-C(1)-Ge(1A): 94.9(3)
P(1)-C(10): 1.872(3)	Ge(1)-C(1)-P(1): 121.9(3)
Ge(1)-C(2): 1.93(2)	C(1)-Ge(1)-C(1A)-Ge(1A): 0
P(1)-S(1): 1.937(2)	C(1)-Ge(1)-C(1A)-P(1A): 180
Ge(1)···Ge(1A): 2.956	
C(1)···C(1A): 2.712	

The bond distances and angles are in the expected range of the values reported in the literature. The planarity of the digermacyclobutane ring is kept, despite the steric congestion around it. The phosphorus atom has as expected, a trigonal planar geometry, with angles a bit deviated from the ideal values. In both cases, the S1-P1-C10 is smaller (around 116°) and the C1-P1-S1 angle is wider (~125°). This is not the consequence of the crystal packing, but rather of the bulkiness of the *tert*-butyl groups on the ring. The Ge···Ge distance increases by comparison with the analogue non-sulfurated derivatives, and as a consequence, the C1-C1A distance decreases. The sulfur atom is about 4 degrees out of the digermabutane-cycle plan in the case of the *cis* derivative, but coplanar with the ring for the *trans* isomer.

5) Theoretical investigation of compounds 5 and 8

Quantum-chemical calculations using the Spartan package of programs [21] were carried out on model compounds of **5a,b**, represented in scheme III.11. Geometry optimizations were performed and the total energies obtained by B3LYP/6-31G(d) [22] calculations are given in table III.8 (for model compounds of **5**).



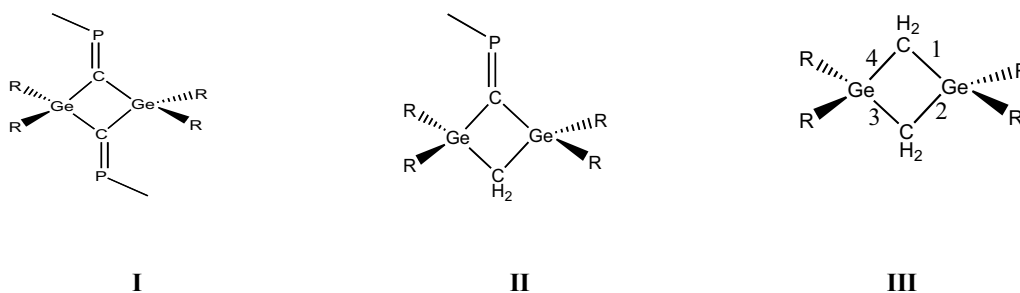
Scheme III.11

Table III.8. Calculated energies for model compounds of **5**

	E 5'a (a.u) <i>cis</i>	E 5'b (a.u) <i>trans</i>	Relative energy of 5'a (kcal/mol)
R = H	-4915.9629454	-4915.9629869	+0.01
R = Me	-5073.2640401	-5073.2643163	+0.09
R = <i>t</i> -Bu*	-5544.9853568	-5544.989180	+2.40

It can be seen that the *trans* isomer is barely lower in energy in all cases. The experimental ratio in favor of the *cis* isomer can be explained by solvating effects not taken into account by the calculations. Geometrical parameters for both isomers are very similar, as it was the case for the experimentally determined X-ray structures.

A possible conjugation between the C=P bonds through the germanium atoms should also be considered. In order to determine whether such conjugation exists, calculations were carried out on model compounds **I-III**, shown in scheme III.12. The four Ge-C bonds in the 4-atom ring should give us some insight into this matter. Table III.9 presents the calculated values of the Ge-C bonds.



Scheme III.12

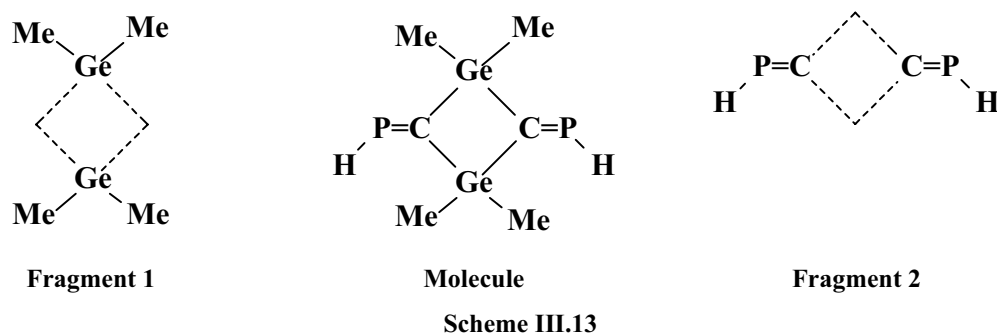
Table III.9. B3LYP/6-31G(d) Calculated ring geometries for model 5 and related systems

	P=C	CGe(1)	CGe(2)	CGe(3)	CGe(4)
R = H	1.672	1.987	1.989	1.987	1.989
I	1.672				
II	1.671	1.994	2.000	1.997	1.998
	-				
III	-	2.002	2.002	2.002	2.002
R = Me	1.673	1.992	1.996	1.992	1.996
I	1.673				
II	1.673	2.001	2.004	2.001	2.004
	-				
III	-	2.010	2.010	2.010	2.010
R = <i>t</i> -Bu	1.678	2.012	2.009	2.012	2.009
I	1.678				
II	1.678	2.019	2.018	2.015	2.013
	-				
III	-	2.020	2.020	2.020	2.020

The absence of P=C bonds in structure III causes a lengthening of the Ge-C bonds, compared to the other rings. Going from III to II, a shortening up to 0.007 Å can be noticed. For structure I, where two P=C units are present, the values of the Ge-C bonds are even smaller, while the length of the double P=C bond remains essentially the same.

However, this cannot be a sufficient prove for a conjugation extended throughout the cycle, because this shortening can be attributed to the change in the hybridization of the carbon atom, from sp^3 to sp^2 .

The molecular orbitals of **I** (R = Me) were analyzed using the AOMIX package [23]. To this purpose, single-point calculations were run with Gaussian 98 [24] at the B3LYP/6-31G(d) level of the theory on the entire molecule, and the two corresponding fragments, represented in scheme III.13.



The C_{2v} symmetry of the molecule allows for four types of symmetry-adapted fragment-orbitals (A_1 , A_2 , B_1 , and B_2). Figure III.7 details the interaction diagram for the frontier orbitals.

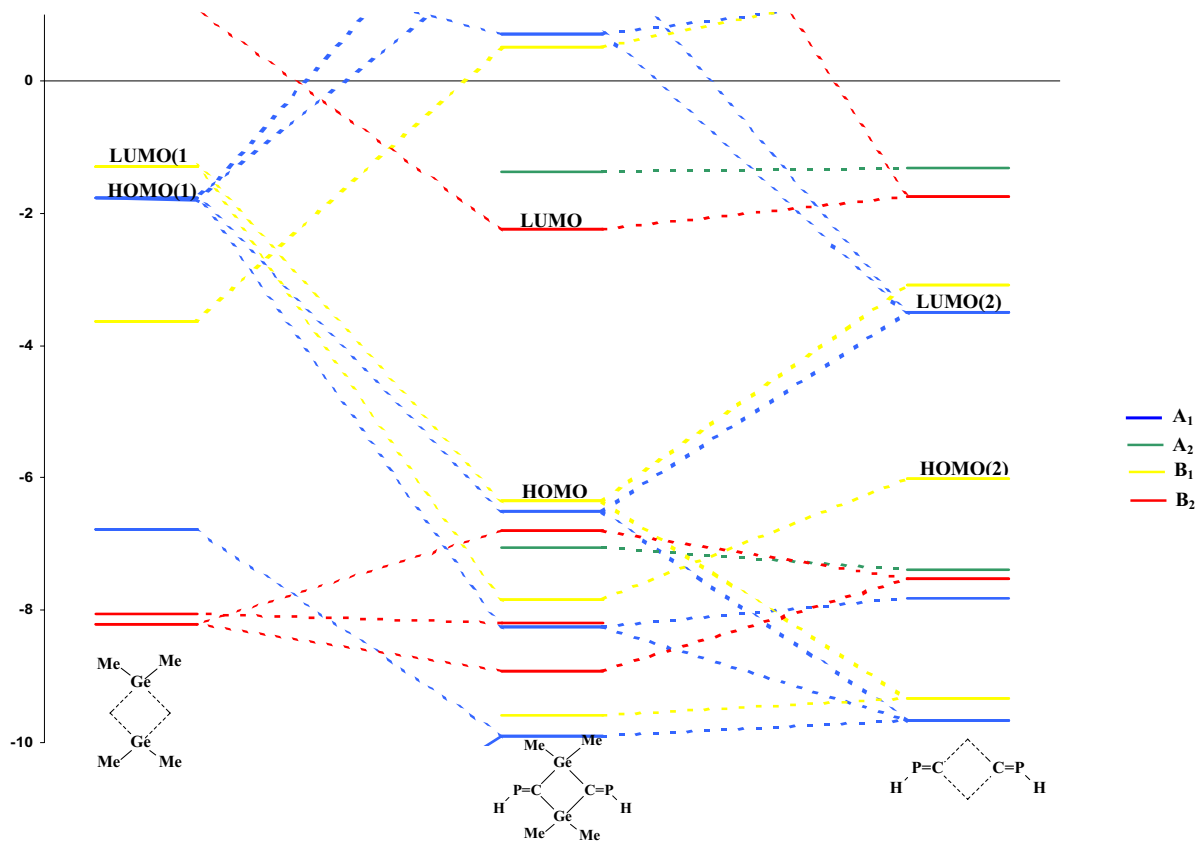


Figure III.7. Molecular orbital diagram for the interaction of 2 Me_2Ge (on the left) and 2 H-P=C (on the right) fragment-orbitals

An important stabilizing contribution can be noticed within the A_1 set of orbitals and comes from the 2-electron-2-orbital interaction of the HOMO(1) (the lone pairs on the GeMe_2 fragment) with the LUMO(2) (localized on the $\text{P}=\text{C}$ double bonds). Some relevant interactions within this symmetry-adapted class of orbitals are given in Figure III.8.

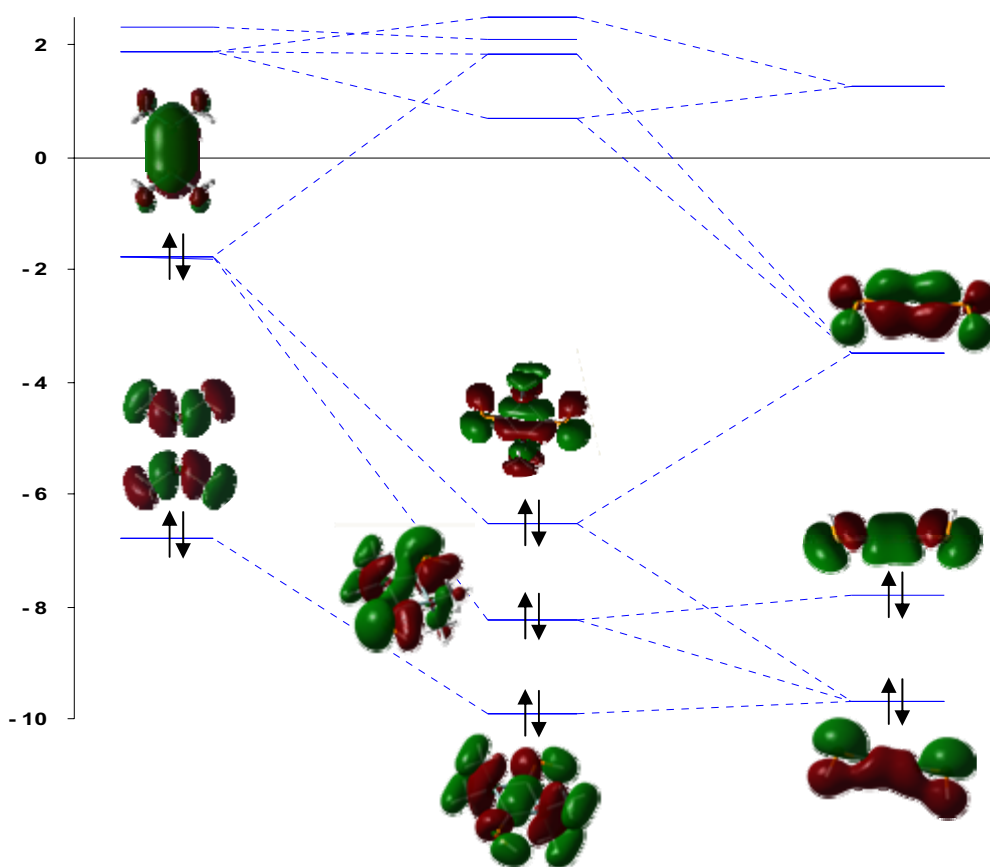


Figure III.8. Stabilizing interactions within the A_1 set of fragment-orbitals

Other stabilizing interactions occur between the HOMO of the Me_2Ge fragment and the corresponding symmetry-adapted LUMO from the two $\text{HP}=\text{C}$ units. Figure III.9 represents the interactions within the B_1 set of orbitals and the resulting molecular orbitals.

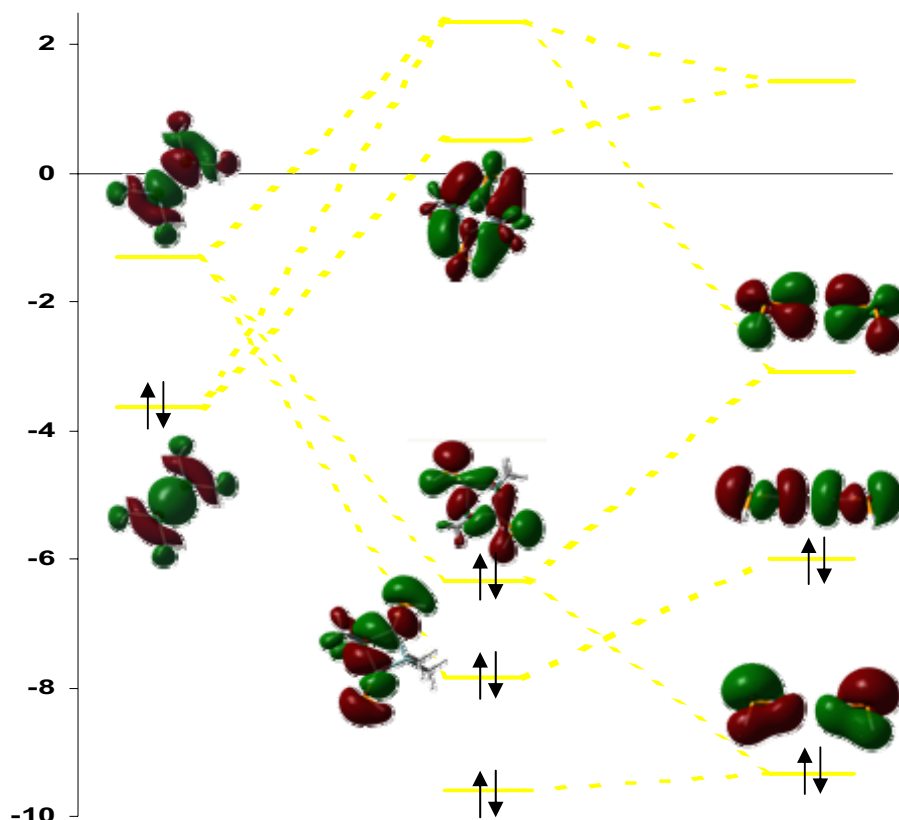


Figure III.9. Stabilizing interactions within the B_1 set of fragment-orbitals

The possibility of the conjugation between the two P=C bonds can also be estimated by assessing the aromaticity of the cycle. Schleyer proposes the use of nucleus independent magnetic shielding (NICS) as a criterion for the aromaticity of rings [25]. He proves that there is a correlation between the absolute magnetic shielding calculated at a point coinciding with the ring centre and their aromatic stabilization energies. The NICS is given by the negative value of the calculated absolute magnetic shielding. In order to eliminate the influence of sigma electron-bonding and to assess only the π orbitals, the NICS can be calculated at certain distances from the centre of the cycle (usually at 0.5 and 1 Å). According to this model, negative values of the NICS denote aromaticity, while positive values are indicative of an antiaromatic character. Most current quantum

chemistry software allows the calculation of magnetic shielding tensors. Using Gaussian 98, we estimated the NICS at the centre of the 4-atom ring of the geometry-optimized model molecule $[\text{Me}_2\text{Ge}-\text{C}(=\text{PH})]_2$ and at several distances above it. Table III.10 shows the calculated values at the B3LYP/6-31G(d) level of the theory. For comparison, the calculated NICS for benzene (using the same method and basis set) are given.

Table III.10. B3LYP/6-31G(d) calculated NICS values for model compound of **5** and benzene

Molecule	ring centre	at 0.5 Å	at 1 Å	at 1.5 Å	at 2 Å	at 2.5 Å
$\text{Me}_2\text{Ge}[\text{C}=\text{PH}]_2$	7.222	4.117	0.488	-0.392	-0.308	-0.147
benzene	-9.681	-11.437	-11.206	-7.839	-4.741	-2.860

The values of the NICS account for a non-aromatic character of the four-atom ring, rather than the conjugation of the P=C bonds suggested by the molecular orbital diagram.

The same considerations were applied for model compounds of **8**. The geometry of the model compound $[\text{Me}_2\text{Ge}-\text{C}(=\text{P}(\text{H})=\text{S})]_2$ was optimized using B3LYP/6-31G(d) and a single point calculation was run on Gaussian 98. The molecular orbital diagram resulted from the interaction of the 2 Me_2Ge and 2 $\text{H}-\text{P}(=\text{S})=\text{C}$ fragment-orbitals is shown in figure III.10; a more detailed account of these interactions is given in annex 3.

The aromaticity of the ring was assessed by the same NICS method, estimating the magnetic shielding at points in the centre of the rings, and at 0.5, 1, and 1.5 Å above it. The small negative values of the magnetic shielding (and positive values of the NICS) also point to the non-aromatic character of the cycle.

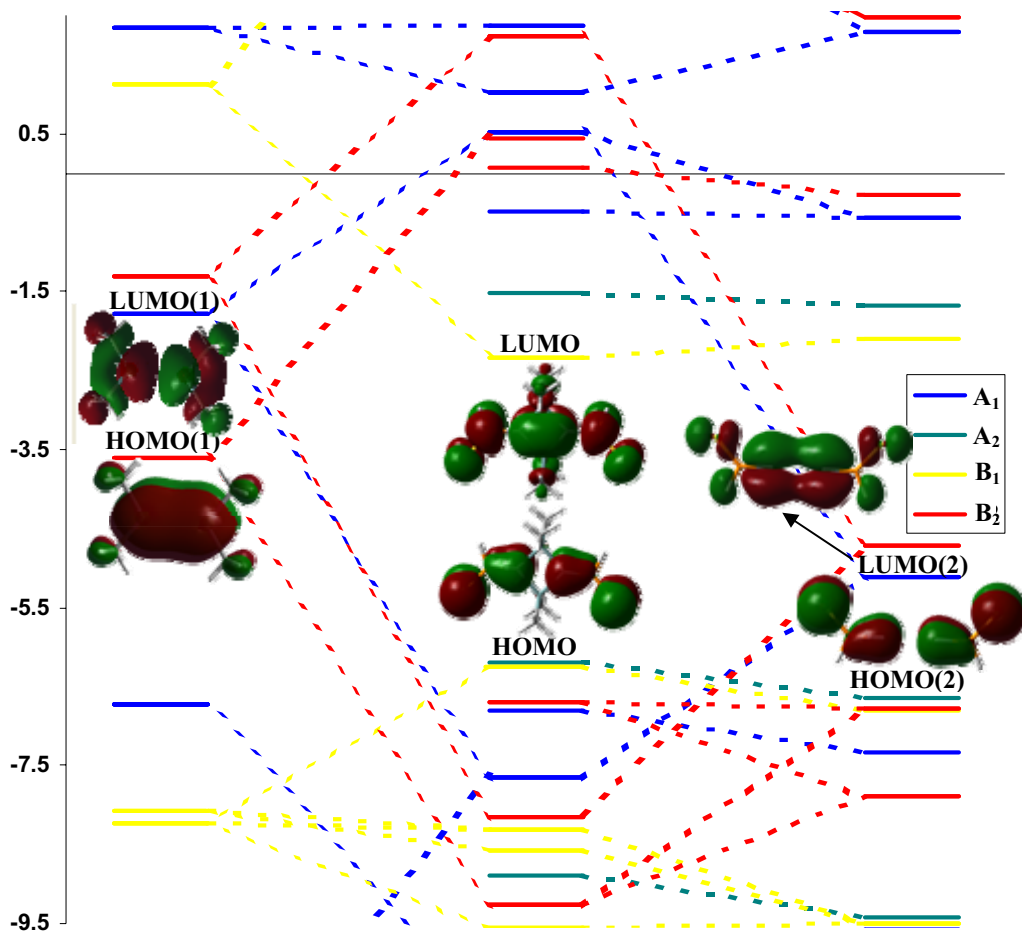


Figure III.10. Molecular orbital diagram for $[\text{Me}_2\text{Ge}(\text{C}(=\text{P}(\text{H})=\text{S}))_2]$

In conclusion, although there seems to be no effective conjugation between the two P=C bonds throughout the cycle, the high stability of compounds **5a,b** can be explained through stabilizing interactions throughout the 4-atom ring and the doubly-bonded phosphorus atom. Also, small energetic difference between the *cis* and *trans* isomers were found.

Experimental Part

General procedures

All experiments were carried out in flame-dried glassware under an argon atmosphere using high-vacuum-line techniques. Solvents were dried and freshly distilled from sodium benzophenone ketyl and carefully deoxygenated on a vacuum line by several “freeze-pump-thaw” cycles. NMR spectra were recorded in CDCl₃ on the following spectrometers: ¹H, Bruker Avance 300 (300.13 MHz) and Avance 400 (400.13 MHz); ¹³C{¹H}, Bruker Avance 300 (75.47 MHz) and Avance 400 (100.62 MHz) (reference TMS), ³¹P, Bruker AC200 at 81.02 MHz (reference H₃PO₄), ¹⁹F Avance 400 (188.3 MHz, reference CFCl₃). Melting points were determined on a Wild Leitz-Biomed apparatus. Mass spectra were obtained on a Hewlett-Packard 5989A spectrometer by EI at 70 eV.

1) Synthesis of Mes*P=C(Cl)Ge(F)tBu₂ 4

To 1.0 g of dichlorophosphaalkene **2** (2.7 mmol) in 30 mL of THF cooled at -90 °C were added dropwise 1.9 mL of nBuLi 1.6 M in hexane (1 eq). After half an hour at -85 °C, 0.62 g (2.7 mmol) of *t*Bu₂GeF₂ in 20 mL of THF were cannulated. The reaction mixture was then allowed to warm up to room temperature and the solvent was removed under vacuum and replaced by pentane. Lithium salts were removed by filtration. **4** precipitated from methanol as a white solid (1.47 g 78%, mp = 118 °C). Only the *E*-isomer was obtained.

NMR data for 4 (solvent CDCl₃, ppm):

δ¹H (300 MHz): 1.23 (d, ⁴J_{HF} = 1.2 Hz, *t*BuGe), 1.29 (s, *p*-tBu), 1.47 (s, *o*-tBu), 7.38 (d, ⁴J_{PH} = 1.4 Hz, arom H.);

δ¹³C (75.5 MHz): 28.10 (Me₃C of *t*BuGe), 31.33 (*p*-Me₃C of Mes*P), 32.94 (d, ⁴J_{CP} = 6.7 Hz, *o*-Me₃C of Mes*P), 33.00 (dd, ²J_{C-F} and ³J_{C-P} = 3.3 and 8.3 Hz, Me₃C of *t*Bu), 35.03, (s, *p*-Me₃C of Mes*P), 37.85 (*o*-Me₃C of Mes*P), 122.00 (*m*-C of Mes*), 134.19

(dd, ipso-C, $^1J_{CP} = 67.15$, $^4J_{CF} = 2.3$ Hz), 150.60 (p-C of Mes*), 153.54 (d, o-C of Mes*, $^2J_{CP} = 2.3$ Hz), 165.27 (dd, $^1J_{CP} = 91.0$ Hz, $^2J_{CF} = 4.5$ Hz, C=P);

$\delta^{19}\text{F}$ (188.3 MHz, CFCl_3): -135.4;

$\delta^{31}\text{P}$ (121.5 MHz): 293.5 (d, $^3J_{PF} = 45.8$ Hz).

MS (EI, m/z): 515 ($\text{M}^+ - \text{Me}$), 1), 473 ($\text{M} - t\text{Bu}$, 3), 417 ($\text{M} - 2t\text{Bu} + 1$, 10), 323 ($\text{Mes}^*\text{P}=\text{CCl}$, 8), 289 ($\text{Mes}^*\text{P}=\text{CH}$, 60), 57 ($t\text{Bu}$, 100)

Found: C 61.02; H, 9.04, $\text{C}_{27}\text{H}_{47}\text{ClFGeP}$ requires C 61.22; H, 8.94%

2) Synthesis of 2,4-diphosphenylidene-1,3-digermacyclobutane 5

To 1.0 g (1.89 mmol) of **4** in 20 mL of THF cooled at $-95\text{ }^\circ\text{C}$, 1.38 mL of $t\text{BuLi}$ 1.5M in hexane (10% excess) were added dropwise. The reaction mixture was left at low temperature for 15 minutes and then allowed to slowly warm up to room temperature. After removal of the lithium salts and of the solvents, 20 mL of pentane were added. A mixture of **5a/5b** precipitated (0.67 g, 75 %). The yellow mixture was dissolved in 20 mL of THF. Yellow acicular crystals of the *trans* isomer of **5** were obtained after a few days at $-20\text{ }^\circ\text{C}$ while the *cis* isomer crystallized from pentane through slow evaporation.

m.p. = $309\text{ }^\circ\text{C}$ (**5a**), m.p. = $301\text{ }^\circ\text{C}$ (**5b**).

NMR data for 5 (solvent CDCl_3 , ppm)

$\delta^1\text{H}$ (300 MHz): 0.56 (s, tBuGe), 1.23 and 1.32 (2s, p-tBu and tBuGe), 1.47 (s, o-tBu), 7.07 (s, H_{arom});

$\delta^{31}\text{P}$ (121.5 MHz): 367.4.

3b $\delta^1\text{H}$ (300 MHz): 0.94, 1.19 and 1.50 (3s, tBu), 7.13 (s, arom H)

$\delta^{31}\text{P}$ (121.5 MHz): 367.7.

$\delta^{13}\text{C}$ (75.5 MHz) mixture of **5a/5b**: 31.32, 31.39, 31.47, 31.62, 31.68 and 35.11 (Me₃C), 34.22, 34.51, 34.57, 34.74 and 39.04 (Me₃CC), 119.51, 121.47 and 121.64 (m-C of Mes*), 148.42, 149.96, 153.12 and 153.19 (arom C), 204.0 (dd, $^1J_{CP} = 96.6$ Hz, $^3J_{CP} = 25.7$ Hz, C=P) (**3a**), 204.3 (dd, $^1J_{CP} = 92.0$ Hz, $^3J_{CP} = 24.9$ Hz, C=P) (**5b**).

MS (EI, m/z): 893 ($M^+ - t\text{Bu}$, 8), 721 ($M - 4t\text{Bu} - 1$, 5), 705 ($M - \text{Mes}^* 2$), 665 ($M - 5t\text{Bu}$, 5), 649 ($M - 5t\text{Bu} - \text{MeH}$, 5), 605 ($M - \text{Mes}^*\text{P}=\text{C} - t\text{Bu}$, 20), 275 ($\text{Mes}^*\text{P} - 1$, 10), 57 ($t\text{Bu}$, 100).

Found: C 68.03 ; H, 10.04, $\text{C}_{54}\text{H}_{94}\text{Ge}_2\text{P}_2$ requires C 68.24 ; H, 9.97%.

Table III.12. Crystal data and structure refinement for **5a**

Empirical formula	$C_{54}H_{94}Ge_2P_2$	
Formula weight	950.41	
Temperature	173(2) K	
Wavelength	0.71073 Å	
Crystal system	Monoclinic	
Space group	C2/c	
Unit cell dimensions	$a = 33.039(3)$ Å	$\alpha = 90^\circ$.
	$b = 10.8738(11)$ Å	$\beta = 115.321(2)^\circ$.
	$c = 17.1736(17)$ Å	$\gamma = 90^\circ$.
Volume	$5577.0(10)$ Å ³	
Z	4	
Density (calculated)	1.132 Mg/m ³	
Absorption coefficient	1.166 mm ⁻¹	
F(000)	2048	
Crystal size	0.1 x 0.2 x 0.5 mm ³	
Theta range for data collection	2.22 to 26.43°.	
Index ranges	$-40 \leq h \leq 41$, $-12 \leq k \leq 13$, $-21 \leq l \leq 17$	
Reflections collected	16226	
Independent reflections	5722 [R(int) = 0.0595]	
Completeness to theta = 26.43°	99.6 %	
Absorption correction	Semi-empirical	
Max. and min. transmission	1.000000 and 0.749303	
Refinement method	Full-matrix least-squares on F ²	
Data / restraints / parameters	5722 / 90 / 354	
Goodness-of-fit on F ²	1.036	
Final R indices [I > 2sigma(I)]	R1 = 0.0343, wR2 = 0.0945	
R indices (all data)	R1 = 0.0435, wR2 = 0.0997	
Largest diff. peak and hole	1.584 and -0.336 e.Å ⁻³	

Table III.13. Crystal data and structure refinement for **5b**

Empirical formula	$C_{58}H_{104}Ge_2OP_2$ (THF in the unit cell)	
Formula weight	1024.54	
Temperature	173(2) K	
Wavelength	0.71073 Å	
Crystal system	Monoclinic	
Space group	C2/c	
Unit cell dimensions	$a = 35.416(2)$ Å	$\alpha = 90^\circ$.
	$b = 10.6099(7)$ Å	$\beta = 101.1090(10)^\circ$.
	$c = 16.2868(11)$ Å	$\gamma = 90^\circ$.
Volume	$6005.3(7)$ Å ³	
Z	8	
Density (calculated)	1.133 Mg/m ³	
Absorption coefficient	1.089 mm ⁻¹	
F(000)	2216	
Crystal size	0.05 x 0.3 x 0.3 mm ³	
Theta range for data collection	5.10 to 24.71°.	
Index ranges	$-41 \leq h \leq 41$, $-12 \leq k \leq 11$, $-19 \leq l \leq 13$	
Reflections collected	14909	
Independent reflections	5077 [R(int) = 0.0577]	
Completeness to theta = 24.71°	99.0 %	
Absorption correction	Semi-empirical	
Max. and min. transmission	1.000000 and 0.730951	
Refinement method	Full-matrix least-squares on F ²	
Data / restraints / parameters	5077 / 88 / 345	
Goodness-of-fit on F ²	0.997	
Final R indices [I > 2sigma(I)]	R1 = 0.0386, wR2 = 0.0748	
R indices (all data)	R1 = 0.0726, wR2 = 0.0847	
Largest diff. peak and hole	0.386 and -0.290 e.Å ⁻³	

3) Synthesis of 2,4-bis(thioxophosphoranylidene)-1,3-digermacyclobutane **8**

To 0.60 g (0.63 mmol) of a mixture of *cis/trans* **5** in 10 mL of THF, were added 3 equivalents of sulfur; the reaction mixture was refluxed for three hours. The NMR study showed the quantitative formation of **8**. After removal of THF, 20 mL of pentane were added and the reaction mixture filtered to eliminate the excess of sulfur; a mixture of **8a/8b** was isolated (0.52 g, 81 %). Crystals of the *trans* isomer were obtained from the THF solution at -20 °C, while the *cis* isomer crystallized from pentane.

NMR data for 8 (solvent CDCl₃, ppm)

$\delta^1\text{H}$ (300 MHz): 0.61, 1.13, 1.25, 1.26, 1.53 and 1.67 (6s, 90H, Me₃C), 7.24 – 7.46 (m, 4H, arom H).

$\delta^{13}\text{C}$ (75.5 MHz): 31.03, 31.55, 31.65, 32.47, 33.31, 33.93 and 34.17 (Me₃C), 32.72, 34.81, 34.95, 35.02 and 35.93 (Me₃C), 119.49, 120.998 and 122.60 (m-C of Mes*), 149.92, 150.82, 152.83, 153.25 and 156.75 (arom C), 159.3 – 164.2 (m, C=P).

$\delta^{31}\text{P}$ (121.5 MHz): 184.4 (**8a**), 183.7 (**8b**)

MS (EI, m/z): 957 (M⁺ – *t*Bu, 10), 941 (M – *t*Bu – MeH, 5), 737 (M – Mes* - S), 509 (M/2 + 1, 10), 275 (Mes*P – 1, 20), 57 (*t*Bu, 100).

Found: C 64.05 ; H, 9.14, C₅₄H₉₄Ge₂P₂S₂ requires C 63.93 ; H, 9.34%.

Table III.14. Crystal data and structure refinement for **8a**

Empirical formula	$C_{54}H_{94}Ge_2P_2S_2$	
Formula weight	1014.53	
Temperature	173(2) K	
Wavelength	0.71073 Å	
Crystal system	Monoclinic	
Space group	C2/c	
Unit cell dimensions	$a = 33.160(3)$ Å	$\alpha = 90^\circ$.
	$b = 11.3364(10)$ Å	$\beta = 118.224(2)^\circ$.
	$c = 17.1891(15)$ Å	$\gamma = 90^\circ$.
Volume	$5693.4(9)$ Å ³	
Z	4	
Density (calculated)	1.184 Mg/m ³	
Absorption coefficient	1.217 mm ⁻¹	
F(000)	2176	
Crystal size	0.1 x 0.2 x 0.2 mm ³	
Theta range for data collection	2.15 to 26.40°.	
Index ranges	$-39 \leq h \leq 38$, $-14 \leq k \leq 7$, $-17 \leq l \leq 21$	
Reflections collected	13514	
Independent reflections	5717 [R(int) = 0.0227]	
Completeness to theta = 26.40°	97.8 %	
Absorption correction	Semi-empirical	
Max. and min. transmission	1.000000 and 0.731643	
Refinement method	Full-matrix least-squares on F ²	
Data / restraints / parameters	5717 / 0 / 287	
Goodness-of-fit on F ²	1.035	
Final R indices [I > 2σ(I)]	R1 = 0.0290, wR2 = 0.0715	
R indices (all data)	R1 = 0.0394, wR2 = 0.0768	
Largest diff. peak and hole	0.636 and -0.269 e.Å ⁻³	

Table III.15. Crystal data and structure refinement for **8b**.

Empirical formula	$C_{62}H_{110}Ge_2O_2P_2S_2$ (2 THF in the unit cell)	
Formula weight	1158.74	
Temperature	173(2) K	
Wavelength	0.71073 Å	
Crystal system	Orthorhombic	
Space group	Ibam	
Unit cell dimensions	$a = 20.440(3)$ Å	$\alpha = 90^\circ$.
	$b = 16.670(2)$ Å	$\beta = 90^\circ$.
	$c = 19.133(3)$ Å	$\gamma = 90^\circ$.
Volume	$6519.2(15)$ Å ³	
Z	8	
Density (calculated)	1.181 Mg/m ³	
Absorption coefficient	1.073 mm ⁻¹	
F(000)	2496	
Crystal size	0.1 x 0.1 x 0.5 mm ³	
Theta range for data collection	5.11 to 23.53°.	
Index ranges	$-22 \leq h \leq 22$, $-18 \leq k \leq 18$, $-14 \leq l \leq 21$	
Reflections collected	14548	
Independent reflections	2491 [R(int) = 0.1131]	
Completeness to theta = 23.53°	98.8 %	
Absorption correction	Semi-empirical	
Max. and min. transmission	1.000000 and 0.617438	
Refinement method	Full-matrix least-squares on F ²	
Data / restraints / parameters	2491 / 260 / 273	
Goodness-of-fit on F ²	1.049	
Final R indices [I > 2σ(I)]	R1 = 0.0504, wR2 = 0.1037	
R indices (all data)	R1 = 0.0940, wR2 = 0.1217	
Largest diff. peak and hole	0.492 and -0.710 e.Å ⁻³	

All data for all structures represented in this paper were collected at low temperatures using an oil-coated shock-cooled crystal on a Bruker-AXS CCD 1000 diffractometer with MoK α radiation ($\lambda = 0.71073$ Å). The structures were solved by direct methods [26] and all non hydrogen atoms were refined anisotropically using the least-squares method on F^2 [27].

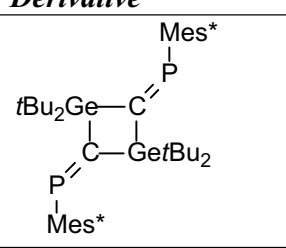
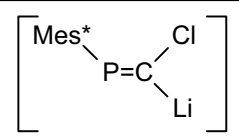
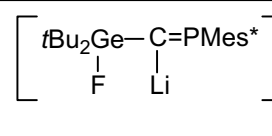
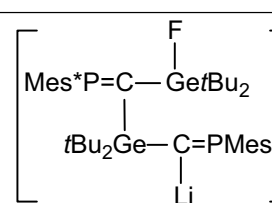
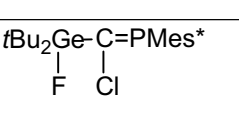
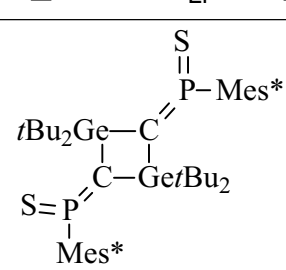
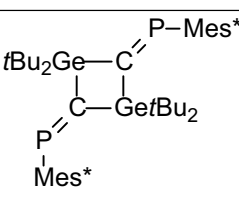
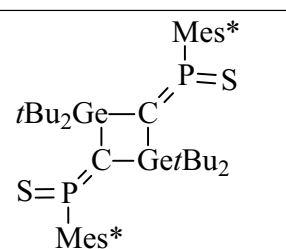
References

1. Escudié, J.; Ranaivonjatovo, H.; *Organometallics*, **2007**, *26*, 1542.
2. Cretiu Nemes, G.; Ranaivonjatovo, H.; Escudié, J.; Silaghi-Dumitrescu, I.; Silaghi-Dumitrescu, L.; Gornitzka, H. ; *Eur. J. Inorg. Chem.*, **2005**, 1109.
3. Huheey, Keiter and Keiter, *Chimie Inorganique*, De Boeck Université, Bruxelles, **1996**, Appendix E.
4. a) Goede, S.; Bickelhaupt, F.; *Chem. Ber.*, **1991**, *124*, 2677; b) Yoshifuji, M.; Shima, I.; Inamoto, N.; *J. Am. Chem. Soc.*, **1981**, *103*, 4587.
5. Ranaivonjatovo, H.; Escudié, J.; Couret, C.; Satgé, J.; Draeger, M.; *New Journal of Chemistry*, **1989**, *13*, 389
6. Petrar, P. M.; Nemes, G.; Silaghi-Dumitrescu, I.; Ranaivonjatovo, H.; Gornitzka, H.; Escudié, J.; *Chem. Commun.*, **2007**, *40*, 4149.
7. Rigon, L.; Ranaivonjatovo, H.; Escudié, J.; Dubourg, A.; Declercq, J. P.; *Chem. Eur. J.*, **1999**, *5*, 774.
8. Ramdane, H.; Ranaivonjatovo, H.; Escudié, J.; Mathieu, S.; Knouzzi, N.; *Organometallics*, **1996**, *15*, 3070.
9. a) Gusev, A. I.; Gar, T. K.; Los, M. G.; Alexeev, N. V.; *Zh. Strukt. Khim.*, **1976**, *17*, 736; b) Toltl, N. P.; Stradiotto, M.; Morkin, T. L.; Leigh, W. J.; *Organometallics*, **1999**, *18*, 5643; c) Wiberg, N.; Passler, T.; Wagner, S.; Polborn, K.; *J. Organomet. Chem.*, **2000**, *598*, 292.
10. El Harouch, Y.; Gornitzka, H.; Ranaivonjatovo, H.; Escudié, J.; *J. Organomet. Chem.*, **2002**, *643-644*, 202.
11. a) Weber, L.; *Angew. Chem, Int. Ed. Engl.*, **2002**, *41*, 563; b) Daugulis, O.; Brookhart, M.; White, P.S.; *Organometallics*, **2002**, *21*, 5935; c) Ozawa, F.; Okamoto, H.; Kawagishi, S.; Yamamoto, S.; Minami, T.; Yoshifuji, M.; *J. Am. Chem. Soc.*, **2002**, *124*, 10968; d) Ikeda, S.; Ohhata, F.; Kawagishi, S.; Yamamoto, S.; Minami, T.; Ozawa, F.; Yoshifuji, M.; *Angew. Chem, Int. Ed. Engl.*, **2000**, *39*, 4512.
12. Appel, R.; Casser, C.; *Tetrahedron Lett.*, **1984**, *25*, 4109.
13. Niecke, E.; Wildbrecht, D.-A.; *J. Chem. Soc. Chem. Comm.*, **1981**, 72.

14. Van Der Knaap, Th. A.; Klebach, Th. C.; Lourens, R. ; Vos, M. ; Bickelhaupt, F.; *J. Am. Chem. Soc.*, **1983**, *105*, 4026.
15. Van Der Knaap, Th. A.; Bickelhaupt, F. ; *Tetrahedron*, **1983**, *39*, 3189.
16. Caira, M. ; Neilson, R. H. ; Watson, W.H. ; Wisian-Neilson, P. ; Xie, Z.M.; *J. Chem. Soc. Chem. Comm.*, **1984**, 698.
17. Toyota, K. ; Shimura, K. ; Takahashi, H. ; Yoshifuji, M. ; *Chem. Lett.*, **1994**, 1927.
18. Toyota, K.; Takahashi, H.; Shimura, K.; Yoshifuji, M.; *Bull. Chem. Soc. Jpn.*, **1996**, *69*, 141.
19. Yoshifuji, M.; Takahashi, H.; Shimura, K.; Toyota, K.; Hirotsu, K.; Okada, K.; *Heteroatom. Chem.*, **1997**, *8*, 375.
20. Nakamura, A.; Kawasaki, S.; Toyota, K.; Yoshifuji, M.; *J. Organomet. Chem.*, **2007**, *692*, 70.
21. Wavefunction Inc.18401 Von Karman Avenue, Suite 370 Irvine, CA 92612.
22. a) Becke, A.D.; *J. Chem. Phys.*, **1993**, *98*, 5648; b) Lee, C.; Yang, W.; Parr, R.G.; *Phys. Rev. B*, **1988**, *37*, 785; c) Vosko, S. H.; Wilk, L.; Nusair, M.; *Can. J. Phys.*, **1980**, *58*, 1200; d) Stephens, P. J.; Devlin, F. J.; Chabalowski, C. F. ; Frisch, M. J.; *J. Phys. Chem.*, **1994**, *98*, 11623.
23. a) Gorelsky, S.I.; *AOMix: Program for Molecular Orbital Analysis*; York University: Toronto, **1997**, <http://www.sg-chem.net/>; b) Gorelsky, S.I.; Lever, A.B.P.; *J. Organomet. Chem.*, **2001**, *635*, 187.
24. *Gaussian 98, Revision A.11.3*, Frisch, M. J.; Trucks, G. W.; Schlegel, H. B.; Scuseria, G. E.; Robb, M. A.; Cheeseman, J. R.; Zakrzewski, V. G.; Montgomery Jr., J. A.; Stratmann, R. E.; Burant, J. C.; Dapprich, S.; Millam, J. M.; Daniels, A. D.; Kudin, K. N.; Strain, M. C.; Farkas, O.; Tomasi, J.; Barone, V.; Cossi, M.; Cammi, R.; Mennucci, B.; Pomelli, C.; Adamo, C.; Clifford, S.; Ochterski, J.; Petersson, G. A.; Ayala, P. Y ; Cui, Q.; Morokuma, K.; Malick, D. K.; Rabuck, A. D.; Raghavachari, K.; Foresman, J. B.; Cioslowski, J.; Ortiz, J. V.; Baboul, A. G.; Stefanov, B. B.; Liu, G.; Liashenko, A; Piskorz, P.; Komaromi, I.; Gomperts, R.; Martin, R. L.; Fox, D. J.; Keith, T.; Al-Laham, M. A.; Peng, C. Y.; Nanayakkara., A.; Gonzalez, C.; Challacombe, M.; Gill, P. M. W.; Johnson, B.; Chen, W.; Wong, M. W.; Andres, J. L.; Gonzalez, C.; Head-Gordon, M.; Replogle, E. S.; Pople, J. A.; Gaussian, Inc., Pittsburgh PA, **2002**.

25. Schleyer, P.R.; Maerker, C.; Dransfeld, A.; Jiao, H.; Hommes, N.J.; *J. Am. Chem. Soc.*, **1996**, *118*, 6317.
26. SHELXS-97, G. M. Sheldrick; *Acta Crystallogr.*, **1990**, *A46*, 467.
27. SHELXL-97, Program for Crystal Structure Refinement, G. M. Sheldrick, University of Göttingen, **1997**.

Chapter III- Recapitulative list of synthesized compounds

<i>Derivative</i>	<i>Number</i>	<i>Derivative</i>	<i>Number</i>
Mes*P=CCl ₂	1		<u>5b</u>
	2		<u>6</u>
<i>t</i> Bu ₂ GeF ₂	3		<u>7</u>
	<u>4</u>		<u>8a</u>
	<u>5a</u>		<u>8b</u>

N – novel compounds

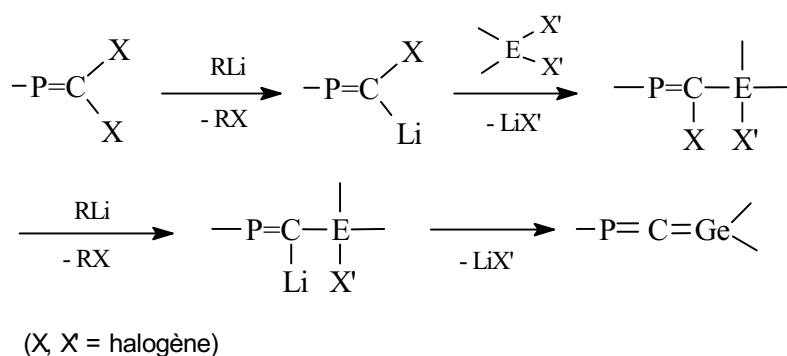
CHAPTER IV

*PHOSPHAGERMA-, PHOSPHASILA- AND
PHOSPHASTANNAPROPENES*

Chapitre IV

Phosphagerma-, phosphasila- et phosphastannapropènes

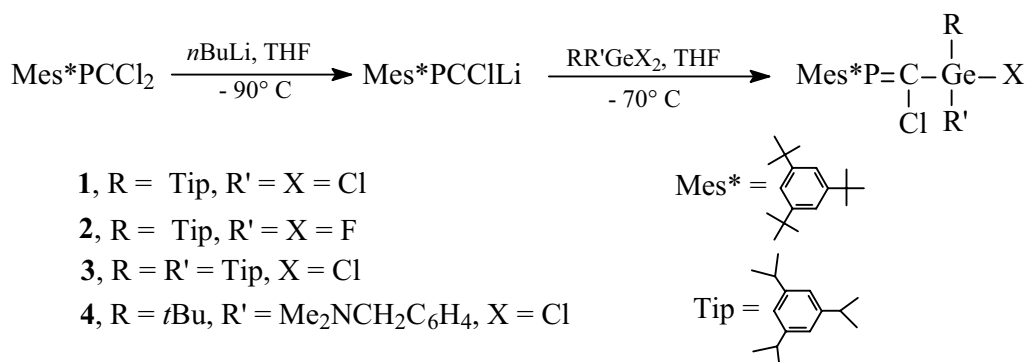
Le quatrième chapitre de la thèse présente la synthèse de précurseurs d'hétéroallènes, leur caractérisation en solution et les tentatives pour obtenir les hétéroallènes par action d'un organolithien. La voie générale de synthèse aboutissant à des composés non saturés contenant l'unité $E_{14}=C=P-$ ($E_{14} = Si, Ge, Sn$) implique la préparation de phosphaalcènes substitués par le métal 14, selon le schéma IV.1. L'action de *t*BuLi sur ces dérivés devrait ensuite conduire aux allènes correspondants par élimination d'halogénure de lithium.



Schema IV.1

1) Synthèse et caractérisation d'halogégermylchlorophosphapropènes - $P=C(X)-Ge<$

Plusieurs dihalogénophosphagermapropènes ont été obtenus à partir de $Mes^*P=CCl_2$, du n-butyllithium et des dérivés halogénés du germanium (voir schéma IV.2). Des groupes organiques encombrants sur les atomes de germanium et de phosphore ont été utilisés afin de permettre une meilleure protection stérique de la double liaison $Ge=C$, liaison supposée être la plus réactive dans le phosphagermaallène $-P=C=Ge<$. Nous avons également envisagé l'utilisation d'un groupement portant un bras CH_2NMe_2 ; une complexation du germanium par la paire libre de l'azote pourrait permettre de stabiliser la double liaison $Ge=C$; de telles coordinations ont été utilisées avec succès dans le cas d'autres espèces à basse coordinence du germanium.

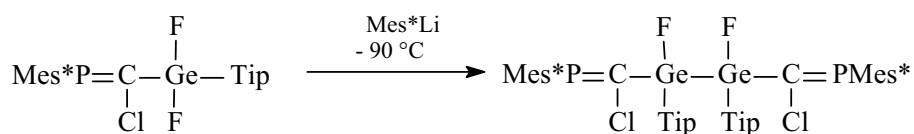


Scheme IV.2

Les dérivés **1-4** ont été caractérisés en solution par RMN ¹H, ³¹P et ¹³C et la structure à l'état solide du composé **4** a été déterminée par diffraction des rayons X. Cette étude montre comme attendu une coordination, cependant faible, entre les atomes de germanium et d'azote.

2) Action de dérivés lithiés sur les dihalogénophosphagermapropènes

L'action d'organolithiens tels que *n*-BuLi et *t*-BuLi sur les composés décrits précédemment n'a pas conduit aux allènes stables désirés; dans chaque cas, plusieurs produits de réaction ont été obtenus et leur séparation et purification n'ont pas été possibles. L'action sur **2** d'un lithien extrêmement encombré, tel que Mes*Li, conduit de façon surprenante, par un mécanisme de transfert monoélectronique, à la formation d'un nouveau digermane portant deux entités phosphaalcènes, (schéma IV.3).



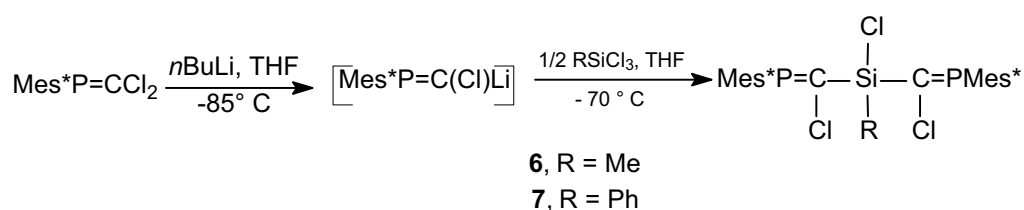
Schema IV.3

L'utilisation de ce digermane en tant que précurseur potentiel de cumulènes du germanium est en cours.

3) Synthèse et caractérisation de dihalogénophosphasilapropènes -P=C(X)Si<

Seul un phosphasilaallène transitoire -P=C=Si< a été synthétisé jusqu'ici. Les substituants utilisés pour stabiliser leurs analogues germaniés n'ont pas permis d'obtenir

des phosphasilaallènes stables. Au cours de ce travail, nous avons envisagé la préparation d'un phosphasilaallène d'un nouveau type qui pourrait être stabilisé à la fois par des effets stériques et électroniques notamment par une possible conjugaison entre l'unité allénique et la double liaison C=P, ce qui conduirait à un dérivé de type $-P=C=Si(R)-R'C(X)=P-$. Les précurseurs potentiels de ces phosphasilaallènes ont été synthétisés selon le schéma IV.4: Les analyse physicochimiques ont montré que ces réactions étaient stéréosélectives, avec formation de l'isomère *Z,Z*.



Schema IV.4

L'action de *t*BuLi sur ces dérivés conduit à plusieurs produits de réaction comportant des doubles liaisons P=C. Leur séparation par cristallisation fractionnée est en cours afin de déterminer leur structure.

4) Synthèse et caractérisation de précurseurs de phosphastannaallènes

Les phosphastannaallènes $-P=C=Sn<$ n'ont encore jamais pu être isolés ni même caractérisés par voie chimique ou physicochimique. Plusieurs de leurs précurseurs ont été préparés au cours de ce travail et caractérisés par des méthodes spectroscopiques. Une voie alternative pour la préparation de composés contenant l'unité $-P=C=Sn<$ a été envisagée : elle implique la synthèse de dérivés à double liaison Sn=C comme première étape de la réaction. La synthèse de $\text{Tip}_2\text{Sn}(\text{Br})\text{CBr}_3$, précurseur potentiel d'un tel dérivé, a été effectuée et ce dernier a été entièrement caractérisé.

En conclusion, le choix des substituants sur l'atome lourd semble être le facteur déterminant dans la synthèse des dérivés hétéroalléniques. Même si les hétéroallènes n'ont pas été obtenus, de nombreux nouveaux dérivés ont été préparés et caractérisés.

Dans le futur, nos efforts porteront sur les essais de synthèse des hétéroallènes à partir de ces précurseurs en utilisant d'autres agents de déshalogénéation tels que magnésiens, cuivriques ou zinciques.

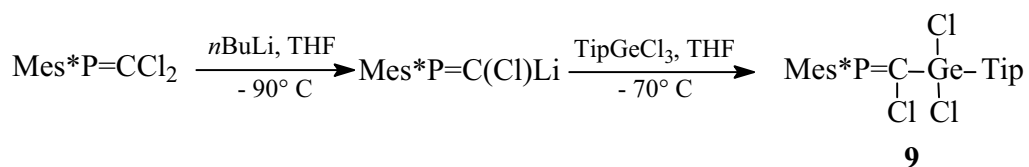
In the precedent chapter, we reported that the attachment of two *t*Bu groups on the germanium atom did not lead to the related phosphagermaallene $\text{Mes}^*\text{P}=\text{C}=\text{Ge}(\textit{t}\text{Bu})_2$. We have therefore turned our attention to different organic bulky groups in order to achieve the stabilization of the $\text{P}=\text{C}=\text{Ge}$ unit.

The synthesis of several phosphagermapropenes was described in this chapter and we also report the synthesis of phosphasila- and phosphastannapropenes, potential precursors of the corresponding phosphametallaallenes.

Phosphagermapropenes

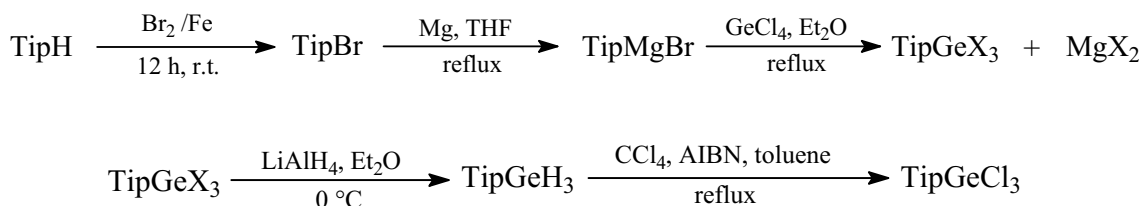
1) Synthesis and characterization of phosphagermapropenes $\text{Mes}^\text{P}=\text{C}(\text{Cl})\text{Ge}(\text{Tip})\text{X}_2$*

The 2,4,6-triisopropylphenyl group (Tip) has been successfully used for the stabilization of silaallenes $>\text{Si}=\text{C}=\text{C}<$ [1, 2] and germaallenes $>\text{Ge}=\text{C}=\text{C}<$ [3]. It has also been previously employed in the steric protection of the $\text{Ge}=\text{C}$ bond of the phosphagermaallene $\text{Mes}^*\text{P}=\text{C}=\text{Ge}(\textit{t}\text{Bu})\text{Tip}$ which has been recently synthesized [4] and proved to be very stable at room temperature under inert atmosphere. We thought that the replacement of the *t*Bu group on the germanium atom by a halogen could allow the functionalization of the phosphagermaallene. The large volume of the Tip group could in theory afford a sufficient protection; we therefore attempted the synthesis of 2-chloro-3,3,3-[dichloro(1,3,5-triisopropylphenyl)germyl]-1,3-phosphagermapropene $\text{Mes}^*\text{P}=\text{C}(\text{Cl})\text{Ge}(\text{Tip})\text{Cl}_2$, starting from $\text{Mes}^*\text{P}=\text{C}\text{Cl}_2$, at low temperature as shown in scheme IV.1.



Scheme IV.1

TipGeCl₃ was obtained in a multiple-step synthesis from 1,3,5-triwasopropylbenzene (scheme IV.2) [5].



Scheme IV.2

The use of Grignard reagents in the case of germanium derivative was more appropriate than the alternative organolithium TipLi, because of the complex reactivity of GeCl₄ towards lithium derivatives. Reduction of the Ge-Cl bond as well as formation of germanium-containing oligomers are generally observed. Although the substitution of only one chlorine atom can be easily induced by controlling the stoichiometry of the reaction, halogen exchanges invariably occur, so the reducing step leading to TipGeH₃ followed by chlorination with CCl₄ in the presence of AIBN becomes necessary to obtain TipGeCl₃ in pure form.

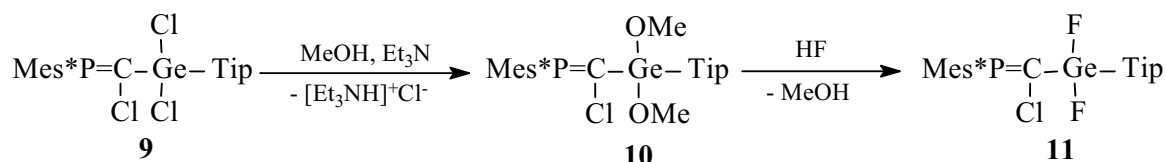
The reaction of TipGeCl₃ with Mes*P=C(Cl)Li occurs with the formation of the sole *E*-isomer with respect to the P=C bond, for the reasons discussed above, as the NMR analysis of the synthesized compound shows only one signal at 303.7 ppm. It can be seen that the presence of the electropositive germanium atom causes a more than 50 ppm shift of the ³¹P signal, relatively to the starting Mes*P=CCl₂ [6].

Reaction with *t*BuLi did not result in the formation of the expected heteroallene Mes*P=C=Ge(Cl)Tip although the bulky Tip substituent was theoretically large enough to afford the steric protection needed for its stabilization. Instead, several compounds were obtained in low yields, resonating in the range of 297 ppm to 430 ppm in ³¹P NMR

spectroscopy. Thus the presence of the chlorine atoms does not allow a good control of the reactivity towards lithium derivatives; so the synthesis of the fluorinated analogue $\text{Mes}^*\text{P}=\text{C}(\text{Cl})\text{Ge}(\text{Tip})\text{F}_2$ was also carried out.

As said previously, better results are generally obtained with a fluorine atom instead of chlorine since the stronger Ge-F bond (about 115 kcal/mol in GeF_4 versus 80 for GeCl in GeCl_4) [7] prevents side reactions such alkylation or reduction.

Direct fluorination of $\text{Mes}^*\text{P}=\text{C}(\text{Cl})\text{Ge}(\text{Tip})\text{Cl}_2$ with HF does not lead to the expected product; so a germanium methoxylation step followed by a treatment with aqueous HF was needed (scheme IV.3). $\text{Mes}^*\text{P}=\text{C}(\text{Cl})\text{Ge}(\text{Tip})\text{F}_2$ **11** can also be obtained by another route starting from TipGeX_3 ($\text{X}_3 = \text{Cl}_3, \text{Cl}_2\text{Br}, \text{ClBr}_2, \text{Br}_3$). Successive reaction of this mixture of halogermanes with MeOH and Et_3N led to $\text{TipGe}(\text{OMe})_3$ and with $\text{Mes}^*\text{P}=\text{C}(\text{Cl})\text{Li}$ to $\text{Mes}^*\text{P}=\text{C}(\text{Cl})\text{Ge}(\text{Tip})(\text{OMe})_2$ **10** in an excellent yield. This route to finally get the dimethoxy compound was faster, since it does not need the reduction and rechlorination steps. After drying and elimination of all the residual hydrofluoric acid, **11** must be kept in an inert atmosphere to avoid the formation of $\text{Mes}^*\text{P}=\text{C}(\text{Cl})\text{Ge}(\text{OH})\text{F}$ by hydrolysis of one GeF bond. The NMR analysis shows the presence of only one isomer, probably the *E* isomer.



Scheme IV.3

Relevant NMR data of phosphagermapropenes **9** – **11** are given in table IV.1.

Table IV.1. NMR data for phosphagermapropenes **9** - **11**

Compound	^{19}F NMR	^{31}P NMR	^{13}C NMR
9	-	303.7 ppm	166.6 ppm, (d, $^1J_{\text{CP}} = 92$ Hz, P=C)
10	-	301.0 ppm	166.7 ppm (d, $^1J_{\text{CP}} = 85.9$ Hz, P=C)
11	-74.3 ppm (d)	311.7 ppm (t, $^3J_{\text{PF}} = 24.6$ Hz)	161.1 ppm (t, $^1J_{\text{CP}} = 75.3$ Hz, P=C) $^2J_{\text{CF}} = 11.1$ Hz

In an attempt to synthesize $\text{Mes}^*\text{P}=\text{C}=\text{Ge}(\text{Tip})\text{F}$, compound **11** was allowed to react with *tert*-butyllithium at low temperature. The target phosphagermaallene was not obtained; instead, several reaction products resulted.

As a fractional crystallization was unsuccessful, only ^{31}P and ^{19}F NMR could allow the identification of some products:

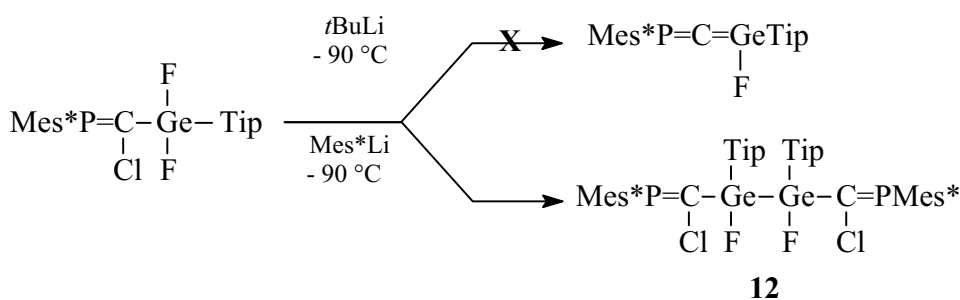
- $\text{Mes}^*\text{P}=\text{C}(\text{Cl})\text{Ge}(t\text{Bu})(\text{Tip})\text{F}$ which displays a doublet at 297.7 ppm in ^{31}P NMR with a PF coupling constant of 30.8 Hz. This derivative has previously been obtained by another route involving the addition of $(\text{Tip})(t\text{Bu})\text{GeF}_2$ to $\text{Mes}^*\text{P}=\text{C}(\text{Cl})\text{Li}$ [1].

- $\text{Mes}^*\text{P}=\text{C}(\text{H})\text{Ge}(t\text{Bu})(\text{Tip})\text{F}$ with a doublet at 338 ppm ($^3J_{\text{PF}} = 34.5$ Hz) which gives a doublet of doublet in the spectrum without proton decoupling. This product could arise from the hydrolysis of the lithium compound $\text{Mes}^*\text{P}=\text{C}(\text{Li})\text{Ge}(t\text{Bu})\text{TipF}$ or from the reduction of the CCl bond by *t*BuLi.

- the starting compound **11**.

A change in the reaction conditions (temperature, solvent, concentration) did not lead to a cleaner reaction.

In order to better control the reaction outcome, the more sterically crowded Mes^*Li was used to induce intramolecular elimination of LiF and avoid the direct alkylation of Ge. In this case, a Ge-Ge coupling was observed, with derivative **12** as the final minor product with some other unidentified derivatives (scheme IV.4).



Scheme IV.4

Compound **12** was obtained in the form of two diastereoisomers in the ratio 50/50 and one of them could be purified by fractional crystallization. However it was obtained

only in a low yield (about 10%). Its structure was determined by ^1H , ^{13}C , ^{19}F and ^{31}P NMR and mass spectrometry.

A triplet was observed in both ^{19}F and ^{31}P NMR spectra at -65.4 ppm and 300.4 ppm respectively (other diastereoisomer: 301.2 ppm) due to the equal magnitude of $^3J_{\text{PF}}$ and $^4J_{\text{PF}}$ (17.4 Hz). In ^{13}C NMR, a triplet was also observed for the *ipso*-C of the Tip group at 127.23 ppm ($^2J_{\text{CF}} = ^3J_{\text{CF}} = 4.1$ Hz), but for the sp^2 carbon atom bonded to P and Ge, the $^2J_{\text{CF}}$ (6.1 Hz) and $^3J_{\text{CF}}$ (5.1 Hz) were slightly different. The similarity of 3J and 4J or of 2J and 3J coupling constants was not surprising: such phenomenon generally occurs in symmetrical derivatives.

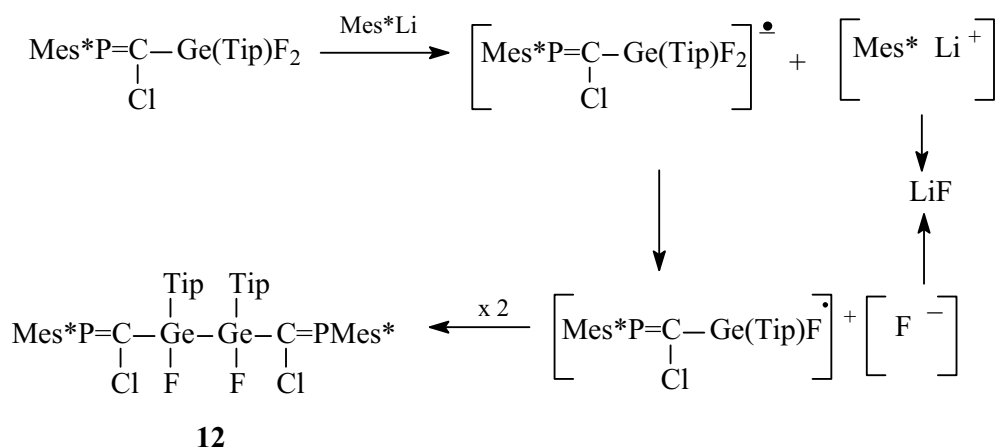
For example, this has previously been observed in derivative **13** in which $^3J_{\text{PH}}$ and $^4J_{\text{PH}}$ (H on *t*Bu) are identical [8]. By contrast in **14**, such coupling constants are different (scheme IV.5).



Scheme IV.5

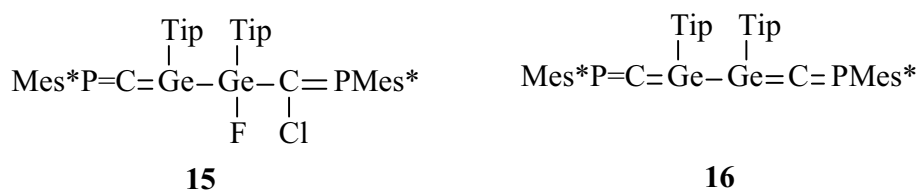
Compound **12** probably does not arise from a reaction between $\text{Mes}^*\text{P}=\text{C}(\text{Cl})\text{Ge}(\text{Tip})\text{F}_2$ and $\text{Mes}^*\text{P}=\text{C}(\text{Cl})\text{Ge}(\text{Tip})(\text{Li})\text{F}$ since it should involve F/Li exchange on the Ge atom which was unknown.

Thus, it seems that the more probable mechanism involves a coupling between two radicals $\text{Mes}^*\text{P}=\text{C}(\text{Cl})\text{Ge}^\bullet(\text{Tip})\text{F}$: we can postulate a single-electron transfer mechanism, which occurs frequently when there is a high steric congestion:



Scheme IV.6

The digermane **12** could be a very interesting precursor of phosphagermaallene **15** or bis(phosphagermaallene) **16** (scheme IV.7).



Scheme IV.7

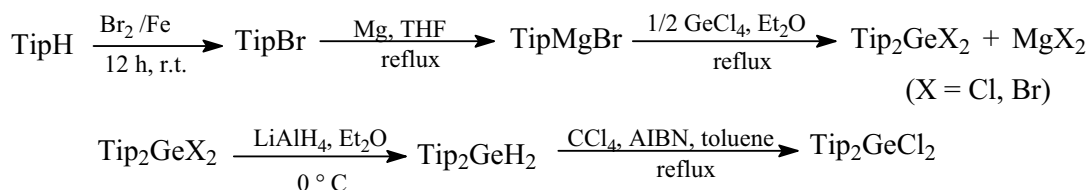
However, it was obtained in a too poor yield in this reaction. Thus, some efforts should be made to prepare **12** by another way, for example involving the first formation of the digermane skeleton X-Ge(Tip)F-Ge(Tip)F-X.

2) Synthesis and characterization of the phosphagermapropene Mes*P=C(Cl)-Ge(Tip)₂X (X = Cl, F)

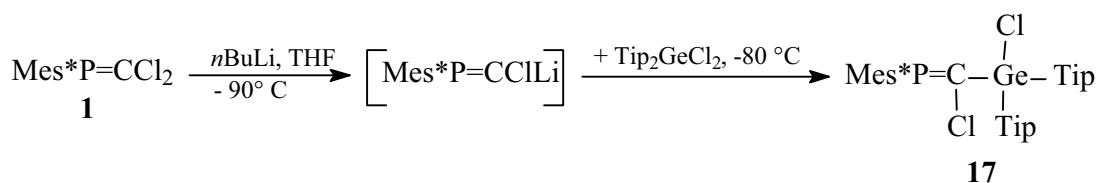
The formation of many unidentified products along with digermane **12** in the reaction of Mes*P=C(Cl)Ge(Tip)X₂ (X = F, Cl) with organolithium derivatives showed that the presence of 2 halogen atoms on the germanium atom is a problem: it allows an

easy alkylation, there are more possibility of reactions and the steric protection around the germanium was not sufficient. This reaction led us to the conclusion that the more sterically protected Mes*P=C(Cl)-Ge(Tip)₂Cl should be a more appropriate precursor of phosphagermaallene.

Note than the phosphagermaallene Mes*P=C=Ge(Tip)*t*Bu has already been synthesized. However, the presence of two different groups on the Ge atom which is prochiral complicates the analysis of the reaction by the formation, in many cases, of diastereoisomers. Thus, such a problem would be avoided by the use of the same groups. This derivative should theoretically be obtained starting from the dichlorogermane Tip₂GeCl₂ [9] synthesised through a series of reactions similar to those discussed above for the monochlorinated analogue (scheme IV.8), followed by the reaction described in scheme IV.9:



Scheme IV.8



Scheme IV.9

Unfortunately **17** is formed in a very poor yield (5%) and the changes in the reaction conditions (temperature, solvent, concentrations) did not allow the increase of the yield. This was probably due to the very important steric hindrance which prevents the approach of the two reactants. Thus the further reaction with *t*BuLi in order to obtained the phosphagermaallene Mes*P=C=GeTip₂ was not attempted. However, the structure of **17** could be determined by a NMR analysis.

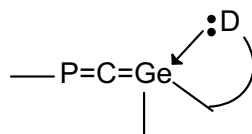
The formation of the sole **17** *E* isomer was observed in the ^{31}P NMR spectrum, with a chemical shift of 304.7 ppm, very close to that of the related $\text{Mes}^*\text{P}=\text{C}(\text{Cl})\text{GeCl}_2\text{Tip}$ (303.7 ppm). It can be seen that the replacement of the electronegative chlorine with the aromatic substituent Tip does not affect too much the electronic environment at the P atom. In the ^{13}C NMR spectrum however, a greater shift of the signal for the unsaturated carbon atom was noticed: from 166.6 ppm for **9** to 176.6 ppm for derivative **17**.

In ^1H NMR, one singlet was observed for the *t*Bu groups of the Mes* group which proves their rotation is not hindered. By contrast, more complex signals appear for the Tip groups: between 1.12 and 1.28 ppm, a broad multiplet was present corresponding to all *ortho* and *para* methyl groups. In the aromatic area, three singlets are observed for the *m*-CH, one at 6.87 ppm (2 H), and the two other ones slightly broad, at 6.98 and 7.12 ppm (2x1H). We can conclude that the 2 Tip groups are unequivalent, due to the hindered rotation around P=C-Ge bond and that one of the Tip groups presents a free rotation around the Ge-Tip bond (one singlet for the equivalent *m*-CH) and the other one a hindered rotation around Ge-Tip bond (two broad singlet for the unequivalent *m*-CH). This assumption was also proved by the ^{13}C NMR spectrum which presents two singlets for the *m*-CH carbon atom at 121.62 and 122.12 ppm for one Tip group and only one singlet at 122.31 ppm for the other one.

As a perspective, the use of bromine instead of chlorine on the germanium atom, which is a better leaving group, could be tried in order to be successful in the coupling reaction between $\text{Mes}^*\text{P}=\text{C}(\text{Cl})\text{Li}$ and $\text{Tip}_2\text{GeBr}_2$ to obtain $\text{Mes}^*\text{P}=\text{C}(\text{Cl})\text{-Ge}(\text{Tip})_2\text{Br}$.

3) Synthesis and characterization of $\text{Mes}^*\text{P}=\text{C}(\text{Cl})\text{-GeCl}(\text{t-Bu})\text{C}_6\text{H}_4\text{-ortho-CH}_2\text{-NMe}_2$

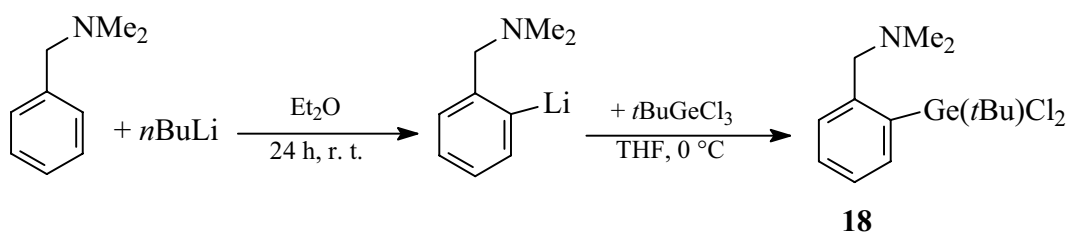
While exploring new ways to further stabilize the P=C=Ge unit in phosphagermaallenes, we have envisaged to increase the electron density on the germanium atom through its coordination with an electron-donor atom (scheme IV.10). The electronic influence, combined with the steric hindrance afforded by the coordinating atom can be increased by a chelate effect.



Scheme IV.10

This can be realized by functionalizing the germanium precursor with a pendant arm ligand containing a nitrogen atom as electron-donor atom and already allowed the stabilization of various doubly-bonded compounds of germanium such as germathiones $>\text{Ge}=\text{S}$ [10], germaselones $>\text{Ge}=\text{Se}$ [11] and germatellones $>\text{Ge}=\text{Te}$ [11].

We planned to use as a pendant arm ligand the *N,N*-dimethylaminomethylphenyl group. To this purpose we have carried out the synthesis of dichloro(*N,N*-dimethylaminomethyl)phenyl-*tert*-butylgermane **18** through the series of reactions represented in scheme IV.11. We have first prepared the *ortho*-lithium benzylamine according to the method of Noltes [12]. The selectivity of the *ortho*-lithiation was explained by a strong coordination between the nitrogen and lithium atoms. Addition to *t*BuGeCl₃ [13] afforded **18** in a good yield.

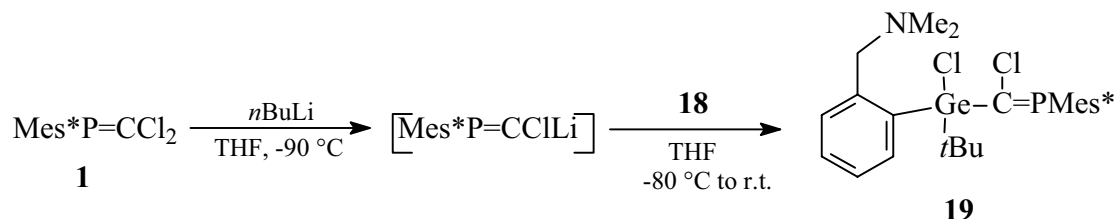


Scheme IV.11

A by-product of the reaction depicted in scheme IV.11 was the germane $(\text{Me}_2\text{NCH}_2\text{C}_6\text{H}_4)_2(\textit{t}\text{Bu})\text{GeCl}$.

Derivative **18** was characterized through its proton (singlet at 3.61 ppm) and carbon NMR spectra. From the NMR spectra it was impossible to determine if the nitrogen atom was coordinated to the germanium atom since in all cases (coordination or not) the two Me group and the two methylenic protons are equivalent.

Reaction of the dichlorogermene **18** with the lithium derivative of compound **1** at low temperature led to the phosphagermapropene **19** in a poor yield (scheme IV.12).



Scheme IV.12

One of the major by-product was $\text{Mes}^*\text{P}=\text{C}(\text{Cl})\text{H}$, due to the final hydrolysis of $\text{Mes}^*\text{P}=\text{C}(\text{Cl})\text{Li}$ which had not reacted with **18**. The formation of **19** was evidenced through ^{31}P NMR spectroscopy. The signal appears at 300.4 ppm, as expected for a phosphagermapropene, along with the characteristic peak for $\text{Mes}^*\text{P}=\text{C}(\text{Cl})\text{H}$, in a 3.6:1 ratio. Although attempts to isolate compound **19** failed, its ^1H NMR spectrum shows a broad signal for the methylenic group on the pendant arm indicating in this case the coordination of the nitrogen atom to the germanium.

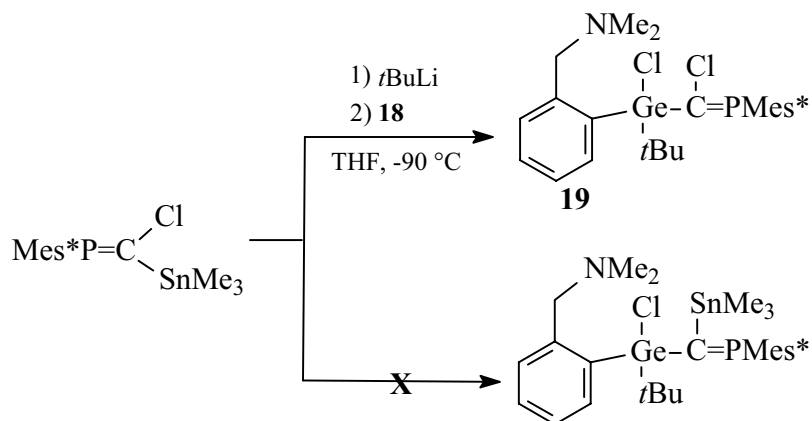
This coordination $\text{N} \rightarrow \text{Ge}$, should be less favorable in **19** than **18** for two reasons: the greater steric congestion which can prevent the approach of the NMe_2 moiety and the less electrophilic character of the germanium atom substituted by only one chlorine atom instead of two. As the coordination was proved in the case of **19**, we can reasonably postulate that such a coordination also exists in **18** [14].

An alternative synthetic route involved the preparation of $\text{Mes}^*\text{P}=\text{C}(\text{SnMe}_3)\text{Cl}$, as indicated in scheme IV.13, to obtain the phosphagermaallene precursor $\text{Mes}^*\text{P}=\text{C}(\text{SnMe}_3)-\text{Ge}(\text{Me}_2\text{NCH}_2\text{C}_6\text{H}_4)(t\text{Bu})\text{Cl}$. The latter could eliminate Me_3SnCl to afford the $\text{P}=\text{C}=\text{Ge}$ unit without using a lithium compound.



Scheme IV.13

Mes*P=C(SnMe₃)Cl was evidenced by ³¹P NMR (with a chemical shift at 280.5 ppm) and the resulting reaction mixture was used without further purification. Treatment with *t*BuLi and the subsequent addition of (Me₂NCH₂C₆H₄)(*t*Bu)GeCl₂ does not lead to the expected stannylated-phosphagermapropene, but affords a mixture of **19** and Mes*P=C(Cl)H, in about the same ratio as observed in the case of the previously described synthetic route (see scheme IV.14).



Scheme IV.14

The formation of **19** can be explained by the preliminary cleavage reaction of the weak C-Sn bond by *t*BuLi, leading to Me₃SnBu and Mes*P=C(Cl)Li followed by the subsequent reaction with **18** and hydrolysis.

*Study of germane (Me₂NCH₂C₆H₄)₂(*t*Bu)GeCl 20*

The structure of compound **20**, obtained as a by-product in the reaction between C₆H₄(Li)CH₂NMe₂ and *t*BuGeCl₃, was determined by X-ray (figure IV.1) diffraction showing shows that two halogen atoms of *t*BuGeCl₃ have been replaced by two Me₂NCH₂C₆H₄ moieties. The Ge(1)-C(1) (1.919(11) Å) and Ge(1)-C(10) (1.931(10) Å) distances lie in the normal range for such bonds between a germanium atom and the *ipso*-carbon of an aromatic ring. By contrast, the Ge(1)-C(19) distance was slightly elongated to 1.993(14) Å due to the steric hindrance of the *t*Bu group.

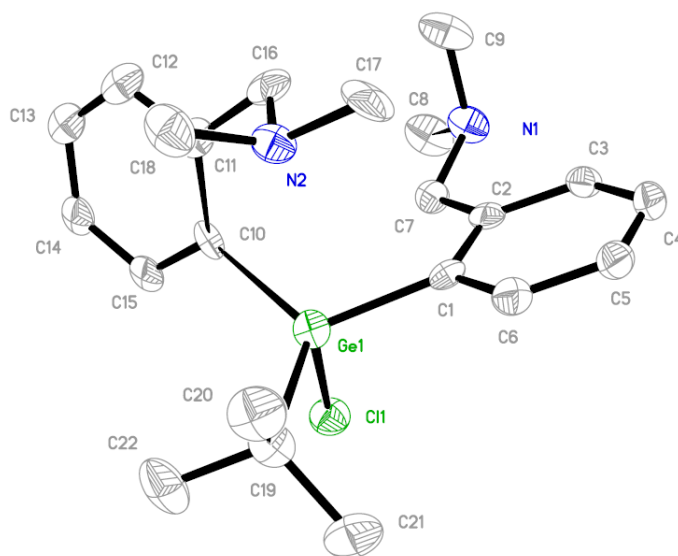


Figure IV.1. Molecular structure of **20** (thermal ellipsoids drawn at the 50% probability level); hydrogen atoms are omitted for clarity; selected bond lengths (Å) and angles (°).

Ge(1)-C(10): 1.919(11); Ge(1)-C(1): 1.931(10); Ge(1)-C(19): 1.993(14); Ge(1)-Cl(1) 2.253(4);
 C(2)-C(7): 1.515(14); C(7)-N(1): 1.451(16); C(11)-C(16): 1.517(15); C(16)-N(2): 1.473(14);
 C(10)-Ge(1)-C(1): 117.5(5); C(10)-Ge(1)-C(19): 117.3(5); C(1)-Ge(1)-C(19): 115.7(5); C(10)-
 Ge(1)-Cl(1): 100.6(4); C(1)-Ge(1)-Cl(1): 100.8(3); C(19)-Ge(1)-Cl(1): 99.6(4); Ge(1)-N(1):
 4.724; Ge(1)-N(2): 3.107.

The most interesting feature was the presence of a distorted tetrahedral geometry around the germanium atom: the sum of angles C(1)Ge(1)C(10), C(1)Ge(1)C(19) and C(10)Ge(1)C(19) was 350.5°, not too far from 360° for a planar geometry. In a tetrahedral structure, the sum of these angles should be 327.7°. The distance of the Ge atom to the C(1)C(10)C(19) plane was only 0.35 Å. Thus, the four atoms C(1), C(10), C(19) and Ge(1) are roughly in a plane. The Ge(1)-Cl(1) bond length (2.253 Å) is slightly elongated compared to standard Ge-Cl distances (2.09 to 2.21 Å) [14b]. The nitrogen atom N(1) is far from the germanium atom (4.724 Å), but the nitrogen atom N(2) is closer (3.107 Å). Even if the distance is long for an interaction between the Ge and N(2) atoms, the long Ge-Cl bond and the rather planar geometry for the GeC₃ skeleton are in agreement with a weak coordination.

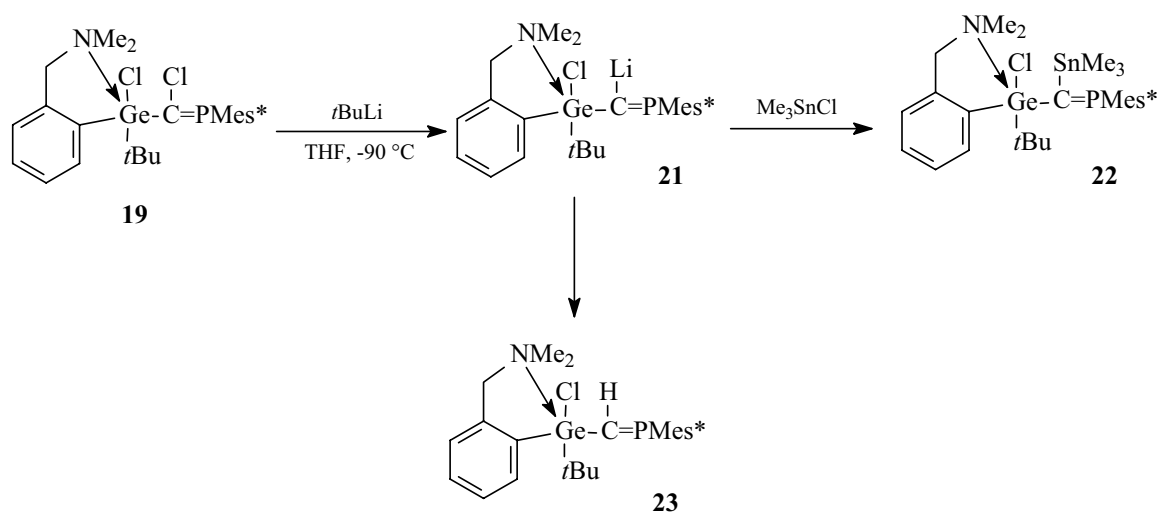
Action of *t*BuLi on derivative **19**

The reaction of **19** with *tert*-butyllithium was followed by ^{31}P NMR techniques. After the addition of the lithium reagent and warming up to room temperature, the signal corresponding to the phosphagermapropene **19** disappears and two other peaks appear at 403.3 and 322.2 ppm (d, $J_{\text{PH}} = 24.85$ Hz). The more deshielded signal at 403 ppm could reasonably correspond to the lithium compound **21** (scheme IV.15), stabilized by a possible interaction with the amino group (such a deshielded signal (441.4 ppm) was observed in a phosphasilapropenyl derivative with the rather similar $\text{Mes}^*\text{P}=\text{C}(\text{Li})\text{SiCl}$ skeleton [15]).

When the reaction mixture was kept under an inert atmosphere, the amount of the compound corresponding to the signal at 322 ppm increases.

Although attempts to separate the mixture and further analyze the two derivatives are still in progress, we have assigned the signal at 322 ppm to **23**, the hydrolysis product of **21**.

Subsequent treatment of **21** with Me_3SnCl led to the shift of the signal to a higher field (392.6 ppm), which could be explained by the formation of **22** (scheme IV.15).



Scheme IV.15

A signal at this field was characteristic of a $\text{Mes}^*\text{P}=\text{C}$ derivative, with two electropositive groups on the doubly bonded carbon atom. For example

$\text{Mes}^*\text{P}=\text{C}(\text{SiMe}_3)_2$ with two SiMe_3 group which have about the same electronic properties as Me_3Sn and $\text{R}(t\text{Bu})\text{ClGe}$ gives a signal at 393 ppm [16] and the rather similar derivative $\text{Mes}^*\text{P}=\text{C}(\text{SnMe}_3)_2$ gives a signal at 386.7 ppm [17].

Heating **21** or **22** to get the expected phosphagermaallene by elimination of LiCl or Me_3SnCl was unsuccessful. However, new attempts are now planned using other solvents or involving heating in a sealed tube.

Phosphasilapropenes

The synthesis of phosphasilaallenes $-\text{P}=\text{C}=\text{Si}<$ proved to be a challenge, partially due, no doubt, to the smaller size of the silicon atom, which makes the choice of the appropriate protective groups rather difficult: the usual bulky groups used for germanium in the synthesis of stable phosphagermaallenes failed for the preparation of the $\text{P}=\text{C}=\text{Si}$ unit.

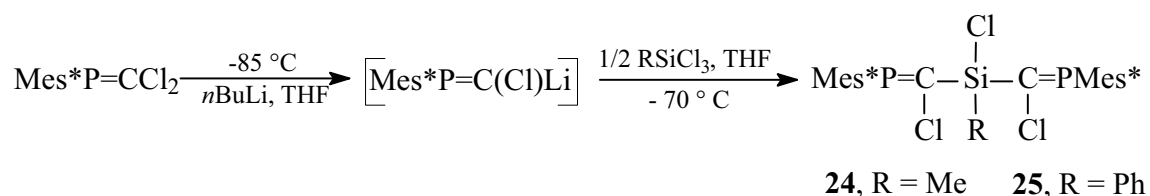
For example, as previously said in the Chapter I, the *Tip* and *tBu* group on germanium allowed the synthesis and stabilization of phosphagermaallene $\text{Mes}^*\text{P}=\text{C}=\text{Ge}(\text{Tip})t\text{Bu}$ [4] and with two mesityl groups, the corresponding allene $\text{Mes}^*\text{P}=\text{C}=\text{GeMe}_2$ [18] could be characterized by NMR and trapping reactions.

Previous attempts showed that the use of such group was impossible in the case of silicon, since the coupling between the phosphorus and the silicon moiety was impossible, probably for steric reasons. Only a transient phosphasilaallene with phenyl and *Tip* groups on the silicon atom was characterized until now [19].

So we tried to prepare a phosphasilaallene of a new type which could be stabilized both by steric and electronic effects: in this case the steric hindrance does not need to be so important, and the additional electronic effect could be sufficient enough for the stabilization. Thus, we thought to a conjugation between the allenic moiety and a $\text{C}=\text{P}$ double bond and we planned to prepare a phosphasilaallene of the type $-\text{P}=\text{C}=\text{Si}(\text{R})-\text{R}'\text{C}=\text{P}-$. The obvious choice for the group on the phosphorus atom was the Mes^* group, and less hindered substituents, like methyl or phenyl can be used on silicon.

It would also be interesting to evaluate the electronic effect of the P=C bond on the stabilization of the allenic unit.

The reaction of RSiCl₃ (R = Me, Ph) with two equivalents of Mes*P=C(Cl)Li led to the formation of the sterically hindered phosphasilapropenes **24** and **25**, as described in scheme IV.16:



Scheme IV.16

Derivative **24** was characterized through NMR spectroscopy; relevant data are given in Table IV.2.

Table IV.2. NMR data for derivative **24**

Compound	¹ H NMR	³¹ P NMR	¹³ C NMR
24	0.88 ppm (s, 3H, Me), 1.33 ppm, (s, 9H, <i>p</i> -tBu), 1.44 (s, 18H, <i>o</i> -tBu), 7.41 ppm (s, 2H, H _{arom})	313.6 ppm (² J _{SiP} = 44.6 Hz)	162.90 ppm (dd, ¹ J _{CP} = 75.5 Hz, ³ J _{CP} = 5.5 Hz), P=C 134.37 ppm (d, ² J _{CP} = 64.1 ppm, <i>ipso</i> C Mes*)

The ²⁹Si NMR spectrum showed a triplet at -1.61 ppm, with a J_{PSi} coupling constant of 47.7 Hz, in agreement with the data obtained from the ³¹P NMR spectrum.

Only one isomer was obtained. As the formation of the lithium compound Mes*P=C(Cl)Li is stereoselective, we can postulate that the sole isomer formed in this reaction was the *Z,Z*-isomer.

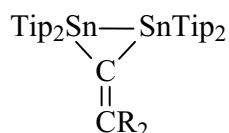
The formation of compound **25** was evidenced through ³¹P NMR spectroscopy, in a 50% yield, but several other by-products resulted from the reaction and **25** could not be obtained in a pure form by fractional crystallization. The major signal appeared at 322.5 ppm and was assigned, as for **24**, to the *Z,Z*-isomer of **25**, on the basis of the *trans*-Mes* orientation shown by **1** in lithiation reactions. Another close signal (20%) at 321.4 ppm

was observed. As the Li/Cl exchange is stereoselective, and normally only the *Z,Z*-isomer must be formed, we can postulate that this signal could correspond to the monosubstituted derivative $\text{Mes}^*\text{P}=\text{C}(\text{Cl})\text{-Si}(\text{Ph})\text{Cl}_2$.

For comparison, the already reported $\text{Mes}^*\text{P}=\text{C}(\text{Cl})\text{-Si}(\text{Cl})\text{PhTip}$ has a ^{31}P NMR chemical shift of 319.7 ppm [19] and the values for the carbon involved in the double bond are also similar. Unfortunately, it has been impossible to separate and to purify these products by fractional crystallization: thus only hypotheses about the structures of these derivatives can be formulated. As **25** was not obtained in a pure state, the synthesis of phosphasilaallene could not be attempted since both products (mono- and bisubstituted) should react with BuLi. Thus, the synthesis of phosphasilaallene was tried only on the phosphasilapropene **24**. However, addition of *n*BuLi to a solution of **24** in ether at low temperature led only to a mixture of several compounds which could not be separated. Change in the experimental conditions (temperature, solvent, and *t*BuLi instead of *n*BuLi) did not allow a clean reaction. The signals between 200 and 300 ppm in ^{31}P NMR correspond to derivatives with a P=C double bond. The lack of signal in the expected area (close to 150 ppm) shows that no phosphasilaallene was present in the reaction mixture; however its transient formation followed by a reaction (with BuLi rearrangement or dimerization) cannot be excluded to form derivatives giving signals between 200 at 300 ppm.

Phosphastannapropenes

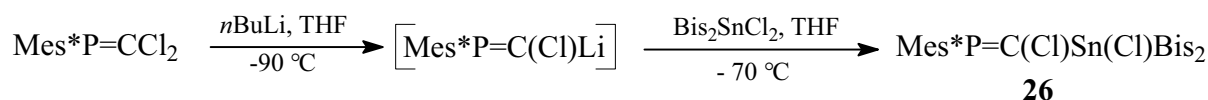
There are no phosphastannaallenes or stannaallenes described to date in the literature, even transient ones. The formation of $\text{Tip}_2\text{Sn}=\text{C}=\text{CR}_2$ (CR_2 = fluorenylidene) has been postulated as an intermediate in the synthesis of the first stable distannirane [20] (scheme IV.17).



Scheme IV.17.

The lower tendency of tin relative to its group 14 analogues to form stable double bonds was mainly due to the poor orbital overlapping of the π bond. It was well known that in some group, the stabilization is more and more difficult going down the group. For example, whereas many compounds with a $\text{Si}=\text{C}$ are stable, much less $\text{Ge}=\text{C}$ derivatives have been obtained and only a few compounds containing the $\text{Sn}=\text{C}$ bond.

The synthesis of a phosphastannaallene $-\text{P}=\text{C}=\text{Sn}<$ thus appears to be a great challenge. For the stabilization this type of compounds, a great steric hindrance is necessary. We use the supermesityl group on the phosphorus atom and the bulky bis(trimethylsilyl)methyl group $\text{CH}(\text{SiMe}_3)_2$ (Bis) on the tin, which can also sterically protect the $\text{Sn}=\text{C}$ bond. We have thus attempted the synthesis of the phosphastannaallene $\text{Mes}^*\text{P}=\text{C}=\text{Sn}(\text{Bis})_2$, starting from $\text{Mes}^*\text{P}=\text{CCl}_2$ and $\text{Bis}_2\text{SnCl}_2$ [21], as depicted in scheme IV.18:



Scheme IV.18

Surprisingly, derivative **26** was obtained as a mixture of *E/Z* isomers, in a relative ratio of 4:1. The *E* isomer showed a doublet at 43.6 ppm ($^3J_{\text{P-Sn}} = 363.7$ Hz) in the ^{119}Sn

NMR spectrum and a singlet in the ^{31}P spectrum at 305.5 ppm. The *Z* isomer gives signals at 306.1 ppm in ^{31}P NMR spectrum and 12.1 ppm (d, $^3J_{\text{P-Sn}} = 374.9$ Hz) in ^{119}Sn NMR respectively. The structure of the two isomers was confirmed by mass spectroscopy, where all preponderant peaks were assigned for $\text{Mes}^*\text{P}=\text{C}(\text{Cl})\text{Sn}(\text{Cl})\text{Bis}_2$. The *E* isomer should be formed in higher ratio, because of the selective reactivity behavior of the $\text{Mes}^*\text{P}=\text{C}$ moiety for the reasons which we have already mentioned.

Compound **26** has also been characterized through ^{29}Si -NMR spectroscopy and the spectrum exhibits a doublet at -5.65 ppm with a silicon-phosphorus coupling constant of 58 Hz for the major compound.

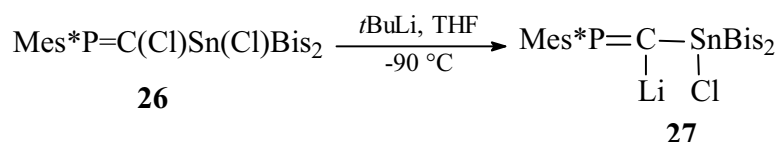
The two Me_3Si groups of a $(\text{Me}_3\text{Si})_2\text{CH}$ unit are diastereotopic and display two singlets in ^1H NMR. Table IV.3 summarizes the most relevant NMR data of compound **26**.

Table IV.3. NMR data for derivative **26**

	^1H NMR	^{31}P NMR	^{13}C NMR
26	0.24 ppm (s, 9H, Me_3Si)	305.5 ppm ($^2J_{\text{PSn}} =$	4.40 ppm, (broad signal, $\underline{\text{C}}\text{H}_3\text{Si}$)
	0.27 ppm (s, 9H, Me_3Si)	365.6 Hz)	14.42 ppm (s, $\underline{\text{C}}\text{HSn}$)
	7.40 ppm (s, 2H, H_{arom})		174.25 ppm (d, $^2J_{\text{PC}} = 102,8$ Hz)

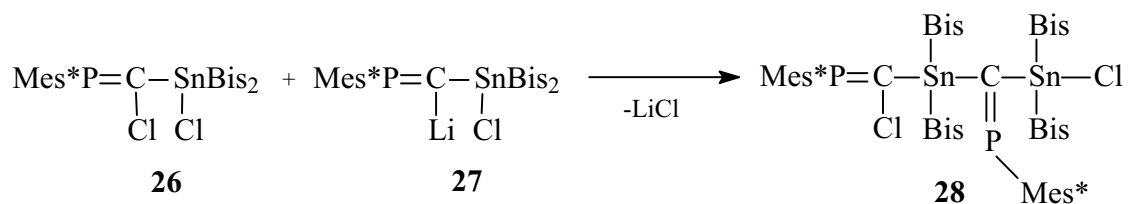
*Treatment of 26 with *t*BuLi*

The reaction of **26** with *t*BuLi was monitored by ^{31}P NMR spectroscopy. The presence at 409.8 ppm of a phosphorus signal (s, $J_{\text{PSn}} = 982.5$ Hz) was assigned to the formation of the lithium derivative $\text{Mes}^*\text{P}=\text{C}(\text{Li})\text{-Sn}(\text{Cl})\text{Bis}_2$, as shown in scheme IV.19:



Scheme IV.19

After some hours, the signal at 409.8 ppm disappeared and the postulated compound **27** led to a derivative (about 30% ratio) that showed two doublets in the ^{31}P NMR spectra at 327.1 ppm and 451.4 ppm ($J_{\text{PP}} = 33.6$ Hz). Based on these considerations, we postulate that rather than undergoing intramolecular elimination of LiCl, the lithium halide was eliminated intermolecularly as the result of a condensation between **26** and derivative **27**, according to scheme IV.20.



Scheme IV.20

The proposed structure of **28** would account for the up-field value of 451.4 ppm for the phosphorus atom in the P=C unit bonded to two tin atoms. Both P signals show satellites at high values of the $J_{\text{P-Sn}}$ coupling constant (see table IV.4).

Table IV.4. NMR data for derivatives 27-28

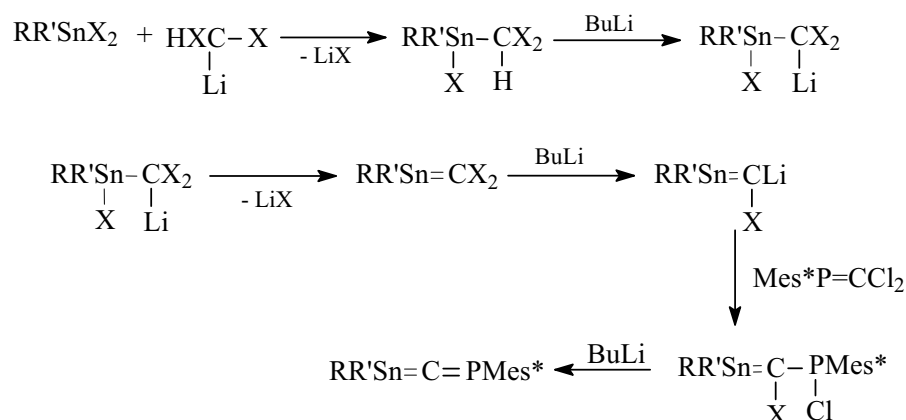
	^{31}P NMR	$^4J_{\text{PP}}$	J_{PSn}
27	409.8ppm	-	$^2J_{\text{PSn}} = 982.5$ Hz
28	327.1 ppm		$^2J_{\text{PSn}} = 365.1$ Hz
	451.4 ppm	33.6 Hz	$^2J_{\text{PSn}} = 415.1$ Hz

Besides the signals of the starting **26**, three other strong signals were detected in the ^{31}P NMR at 292.5 ppm ($J_{\text{PSn}} = 250.1$ Hz), 342.2 ($J_{\text{PSn}} = 363$ Hz) and 342.7 ppm ($J_{\text{PSn}} = 360$ Hz).

Addition of a second equivalent of BuLi led to many derivatives and did not afford the expected phosphastannaallene, since no signal could be detected at about 150 ppm.

Synthesis of a precursor of a stannaallene

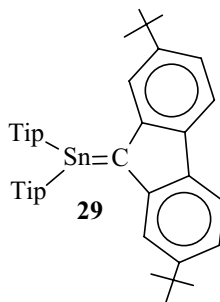
The attempts made so far to synthesize a phosphastannaallene by a route involving the first formation of the P=C double bond were unsuccessful. An alternative to the synthetical route described above for phosphasila- and phosphagermaallenes would be the creation of the C=Sn bond first, as described in scheme IV.21.



Scheme IV.21

We have attempted the synthesis and characterization of two potential precursors of stannaalkenes and -allenes, starting from the sterically hindered tin derivative Tip_2SnF_2 [22].

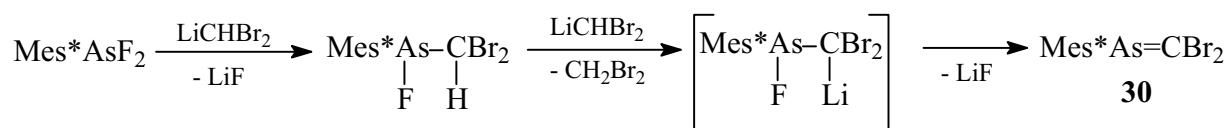
The choice of the starting material in the synthesis of doubly bonded tin derivatives was important, because of the protection role that the organic groups on the tin atom will play in the case of the Sn=C bond. Bulky groups, like Tip (2,4,6-*i*Pr₃-C₆H₂), afford steric stabilization of the very reactive tin-carbon bond. For example the stannene **29** has been stabilized by these groups [23] (scheme IV.22):



Scheme IV.22

The efficiency of Tip as a protection group has already been proven for other doubly bonded compounds [2, 3].

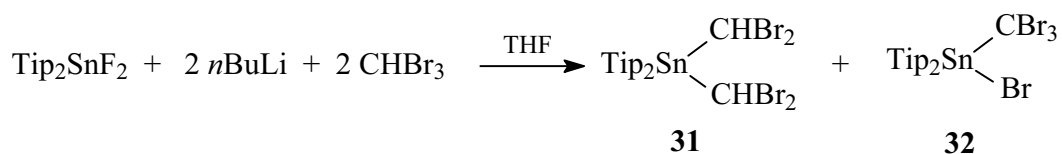
The reaction of Mes*EX₂ derivatives (E = P, As) with chloroform or bromoform in the presence of lithium derivatives leads to the formation of Mes*E=CX₂ compounds. [17, 24]. For example the C,C-dibromoarsaalkene **30** has been obtained by the following route using CHBr₃ [24] (Scheme IV.23):



Scheme IV. 23

It was therefore interesting to explore the reactivity of halostannanes towards bromoform, in the hope of obtaining the corresponding stannaalkenes RR'Sn=CBr₂. Such compounds should be extremely interesting in tin chemistry since owing to the possibility of exchange Li/Br, this compound could be functionalized.

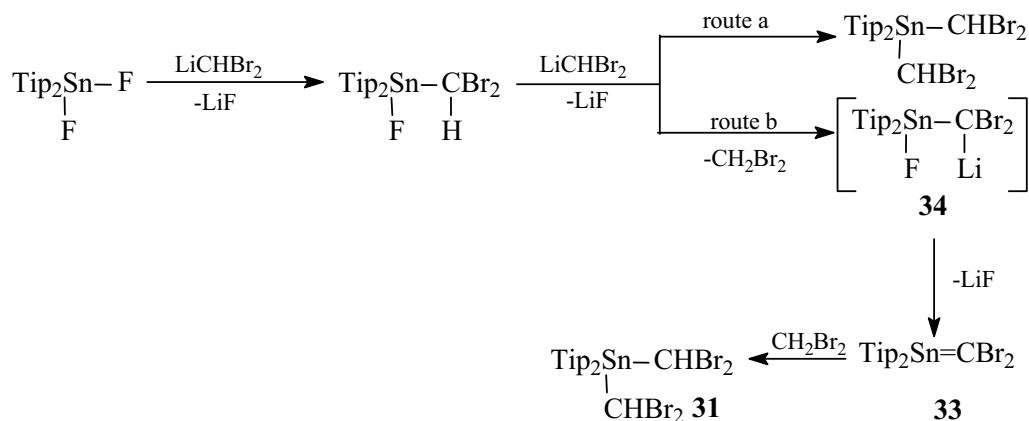
However, the behavior of dihalosubstituted group 14 derivatives in such reactions was quite different from that of similar group 15 compounds: the reaction of Tip₂SnF₂ with two equivalents of CHBr₂ and *n*BuLi performed at -90°C, in THF led to the formation of two main compounds **31** and **32** in a 4:1 ratio (scheme IV.24).



Scheme IV.24

As reported in the literature [25], both CLiHBr₂ and CLiBr₃ can be formed by the reaction of lithium derivatives with bromoform.

The formation of **31** probably arises from a double alkylation reaction (route a) (scheme IV.25), but it could also involve the expected C,C-dibromostannaalkene intermediate **33** (route b), formed from **34**, followed by addition of CH₂Br₂.



Scheme IV.25

The Sn-C double bond is extremely reactive; the addition of the poorly reactive CH bond of dibromomethylene seems less likely.

To explain the formation of compound **32**, we supposed the first formation of Tip₂Sn(F)CBr₃ by alkylation with CLiBr₃ in the first step of the reaction, followed by a fluorine-bromine exchange with the LiBr formed *in situ*.

Compounds **31** and **32** have been characterized by multinuclear NMR spectroscopy. The relevant NMR data for **31** are given in Table IV.5.

Table IV.5. NMR data for Tip₂Sn(CHBr₂)₂

¹ H NMR	¹¹⁹ Sn NMR	¹³ C NMR
1.18 ppm (d, ³ J _{HH} = 6.4 Hz, 12H, CH ₃ , <i>p-iPr</i>)	-134.2 ppm	23.9 ppm (CH ₃ , <i>o-iPr</i>)
1.50 ppm (d, ³ J _{HH} = 6.4 Hz, 24H, CH ₃ , <i>o-iPr</i>)	(² J _{SnBr} = 11.8 Hz)	24.7 ppm (CH ₃ , <i>p-iPr</i>)
2.58 (sept, ³ J _{HH} = 6.4 Hz, 4H, CH, <i>o-iPr</i>)		32.5 ppm (CH, <i>o-iPr</i>)
2.82 (sept, ³ J _{HH} = 6.4 Hz, 2H, CH, <i>p-iPr</i>)		34.3 ppm (CH, <i>p-iPr</i>)
5.80 (s, 2H, CHBr ₂)		40.1 ppm (CHBr ₂)
6.96 (s, 4H, <i>m-CH</i> Tip).		122.6 (<i>m-CH</i> Tip), 150.9 and 151.6 ppm (<i>o-</i> and <i>p-C</i> Tip).

Surprisingly the ^{119}Sn NMR with proton decoupling spectrum of compound **31** shows a multiplet (13 peaks). This result can only be understood by the coupling with the four bromine atoms: ^{79}Br and ^{81}Br (natural abundance 50.54 and 49.46 % respectively) have a spin of 3/2 and the coupling constant between ^{119}Sn and the two bromine isotopes should be rather the same (figure IV.2). Such signals are usually broad and the coupling constant was not observed; to our best knowledge, it was the first time that the coupling of tin with such a great number of bromine atoms resulted in an observed hyperfine splitting of the signal and not just in its widening.

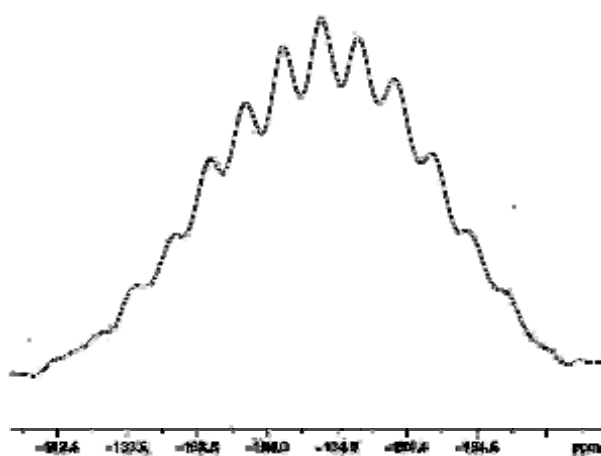


Figure IV.2. ^{119}Sn NMR signal for $\text{Tip}_2\text{Sn}(\text{CHBr}_2)_2$

NMR data for **32** do not show any special features; the only interesting characteristic is the presence of two signals for the diastereotopic Me of the *i*Pr groups; the position of the signals are given in the Experimental section

Compound **32**, $\text{Tip}_2\text{Sn}(\text{Br})\text{CBr}_3$, was characterized in the solid state through X-ray diffraction on single crystal. An ORTEP drawing of the molecular structure is shown in Figure IV.2. Some geometrical data are also given in table IV.6. The presence of the heavy bromine atoms makes the refinement of the structure difficult. Two equivalent positions atom are possible for the CBr_3 groups, as well as for the Br1 atom, with respect to an axis containing the central tin and acting as a two-fold symmetry axis for the Tip groups. The Sn-Br distance (2.714 Å) is remarkably larger than those found in similar compounds (2.50 - 2.60 Å) [26, 27]. As expected, the geometry about the tin atom is distorted tetrahedral, with wider angles for atoms belonging to the CBr_3 group.

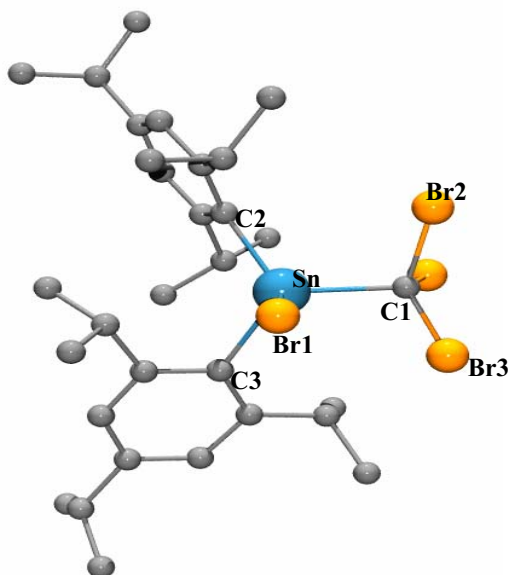
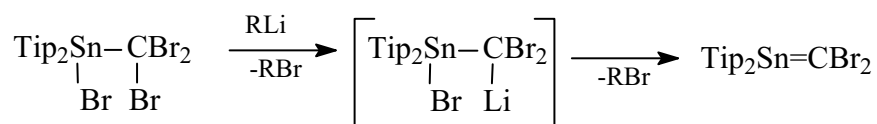


Figure IV.3. Molecular structure of $\text{Tip}_2\text{Sn}(\text{Br})\text{CBr}_3$ (hydrogen atoms were omitted for clarity)

Table IV.6. Geometrical data for $\text{Tip}_2\text{Sn}(\text{Br})\text{CBr}_3$

Bond lengths (Å)		Bond angles (°)	
Sn-C1	2.227	Br1-Sn-C1	94.19
Sn-C2	2.156	C2-Sn-C3	110.81
Sn-Br1	2.714	C1-Sn-C3	122.70
C1-Br2	1.932	Br2-C1-Sn	104.52
C1-Br3	1.940	Br1-C1-Br2	114.98

Several attempts have been performed in order to obtain the stannene $\text{Tip}_2\text{Sn}=\text{CBr}_2$ from $\text{Tip}_2\text{Sn}(\text{Br})\text{CBr}_3$ **32** by the expected mechanism described in scheme IV.26:



Scheme IV.26

Unfortunately, addition of *n*BuLi or *t*BuLi in Et₂O or THF, at -78°C or -100 °C and various concentrations, led to many unidentified derivatives as displayed by the ¹¹⁹Sn NMR spectrum. This was due to the multiple possibilities of reaction with lithium compound such as an exchange Br/Li on the carbon atom, followed by elimination of LiBr to form the transient stannene Tip₂Sn=CBr₂ which can duplicate or rearrange. An intermolecular elimination of LiBr can also occur between two molecules of **33** as well as an elimination of LiBr on the carbon atom leading to a transient carbene. Thus, by this route, it has not been possible to obtain neither the functional Tip₂Sn=CBr₂, nor the precursor of the phosphastanaallene Tip₂Sn=C(Br)-P(Cl)Mes*.

In conclusion, we have prepared some new phosphasila-, phosphagerma- and phosphastannaalkenes, differently substituted. However, we have been unsuccessful in the synthesis of the corresponding allenes.

One of the great difficulties encountered in this study was the formation of many derivatives (generally due to the multiple possibilities of reaction) which could not be separated by fractional crystallization. The study also shows that the choice of substituents to obtain low coordinate heteroallenic compounds appears to be extremely difficult, since they must not be too large in order to allow the synthesis of the precursor (case of $\text{Mes}^*\text{P}=\text{C}(\text{Cl})\text{Ge}(\text{Cl})\text{Tip}_2$ obtained in a very poor yield), but large enough to be able to stabilize the doubly bonded species.

In the perspective, we plan to use other types of substituents, like silyl group such as $t\text{Bu}_2\text{MeSi}$ recently used for the successful stabilization of various doubly bonded species and to vary both the steric and the electronic effects of the groups both on the phosphorus and the group 14 element.

Experimental Section

General procedures

All experiments were carried out in flame-dried glassware under an argon atmosphere using high-vacuum-line techniques. Solvents were dried and freshly distilled from sodium benzophenone ketyl and carefully deoxygenated on a vacuum line by several “freeze-pump-thaw” cycles. NMR spectra were recorded in CDCl₃ on the following spectrometers: ¹H, Bruker Avance 300 (300.13 MHz) and Avance 400 (400.13 MHz); ¹³C{¹H}, Bruker Avance 300 (75.47 MHz) and Avance 400 (100.62 MHz) (reference TMS), ³¹P, Bruker AC200 at 81.02 MHz (reference H₃PO₄). Melting points were determined on a Wild Leitz-Biomed apparatus. Mass spectra were obtained on a Hewlett-Packard 5989A spectrometer by EI at 70 eV.

1) Synthesis of 1-bromo-2,4,6-triisopropylbenzene (TipBr)

A solution of Br₂ (82 g; 0.15 mol) in 100 ml of CCl₄ was added dropwise to a mixture of TipH (100 g; 0.49 mol), CCl₄ (60 ml) and iron powder (4 g), at -15 °C. The mixture was kept away at dark and under stirring for 24 hours; then 200 ml of water and 100 ml of NaOH 20 % were added. After separating the phases and drying the organic phase on Na₂SO₄, CCl₄ was removed and TipBr (115.13 g) was purified by vacuum distillation (η = 83 %)

$\delta^1\text{H}$ (300 MHz, CDCl₃): 1.26 (d, ³J_{HH} = 6,4 Hz, 18H, *o*- and *p*-CHMe₂); 2.80 (m, ³J_{HH} = 6,4 Hz, 1H, *p*-CHMe₂); 3.50 (m, ³J_{HH} = 6,4 Hz, 2H, *o*-CHMe₂); 7.00 (s, 2H, arom H)

2) Synthesis of trichloro(2,4,6-trisopropylphenyl)germane TipGeCl₃

Synthesis of TipGeX₃

A solution of TipBr (29.44 g; 0.104 mol) in 50 ml of THF was added dropwise to 2.73 g (0.113 mol) of Mg turnings in 10 ml of THF. After the addition, the reaction

mixture was refluxed for 2 hours. The Grignard reagent TipMgBr was then cannulated dropwise to a solution of GeCl₄ (22.32 g; 0.104 mols) in 70 ml of ethylic ether at 0 °C. The mixture was then refluxed for another one hour. After treatment with HCl (10 %), phase separation and drying the organic phase on Na₂SO₄, TipGeX₃ was isolated (28.6 g, X = Cl, Br).

Reduction of TipGeX₃

The TipGeX₃ mixture in 100 ml ether, was added dropwise to 10.04 g of LiAlH₄ (0.26 mol) in 50 ml of THF. The reaction mixture was refluxed for 2 hours. After treatment with water and then diluted HCl, phase separation and drying of the organic phase on Na₂SO₄, TipGeH₃ was purified by distillation (16.62 g; η = 79 %)

$\delta^1\text{H}$ (300 MHz, CDCl₃): 1.25 (d, $^3J_{\text{HH}} = 6.8$ Hz, 18H, *o* and *p*-CHMe₂); 2.87 (sept, $^3J_{\text{HH}} = 6.8$ Hz, 2H, *p*-CHMe₂); 3.2 (sept, $^3J_{\text{HH}} = 6.8$ Hz, 1H, *o*-CHMe₂); 4.24 (s, 3H, GeH); 7.03 (s, 2H, arom H)

Synthesis of TipGeCl₃

A solution of TipGeH₃ (16.62 g; 0.059 mol) in 70 ml of toluene was added dropwise to a mixture of 30 ml of CCl₄ and 0.4 g AIBN in 20 ml of toluene. The reaction mixture was refluxed for one hour. The solvent was then removed under vacuum and replaced by pentane, from which 15.5 g of TipGeCl₃ were crystallized (η = 68 %).

$\delta^1\text{H}$ (300 MHz, CDCl₃): 1.29 (d, $^3J_{\text{HH}} = 6.6$ Hz, 12H, *o*-CHMe₂); 1.25 (d, $^3J_{\text{HH}} = 6.8$ Hz, 6H, *p*-CHMe₂); 2.91 (sept, $^3J_{\text{HH}} = 6.8$ Hz, 1H, *p*-CHMe₂); 3.70 (sept, $^3J_{\text{HH}} = 6.6$ Hz, 2H, *o*-CHMe₂); 7.11 (s, 2H, arom H).

3) Synthesis of Mes*P=C(Cl)Ge(Tip)Cl₂ 9

A solution of 3.8 ml *n*-BuLi 1,6 M in hexane (5.9 mmol) was added at -85 °C to a solution of Mes*P=CCl₂ (2.03 g; 5.65 mmol) in 60 ml of THF; the reaction mixture was kept below -70 °C for an hour to ensure the formation of **2** and then a solution of TipGeCl₃ (2.2 g; 5.7 mmol) in 60 ml de THF was added. The mixture was allowed to slowly warm up to room temperature and then THF was removed under vacuum and

replaced with 30 ml of pentane. Lithium salts were removed by filtration. White crystals of Mes*P=C(Cl)Ge(Tip)Cl₂ (2.78 g, η = 72 %, m.p. =161-166 °C) crystallized after a while.

$\delta^1\text{H}$ (300 MHz, CDCl₃): 1.25 (d, $^3J_{\text{HH}}$ = 6.9 Hz, 6H, *p*-CHMe₂); 1.28 (d, $^3J_{\text{HH}}$ = 7.3 Hz, 12H, *o*-CHMe₂); 1.33(s, 9H, *p*-*t*Bu); 1.49(s, 18H, *o*-*t*Bu); 2.89 (sept, $^3J_{\text{HH}}$ = 7.1 Hz, 1H, *p*-CHMe₂); 3.49 (sept, $^3J_{\text{HH}}$ = 6.5 Hz, 2H, *o*-CHMe₂); 7.1 (s, 2H, arom H of Tip); 7.43 (d, $^4J_{\text{HP}}$ = 1.7 Hz, 1H, arom H of Mes*).

$\delta^{31}\text{P}$ (121.5 MHz): 303.7 ppm.

$\delta^{13}\text{C}$ (75.5 MHz): 23.78 (*p*-CHMe₂); 25.39 (*o*-CHMe₂); 31.36 (*p*-Me₃C); 32.95 (d, $^4J_{\text{CP}}$ = 6.8 Hz, *o*-Me₃C); 34.31 (*p*-CHMe₂); 34.64 (*o*-CHMe₂); 35.15 (*p*-Me₃C); 37.89 (*o*-Me₃C); 122.42 and 123.22 (*m*-CH (Mes*, Tip)); 128.38 (d, $^3J_{\text{CP}}$ = 1.7 Hz, *ipso*-C Tip); 132.96 (d, $^1J_{\text{CP}}$ = 63.4 Hz, *ipso*-C Mes*); 151.42 and 152.92 (*p*-C Tip and *p*-C Mes*); 153.78 (d, $^2J_{\text{CP}}$ = 2.3 Hz, *o*-C Mes*); 154.94 (*o*-C Tip); 166.57 (d, $^1J_{\text{CP}}$ = 92.1 Hz, P=C-Ge).

MS (m/z, %): 670 (M, 5); 655 (M - Me, 7); 635 (M - Cl, 10); 627 (M - *i*Pr, 10); 613 (M - *t*Bu, 3); 591 (M - *i*Pr - Cl - 1, 3); 435 (M - 2*i*Pr - 2*t*Bu - Cl, 5); 425 (M - Mes*, 1); 323 (Mes*P=C(Cl, 15); 275 (Mes*P - 1, 80); 245 (Mes*, 2); 203 (Tip, 2); 57 (*t*Bu, 100).

4) Synthesis of Mes*P=C(Cl)Ge(Tip)(OMe)₂ 10

To a solution of 19.5 g Mes*P=C(Cl)Ge(Tip)Cl₂ (29 mmol) in 200 ml toluene and 24 ml methanol, 13 ml Et₃N were added. The reaction mixture was refluxed for one and a half hours. The solvent was then removed under vacuum and replaced by pentane, and Et₃NHCl was separated by filtration; 12.43 g of white crystals of **10** were obtained by crystallization (η = 64 % m.p. = 150 - 152 °C)

$\delta^1\text{H}$ (300 MHz, CDCl₃): 1.24 (d, $^3J_{\text{HH}}$ = 6.6 Hz, 6H, *p*-CHMe₂); 1.25 (d, $^3J_{\text{HH}}$ = 6.6 Hz, 12H, *o*-CHMe₂); 1.31 (s, 9H, *p*-*t*Bu); 1.46 (d, $^5J_{\text{HP}}$ = 0.6 Hz, 18H, *o*-*t*Bu); 2.89 (sept, $^3J_{\text{HH}}$ = 6.9 Hz, 1H, *p*-CHMe₂); 3.50 (sept, $^3J_{\text{HH}}$ = 6.6 Hz, 2H, *o*-CHMe₂); 3.70 (s, 6H, Ge-OMe); 7.08 (s, 2H, arom H of Tip); 7.42 (d, $^4J_{\text{HP}}$ = 1.5 Hz, 2H, arom H of Mes*)

$\delta^{31}\text{P}$ (121.5 MHz): 301.0 ppm

$\delta^{13}\text{C}$ (75.5 MHz): δ 23.83 (*p*-CHMe₂); 25.55 (*o*-CHMe₂); 31.36 (*p*-Me₃C); 32.78 (d, $^4J_{\text{CP}} = 6.6$ Hz, *o*-Me₃C); 34.24 (*o* and *p*-CHMe₂); 35.09 (*p*-Me₃C); 37.77 (*o*-Me₃C); 52.85 (Ge-OMe); 122.06 and 122.15 (*m*-CH (Mes* and Tip)); 125.5 (*ipso*-C Tip); 134.2 (d, $^1J_{\text{CP}} = 64.3$ Hz, *ipso*-C Mes*); 150.87 and 151.47 (*p*-C Tip and *p*-C Mes*); 153.41 (d, $^2J_{\text{CP}} = 2.1$ Hz, *o*-C Mes*); 156.08 (*o*-C Tip); 166.7 (d, $^1J_{\text{CP}} = 85.9$ Hz, P=C-Ge)

MS (m/z, %): 662 (M, 1); 631 (M - OMe, 8); 627 (M - Cl, 6); 589 (M - *i*Pr - OMe + 1, 5); 307 (TipGeOMe - 1, 10); 275 (Mes*P - 1, 20); 245 (Mes*, 30); 231 (Mes* - Me, 10); 57 (*t*Bu, 100).

5) Synthesis of Mes*P=C(Cl)Ge(Tip)F₂ 11

A solution of HF 40% (15 ml, large excess) was added to 12.73 g of ArP=C(Cl)Ge(Tip)(OMe)₂ (18 mmol) in 60 ml of benzene; the reaction mixture was then refluxed for 45 minutes. After returning to room temperature, the solvents were eliminated and the organic phase was extracted in ether and dried on Na₂SO₄, 8.12 g of **11** were separated. ($\eta = 68\%$, m.p. = 122 - 124 °C)

$\delta^1\text{H}$ (300 MHz): 1.27 (d, $^3J_{\text{HH}} = 6.8$ Hz, 6H, *p*-CHMe₂); 1.32 (d, $^3J_{\text{HH}} = 6.8$ Hz, 12H, *o*-CHMe₂); 1.33 (s, 9H, *p*-*t*Bu); 1.46 (s, 18H, *o*-*t*Bu); 2.92 (sept, $^3J_{\text{HH}} = 6.8$ Hz, *p*-CHMe₂); 3.15 (m, $^3J_{\text{HH}} = 6.8$ Hz, $^5J_{\text{HF}} = 2.0$ Hz, 12H, *o*-CHMe₂); 7.14 (s, 2H, arom H Tip); 7.44 (d, $^4J_{\text{HP}} = 1.6$ Hz, 2H, arom H Mes*).

$\delta^{31}\text{P}$ (121.5 MHz): 311.7 ppm (t, $^3J_{\text{PF}} = 24.6$ Hz)

$\delta^{19}\text{F}$ (188.3 MHz): -74.32 ppm (d, $^3J_{\text{FP}} = 24.6$ Hz)

$\delta^{13}\text{C}$ (75.5 MHz): 23.83 (*p*-CHMe₂); 25.20 (*o*-CHMe₂); 31.36 (*p*-Me₃C); 32.81 (d, $^4J_{\text{CP}} = 6.5$ Hz, *o*-Me₃C); 34.51 (*p*-CHMe₂); 35.18 (*p*-Me₃C); 35.80 (*o*-CHMe₂); 37.77 (*o*-Me₃C); 122.39 (*m*-CH (Tip and Mes*)); 123.71 (t, $^2J_{\text{CF}} = 6.9$ Hz, C-*ipso* Tip); 132.12 (d, $^1J_{\text{CP}} = 62.4$ Hz, C-*ipso* Mes*); 151.66 (*p*-C Tip); 153.63 (*p*-C Mes* and *p*-C Tip); 155.54 (*o*-C Mes*); 161.1 (d, $^1J_{\text{CP}} = 75.3$ Hz, $^2J_{\text{CF}} = 11.1$ Hz, P=C-GeF₂)

MS (m/z, %): 638 (M, 33); 623 (M - Me, 75); 595 (M - *i*Pr, 37); 580 (M - *i*Pr - Me, 33); 435 (M - Tip, 9); 393 (M - Mes*, 7); 275 (Mes*P - 1, 77); 203 (Tip, 8); 57 (*t*Bu, 100).

6) Action of Mes*Li on Mes*P=C(Cl)Ge(Tip)F₂ 11

A solution of 3.3 mmol *n*BuLi (2.1 ml, 1.6 M in hexane) was added dropwise at -85 °C to 1.05 g Mes*Br (3.2 mmol) in 5 ml of THF; the reaction mixture was kept under stirring for 3 hours at -80 °C, and 2.02 g of Mes*P=C(Cl)Ge(Tip)F₂ (3.2 mmol) in 10 ml THF was added and then allowed to gradually warm up to room temperature. THF was removed under vacuum and replaced with 30 ml pentane. Lithium salts were removed by filtration. White crystals of **12** were obtained from ether (1.6 g, η = 38% , m.p. > 400 °C).

$\delta^1\text{H}$ (300 MHz): 1.24 (d, $^3J_{\text{HH}} = 7.0$ Hz, 36H, CHMe₂); 1.29, 1.30 and 1.37 (3s, *p* and *o*-*t*Bu); 2.88 (sept, $^3J_{\text{HH}} = 6.7$ Hz, *p*-CHMe₂); 3.42 (sept, $^3J_{\text{HH}} = 6.8$ Hz, *o*-CHMe₂); 7.04 (s, 4H, arom H Tip); 7.33 (d, $^4J_{\text{HP}} = 1.3$ Hz, 4H, arom H Mes*).

$\delta^{31}\text{P}$ (121.5 MHz): δ 300.39 ppm (t, $^3J_{\text{PF}} = ^4J_{\text{PF}} = 17.4$ Hz).

$\delta^{19}\text{F}$ (188.3 MHz): -65.4 ppm (t, $^3J_{\text{FP}} = ^4J_{\text{FP}} = 17.4$ Hz).

$\delta^{13}\text{C}$ (75.5 MHz): 24.24 (*p*-CHMe); 24.25 (*p*-CHMe'); 25.27 (*o*-CHMe); 25.61 (*o*-CHMe'); 31.3 (*p*-Me₃C); 32.95 and 33.10 (2d, $^4J_{\text{CP}} = 6.2$ Hz, *o*-Me₃C); 34.71 (*p*-CHMe₂); 35.28 (*o*-CHMe₂); 35.41 (*p*-Me₃C); 38.00 and 38.08 (2s, *o*-Me₃C); 122.30 and 122.36 (2s, *m*-CH (Mes*)); 122.51 (*m*-CH (Tip)); 127.23 (t, $^2J_{\text{CF}} = ^3J_{\text{CF}} = 4.1$ Hz, *ipso*-C Tip); 134.2 (d, $^1J_{\text{CP}} = 63.4$ Hz, *ipso*-C Mes*); 151.1 and 152.25 (*p*-C Tip and *p*-C Mes*); 153.78 and 153.9 (2s, *o*-C Mes*); 155.78 (*o*-C Tip); 166.53 (ddd, $^1J_{\text{CP}} = 79.5$ Hz, $^2J_{\text{CF}} = 6.1$ Hz, $^3J_{\text{CF}} = 5.1$ Hz, P=C-Ge).

MS (Z/e): 1253 (M + 17, 100); 1235 (M - 1, 95); 1217 (M - F, 20); 1051 (M - Tip + 17 + 1, 20); 1009 (M - Ar + 17 + 1, 50); 942 (M - ArP=C(Cl) + 29, 16); 635 (M/2 + 17 - 1, 10); 617 (M/2 - F + 17, 15).

7) Synthesis of Mes*P=C(Cl)Ge(Cl)Tip₂ 17

To a solution of 2.6 g Mes*PCCl₂ (7.2 mmol) in 30 ml of THF, 5 ml of *n*BuLi 1.6M were added at -90 °C. The reaction mixture was stirred for an hour at -85 °C and then a solution of 4 g of Tip₂GeCl₂ (7.2 mmol) in 30 ml THF, cooled at -70 °C, were cannulated slowly on the lithium derivative **2**. The solution was allowed to warm up at

room temperature and the solvent was removed under vacuum and replaced with pentane. LiCl was removed by filtration. Several attempts to obtain a crystalline product failed but after a few days at -25 °C, derivative **17** precipitated as a white solid ($\eta = 52\%$).

$\delta^1\text{H}$ (300 MHz): 1.22-1.32 (wide signal, 36H, *o*- and *p*-CHMe₂); 1.42 (s, 9H, *p*-*t*Bu); 1.57 (s, 18H, *o*-*t*Bu); 2.85 (m, 2H, *p*-CHMe₂); 3.2 (m, 4H, *o*-CHMe₂); 6.94 (s, 1H, *m*- arom H of Tip); 7.05 ppm (s, 1H, *m*- arom H of Tip); 7.50 (s, 2H, arom H of Mes*).

$\delta^{31}\text{P}$ (121.5 MHz): 304.67 ppm

$\delta^{13}\text{C}$ (75.5 MHz): 176.57 ppm (d, $^3J_{\text{CP}} = 95$ Hz, P=C-Ge)

8) Synthesis of dichloro(*N,N*-dimethylbenzylideneamine)-*tert*-butyl-germane **18**

To 4.5 ml (4 g, 29 mmol, 10% excess) of PhCH₂NMe₂ in 30 ml of ether, 16.25 ml *n*BuLi 1.6 M (26 mmol) were added dropwise and then the reaction mixture was stirred at room temperature for 24 hours, when a white precipitate appeared, and then it was cooled down to 0 °C. A solution of 6.25 g of *t*BuGeCl₃ (26 mmol) in 40 ml of THF was cooled to 0 °C and then cannulated drop by drop to the lithium derivative of the amine. The mixture was allowed to react for ½ hours and then the solvents were removed under vacuum and replaced with 40 ml of pentane. Lithium salts were separated by filtration and the solution was stored at -25 °C for 24 hours. The solution was concentrated until **15** precipitates as a white solid (7 g, $\eta = 60\%$).

$\delta^1\text{H}$ (300 MHz): 1.33 (s, 9H, *t*Bu, C(CH₃)₃); 2.17 (s, 6H, methyl, CH₃); 3.61 (s, 2H, methylene, CH₂); 7.39-8 (m, 4H, arom H)

$\delta^{13}\text{C}$ (75.5 MHz): 27.08 (*t*Bu, C(CH₃)₃) 38.26(*t*Bu, C(CH₃)₃); 45.35 (Me, CH₃); 63.43(methylene, CH₂); 127.30-144.84 (arom C)

9) Synthesis of (Me₂NCH₂C₆H₄)*t*BuGe(Cl)C(Cl)=PMes* **19**

To 2.6 g (7.2 mmol) of **1** in 40 mL of THF cooled at -95 °C, 4.95 mL of *n*BuLi 1.6 M in hexane (10% excess) were added dropwise. The reaction mixture was stirred at

low temperature (-75 °C) for 45 minutes. A solution of 2.4 g of **18** in 30 ml of THF was cannulated slowly on to the lithium derivative **2**, after it had been previously cooled down to -70 °C. The reaction mixture was then allowed to gradually warm up to room temperature and THF was removed under vacuum. Replacement with pentane allowed for the precipitation and separation of the lithium salts. ³¹P-NMR spectra indicates the formation of **19**, which could not be separated from the by-product Mes*P=CHCl. The estimated yield (in ³¹P NMR) was 40%.

$\delta^{31}\text{P}$ (121.5 MHz): 300.3 ppm

Transparent crystals are obtained from a pentane solution stored at room temperature and were later identified by X-ray crystallography as derivative **20**.

$\delta^1\text{H}$ (300 MHz, C₆D₆): 1.48 (s, 9H, *t*Bu, C(CH₃)₃), 1.70 (s, 12H, NCH₃), 2.92 (d, 2H, CH₂, ²J_{HH} = 12 Hz), 3.26 (d, 2H, CH₂, ²J_{HH} = 12 Hz), 7.15-7.20, 8.13-8.19 (broad signals, 8H, arom H)

*10) Attempted Synthesis of (Me₂NCH₂C₆H₄)*t*BuGe(Cl)C(SnMe₃)=PMes* 22*

To a solution of 2.6 ml of **2** in 20 ml THF, prepared as described above, 10 ml of a THF solution of Me₃SnCl₂ (0.52 g, 2.6 mmol) were added dropwise at -70 °C. The resulting mixture was used without any further purification; as Mes*PCCl(SnMe₃) was identified by ³¹P NMR to form in almost quantitative yield. 2 ml of *t*BuLi 1.5M in hexane were then added at low temperature and after 15 minutes, 0.9 g (2.6 mol) of **19** in 15 ml THF were cannulated. The solution was allowed to slowly warm up at room temperature. The formation of the expected Mes*P=C(SnMe₃)Ge(Me₂NCH₂C₆H₄)(Cl)*t*Bu was not evidenced, instead, derivative **19** was formed:

$\delta^{31}\text{P}$ (121.5 MHz): 300.3 ppm

11) Action of *t*BuLi on 19

To the THF solution of a mixture of 16 and Mes*P=CHCl (1.55 g, in a 3.6:1 molar ratio), 2 ml *t*BuLi 1.5M in pentane were added at -90 °C. The solution was allowed to warm up to room temperature, and then the reaction products were characterized by ³¹P-NMR and the lithioderivative of **19** was assigned the peak at 403 ppm. At room temperature, only the hydrolysis product of the lithioderivative, compound **23**, was observed in phosphorus NMR (δ ppm: 322.2 ppm (d, $J_{\text{PH}} = 24.85$ Hz)). Upon adding an excess of Me₃SnCl to a sample solution of **21**, the signal shifted at higher fields, which was consistent with the formation of **22**.

$\delta^{31}\text{P}$ (121.5 MHz): 147 ppm

12) Synthesis of bis[1-chloro-2-(1,3,5-tri-*tert*-butyl-phenyl)phosphaalkene] methyl-chlorosilane 24

To a solution of 2 g Mes*PCCl₂ (5.4 mmol) in 30 mL of THF 3.8 mL of *n*BuLi 1.6M was added at -90 °C. The reaction mixture was stirred for an hour at -85 °C and then added dropwise to a solution of 0.40 g Me₃SiCl (2.7 mmol) in 15 ml of THF, cooled at -70 °C. The solution was allowed to warm up at room temperature and the solvent was removed under vacuum and replaced with pentane. LiCl was removed by filtration. Attempts to obtain crystalline product failed. By removing the pentane a light-yellow solid mixture was obtained from which compound **24** was identified through NMR data.

$\delta^{31}\text{P}$ (121.5 MHz): 321.6 ppm

13) Synthesis of {[Bis(bis-trimethylsilylmethyl)chlorostannyl]-chloromethylene}-(2,4,6-tri-*tert*-butyl-phenyl)phosphane 26

To a solution of 2.12 g Mes*P=CCl₂ (5.9 mmol) in 30 ml of THF 3.3 ml of *n*BuLi 1.6M were added at -90 °C. The reaction mixture was stirred for an hour at -85 °C and

then added dropwise to a solution of 3 g of Bi_2SnCl_2 (5.9 mmol) in 30 ml of THF, cooled at $-70\text{ }^\circ\text{C}$. The solution was allowed to warm up at room temperature and the solvent was removed under vacuum and replaced with pentane. LiCl was removed by filtration. Several attempts to obtain a crystalline product failed but by eliminating the pentane, a white solid mixture was obtained from which compound **26** was identified only by ^{31}P NMR in a fairly poor yield ($\eta = 50\%$ from ^{31}P NMR)

$\delta^1\text{H}$ (300 MHz): 0.24 ppm (s, 3H, Me_3Si); 0.27 ppm (s, 3H, Me_3Si), 1.33 ppm (s, 9H, *p*-*t*Bu); 1.49 ppm (s, 18H, *o*-*t*Bu), 7.40 ppm (s, 2H, arom H)

$\delta^{31}\text{P}$ (121.5 MHz): 305.49 ppm (s, $^2J_{\text{PSn}} = 365.66\text{ Hz}$)

$\delta^{13}\text{C}$ (75.5 MHz): 174.25 ppm (d, $^2J_{\text{PC}} = 102.85\text{ Hz}$)

$\delta^{119}\text{Sn}$: 43.60 ppm (d, $^2J_{\text{PSn}} = 363.74\text{ Hz}$)

14) Action of *t*BuLi on 26

A solution of 3.77 g of **22** (4.7 mmol) in 50 ml THF was cooled down to $-80\text{ }^\circ\text{C}$ and then 3.4 ml *t*BuLi 1.5M in hexane (10 % excess) were added dropwise. The reaction mixture was allowed to warm up slowly to room temperature and the THF was removed under vacuum and replaced with pentane. The lithium salts were removed by filtration. Attempts to separate the derivative **27** failed, but the compound was identified through ^{31}P and ^{119}Sn NMR. The lithium derivative was also identified in ^{31}P NMR (409.8 ppm, $^2J_{\text{PSn}} = 982\text{ Hz}$)

$\delta^{31}\text{P}$ (121.5 MHz): 327.12 ppm (d, $^4J_{\text{PP}} = 33,56\text{ Hz}$, $^2J_{\text{PSn}} = 365,05\text{ Hz}$)

451.35 ppm (d, $^4J_{\text{PP}} = 33,56\text{ Hz}$, $^2J_{\text{PSn}} = 415,05\text{ Hz}$)

$\delta^{119}\text{Sn}$: 176.7 (d, $^2J_{\text{PSn}} = 415.1\text{ Hz}$)

43.9 ppm (d, $^2J_{\text{PSn}} = 365.1\text{ Hz}$)

15) Synthesis of bis-dibromomethyl-bis-(2,4,6-triisopropylphenyl)stannane 31 and tribromomethyl-bis-(2,4,6-triisopropylphenyl)bromostannane 32

A mixture of 2 g (0.0035 mol) Tip_2SnF_2 and 1.77 g CHBr_3 (0.007 mols) in 70 ml THF was cooled at $-90\text{ }^\circ\text{C}$ and 4.5 ml $n\text{BuLi}$ 1.6 M (0.0072 mols) were added dropwise. The reaction mixture was stirred for half an hour at $-90\text{ }^\circ\text{C}$ and then it was allowed to warm up at room temperature. The solvent was removed under vacuum and replaced with 20 ml pentane. Lithium salts were removed by filtration and the filtrate was stored at $-25\text{ }^\circ\text{C}$. After 24 hours, compound **31** was isolated by filtration as a white powder with a 45% yield. The remaining solution was further concentrated under vacuum and stored at $-25\text{ }^\circ\text{C}$. Transparent crystals of **32** were isolated after a few hours with a 11% yield.

31: $\delta^1\text{H}$ (300 MHz): 1.50 ppm (d, $^3J_{\text{HH}} = 6.4\text{ Hz}$, 24H, CH_3 , *o*-iPr); 1.18 ppm (d, $^3J_{\text{HH}} = 6.4\text{ Hz}$, 12H, CH_3 , *p*-iPr); 2.58 (sept, $^3J_{\text{HH}} = 6.4\text{ Hz}$, 4H, CH , *o*-iPr); 2.82 (sept, $^3J_{\text{HH}} = 6.4\text{ Hz}$, 2H, CH , *p*-iPr); 5.80 (s, 2H, CHBr_2); 6.96 (s, 4H, meta- CH Tip).

$\delta^{13}\text{C}$ (75.5 MHz): 23.9 ppm (CH_3 , *o*-iPr); 24.7 ppm (CH_3 , *p*-iPr); 32.5 ppm (CH , *o*-iPr) 34.3 ppm (CH , *p*-iPr); 40.1 ppm (CHBr_2); 122.6 (*m*- CH Tip); 150.9 and 151.6 ppm (*o* and *p*-C Tip).

MS (Z/e): 697 (M- CHBr_2), m.p. = $177\text{ }^\circ\text{C}$

32: $\delta^1\text{H}$ (300 MHz): 1.05 ppm (d, $^3J_{\text{HH}}=6.2\text{ Hz}$, 6H, CH_3 , *o*-iPr); 1.080 ppm (d, $^3J_{\text{HH}}=5.8\text{ Hz}$, 6H, CH_3 , *o*-iPr); 1.194 ppm (d, $^3J_{\text{HH}}=7\text{ Hz}$, 6H, CH_3 , *p*-iPr); 2.567 ppm (m, 1H, CH , *p*-iPr); 3.35 ppm (m, 2H, CH , *o*-iPr), 7.080 ppm (s, 4H, *m*- CH of Tip).

Table IV.7. Crystal data and structure refinement for **20**

Empirical formula	C ₂₂ H ₃₃ ClGeN ₂	
Formula weight	433.54	
Temperature	173(2) K	
Wavelength	0.71073 Å	
Crystal system	Monoclinic	
Space group	P2(1)/c	
Unit cell dimensions	a = 9.169(9) Å	α = 90°.
	b = 10.927(11) Å	β = 94.116(18)°.
	c = 22.145(17) Å	γ = 90°.
Volume	2213(4) Å ³	
Z	4	
Density (calculated)	1.301 Mg/m ³	
Absorption coefficient	1.513 mm ⁻¹	
F(000)	912	
Crystal size	0.1 x 0.4 x 0.4 mm ³	
Theta range for data collection	5.24 to 23.25°.	
Index ranges	-6 ≤ h ≤ 9, 0 ≤ k ≤ 12, -20 ≤ l ≤ 11	
Reflections collected	2871	
Independent reflections	2305 [R(int) = 0.1621]	
Completeness to theta = 23.25°	72.5 %	
Absorption correction	None	
Refinement method	Full-matrix least-squares on F ²	
Data / restraints / parameters	2305 / 205 / 242	
Goodness-of-fit on F ²	0.879	
Final R indices [I > 2σ(I)]	R1 = 0.0701, wR2 = 0.1189	
R indices (all data)	R1 = 0.1777, wR2 = 0.1485	
Largest diff. peak and hole	0.646 and -0.463 e.Å ⁻³	

Resolution of the structure of 20

2305 independent reflections were collected at low temperatures (T = 173(2) K) using an oil-coated shock-cooled crystal on a Bruker-AXS CCD 1000 diffractometer with MoK α radiation (λ = 0.71073 Å). The structure was solved by direct methods [28] and 242 parameters were refined using the least-squares method on F^2 [29]. All non hydrogen atoms were refined anisotropically.

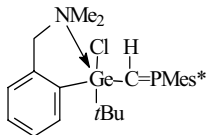
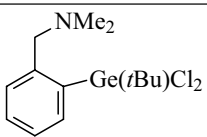
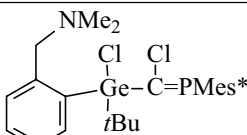
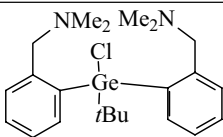
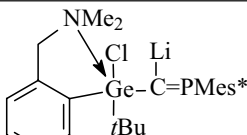
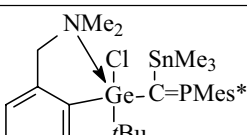
The largest electron density residue is $0.646 \text{ e}\text{\AA}^{-3}$ and R_1 (for $I > 2\sigma(I)$) = 0.0798 and $wR_2 = 0.1189$ (all data) with $R_1 = \Sigma||F_o| - |F_c|| / \Sigma|F_o|$ and $wR_2 = (\Sigma w(F_o^2 - F_c^2)^2 / \Sigma w(F_o^2)^2)^{0.5}$.

References

1. For reviews on heteroallenes, see: a) Escudié, J.; Ranaivonjatovo, H.; Rigon, L.; *Chem. Rev.*, **2000**, *100*, 3639; b) Eichler, B.; West, R.; *Adv. Organomet. Chem.*, **2001**, *46*, 1; c) Escudié, J.; Ranaivonjatovo, H.; *Organometallics*, **2007**, *26*, 1542
- 2.a) Trommer, M.; Miracle, G. E.; Eichler, B. E.; Powell, D. R.; West, R.; *Organometallics*, **1997**, *16*, 5737; b) Eichler, B. E.; Miracle, G. E.; Powell, D. R.; West, R.; *Main Group Met. Chem.*, **1999**, *22*, 147.
3. Eichler, B. E.; Powell, D. R.; West, R.; *Organometallics*, **1998**, *17*, 2142.
4. El Harouch, Y.; Gornitzka, H.; Ranaivonjatovo, H.; Escudié, J.; *J. Organomet. Chem.*, **2002**, *643-644*, 202.
5. Chaubon, M. A.; Dittrich, B.; Escudié, J.; Ramdane, H.; Ranaivonjatovo, H.; Satgé, J.; *Synth. React. Inorg. Met.-Org. Chem.*, **1997**, *27*, 519.
6. For a review on ^{31}P chemical shifts in $-\text{P}=\text{C}<$ derivatives, see Lochschmidt, S.; Schmidpeter, A.; *Phosphorus and Sulfur*, **1986**, *29*, 73.
7. Purcell and Kotz, *Inorganic Chemistry*, Ed. W.B. Sanders, **1977**.
8. Escudié, J.; Couret, C.; Andriamizaka, J.D.; Satgé, J. *J. Organomet. Chem.* **1982**, *C76*, 228.
9. Ando, W.; Itoh, H.; Tsumuraya, T.; *Organometallics*, **1989**, *8*, 2759.
10. a) Leung, W.-P.; Chong, K.-H.; Wu, Y.-S.; So, C.-W.; Mak, T. C. W.; *Eur. J. Inorg. Chem.* **2006**, *4*, 808; b) Leung, W.-P.; Chong, K.-H.; Zhou, Z.-Y.; Mak, T. C. W.; *Organometallics*, **2000**, *19*, 293.
- c) Veith, M.; Rammo, A.; *Z. Anorg. Allg. Chem.*, **1997**, *623*, 861.
11. Ossig, G.; Meller, A.; Brönneke, C.; Müller, O.; Schafer, M.; Herbst-Irmer, R.; *Organometallics*, **1997**, *16*, 2116.
12. Van Koten, G.; Jastrzebski, J. T. B. H.; Noltes, J. G.; Pontenagel, W. M. G. F.; Kroon, J.; Spek, A.L.; *J. Am. Chem. Soc.*, **1978**, *100*, 5021.
13. Puff, H.; Franken, S.; Schuh, W.; Schwab, W.; *J. Organomet. Chem.*, **1983**, *254*, 33.
14. a) Brelière, C.; Carré, F.; Corriu, R. J. P.; De Saxce, A.; Poirier, M.; Royo, G.; *J. Organomet. Chem.*, **1981**, *205*, C1; b) Baines, K. M.; Stibbs, W. G.; *Coord. Chem. Rev.*, **1995**, *145*, 157.

15. Nemes, G.; Ranaivonjatovo, H.; Escudié, J.; Silaghi-Dumitrescu, I.; Silaghi-Dumitrescu, L.; Gornitzka, H.; *Eur. J. Inorg. Chem.*, **2005**, 1109.
16. Cowley, A. H.; Jones, R. A.; Lasch, J. G.; Norman, N. C.; Stewart, C. A.; Stuart, A. L.; Atwood, J. L.; Hunter, W. E.; Zhang, H.-M.; *J. Am. Chem. Soc.*, **1985**, *106*, 7015.
17. Goede, S. I.; Bickelhaupt, F.; *Chem. Ber.*, **1991**, *124*, 2677.
18. Ramdane, H.; Ranaivonjatovo, H.; Escudié, J.; *Organometallics*, **1996**, *15*, 3070.
19. Rigon, L.; Ranaivonjatovo, H.; Escudié, J.; Dubourg, A.; Declercq, J.-P.; *Chem. Eur. J.*, **1999**, *5*, 774.
20. Baiget, L.; Ranaivonjatovo, H.; Escudié, J.; Gornitzka, H.; *J. Am. Chem. Soc.*, **2004**, *126*, 11792.
21. Wiberg, N.; Wagner, G.; *Chem. Ber.*, **1986**, *119*, 1455.
22. Anselme, G.; Ranaivonjatovo, H.; Escudié, J.; Couret, C.; Satgé, J.; *Organometallics*, **1992**, *11*, 2748.
23. Abdul Fatah; El Ayoubi, R.; Escudié, J.; Ranaivonjatovo, H.; Gornitzka, H.; *private communication*.
24. Ramdane, H.; Ranaivonjatovo, H.; Escudié, J.; Knouzi, N.; *Organometallics*, **1996**, *15*, 2683.
25. Goede, S. J.; Bickelhaupt, F.; *Chem. Ber.*, *124*, **1991**, 2677.
- 26.a) Preut, H.; Huber, F.; *Acta Crystallogr., Sect. B: Struct. Crystallogr. Cryst. Chem.* **1979**, *35*, 744; b) Saito, M.; Haga, R.; Yoshioka, M.; *Heteroat. Chem.*, **2001**, *12*, 349; c) Alcock, N.W.; Sawyer, J. F.; *J. Soc., Dalton Trans.*, **1977**, 1090; d) Brown, P.; Mahon, M. F.; Molloy, K. C.; *J. Organomet. Chem.*, **1992**, *435*, 265.
27. a) Konig, U. C.; Berkei, M.; Neikes, F.; Preut, H.; Mitchell, T.N.; *Acta Crystallogr., Sect. C: Cryst. Struct. Commun.*, **2000**, *56*, 53; b) Bajue, S. A.; Bramwell, F. B.; Charles, M.; Cervantes-Lee, F.; Pannell, K.; *Inorg. Chim. Acta*, **1992**, *197*, 83; c) Tang, L. F.; Wang, Z.H.; Jia, W.L.; Xu, Y.M.; Wang, J.T.; *Polyhedron*, **2000**, *19*, 381.
28. SHELXS-97, Sheldrick, G. M.; *Acta Crystallogr.* **1990**, *A46*, 467.
29. SHELXL-97, Program for Crystal Structure Refinement, Sheldrick, G. M.; University of Göttingen, **1997**.

Chapter IV- Recapitulative list of synthesized compounds

Derivative	Number	Derivative	Number
$\text{Mes}^*\text{P}=\text{C} \begin{array}{c} \text{Cl} \\ \\ \text{C}-\text{Ge}-\text{Tip} \\ \quad \\ \text{Cl} \quad \text{Cl} \end{array}$	9		<u>23</u>
$\text{Mes}^*\text{P}=\text{C} \begin{array}{c} \text{OMe} \\ \\ \text{C}-\text{Ge}-\text{Tip} \\ \quad \\ \text{Cl} \quad \text{OMe} \end{array}$	10	$\text{Mes}^*\text{P}=\text{C} \begin{array}{c} \text{Cl} \\ \\ \text{C}-\text{Si}-\text{C}=\text{PMes}^* \\ \quad \quad \\ \text{Cl} \quad \text{Me} \quad \text{Cl} \end{array}$	<u>24</u>
$\text{Mes}^*\text{P}=\text{C} \begin{array}{c} \text{F} \\ \\ \text{C}-\text{Ge}-\text{Tip} \\ \quad \\ \text{Cl} \quad \text{F} \end{array}$	11	$\text{Mes}^*\text{P}=\text{C} \begin{array}{c} \text{Cl} \\ \\ \text{C}-\text{Si}-\text{C}=\text{PMes}^* \\ \quad \quad \\ \text{Cl} \quad \text{Ph} \quad \text{Cl} \end{array}$	<u>25</u>
$\text{Mes}^*\text{P}=\text{C} \begin{array}{c} \text{Tip} \quad \text{Tip} \\ \quad \\ \text{C}-\text{Ge}-\text{Ge}-\text{C}=\text{PMes}^* \\ \quad \quad \quad \\ \text{Cl} \quad \text{F} \quad \text{F} \quad \text{Cl} \end{array}$	<u>12</u>	$\text{Mes}^*\text{P}=\text{C}(\text{Cl})\text{Sn}(\text{Cl})\text{Bis}_2$	<u>26</u>
$\text{Mes}^*\text{P}=\text{C} \begin{array}{c} \text{Cl} \\ \\ \text{C}-\text{Ge}-\text{Tip} \\ \quad \\ \text{Cl} \quad \text{Tip} \end{array}$	<u>17</u>	$\text{Mes}^*\text{P}=\text{C} \begin{array}{c} \text{Li} \quad \text{SnBis}_2 \\ \quad \\ \text{C}-\text{Sn} \\ \quad \\ \text{Li} \quad \text{Cl} \end{array}$	<u>27</u>
	<u>18</u>	$\text{Mes}^*\text{P}=\text{C} \begin{array}{c} \text{Bis} \quad \text{Bis} \\ \quad \\ \text{C}-\text{Sn}-\text{C}-\text{Sn}-\text{Cl} \\ \quad \quad \quad \\ \text{Cl} \quad \text{Bis} \quad \text{P} \quad \text{Bis} \\ \quad \quad \quad \\ \quad \quad \quad \text{Mes}^* \end{array}$	<u>28</u>
	<u>19</u>	$\text{Mes}^*\text{As}=\text{CBr}_2$	30
	<u>20</u>	$\text{Tip}_2\text{Sn} \begin{array}{c} \text{CHBr}_2 \\ \\ \text{CHBr}_2 \end{array}$	<u>31</u>
	<u>21</u>	$\text{Tip}_2\text{Sn} \begin{array}{c} \text{CBr}_3 \\ \\ \text{Br} \end{array}$	<u>32</u>
	<u>22</u>		

N – novel compounds

CHAPTER V

***A NEW PHOSPHAARSAALLENE: THE
ARSENYLIDENE BIS(METHYLENEPHOSPHORANE)***



Chapitre V

Un nouveau phospharsaallène: L'arsenylidenebis(méthylène)phosphorane



Le premier composé stable à liaisons multiples du phosphore contenant l'unité $\text{C}=\text{P}=\text{C}$ a été décrit pour la première fois en 1982. Ce type de dérivés présente un grand intérêt comme briques moléculaires en chimie du phosphore ; de plus ses multiples possibilités de coordination en font des ligands polyvalents dans la synthèse des complexes de métaux de transition. Nos recherches ont porté sur la fonctionnalisation de cette structure grâce à des substituants comportant des éléments de groupes 14 et 15, qui par leurs effets électroniques peuvent modifier les propriétés de cette unité. Nous avons également tenté la synthèse d'hétérocumulènes du type $\text{E}=\text{C}=\text{PR}=\text{C}<$ (E = éléments de groupes 14 et 15).

Ce chapitre décrit la synthèse et la caractérisation du premier bis(méthylène)phosphorane **2** substitué par un groupement arsanyle, à partir du dichlorobis(méthylène)phosphorane **1** (schéma V.1).

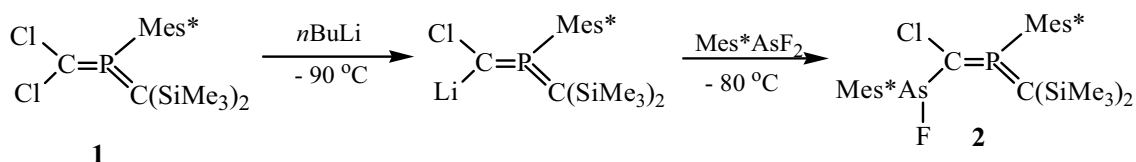


Schéma V.1

Un seul signal est observé dans le spectre de RMN ^{31}P du composé **2**, car seul l'isomère *E* est formé, avec l'atome de chlore dans une position *trans* par rapport au groupement Mes^* , indiquant une attaque de $n\text{BuLi}$ du côté le moins encombré de la double liaison $\text{P}=\text{C}$. La structure de **2** en solution a été élucidée par spectroscopie de RMN ^1H , ^{31}P et ^{19}F .

Le composé **2** a été isolé sous forme d'aiguilles jaunes et transparentes et caractérisé par diffraction des rayons X. Sa structure moléculaire est représentée dans la figure V.1, avec les valeurs les plus importantes des paramètres géométriques.

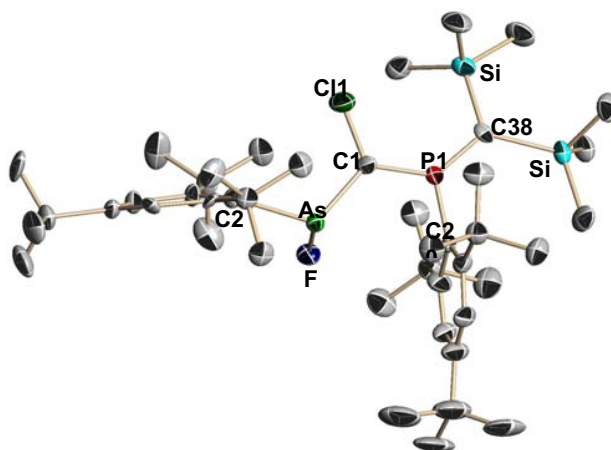


Figure V.1. Structure moléculaire de $(\text{Me}_3\text{Si})_2\text{C}=\text{P}(\text{Mes}^*)=\text{C}(\text{Cl})-\text{As}(\text{F})\text{Mes}^*$. Longueurs des liaisons (Å) et angles ($^\circ$) sélectionnés. As-F: 1.783(8); As-C(2): 1.999(9); As-C(1): 1.951(9); C(1)-Cl: 1.730.8; C(1)-P: 1.684(8); P-C(20):1.803(7); P-C(3): 1.661(8); C(38)-Si(1): 1.884(8); C(38)-Si(2): 1.857(8); FAsC(1) : 101.3(4) ; AsC(1)Cl: 119.0(4); ClC(1)P: 119.8(5); C(1)PC(20): 106.7(4); C(1)PC(38): 129.6(4); C(20)PC(38): 123.6(4); AsC(1)PC(38): 175.4; FAsC(1)Cl: 120.7; FAsC(1)P: 63.8; ClC(1)PC(38): 9.2.

La réaction de dérivé **2** avec *t*BuLi a été suivie en RMN ^{31}P . Seulement 50% de l'arsanylbis(méthylène)phosphorane a été converti en un dérivé caractérisé par un déplacement chimique de 132.4 ppm. Bien qu'il n'ait pas encore été clairement identifié, ce composé pourrait être le premier 2-phospha-4-arsabutatriène **3** connu à ce jour (schéma V.2). Le traitement ultérieur de **3** avec du méthanol déplace le signal observé en RMN ^{31}P à champ faible ($\delta = 164.1$ ppm). Nous pouvons postuler la formation du composé **4** par addition de MeOH sur la double liaison As=C, qui est polarisée $\text{As}^{\delta+}-\text{C}^{\delta-}$. Le spectre de RMN ^{31}P du dérivé **4** présente à peu près le même déplacement chimique que celui de **2** en raison d'une grande similitude de structures (atome de F remplacé par un groupe OMe).

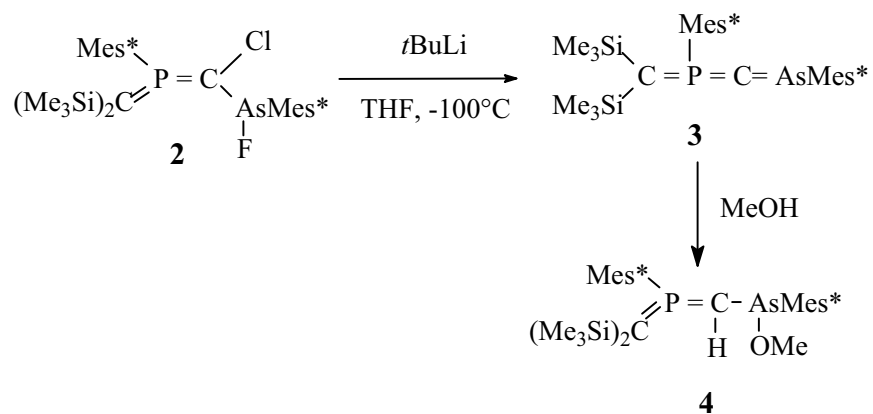
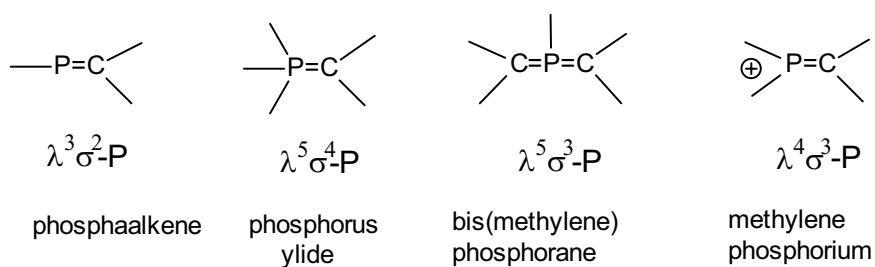


Schéma V.2

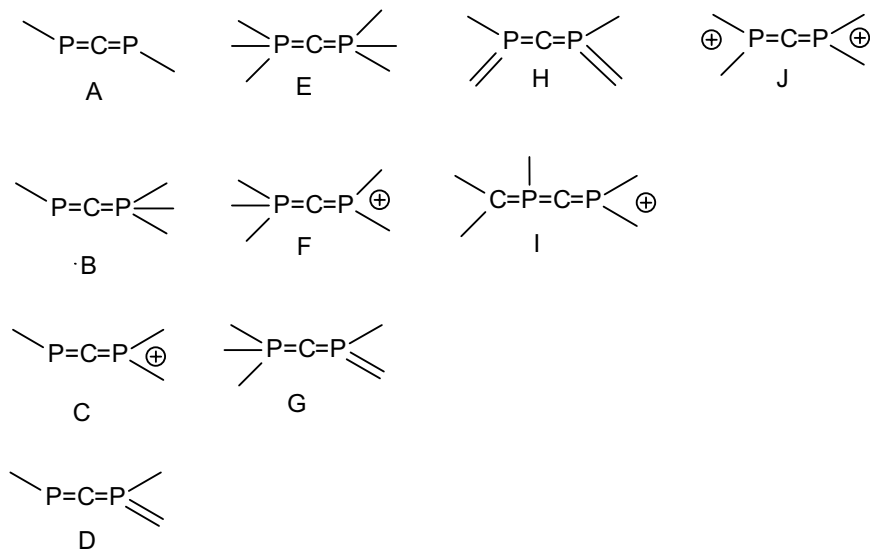
En conclusion, il existe des constatations convergentes en faveur de la formation du premier composé comportant trois doubles liaisons cumulés C=P=C=As même si davantage de caractérisations sont nécessaires afin de confirmer entièrement sa structure.

The phosphorus atom can adopt several coordination numbers, so various types of P=C double bonds could be envisaged (Scheme V.1):



Scheme V.1

Thus, 10 different structures of phosphorus cumulenes can be imagined (Scheme 2):



Scheme V.2

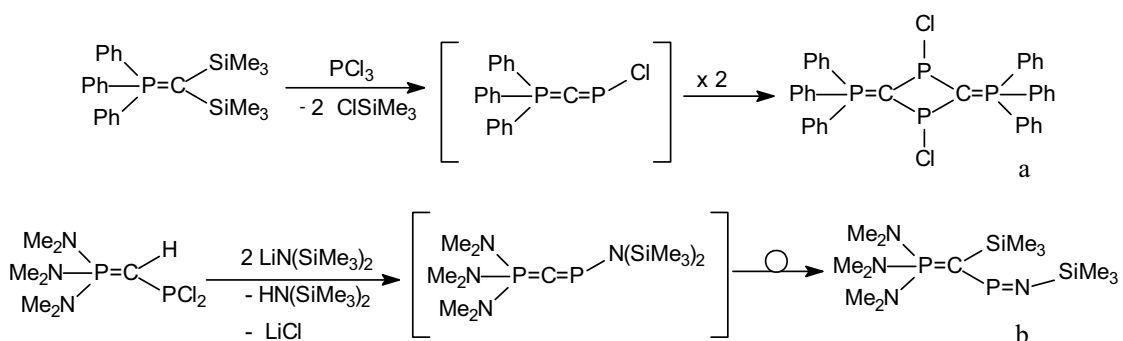
Among the uncharged diphosphaallenes A, B, D, E, G and H, only structures A, B, E and G have been characterized or isolated.

- structure A

Many diphosphaallenes have been obtained as previously said in chapter I [1a, 1b]. Their arsenic analogues $-P=C=As-$ and $-As=C=As-$ are also known [1a, 1b].

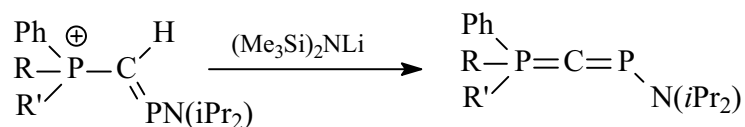
- structure B

Such cumulenes were postulated as intermediates some years ago by Schmidpeter [2a] (Scheme V.3.a) and Grützmacher [2b] (Scheme V.3.b)



Scheme V.3

Only recently stable cumulenes containing $1-\sigma^2$, $3-\sigma^4$ -P atoms have been obtained and isolated from phosphonio-phosphaalkenes (Scheme V.4.) [3a, 3b]:

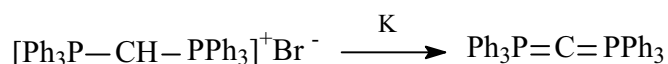


R, R' = Ph, N(*i*Pr₂)

Scheme V.4

- structure E

The first compound of this type, hexaphenylcarbodiphosphorane, was prepared in 1961 by Ramirez (Scheme V.5) [4].

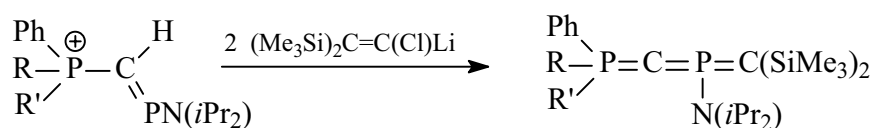


Scheme V.5

Many other derivatives of this type are known to date.

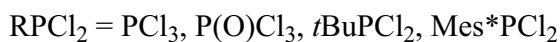
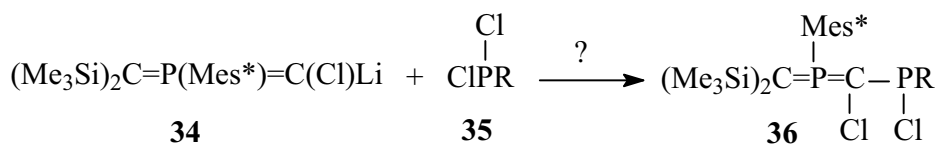
- structure G

Structure G has also been recently prepared by reaction of a phosphonio-phosphaalkene with 2 equivalents of bis(trimethylsilyl)chloromethyl lithium (Scheme V.6.) [3]:



Scheme V.6

Structures D and H are still unknown. A compound with the $-\text{P}=\text{C}=\text{P}(\text{Mes}^*)=\text{O}$ linkage, closely related to the D-type structure, the phosphavinylidene(oxo)phosphorane $\text{Mes}^*\text{P}(\text{O})=\text{C}=\text{P}(\text{Mes}^*)$, has been synthesized recently [5]. Many attempts have been performed by the group of phosphorus chemists of Toulouse (HFA Laboratory) in order to obtain a compound of the type D such as $(\text{Me}_3\text{Si})_2\text{C}=\text{P}(\text{Mes}^*)=\text{C}=\text{PR}$ by the following route (Scheme V.7):



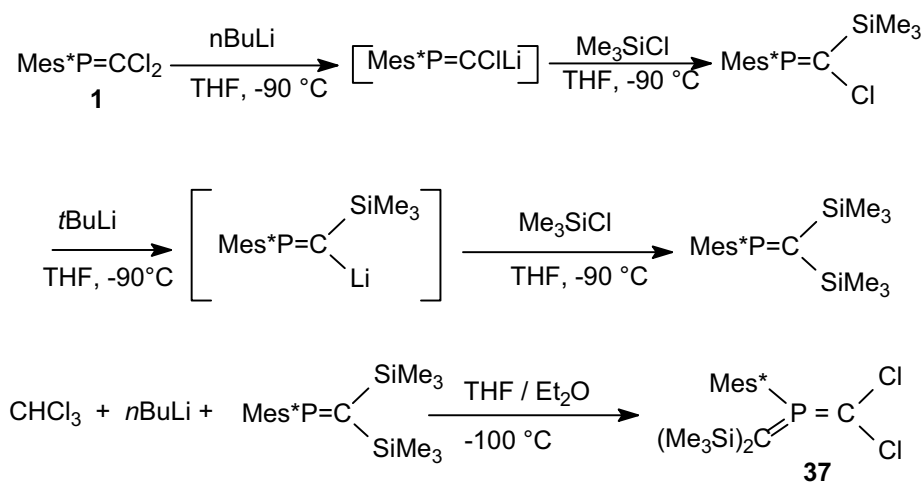
Scheme V.7

The coupling reaction between **34** and PCl_3 , $\text{P}(\text{O})\text{Cl}_3$ and $t\text{BuPCl}_2$ was successful, but other products were formed and purification to obtain **36** was impossible. By contrast, with bulkier Mes^*PCl_2 , no reaction occurred with $(\text{Me}_3\text{Si})_2\text{C}=\text{P}(\text{Mes}^*)=\text{C}(\text{Cl})\text{Li}$, probably for steric reasons.

It seemed then interesting to prepare the arsenic analogue of **D** using Mes^*AsX_2 : in this case, due to longer As-C than P-C bonds, the steric congestion would be less important and the coupling between **34** and Mes^*AsF_2 should be possible.

In this chapter we describe the synthesis of the first arsenylidene-bis(methylene)-phosphorane $(\text{Me}_3\text{Si})_2\text{C}=\text{P}(\text{Mes}^*)=\text{C}=\text{AsMes}^*$, an analogue of compounds with D-type structure presented above.

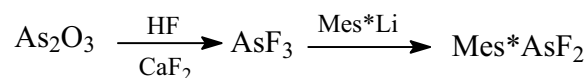
We have envisaged that the already reported bis(methylene)phosphorane $(\text{Me}_3\text{Si})_2\text{C}=\text{P}(\text{Mes}^*)=\text{C}\text{Cl}_2$ **37** would be a good starting point in the synthesis of this compound. The synthesis of **37** was already described in the literature [6], but we modified slightly the procedure (see the experimental section) so that the overall yield of the synthetic route increased from 78% to 92% (scheme V.8): we have added $\text{Mes}^*\text{P}=\text{C}(\text{SiMe}_3)_2$ to the carbenoid LiCCl_3 frozen at $-120\text{ }^\circ\text{C}$, instead of the reverse reaction in which a part of LiCCl_3 decomposes during the cannulation.



Scheme V.8

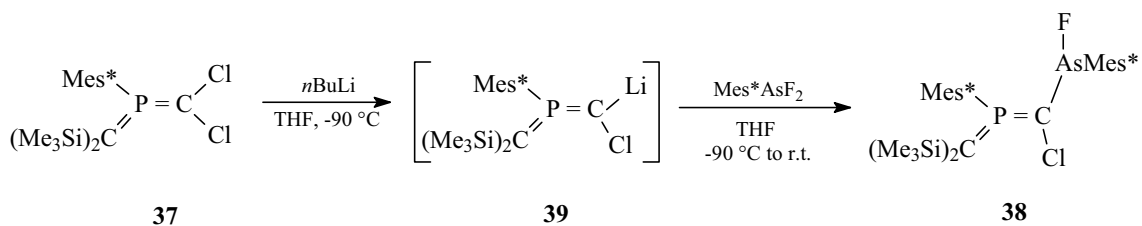
1) Synthesis and characterization of the first arsenylidene-bis(methylene)phosphorane 38

In order to obtain the C=P=C=As unit, the functionalization of **37** with an arsenyl group is necessary, in a similar manner to that described in chapter IV for the synthesis of phosphagermapropenes. Mes*AsF₂ was prepared in a good yield from AsF₃ (obtained from CaF₂ and H₂SO₄) [7] and Mes*Li, as previously described (Scheme V.9.) [8].



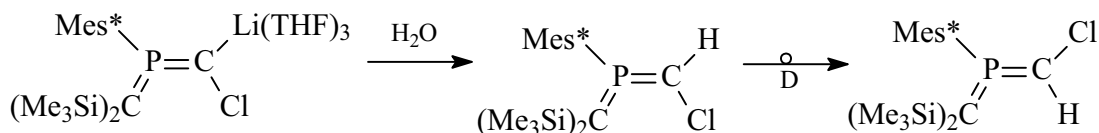
Scheme V.9

Successive additions of *n*-butyllithium and of one equivalent of Mes*AsF₂ to **39** resulted in the formation of the first arsenylbis(methylene)phosphorane **38**, as shown in scheme V.10 [9].



Scheme V.10

A single isomer of **38** was formed according to its NMR spectrum. The X-ray structure studies revealed it to correspond to the *E*-configuration with the arsenic moiety in a *cis* position with respect to the supermesityl group. This finding indicates an attack of *n*-BuLi on the less sterically hindered side of the P=C double bond. The preferential formation of the *Z* isomer **39** was also reported by Niecke [6]. By quenching **39** with water and warming up over 0 °C, it was observed that the resulting *Z* – (Me₃Si)₂C=P(Mes*)=C(Cl)H derivative undergoes a rearrangement into the thermodynamically more stable *E* – derivative (with the H atom in *trans* position with respect to the Mes* group) (scheme V.11):



Scheme V.11

By contrast, in the case of compound **38**, which possesses the very bulky Mes*AsF group instead of the hydrogen atom, such an isomerization did not occur since only the *E* isomer (with the As in a *cis* position with respect to the Mes* group) is observed.

The structure of **38** in solution was confirmed through ¹H and ¹³C NMR spectroscopy which revealed that the rotation around the (Mes*)C-P bond is hindered. In the ¹H NMR spectrum, the non equivalent aromatic protons of the Mes* group bonded to phosphorus appeared as two doublets of doublets due to the coupling with the phosphorus atom (see Figure V.1): the greater coupling constant (4.5 Hz) was attributed to the ⁴J_{HP} by comparison with similar values found in Mes*P(O)=C=PMes* [5]. By contrast, the

aromatic protons on the Mes* group bonded to the arsenic atom gave a singlet indicative of a free rotation around the (Mes*)C-As bond in the NMR time scale. This result is not surprising since the same phenomenon (hindered and free rotation for the Mes* groups bonded to P and As respectively) was observed in the dihalophosphaarsapropene Mes*P=C(Br)-As(F)Mes* [10] which contains a similar Mes*(F)As moiety and a $\lambda^3\sigma^2$ less encumbered phosphorus atom.

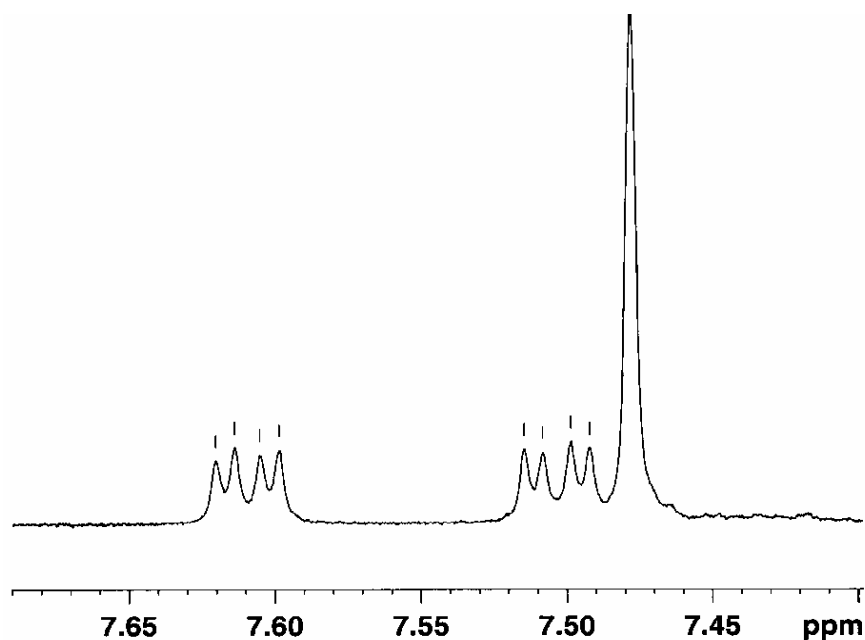


Figure V.1. Detail of the aromatic range in the ^1H -NMR spectrum for derivative **38**

The same non equivalence was observed for the *ortho tert*-butyl groups of the Mes* bonded to P; due to slow or hindered rotation of the Mes* groups, *ortho tert*-butyl groups gave broader signals than did *para tert*-butyl groups allowing an easy assignment.

In the ^{19}F and ^{31}P NMR spectra of **38**, doublets were observed at -151.4 ppm and 157.0 ppm respectively with a $^3J_{\text{PF}}$ coupling constant of 4.5 Hz. Similar chemical shifts have been reported in closely related derivatives (PhP[=C(SiMe₃)₂]₂: $\delta^{31}\text{P}$ =174 ppm [11], Mes*P=C(Br)-As(F)Mes*: $\delta^{19}\text{F}$ = - 175.6 ppm [10]).

The ^{13}C NMR spectrum also pointed to the great steric congestion around the phosphorus atom with two doublets (coupling with P) for the *ortho tert*-butyl groups and the *ortho* and *meta* carbon atoms of the Mes* group on P, whereas only one doublet

(coupling with F) and two singlets were observed for the Mes* groups bonded to As. The different chemical environment of the carbon atoms $\underline{C}(\text{As})$ and $\underline{C}(\text{SiMe}_3)_2$ leads to an asymmetric charge distribution with the negative charge on the latter, since the silyl groups are more capable of stabilizing a negative charge; thus, the corresponding ^{13}C NMR signal was observed at high field (72.33 ppm) with a small $^1J_{\text{CP}}$ coupling constant as previously described for similar derivatives [6].

In mass spectrometry, the molecular peak was observed by electronic impact. The most abundant fragment corresponded to the loss of a Mes* group.

Some relevant NMR data are given in Table V.1.

Table V.1. NMR data for $(\text{Me}_3\text{Si})_2\text{C}=\text{P}(\text{Mes}^*)=\text{C}(\text{Cl})-\text{As}(\text{F})\text{Mes}^*$ **38**

^{13}C NMR	^{19}F NMR	^{31}P NMR
$\delta^{13}\text{C}$: 95.2 ppm (P=C-As), (J_{CF} : 34.1 Hz, J_{CP} : 74.0 Hz),	$\delta^{19}\text{F}$: -151.4 ppm (J_{PF} : 4.5 Hz)	$\delta^{31}\text{P}$: 157.0 ppm (J_{PF} : 4.5 Hz)
$\delta^{13}\text{C}$: 72.3 ppm (P=C(SiMe ₃) ₂), (J_{CP} : 49.0 Hz, J_{CF} : 5.3 Hz).		

Compound **38** was crystallized from pentane as yellow needles and was characterized by X-ray diffraction. Its molecular structure is represented in Figure V.2, together with selected values for significant geometrical parameters.

Like in other bis(methylene)phosphoranes [6], the phosphorus atom has a trigonal-planar arrangement (sum of angles at P: 359.9 °) as have the marginal C atoms C(1) and C(38) in the C=P=C unit. The Mes* group bonded to the phosphorus atom presents an almost orthogonal alignment with regard to the PC₂ unit (torsion angles C(25)C(20)PC(38) = 78.57 ° and C(21)C(20)PC(1) = 93.29 °). The lengths of the PC(1) and PC(38) bonds (1.684(8) and 1.684(8) Å, respectively) are in the normal range for P=C double bonds [12, 13]. The As-C (1.95 Å) bond is also in the standard range for such a derivative, but longer than those in other compounds containing the P=C-As unit with a completely different structure [14, 15].

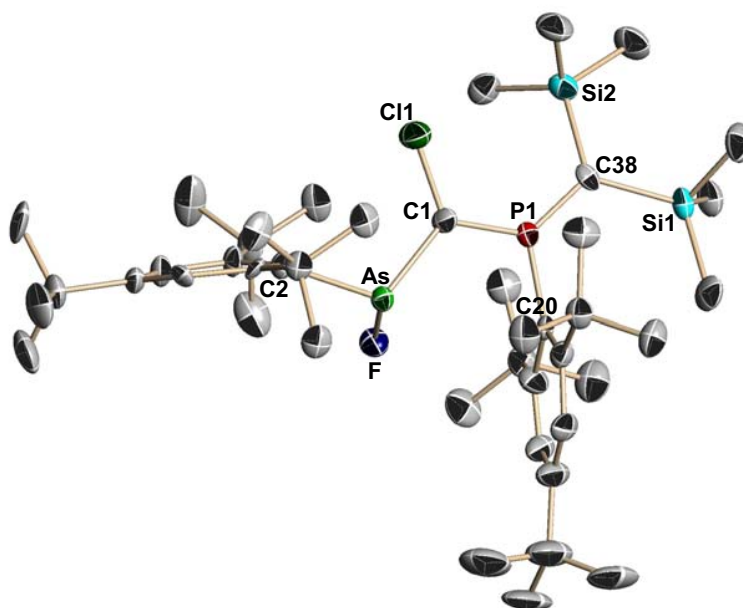


Figure V.2. Molecular structure of $(\text{Me}_3\text{Si})_2\text{C}=\text{P}(\text{Mes}^*)=\text{C}(\text{Cl})-\text{As}(\text{F})\text{Mes}^*$ (thermal ellipsoids drawn at the 50% probability level); hydrogen atoms are omitted for clarity; selected bond lengths (\AA) and angles ($^\circ$). As-F: 1.783(8); As-C(2): 1.999(9); As-C(1): 1.951(9); C(1)-Cl: 1.730.8; C(1)-P: 1.684(8); P-C(20):1.803(7); P-C(38): 1.661(8); C(38)-Si(1): 1.884(8); C(38)-Si(2): 1.857(8); FAsC(1) : 101.3(4) ; AsC(1)Cl: 119.0(4); ClC(1)P: 119.8(5); C(1)PC(20): 106.7(4); C(1)PC(38): 129.6(4); C(20)PC(38): 123.6(4); AsC(1)PC(38): 175.4; FAsC(1)Cl: 120.7; FAsC(1)P: 63.8; ClC(1)PC(38): 9.2.

For example, in the 1-(dichloroarsanylethylidene)triphenylphosphorane $\text{Ph}_3\text{P}=\text{C}(\text{CH}_3)-\text{AsCl}_2$ [15], the carbon-arsenic bond length is 1.83 \AA and 1.89 \AA in $\text{Ph}_3\text{P}=\text{C}(\text{AsCl}_2)_2$. The lengthening of the bond in derivative **38** can be attributed to the great steric hindrance of the bulky Mes^* group, but is also probably due to the different electronic properties of the Mes^* group in relation to the halogen atom.

The analysis of the crystal packing of **38** using the Platon package of programs [16] indicates that weak secondary $\text{F}\cdots\text{H}$ interactions occur between the halogen on the arsenic and *t*Bu protons on the Mes^*P group from a neighboring unit. The interatomic distance is 2.59 \AA , slightly shorter than the sum of the van der Waals radii [17], of 2.67 \AA . These interactions are reinforced by $\text{C}-\text{H}\cdots\pi$ between *t*Bu groups on the Mes^*P unit on one molecule and the center of the Mes^* group on the arsenic atom on the other one. This leads to the creation of distinct units formed of two molecules, as shown in Figure V.3.

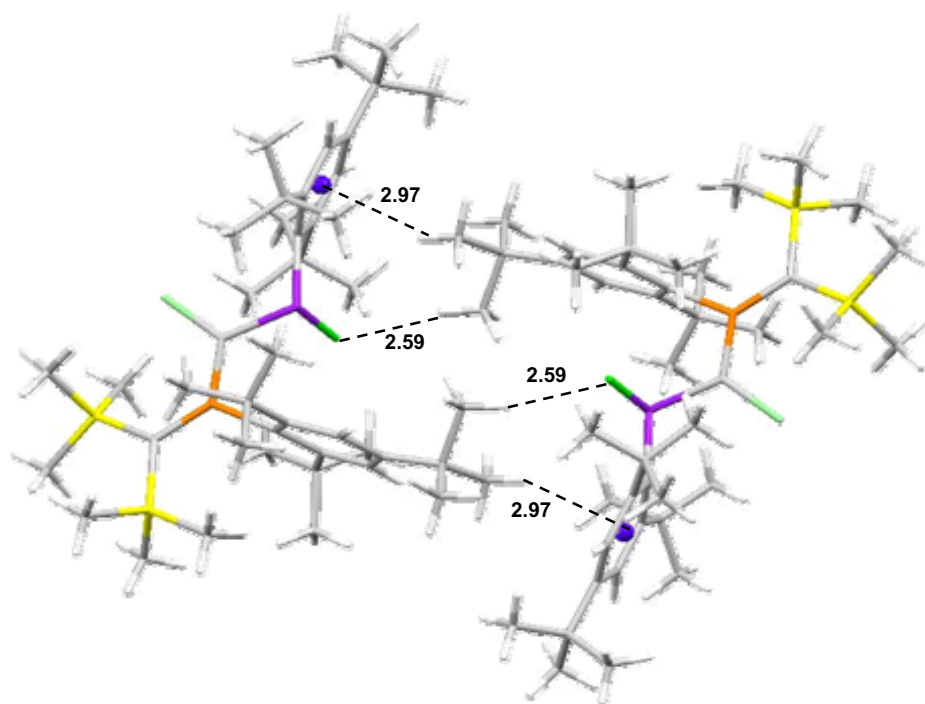


Figure V.3. Distinct units formed through weak interactions in the crystal packing of **38**

These units connect through H...H interactions (2.33 Å) to form zig-zag tridimensional chains, which further pack in layers containing parallel chains through *t*Bu interactions of 2.36 Å (figure V.4).

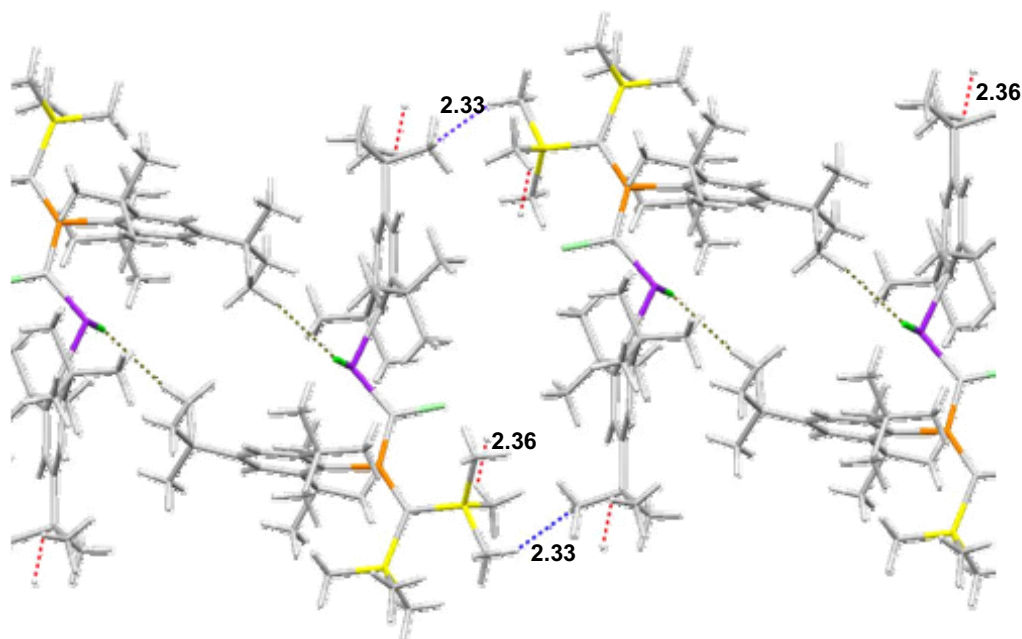


Figure V.4. The crystal packing of **38** in zig-zag chains

It can be noticed that the secondary interactions leading to the pattern described for the crystalline packing of compound **38** has no influence on the As-F bond length, which is in the range reported in the literature for fluoro-substituted organometallic derivatives of arsenic (1.68-1.8 Å) [18]. The P=C-As moiety is also not influenced by the spatial arrangement in the crystal.

2) Action of *t*BuLi on the arsanyl-bis(methylene)phosphorane 38

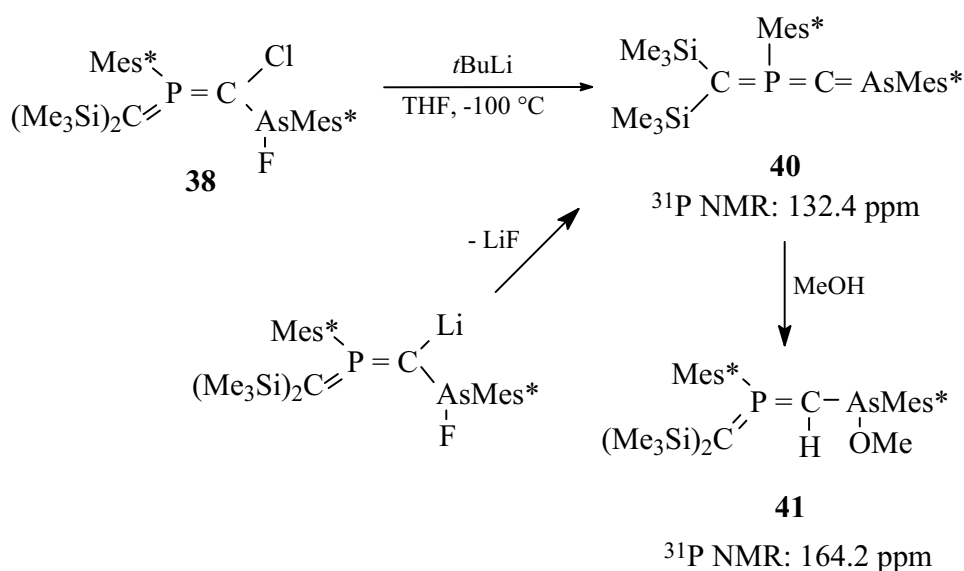
The reaction of derivative **38** with *t*BuLi was followed in ^{31}P NMR. Only 50% of the arsanyl-bis(methylene)phosphorane was converted into a derivative characterized by a chemical shift of 132.4 ppm. This yield was not improved even when two equivalents of *t*BuLi were added, but was increased to almost 75% when a mixture of one equivalent of *n*BuLi and one of *t*BuLi was used.

Although it has not yet been unequivocally identified since it could not be purified, this compound could be the first 2-phospha-4-arsabutatriene known to date; and

its ^{31}P NMR data are convenient for such a structure. It is stable in solution for several days and its stability is similar to that of the arsaphosphaallene $\text{Mes}^*\text{P}=\text{C}=\text{AsMes}^*$ with a $\lambda^3\sigma^2$ phosphorus atom [19]. When exposed to air, degradation was only observed after a couple of hours, with the formation of a still unknown derivative at 88.0 ppm.

Subsequent treatment of **40** with methanol caused the ^{31}P NMR signal to shift from 132.4 ppm towards lower field (164.1 ppm). We can postulate the formation of compound **41** by addition of MeOH to the $\text{As}=\text{C}$ double bond which is polarized $\text{As}^{\delta+}-\text{C}^{\delta-}$. Compound **41** presents about the same ^{31}P chemical shift as the starting **38** due to a close similarity in structures (the F atom is replaced by OMe). Attempts to separate and further characterize by ^1H and ^{13}C NMR the derivative **40** are still in progress.

Scheme V.12 depicts the assignments we have assumed for the course of reaction:



Scheme V.12.

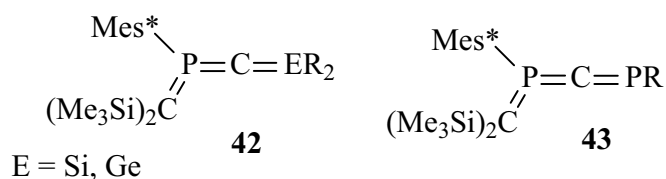
Table V.2 shows the comparison on which we have based our assumptions.

Table V.2. NMR data for compounds **37**, **38**, **40** and **41**

Compound	³¹ P NMR
(Me ₃ Si) ₂ C=P(Mes*)=CCl ₂ 37 [1]	128.61
(Me ₃ Si) ₂ C=P(Mes*)=C(Cl) As(F)Mes* 38	157.0
(Me ₃ Si) ₂ C=P(Mes*)=C=AsMes* 40	132.4
(Me ₃ Si) ₂ C=P(Mes*)=C(H)As(OMe)Mes* 41	164.2

In conclusion, we can postulate the synthesis of the first compound with three cumulenenic double bonds C=P=C=As although more characterizations are necessary to be completely sure of the structure.

One interesting thing we can emphasize is the easy coupling reaction of the lithium compound (Me₃Si)₂C=P=C(Cl)Li to an arsenic moiety. Thus, such a reaction should be generalized to silicon or germanium units in order to prepare new types of phosphacumulenic compounds such as **42** (Scheme V.13).

**Scheme V.13.**

By an adequate choice of group R, the synthesis of **43** should also be possible.

Experimental Section

General procedures

All experiments were carried out in flame-dried glassware under an argon atmosphere using high-vacuum-line techniques. Solvents were dried and freshly distilled from sodium benzophenone ketyl and carefully deoxygenated on a vacuum line by several “freeze-pump-thaw” cycles. NMR spectra were recorded in CDCl₃ on the following spectrometers: ¹H, Bruker Avance 300 (300.13 MHz) and Avance 400 (400.13 MHz); ¹³C{¹H}, Bruker Avance 300 (75.47 MHz) and Avance 400 (100.62 MHz) (reference TMS), ³¹P, Bruker AC200 at 81.02 MHz (reference H₃PO₄). Melting points were determined on a Wild Leitz-Biomed apparatus. Mass spectra were obtained on a Hewlett-Packard 5989A spectrometer by EI at 70 eV.

1) Synthesis of trifluoroarsane [7]

AsF₃ was prepared by distillation at atmospheric pressure of a reaction mixture of 23.40 g of CaCl₂, 19.8 g of As₂O₃ and 98.10 g of H₂SO₄. 16.4 g of ASF₃ (62%, PE 58 °C) were obtained.

2) Synthesis of supermesityldifluoroarsane Mes*AsF₂ [8]

44.7 ml (71.6 mmol) of a solution 1.6 M of n-BuLi in hexane were added dropwise to a solution of Mes*Br (22.16 g, 68.2 mmol) in THF (120 ml) cooled at -78°C. The reaction became yellow and was left for 3 hours under stirring at this temperature. Then the lithium compound Mes*Li was slowly added to a solution of AsF₃ (9.0 g, 68.2 mmol) in THF (20 ml) cooled at -78 °C. After the end of the addition, the reaction mixture was slowly warmed to room temperature, the solvent removed under vacuum. 160 ml of

pentane were added and the lithium salts were eliminated by filtration. Crystallization from pentane at -30 °C afforded 20.50 g (84%) of white crystals of Mes*AsF₂.

$\delta^1\text{H}$ (300 MHz): 1.30 ppm (s, 9H, *t*Bu), 1.47 ppm (s, ${}^6J_{\text{HF}} = 1.0$ Hz, 18H, *o-t*Bu), 7.33 ppm (s, 2H, arom H).

$\delta^{19}\text{F}$ (188.3 MHz): -21.83 ppm.

3) Synthesis of Mes*P=C(SiMe₃)₂

To 5 g (14 mmol) of **1** in 50 mL of THF cooled at -95 °C, 9.5 mL of *n*-BuLi 1.6 M in hexane (10% excess) were added dropwise. The reaction mixture was stirred at low temperature (-75 °C) for 45 minutes to ensure the formation of the lithio derivative **2**, then 1.77 ml of Me₃SiCl (14 mmol) were added dropwise. The solution was allowed to warm up to room temperature and the formation of Mes*P=C(Cl)(SiMe₃) was identified through ³¹P-NMR spectroscopy in almost quantitative yield ($\delta = 287.5$ ppm). Without separating LiCl, the reaction mixture was cooled again at -95 °C and another 9.5 ml of *n*BuLi 1.6M were added. After 15 minutes under stirring at low temperature, 2 ml of Me₃SiCl (15% excess) were added dropwise. After the solution was warmed up to room temperature, THF was removed under vacuum and replaced by 40 ml of pentane, from which LiCl was removed by filtration. Concentrating the obtained solution to 20 ml and keeping it at -25 °C for 24h led to the precipitation of 5.7 g of Mes*P=C(SiMe₃)₂ ($\eta = 94\%$).

$\delta^{31}\text{P}$ (121.5 MHz): 392 ppm

$\delta^1\text{H}$ (300 MHz): -0.40 ppm (s, 9H, Me₃Si), 0.20 (d, 9H, Me₃Si, ${}^4J_{\text{PH}} = 1.5$ Hz), 1.25 ppm (s, 9H, *p-t*Bu), 1.45 ppm (s, 18H, *o-t*Bu), 7.40 (s, 2H, arom H) [20]

4) Synthesis of 2,4,6-tri-*tert*-butylphenyl[bis(trimethylsilyl)methylene]-dichloromethylenephosphorane 37

A solution of 1.2 ml of CHCl₃ (15 mmol) in 20 ml of THF and 5 ml of Et₂O was cooled down at -100 °C and 10 ml of *n*-BuLi 1.6 M in hexane (1 equiv) were added dropwise. The reaction mixture was left under stirring for an hour. The synthesis described in the literature involves cannulating the resulting LiCCl₃ to Mes*P=C(SiMe₃)₂. We found that the reverse addition, thus the dropwise addition of a solution of 6 g of Mes*P=C(SiMe₃)₂ (14 mmol) in 100 ml of Et₂O to a CHCl₃/*n*-BuLi mixture cooled down at -120 °C, increased the yield by 14%.

The resulting mixture was allowed to warm up to room temperature. The solvent was removed under vacuum and replaced by 70 ml of pentane. The lithium salts were filtrated off and the solution was concentrated under vacuum and cooled to -25 °C. After 24 hours, **38** precipitated as a yellow powder ($\eta = 92\%$).

$\delta^{31}\text{P}$ (121.5 MHz): 128 ppm (s).

$\delta^1\text{H}$ (300 MHz): 0.21 ppm (s, 9H, SiCH₃), 0.26 ppm (s, 9H, SiCH₃), 1.26 ppm (s, 9H, *p*-*t*Bu), 1.61 (d, 18H, ⁴J_{PH} = 0.7 Hz, *o*-*t*Bu), 7.49 ppm (d, ⁴J_{PH} = 5.0 Hz, arom H).

5) Synthesis of 2,4,6-tri-*tert*-butylphenyl[bis(trimethylsilyl)methylene][(2,4,6-tri-*tert*-butylphenyl)fluoroarsanyl]chloromethylene]phosphorane 38

A solution of 1g (1.9 mmol) of **37** in 50 ml of THF was cooled down to -90 °C and 1.2 ml *n*-BuLi 1.6 M in hexane (1 equiv) was added dropwise. The mixture was stirred for 15 minutes and then 0.72 g of Mes*AsF₂ (1.9 mmol) in 30 ml of THF were added by canulation. After warming up to room temperature, the solvent was evaporated and replaced by 50 ml of pentane. The salts were removed by filtration and the filtrate was kept at -25 °C. After several hours, yellow crystals of **38** (m.p. = 147 °C) were collected ($\eta = 66\%$).

$\delta^1\text{H}$ (300 MHz, (C₆D₆): 0.21 and 0.43 (2s, 2 x 9H, Me₃Si), 1.09 and 1.20 (2s, 2 x 9H, *p*-*t*Bu of Mes*As and Mes*P), 1.53 (d, J_{HF} = 0.6 Hz, 18H, *o*-*t*Bu of Mes*As), 1.75 and 1.85

(2s, 2 x 9H, *o*-*t*Bu of Mes*P), 7.07 (s, 2H, arom H of Mes*As), 7.50 and 7.61 (2dd, $^4J_{\text{HH}} = 1.8$ Hz, $^4J_{\text{HP}} = 4.5$ Hz, arom H of Mes*P).

$\delta^{13}\text{C}$ (75.5 MHz, THF d_8): 3.54 (d, $^3J_{\text{CP}} = 5.2$ Hz, SiMe₃), 5.21 (d, $^3J_{\text{CP}} = 4.5$ Hz, SiMe₃), 29.67, 30.57 and 34.48 (*p*-Me₃C of Mes*P and Mes*As, *o*-Me₃C of Mes*As), 33.27 (d, $^4J_{\text{CP}} = 4.5$ Hz, *o*-Me₃C of Mes*P), 34.00 (d, $^4J_{\text{CP}} = 3.0$ Hz, *o*-Me₃C of Mes*As), 34.38 and 34.79 (2s, *p*-Me₃C of Mes*As and Mes*P), 38.83 (*o*-Me₃C of Mes*As), 40.58 and 40.97 (2d, $^3J_{\text{CP}} = 2.3$ Hz, *o*-Me₃C of Mes*P), 72.33 (dd, $^1J_{\text{CP}} = 49.1$ Hz, $^4J_{\text{CF}} = 5.3$ Hz, P=C(SiMe₃)₂), 94.96 (dd, $^1J_{\text{CP}} = 74.0$ Hz, $^2J_{\text{CF}} = 24.2$ Hz, P=C-As), 119.39 (d, $^1J_{\text{CP}} = 83.8$ Hz, *ipso*-C of Mes*P), 123.05 (s, *m*-C of Mes*As), 126.63 (d, $^3J_{\text{CP}} = 12.8$ Hz, *m*-C of Mes*P), 127.43 (d, $^3J_{\text{CP}} = 12.1$ Hz, *m*-C of Mes*P), 140.06 (t, $^3J_{\text{CP}}$ and $^2J_{\text{CF}} = 10.2$ Hz, *ipso*-C of Mes*As), 149.85, 153.23 (d, $J_{\text{CP}} = 9.1$ Hz), 153.83 (d, $J_{\text{CP}} = 3.0$ Hz), 155.74 and 156.04 (d, $J_{\text{CP}} = 6.8$ Hz): *o*- and *p*-C of Mes*P and Mes*As

$\delta^{19}\text{F}$ (188.3 MHz): -151.4 ppm (d, $^3J_{\text{PF}} = 4.5$ Hz)

$\delta^{31}\text{P}$ (121.5 MHz): 157.0 ppm (d, $^3J_{\text{PF}} = 4.5$ Hz)

MS (EI, m/z): 820 (M, 5), 800 (M - F - H, 15), 763 (M - *t*Bu, 40), 729 (M - *t*Bu - Cl - H, 25), 656 (M - *t*Bu - Cl - SiMe₃, 25), 641 (M - *t*Bu - Cl - SiMe₃ - Me, 35), 575 (M - Mes*, 100).

Table V.3. Crystal data and structure refinement for **38**

Empirical formula	$C_{44} H_{76} As Cl F P Si_2$	
Formula weight	821.57	
Temperature	173(2) K	
Wavelength	0.71073 Å	
Crystal system	Triclinic	
Space group	P-1	
Unit cell dimensions	$a = 10.206(6)$ Å	$\alpha = 84.565(17)^\circ$.
	$b = 14.094(7)$ Å	$\beta = 86.049(12)^\circ$.
	$c = 16.386(9)$ Å	$\gamma = 88.444(15)^\circ$.
Volume	2340(2) Å ³	
Z	2	
Density (calculated)	1.166 Mg/m ³	
Absorption coefficient	0.900 mm ⁻¹	
F(000)	884	
Crystal size	0.05 x 0.2 x 0.4 mm ³	
Theta range for data collection	5.12 to 21.97°.	
Index ranges	-10 ≤ h ≤ 10, -14 ≤ k ≤ 14, 0 ≤ l ≤ 17	
Reflections collected	5386	
Independent reflections	5386 [R(int) = 0.0000]	
Completeness to theta = 21.97°	94.1 %	
Absorption correction	Semi-empirical	
Max. and min. transmission	1.000000 and 0.628162	
Refinement method	Full-matrix least-squares on F ²	
Data / restraints / parameters	5386 / 552 / 543	
Goodness-of-fit on F ²	1.005	
Final R indices [I > 2σ(I)]	R1 = 0.0798, wR2 = 0.1771	
R indices (all data)	R1 = 0.1375, wR2 = 0.1930	
Largest diff. peak and hole	0.411 and -0.879 e.Å ⁻³	

Resolution of the structure of 38

5386 independent reflections were collected at low temperatures (T = 173(2) K) using an oil-coated shock-cooled crystal on a Bruker-AXS CCD 1000 diffractometer with MoK α radiation ($\lambda = 0.71073$ Å). The structure was solved by direct methods [21] and 543 parameters were refined using the least-squares method on F^2 [22]. All non hydrogen atoms were refined anisotropically.

The largest electron density residue is $0.411 \text{ e}\text{\AA}^{-3}$ and R_I (for $I > 2\sigma(I)$) = 0.0798 and $wR_2 = 0.1930$ (all data) with $R_I = \sum ||F_o| - |F_c|| / \sum |F_o|$ and $wR_2 = (\sum w(F_o^2 - F_c^2)^2 / \sum w(F_o^2)^2)^{0.5}$.

6) Synthesis and characterization of **40**

A solution of 0.5g (0.6 mmol) of **38** in 20 ml of THF was cooled down to $-90 \text{ }^\circ\text{C}$ and 0.44 ml of *t*-BuLi 1.5 M in hexane (10% excess) was added dropwise. After warming up to room temperature, the solvent was evaporated and replaced by 20 ml of pentane. The salts were removed by filtration and the yellow filtrate was kept at $-25 \text{ }^\circ\text{C}$. Several crystals appeared which were identified by NMR as starting derivative **38**. Compound **40** was identified by ^{31}P NMR (132.4 ppm).

7) Synthesis and characterization of **41**

Derivative **41** was obtained in the NMR tube, by adding a drop of methanol to the mixture of **38** and **40** in THF, at room temperature. The reaction mixture was then characterized by ^{31}P NMR. The signal corresponding to **40** is replaced by one at 164.2 ppm attributed to **41**.

References:

1. a) Escudié, J.; Ranaivonjatovo, H.; Rigon, L.; *Chem. Rev.*, **2000**, *100*, 3639 ; b) Escudié, J.; Ranaivonjatovo, H.; *Organometallics*, **2007**, *26*, 1542.
2. a) Schröder, H. P.; Jochem, G.; Schmidpeter, A.; Nöth, H. *Angew. Chem., Int. Ed. Engl.*, **1995**, *34*, 1853, b) Krüger, U.; Pritzkow, H.; Grützmacher, H.; *Chem. Ber.*, **1991**, *124*, 329.
3. a) Martin, D.; Tham, F. S.; Baceiredo, A.; *Chem. Eur. J.* **2006**, *12*, 8444; b) Martin, D.; Gornitzka, H.; Baceiredo, A.; Bertrand, G.; *Eur. J. Inorg. Chem*, **2005**, *13*, 2619.
4. Ramirez, F.; Desai, N. B.; Hansen, B.; McKelvie, N.; *J. Am. Chem. Soc.*, **1961**, *83*, 3539.
5. Septelean, R.; Ranaivonjatovo, H.; Nemes, G.; Escudié, J.; Silaghi-Dumitrescu, I.; Gornitzka, H.; Silaghi-Dumitrescu, L.; Massou, S.; *Eur. J. Inorg. Chem.*, **2006**, 4237.
6. Niecke, E.; Becker, P.; Nieger, M.; Stalke, D.; Schoeller W. W.; *Angew. Chem., Int. Ed. Engl.*, **1995**, *34*, 1849.
7. Hoffman, C. J.; *Inorg. Synth.*, **1953**, *4*, 149.
8. Pakulski, M. P.; Whitlesey, B. R.; Atwood, J. L.; Hunter, W.E.; *Inorg. Chem.*, **1984**, *23*, 2582.
9. Petrar, P.M.; Nemes, G.; Silaghi-Dumitrescu, L.; Silaghi-Dumitrescu, I.; Escudié, J.; Gornitzka, H.; Ranaivonjatovo, H.; *Rev. Roum. Chimie*, **2007**, *52(1-2)*, 45.
10. Ranaivonjatovo, H.; Ramdane, H.; Gornitzka, H.; Escudié, J.; Satgé, J.; *Organometallics*, **1998**, *17*, 1631.
11. Appel, R.; Peters, J.; Westerhaus, A.; *Angew. Chem., Int. Ed. Engl.*, **1982**, *21*, 80.
12. Appel R.; "Multiple Bonding and Low Coordination in Phosphorus Chemistry", Eds: Regitz, M.; Scherer, O. J.; Thieme, **1990**, p 367.
13. Appel, R.; "Multiple Bonds and Low Coordination in Phosphorus Chemistry", Eds: Regitz, M.; Scherer, O. J.; Thieme, **1990**, p 157.
14. Breitsameter, F.; Schmidpeter, A.; Nöth, H.; *Chem.-Eur.J.* , **2000**, *6*, 3531.
15. Schmidbaur, H.; Nusstein, P.; Müller, G.; *Z.Naturforsch.,B:Chem.Sci.* , **1984**, *39*,1456.

16. Spek, A.L., *Acta Crystallogr.*, **1990**, *A46*, C34.
17. Winter, M.; WebElements, the periodic table on the Web, <http://w.w.w.webelements.com>.
18. a) Preut, H.; Kasemann, R.; Naumann, D.; *Acta Crystallogr., Sect. C: Cryst. Struct. Commun.*, **1986**, *42*, 1875; b) Salem, G.; Shaw, G.B.; Willis, A.C.; Wild, S.B.; *J. Organomet. Chem.*, **1993**, *455*, 185; c) Minkwitz, R.; Hirsch, C.; *Z. Anorg. Allg. Chem.*, **1999**, *625*, 1362; d) Avtomonov, E.V.; Megges, K.; Wocadlo, S.; Lorberth, J.; *J. Organomet. Chem.*, **1996**, *524*, 253; e) Augustine, A.; Ferguson, G.; March, F.C.; *Can. J. Chem.*, **1975**, *53*, 1647; f) Kuschel, R.; Seppelt, K.; *J. Fluorine Chem.*, **1993**, *61*, 23; g) Arduengo III, A.J.; Davidson, F.; Krafczyk, R.; Marshall, W.J.; Schmutzler, R.; *Monatsh. Chem.*, **2000**, *131*, 251.
19. Ranaivonjatovo, H.; Ramdane, H.; Gornitzka, H.; Escudié, J.; Satgé, J.; *Organometallics*, **1998**, *17*, 1631.
20. Crowley, A. H.; Jones, R. A.; Lasch, J. G.; Norman, N. C.; Stewart, C. A.; Stuart, A. L.; Atwood, J. L.; Hunter, W. E.; Zhang, H.-M.; *J. Am. Chem. Soc.*, **1984**, *106*, 7015.
21. SHELXS-97, Sheldrick, G. M.; *Acta Crystallogr.*; **1990**, *A46*, 467.
22. SHELXL-97, Program for Crystal Structure Refinement, Sheldrick, G. M.; University of Göttingen, **1997**.

Chapter V- Recapitulative list of synthesized compounds

<i>Derivative</i>	<i>Number</i>
$\begin{array}{c} \text{Mes}^* \\ \diagdown \\ \text{P} = \text{C} \begin{array}{l} \diagup \text{Cl} \\ \diagdown \text{Cl} \end{array} \\ \diagup \\ (\text{Me}_3\text{Si})_2\text{C} \end{array}$	37
$\begin{array}{c} \text{F} \\ \\ \text{AsMes}^* \\ \\ \text{C} \begin{array}{l} \diagup \text{Cl} \\ \diagdown \end{array} \\ \\ \text{P} = \text{C} \begin{array}{l} \diagup \text{Cl} \\ \diagdown \end{array} \\ \diagup \\ \text{Mes}^* \\ \diagdown \\ (\text{Me}_3\text{Si})_2\text{C} \end{array}$	<u>38</u>
$\begin{array}{c} \text{Mes}^* \\ \diagdown \\ \text{P} = \text{C} \begin{array}{l} \diagup \text{Li} \\ \diagdown \text{Cl} \end{array} \\ \diagup \\ (\text{Me}_3\text{Si})_2\text{C} \end{array}$	39
$\begin{array}{c} \text{Mes}^* \\ \\ \text{C} = \text{P} = \text{C} = \text{AsMes}^* \\ \diagup \quad \diagdown \\ \text{Me}_3\text{Si} \quad \text{Me}_3\text{Si} \end{array}$	<u>40</u>
$\begin{array}{c} \text{Mes}^* \\ \diagdown \\ \text{P} = \text{C} - \text{AsMes}^* \\ \diagup \quad \quad \\ (\text{Me}_3\text{Si})_2\text{C} \quad \text{H} \quad \text{OMe} \end{array}$	<u>41</u>

N – novel compounds

Conclusion

Cette étude décrit la synthèse et la caractérisation de précurseurs d'hétéroallènes et d'hétérocumulènes (hétéroéléments = éléments des groupes 14 et 15) et leur réaction avec des organolithiés. Une étude DFT d'hétéroallènes du type $>E_{14}=C=P-$ montre que ces dérivés sont cinétiquement et thermodynamiquement instables et que le facteur principal pour la faible stabilité de la double liaison $E_{14}=C$ est une hyperconjugaison entre la paire libre du phosphore et l'orbitale antiliante localisée sur la double liaison. Des substituants organométalliques possédant un caractère de base ou d'acide de Lewis augmentent cette interaction ; en conséquence, les groupes appropriés pour stabiliser la double liaison $E_{14}=C$ sont les groupes contenant ces éléments. Cette étude théorique a été étendue aux dérivés de formule brute CH_3GeP , CMe_3GeP et CH_3SiP , isomères des hétéroallènes correspondants, pour déterminer lesquels sont les plus stables. Il apparaît ainsi que le dérivé triplement lié $P=Ge-CH_3$ est plus stable que le phosphagermaallène $HP=C=GeH_2$.

Les essais de synthèse d'un nouveau phosphagermaallène, $Mes^*P=C=Ge(tBu)_2$ ($Mes^* = 2,4,6$ -tri-*tert*-butylphényl), on en fait abouti à la formation de ses dimères formels, les 2,4-diphosphinylidène-1,3-digermacyclobutanes, premiers cycles à quatre chaînons digermaniés possédant deux doubles liaisons $C=P$ exocycliques. Les deux isomères *cis* et *trans* (par rapport à l'axe PCCP) ont été isolés et structuralement caractérisés par diffraction de rayons X. Des études par RMN à température variable ont permis de montrer que ces dérivés n'étaient pas obtenus par dimérisation du phosphagermaallène attendu mais probablement par une réaction de couplage intermoléculaire à partir du lithien $Mes^*P=C(Li)-Ge(F)(tBu)_2$.

L'action du soufre sur ces dérivés conduit aux bis(méthyléthioxo)phosphoranes, premiers dérivés possédant deux entités $C=P(S)-$, sous la forme de leurs deux isomères *cis* et *trans*. Ces composés se sont révélés très stables en présence d'eau ou d'oxygène, ainsi que d'un excès de soufre. Ceci est sans doute lié au très gros encombrement stérique puisque généralement, en fonction des substituants sur les atomes de carbone et de phosphore, l'entité $C=P(S)$ se réarrange en thiaphosphirane et subit parfois une addition supplémentaire de soufre. La structure de ces deux dérivés a également été confirmée par rayons X. Une étude théorique par DFT indique qu'il n'y a pas de conjugaison nette entre les deux entités $C=P(S)$ à travers le cycle digermacyclobutane.

De nombreux nouveaux précurseurs d'hétéroallènes, à savoir des phosphagermapropènes, ont également été obtenus par les voies de synthèse déjà décrites dans la littérature. Des substituants de nature différente ont été introduits sur l'atome lourd afin de stabiliser ultérieurement l'hétéroallène $-P=C=E_{14}<$. L'une des principales difficultés dans la préparation des précurseurs des hétéroallènes réside dans le choix des substituants : ceux-ci ne doivent pas être trop volumineux afin de ne pas empêcher l'approche et le couplage des deux entités métallées et phosphorées, mais suffisamment afin de stabiliser l'espèce à basse coordinence. Le choix des groupes sur le métal 14 est primordial. L'action d'un organolithien sur les dihalogénophosphagermapropènes, qui est généralement la meilleure méthode pour éliminer les deux atomes d'halogène, a conduit dans la plupart des cas à plusieurs dérivés. L'élucidation de ces réactions est actuellement en cours.

Ce travail a également permis de synthétiser de nouveaux dihalophosphasilapropènes, caractérisés par RMN multinoyaux 1H , ^{13}C , ^{29}Si et ^{31}P , dans lesquels l'atome de silicium est notamment substitué par deux entités $Mes^*P=C(Cl)$. L'intérêt d'avoir deux motifs de ce type réside dans le fait que les phosphasilaallènes attendus $Mes^*P=C=Si(R)-C(Cl)=PMes^*$ pourraient être stabilisés, de façon inédite, par une conjugaison entre le motif hétéroallénique et la double liaison $C=P$. En fait les tentatives de déshalogénéation par un organolithien n'ont pas conduit à l'hétéroallène attendu mais à plusieurs dérivés dont l'identification est encore en cours. De nouvelles réactions de déshalogénéation sont envisagées avec des organomagnésiens, des cuivriques et des zinciques afin d'obtenir les phosphasilaallènes.

La synthèse d'un dihalogénophosphastannapropène substitué par un groupe supermésityle sur le phosphore et deux groupes bis(triméthylsilyl)méthyles sur l'étain a été effectuée. L'action d'un organolithien a conduit à un stannane substitué par deux groupes $Mes^*P=C(Cl)$ par une réaction de déshalogénéation intermoléculaire. Une nouvelle voie de synthèse d'hétéroallènes a été envisagée, à savoir la création préliminaire de la double liaison $Sn=C$ suivie de celle de la double liaison $P=C$. Les essais de synthèse de précurseurs de type $Tip_2Sn=CX_2$ ($Tip = 2,4,6$ -triisopropylphényle) à partir de Tip_2SnF_2 ont en fait conduit à deux dérivés stannylés : $Tip_2Sn(Br)CBr_3$, caractérisé par une étude aux rayons X, et $Tip_2Sn(CHBr_2)_2$; pour ce dernier, un couplage $Sn-Br$ a été mis en évidence. Notons que c'est la première fois qu'un tel couplage avec un aussi grand nombre d'atomes de brome a été observé.

L'arsanylbis(méthylène)phosphorane $(\text{Me}_3\text{Si})_2\text{C}=\text{P}(\text{Mes}^*)=\text{C}(\text{Cl})-\text{As}(\text{F})\text{Mes}^*$ a été obtenu et caractérisé par une étude aux rayons X. L'action d'un organolithien a conduit au premier cumulène contenant l'entité $>\text{C}=\text{P}(\text{R})=\text{C}=\text{As}-$; ce dernier a été mis en évidence par RMN et réaction avec le méthanol. Nos efforts portent actuellement sur son isolation afin de déterminer ses caractéristiques structurales.

Ce travail est une contribution à la chimie des éléments lourds des groupes 14 et 15, principalement le germanium et le phosphore, mais également le silicium et l'étain. De nombreux nouveaux métallaphosphapropènes ont été synthétisés. Des réactions stéréosélectives ont été mises en évidence à partir du C,C-dichlorophosphaalcène $\text{Mes}^*\text{P}=\text{CCl}_2$ de départ, le groupement organométallique sur le carbone doublement lié étant en *anti* du groupe supermésityle pour des raisons d'encombrement stérique. Les tentatives d'obtention des hétéroallènes correspondants n'ont pas abouti mais de nouvelles études sont en cours en utilisant d'autres réactifs pour effectuer les réactions de déshalogénéation. Les études théoriques ont montré que plusieurs isomères de phosphasilaallènes et de phosphagermaallènes devaient être plus stables que ces derniers, notamment des dérivés possédant une triple liaison GeP, et devraient pouvoir être stabilisés avec des groupements appropriés.

Avec l'apport des résultats déjà décrits dans la littérature, ces études montrent que la présence d'au moins un groupement aromatique sur l'élément E_{14} est nécessaire pour la formation d'un hétéroallène à partir du dihalogénohétéropropène correspondant.

Enfin, ces résultats confirment la grande différence entre les éléments lourds des groupes 14 et 15 ; citons par exemple la synthèse avec un excellent rendement de C,C-dihalogénophospha (ou arsa)alcènes $-\text{P}=\text{CX}_2$ à partir de dihalogénophosphines ou -arsines alors que le même type de réaction à partir de dihalogénostannanes ne conduit pas aux stannènes $>\text{Sn}=\text{CX}_2$.

GENERAL CONCLUSIONS

This study reports the synthesis and characterization of precursors of heteroallenes and heterocumulenes (heteroelement = group 14 and 15 element) and their reaction with lithium compounds. A DFT study of heavier group 14 heteroallenes of the type $>E_{14}=C=P-$ reveals that these compounds are both thermodynamically and kinetically unstable and that the main role in the weakening of the Ge=C bond is played by an hyperconjugative interaction between the lone pair situated on the P atom and the antibonding orbital localized on the double bond. Organometallic substituents of elements bearing lone pairs or vacant *p* orbitals induce other types of charge transfer which also result in the weakening of the Ge=C bond order, thus the appropriate groups to stabilize the Ge=C unit are the ones containing group 14 elements. This also makes a good experimental choice, and is in agreement with the substituents used so far in the synthesis of unsaturated derivatives of this kind.

A theoretical study on the derivatives of the general formula CH_3GeP has been performed; it displays that the triply bonded derivative $P\equiv GeCH_3$ is more stable than the phosphagermaallene $H_2Ge=C=PH$ and could be stabilized with appropriate substituents.

In an attempt to synthesize and structurally characterize a novel phosphagermaallene substituted by two *t*Bu groups on the germanium atom and a supermesityl group on the phosphorus atom, its formal dimers, diphosphinylidene-1,3-digermacyclobutanes were obtained. Both the *cis* and *trans* isomers (relatively to the PCCP axis) were formed and structurally characterized. These derivatives allowed the easy preparation of the first bis(methylenethio)phosphoranones with $C=P(S)Mes^*$ moieties (the corresponding *cis* and *trans* isomers), which displayed a pronounced stability towards oxidation or hydrolysis. This might be due to their high steric congestion since in other instances, depending on the substituents on C and P, the $C=P(S)$ units rearrange to thiaphosphiranes or give a further addition of sulfur. The solid-state structure of the two isomers of these phosphoranones was determined. A theoretical investigation performed at the DFT level indicates that there is no conjugation between the $C=P(S)$ units throughout the digermacyclobutane center.

Several novel precursors of group 14 heteroallenes were also obtained, using the synthetic routes already described in the literature, but varying the nature of the substituents on the heavier atom, in an attempt to find the appropriate method to stabilize the $>E_{14}=C=P$ - unit. The main difficulties in the preparation of heteroallenic precursors arise in the choice of the substituents, not too bulky to allow the coupling of the P and Ge units, but bulky enough in order to stabilize the low coordinate species. In this respect, the influence of the substituents on the heavier group 14 atom seems critical. The subsequent action of *t*BuLi on these derivatives to eliminate the vicinal halogens in order to obtain the heteroallene results in the formation of various products, but still, lithium derivatives remain the best choice. The elucidation of some of these reactions is still in progress. This work opens new perspectives in the chemistry of dihalophosphasila and dihalophosphagermapropenes. The synthesis of unsaturated tin derivatives was also attempted. Two novel organometallic tin compounds have been obtained. Their structure in solution was elucidated through NMR spectroscopy. While the synthetic route employed did not lead to the expected stannaallene, it afforded a potential precursor of doubly bonded derivatives of tin.

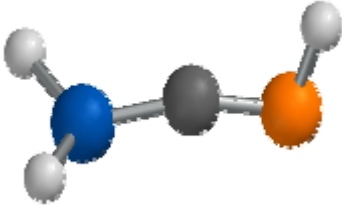
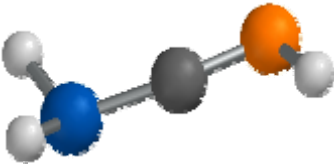
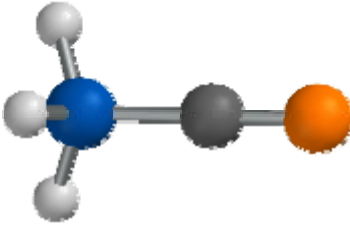
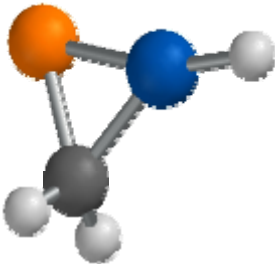
A novel arsanylbis(methylene)phosphorane, an arsenic-containing derivative with two $P=C$ double bonds, was obtained as a stable compound in the solid state. This derivative loses Cl and F by reaction with a lithium derivative to give the first cumulenic compound containing the $>C=P(R)=C=As$ - unit. Although its assignment is not fully sure, spectroscopic data point to its formation.

This work provides a useful insight in the chemistry of organometallic derivatives of group 14 and 15 elements and their ability to lead to unsaturated compounds with cumulated double bonds. Several novel derivatives are reported, some of them being the first of their type and theoretical aspects of heteroallenes and their isomers are also discussed. These studies also prove that the presence of at least one aromatic group on the E_{14} element is necessary to obtain heteroallenes from their halogenophosphapropene precursors.

Annex 1

Correlated methods in the investigation of phosphagermaallene isomers

Table A1. Calculated CCSD/6-31G(d,p) energies and geometrical parameters for HP=C=GeH₂ isomers

Molecule		
	I	Ia
Total Energy (au)	-2453.839071	-2453.725295
ΔE (kcal/mol)	48.74	120.09
Ge-C (Å)	1.784	1.758
P-C (Å)	1.648	1.648
Ge-C-P (°)	164.04	163.97
Molecule		
	II	III
Total Energy (au)	-2453.898196	-2453.869169
ΔE (kcal/mol)	10.93	30.28
Ge-C (Å)	1.917	1.941
P-C (Å)	1.556	1.972
Ge-C-P (°)	179.84	65.30

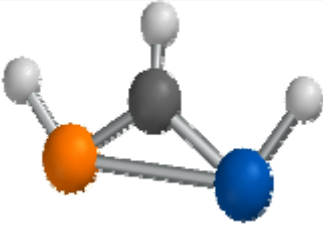
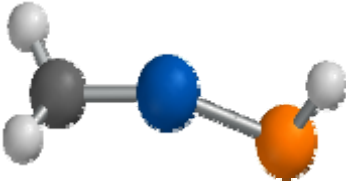
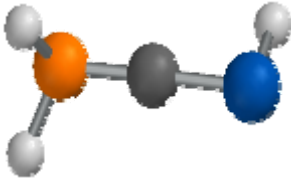
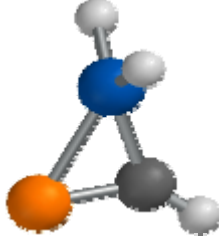
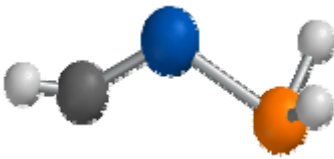
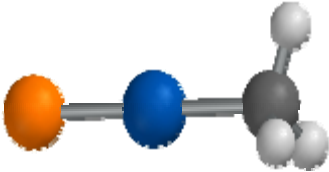
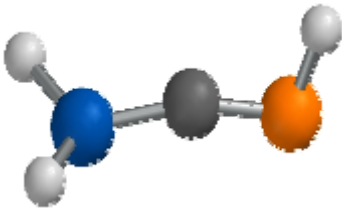
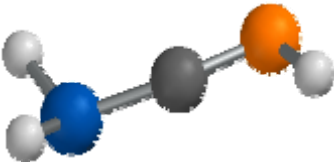
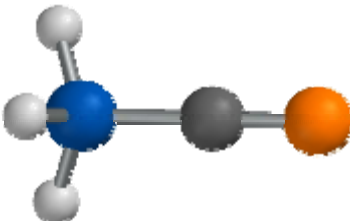
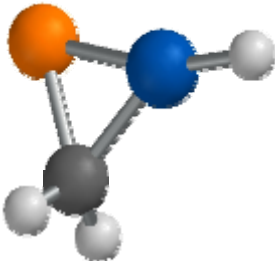
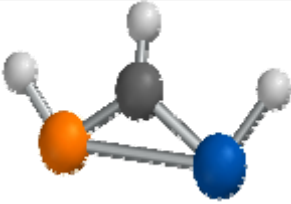
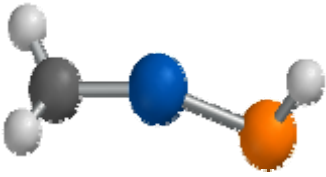
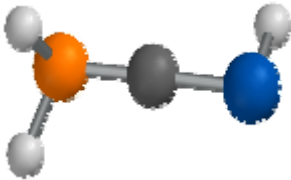
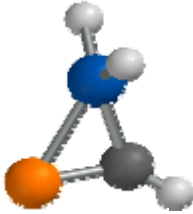
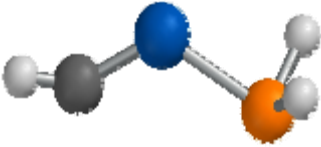
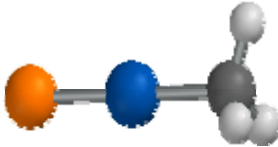
Molecule		
	IV	V
Total Energy (au)	-2453.867485	-2453.869561
ΔE (kcal/mol)	31.33	29.92
Ge-C (Å)	1.972	1.792
P-Ge (Å)	3.105	2.140
P-Ge-C (°)	29.23	157.82
Molecule		
	VI	VII
Total Energy (au)	-2453.811658	-2453.884057
ΔE (kcal/mol)	67.68	20.46
Ge-C (Å)	1.778	1.915
P-C (Å)	1.717	1.686
Ge-C-P (°)	170.35	79.87
Molecule		
	VIII	IX
E (HF)	-2453.823081	-2453.91631
ΔE (kcal/mol)	60.44	0.00
Ge-C (Å)	1.723	1.953
P-Ge (Å)	2.328	2.028
P-Ge-C (°)	129.16	179.92

Table A2. Calculated MP4(SDQ)/6-31G(d,p) energies and geometrical parameters for HP=C=GeH₂ isomers

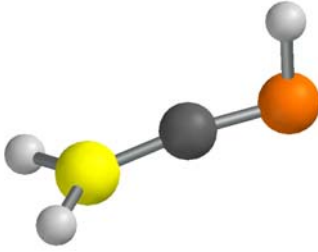
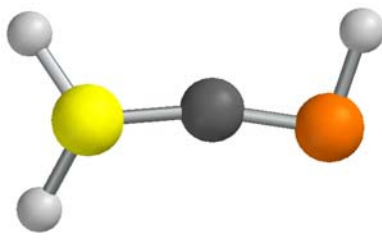
Molecule		
	I	Ia
Total Energy (au)	-2453.838522	-2453.724823
ΔE (kcal/mol)	48.46	119.86
Ge-C (Å)	1.789	1.790
P-C (Å)	1.650	1.645
Ge-C-P (°)	162.56	160.05
Molecule		
	II	III
Total Energy (au)	-2453.898768	-2453.867939
ΔE (kcal/mol)	11.36	29.58
Ge-C (Å)	1.918	1.953
P-C (Å)	1.560	1.987
Ge-C-P (°)	179.82	58.28

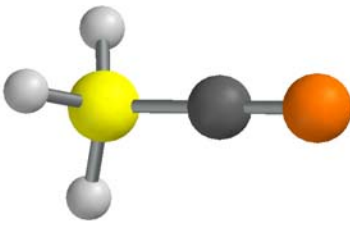
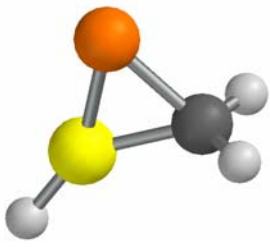
Molecule		
	IV	V
Total Energy (au)	-2453.866262	-2453.868517
ΔE (kcal/mol)	30.63	29.33
Ge-C (Å)	1.971	1.792
P-Ge (Å)	3.099	2.136
P-Ge-C (°)	29.40	156.79
Molecule		
	VI	VII
Total Energy (au)	-2453.808344	-2453.88359
ΔE (kcal/mol)	65.67	20.23
Ge-C (Å)	1.801	1.913
P-C (Å)	1.666	1.687
Ge-C-P (°)	177.84	79.82
Molecule		
	VIII	IX
E (HF)	-2453.819879	-2453.916201
ΔE (kcal/mol)	58.50	0.00
Ge-C (Å)	1.723	1.953
P-Ge (Å)	2.316	2.031
P-Ge-C (°)	136.31	179.91

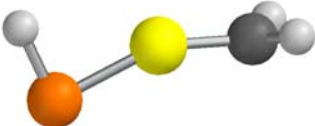
Annex 2

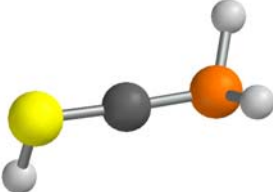
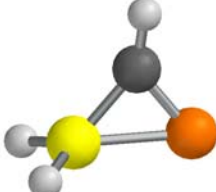
Correlated methods in the investigation of phosphasilallene isomers

Table A1. Calculated MP4(SDQ)/6-31G(d,p) energies and geometrical parameters for HP=C=GeH₂ isomers

Molecule		
	I	I'
Total energy (au)	-669.5074676	-669.5074652
ΔE (kcal/mol)	40.14	40.14
Si-C (Å)	1.705	1.705
P-C (Å)	1.650	1.650
Si-C-P (°)	170.66	170.65

Molecule		
	II	III
Total energy (au)	-669.5714341	-669.5280936
ΔE (kcal/mol)	0.0	27.19
Si-C (Å)	1.850	1.847
P-C (Å)	1.560	2.00
Si-C-P (°)	179.90	63.64

Molecule		
	IV	V
Total energy (au)	-669.5190915	-669.52005
ΔE (kcal/mol)	32.84	32.24
Si-C (Å)	1.889	1.720
P-Si (Å)	3.048	2.074
P-Si-C (°)	29.76	156.53

Molecule		
	VI	VII
Total energy (au)	-669.4676497	-669.5565368
DE (kcal/mol)	65.12	9.35
Si-C (Å)	1.701	1.822
P-C (Å)	1.698	1.691
Si-C-P (°)	176.61	78.24

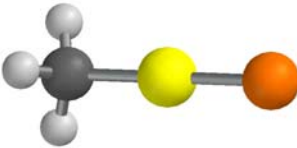
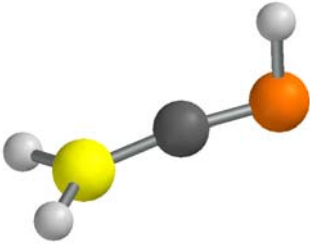
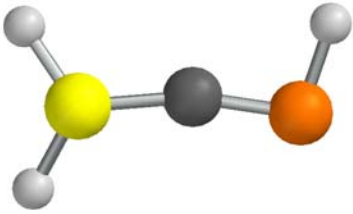
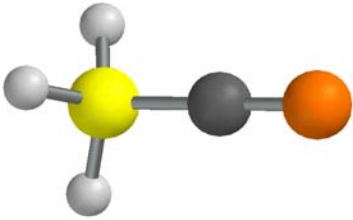
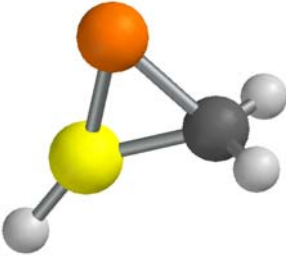
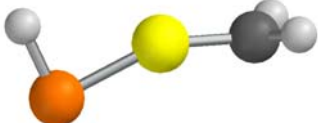
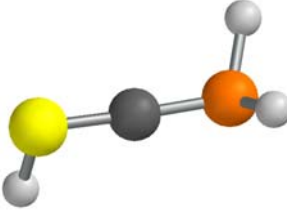
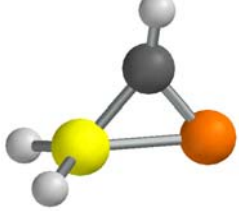
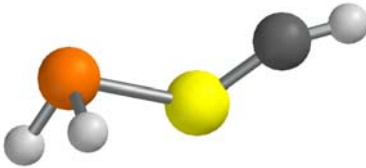
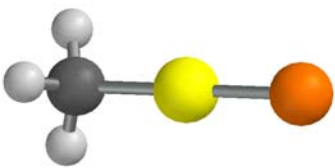
Molecule		
	VIII	IX
Total energy (au)	-669.4774651	-669.5627899
DE (kcal/mol)	58.96	5.42
Si-C (Å)	1.646	1.885
P-Si (Å)	2.252	1.972
P-Si-C (°)	131.54	174.90

Table A2. Calculated CCSD/6-31G(d,p) energies and geometrical parameters for HP=C=GeH₂ isomers

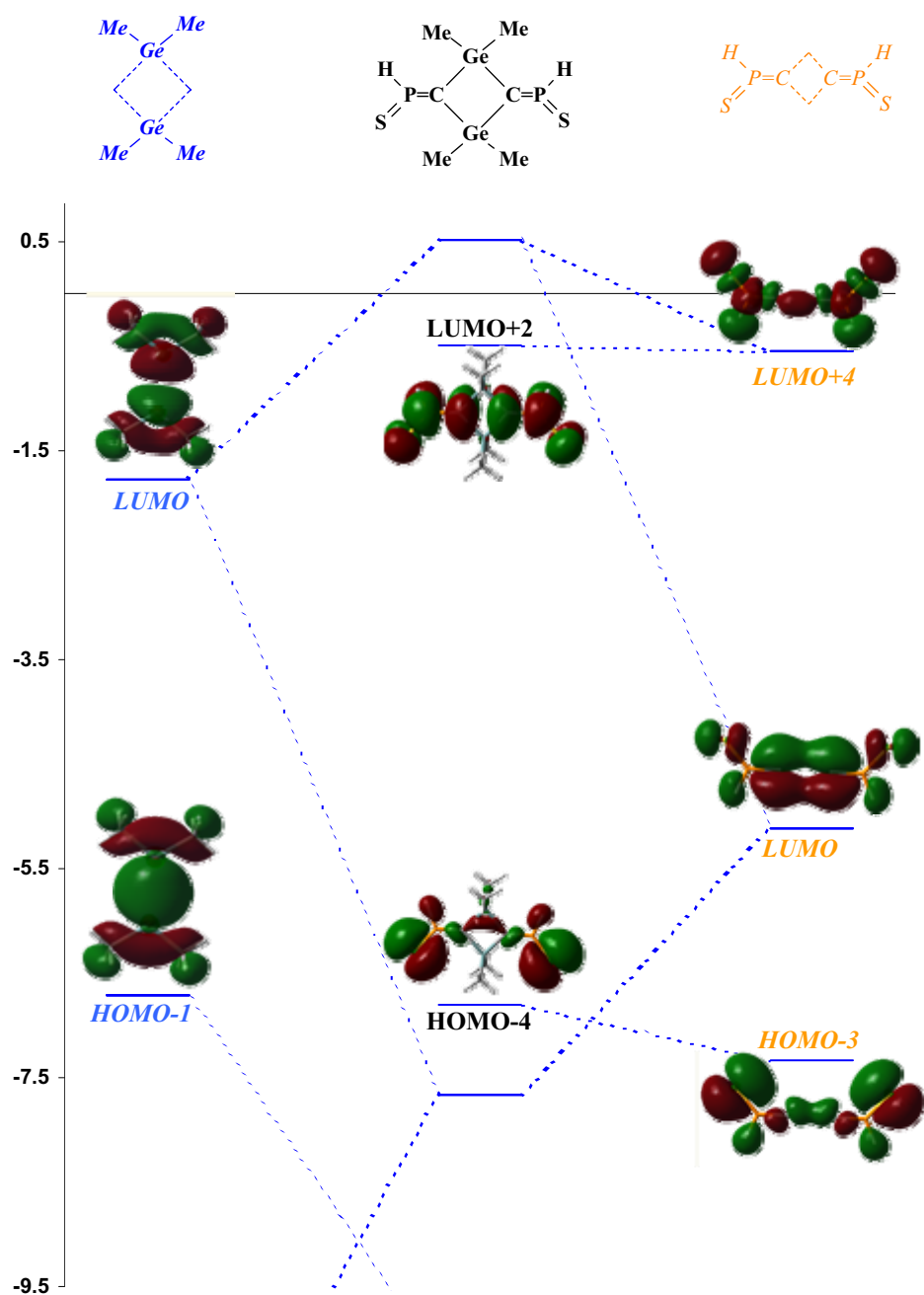
Molecule		
	I	I'
Total energy (au)	-669.5084238	-669.4132685
ΔE (kcal/mol)	39.28	98.99
Si-C (Å)	1.704	1.704
P-C (Å)	1.649	1.649
Si-C-P (°)	171.15	170.97
Molecule		
	II	III
Total energy (au)	-669.5710174	-669.530156
ΔE (kcal/mol)	0.0	25.64
Si-C (Å)	1.850	1.848
P-C (Å)	1.557	1.999
Si-C-P (°)	179.90	63.96

Molecule		
	IV	V
Total energy (au)	-669.5190915	-669.5211743
ΔE (kcal/mol)	32.58	31.28
Si-C (Å)	1.892	1.724
P-Si (Å)	3.114	2.080
P-Si-C (°)	27.73	152.67
Molecule		
	VI	VII
Total energy (au)	-669.4722701	-669.557128
ΔE (kcal/mol)	61.96	8.71
Si-C (Å)	1.692	1.822
P-C (Å)	1.730	1.690
Si-C-P (°)	170.40	78.27
Molecule		
	VIII	IX
Total Energy (au)	-669.4795293	-669.5630016
ΔE (kcal/mol)	57.41	5.03
Si-C (Å)	1.657	1.870
P-Si (Å)	2.264	1.976
P-Si-C (°)	125.00	179.12

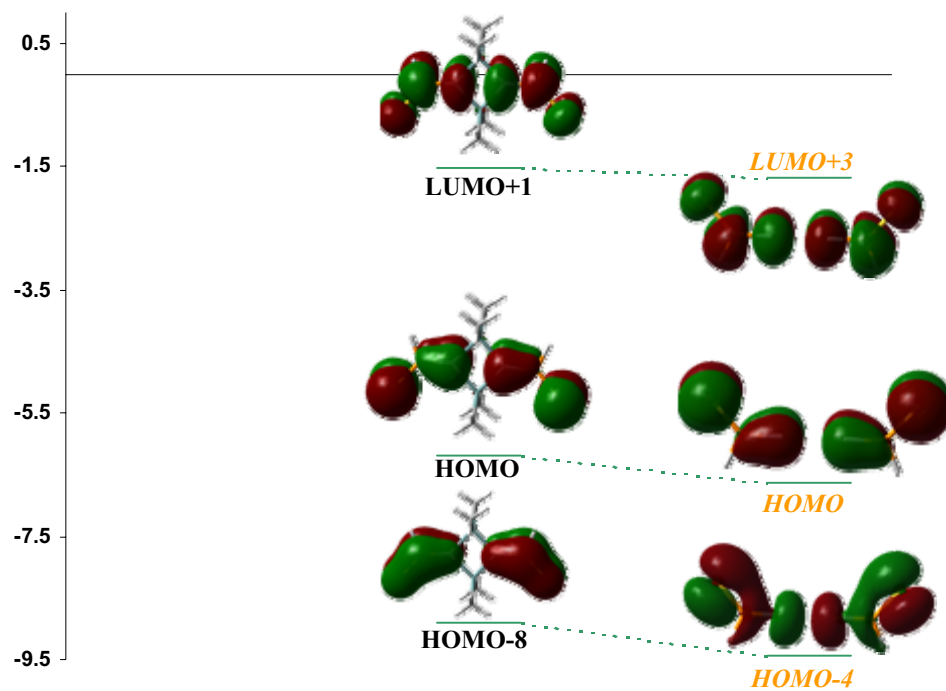
Annex 3

Molecular orbital diagrams for model compounds of 8

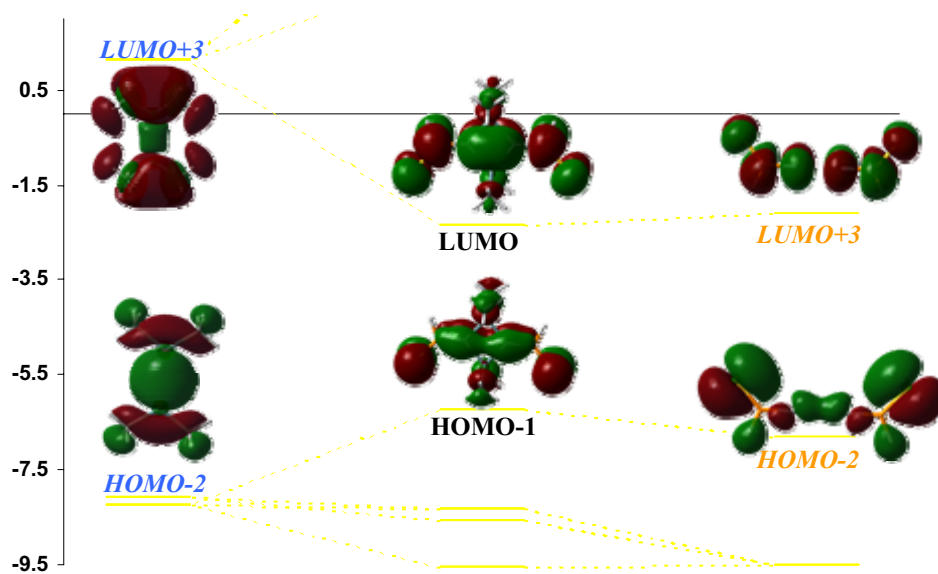
Interactions between symmetry adapted orbitals of $2\text{Me}_2\text{Ge}$ and $2\text{C}=\text{P}(\text{H})=\text{S}$ fragments to form $[\text{Me}_2\text{Ge}(\text{C}=\text{P}(\text{H})=\text{S})]_2$



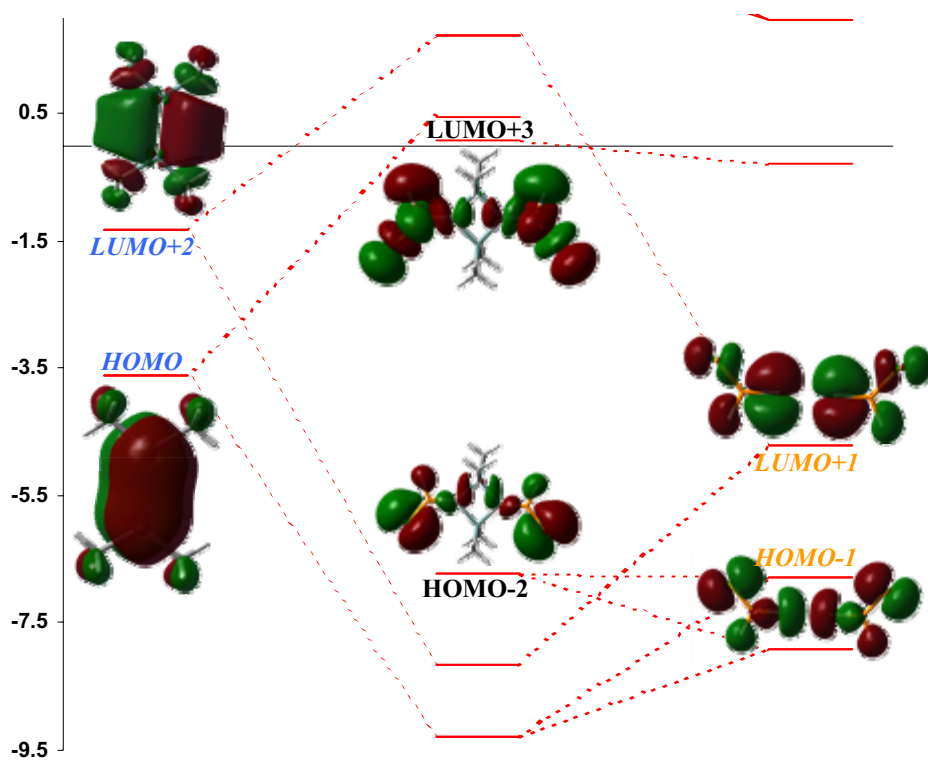
Interactions within the A_1 set of fragment-orbitals



Interactions within the A_2 set of fragment-orbitals



Interactions within the B_1 set of fragment-orbitals



Interactions within the B₂ set of fragment-orbitals